REGULATION OF FACULTATIVE HETEROCHROMATIN IN THE MODEL FUNGUS *NEUROSPORA CRASSA*

by

EDUARDO VICENTE TORRES

(Under the Direction of Zachary A. Lewis)

ABSTRACT

Gene repression by Polycomb Group (PcG) proteins is a conserved mechanism across metazoans and most eukaryotic organisms. Polycomb Repressive Complex 2 (PRC2) maintains gene repression by establishing Histone H3 lysine 27 trimethylation (H3K27me3), a repressive histone post-translational modification (PTM), at target regions across the genome. The mechanisms that underly PRC2 recruitment to these regions remain incompletely understood across all model systems. In this dissertation, I used the model fungus *Neurospora crassa* to study the molecular factors that underly PRC2 localization and activity. The first half describes a model system I developed to assay the kinetics of *de-novo* facultative heterochromatin establishment by PRC2. The second half looks at the role of the conserved, replication-dependent histone chaperone, Chromatin Assembly Factor 1 (CAF-1), in maintaining gene silencing within facultative heterochromatin regions. Collectively, this work deepens our understanding of how PRC2 activity is targeted in fungi and elucidates the role of other chromatin modifying complexes in this process. The findings from these studies may provide insights into how PRC2 function is regulated across all eukaryotes and may be relevant to the

development of therapeutics that target the Polycomb repression pathway to treat cancer and other diseases.

INDEX WORDS: Chromatin Assembly; DNA Replication; Facultative Heterochromatin; Fungal Genetics; Genomics; Polycomb

REGULATION OF FACULTATIVE HETEROCHROMATIN IN THE MODEL FUNGUS *NEUROSPORA CRASSA*

by

EDUARDO VICENTE TORRES

BS, University of North Carolina at Chapel Hill, 2019

A Dissertation Submitted to the Graduate Faculty of The University of Georgia in Partial Fulfillment of the Requirements for the Degree

DOCTOR OF PHILOSOPHY

ATHENS, GEORGIA

2025

REGULATION OF FACULTATIVE HETEROCHROMATIN IN THE MODEL FUNGUS

NEUROSPORA CRASSA

by

EDUARDO VICENTE TORRES

Major Professor:	Zachary A. Lewis
Committee:	Robert J. Schmitz
	Mary Goll
	Michelle Momany
	Kaixiong Ye

Electronic Version Approved:

Ron Walcott
Vice Provost for Graduate Education and Dean of the Graduate School
The University of Georgia
December 2025

DEDICATION

To my parents, who have made endless sacrifices to support me in my academic career.

ACKNOWLEDGEMENTS

I would like to acknowledge Jimena Giudice, Hannah Wiedner, and everyone from my time in the Giudice lab. They were my first mentors who taught me what it means to be a scientist. They also helped me realize my potential and inspired me to pursue a graduate education. I am forever grateful for your role in my development as a scientist and a person.

I would like to thank all my lab mates who supported me in countless ways during my time at UGA. Specifically, Felicia Ebot-Ojong, Quanita Choudhury, Rochelle Yap, and Abigail Deaven, who worked with me for many years and inspired me to be a better scientist every day. The work you do is amazing, and I am grateful for all that you've done to help me complete my degree.

I would like to thank my family and all the friends I've made along the way, from high school to graduate school. We've made countless memories together, and your friendship and support has been central to my success.

I would like to thank Zack and my committee for their continued support, mentorship, and patience as I've navigated the graduate school process

Finally, I would like to thank my girlfriend and best friend Danni. You are the one of the kindest and most selfless people I have ever met. I could not have earned this degree without your help. I am eternally grateful for the love and support you've given me in our time together.

Thank you all.

TABLE OF CONTENTS

LIST OF FIGURES

Page

CHAPTER ONE

INTRODUCTION AND LITERATURE REVIEW

Chromatin Structure and Function

Chromatin is a fundamental unit of biology that is made up of a complex of DNA and histone proteins that form within the nucleus of a cell (Kornberg, 1974; Woodcock & Ghosh, 2010). At its most basic structure, 147 base pairs (bp) of DNA wrap around a histone octamer (made up of two tetramers, each containing an H2A, H2B, H3, and H4 histone protein) in a spool-like fashion to form a nucleosome (Davey et al., 2002; Luger et al., 1997). Nucleosomes are separated by ~30-100 bp of linker DNA and form arrays that have been described as "beads on a string" (Oudet et al., 1975; Woodcock & Ghosh, 2010). This linker DNA is able to interact with histone H1, which allows chromatin to compact into higher-order structures (Weintraub, 1984). In the "beads on a string" conformation, chromatin fibers are ~10 nm in length and further compact to form ~30 nm solenoid-like structures (Finch & Klug, 1976; Robinson et al., 2006). This compaction is the first in a series of steps that ultimately allows DNA to be packaged into a chromosome that can be segregated during mitosis (Kornberg & Lorch, 1999; Woodcock & Ghosh, 2010). Outside of mitosis, chromatin formation plays a critical role in regulating gene expression (Allis & Jenuwein, 2016; Li et al., 2007). The histone binding activity of DNA allows for precise control of its accessibility to transcriptional machinery and other DNA-binding proteins, helping determine which genes are expressed in a given cell (Buenrostro et al., 2013; Li et al., 2007; Lorch et al., 1987). One of the primary biological mechanisms that regulates this

process is epigenetic modification (Bannister & Kouzarides, 2011; Kouzarides, 2007; Strahl & Allis, 2000).

"Epigenetics" was first coined by Conrad Waddington in 1942 and is broadly defined as heritable changes in gene expression or function that do not involve changes to the underlying DNA sequence (Bird, 2007; Waddington, 2012). Epigenetic modifications are made directly to DNA and histone proteins to regulate their biological interactions (Bannister & Kouzarides, 2011; Jones, 2012). Specifically, histones can be modified on their tails at Lysine (K), Arginine (R), and Serine (S) residues with various chemical moieties, including methyl- (me), acyl- (ac), and phospho- (p) groups (Bannister & Kouzarides, 2011; Kouzarides, 2007; Strahl & Allis, 2000). These modifications can serve as scaffolds for binding proteins to interact with chromatin (Bannister et al., 2001; Dhalluin et al., 1999; Min et al., 2003; Musselman et al., 2012; Taverna et al., 2007). Furthermore, acetylation weakens histone-DNA interactions by neutralizing positive lysine charges, thereby inhibiting chromatin compaction and promoting DNA accessibility (Barnes et al., 2019; Oppikofer et al., 2011; Shogren-Knaak et al., 2006). These processes partition the genome into domains that promote or preclude specific protein-chromatin interactions (Dixon et al., 2012; Lieberman-Aiden et al., 2009; Rowley & Corces, 2018; van Steensel & Belmont, 2017; Weintraub & Groudine, 1976). In 1928, Emil Heitz used cytological staining techniques to make the first observations of chromatin that was "densely" or "loosely" packed within a nucleus, which he defined as "heterochromatin" and "euchromatin" respectively (Berger, 2019; Heitz, 1928).

Euchromatin generally localizes within the interior of the nucleus, where it is available to interact with nuclear proteins that carry out transcriptional processes (Gilbert et al., 2004; Lieberman-Aiden et al., 2009; Mahy et al., 2002). These regions are gene-rich and contain the

instructions to produce the proteins necessary for proper cellular function (Gilbert et al., 2004; Mahy et al., 2002). Conversely, heterochromatin aggregates at the nuclear periphery and around the nucleolus, thereby limiting access of DNA binding partners (Towbin et al., 2012; van Steensel & Belmont, 2017; Vertii et al., 2019). Early chromatin research suggested that heterochromatin regions were devoid of genes and primarily functioned to maintain chromatin structure and genomic integrity throughout the cell cycle (Elgin & Reuter, 2013; Janssen et al., 2018). However, recent research that followed the discovery of epigenetic modifications has shown that some heterochromatic regions are enriched for genes whose expression needs to be carefully controlled to maintain cellular function (Bernstein et al., 2006; Lee et al., 2006; Voigt et al., 2013). This ultimately led to further characterization of heterochromatin into gene-poor "constitutive" heterochromatin, and gene-rich "facultative" heterochromatin, due to its ability to decondense in response to molecular, developmental, or environmental signals, and become more permissive to gene expression (Allshire & Madhani, 2018; Bastow et al., 2004; Margueron & Reinberg, 2011; Voigt et al., 2013). Genes within facultative heterochromatin are critical to specific cellular processes, including cell differentiation and stress response among others (Blackledge & Klose, 2021; Boyer et al., 2006; Kim & Roberts, 2016; Lee et al., 2006). The remainder of this introduction will discuss what is known about the biological mechanisms that control facultative heterochromatin formation and describe how my research aims to expand our knowledge of the factors involved in establishing and maintaining the heterochromatin environment.

The History of Polycomb

Polycomb group (PcG) proteins were initially discovered and characterized in the model system *Drosophila melanogaster* due to their role in maintaining homeotic (Hox) gene

repression throughout development (Kassis et al., 2017; Schuettengruber et al., 2017; Simon & Kingston, 2009). This repression acts to prevent homeotic transformations, developmental mutations in which one body part aberrantly develops into another (Kassis et al., 2017; Schuettengruber et al., 2017). Examples of these in *D. melanogaster* include Antennapedia (antennae developing into legs) and the development of extra sex combs on posterior legs (hence the designation "Polycomb") (Kassis et al., 2017; Lewis, 1947; Schneuwly et al., 1987). The first gene mutant with the extra sex combs phenotype, extra sex combs (*esc*), was described in 1942, and several years later, the dominant Polycomb (*Pc*) gene mutation was identified (Lewis, 1947; Slifer, 1942). By the early 1990s, several other gene mutations that resulted in similar phenotypes were discovered, leading to their eventual designation as "PcG" genes (DeCamillis et al., 1992; Duncan, 1982; Franke et al., 1992). Furthermore, the phenomenon of Position-effect variegation (PEV) was discovered in *D. melanogaster* when genes were juxtaposed near a heterochromatic domain, in turn silencing their expression (Elgin & Reuter, 2013; Wakimoto, 1998; Wallrath & Elgin, 1995). These studies provided early evidence that chromatin context can modulate gene expression and while mechanistically distinct from Polycomb repression, PEV helped frame models for heritable gene silencing that informed subsequent PcG studies (Elgin & Reuter, 2013; Kassis, 2002).

The PcG protein Pc was later found to copurify in a complex with the proteins encoded by 3 of these genes, Ph, Psc, and dRING, which became known as Polycomb Repressive Complex 1 (PRC1) (Franke et al., 1992; Shao et al., 1999). Mass-spectrometry and genetic studies expanded PRC1 membership to include proteins such as Scm, helping explain variant PRC1 assemblies observed in later studies (Franke et al., 1992; Levine et al., 2002). In the early 2000s, experiments performed using a recombinant version of the PRC1 complex showed that

the complex was able to maintain gene repression by establishing repressive chromatin structures that are antagonistic to chromatin remodelers, protein complexes that can change nucleosome position to alter accessibility and control gene expression (Francis et al., 2004; Francis et al., 2001; King et al., 2002). Despite this clear mechanistic role for PRC1 in gene repression, the existence of other PcG genes whose roles remained uncharacterized suggested that there was still much that was unknown about this pathway (Birve et al., 2001; Ng et al., 2000).

One such PcG gene was esc, which was mapped and characterized by phenotype early on, but not found to interact with the PRC1 complex (Ng et al., 2000; Shao et al., 1999; Slifer, 1942). It was not until the early 2000s that the first Esc interactor, Enhancer of Zeste (E(z)), was identified as a protein complex that was distinct from PRC1 (Ng et al., 2000). Soon after, a novel PcG gene, Suppressor of zeste 12 (*su(z)12*), was identified, and its protein product was found to be a core interactor with the Esc–E(z) complex (Birve et al., 2001; Muller et al., 2002). Studies performed in vitro using a recombinant version of this complex revealed that it could modify chromatin, and that its enzymatic activity was distinct from that of PRC1 but, still functioned to repress gene expression (Cao et al., 2002; Czermin et al., 2002; Kuzmichev et al., 2002; Muller et al., 2002). This biochemical evidence, in addition to the PcG phenotype characterization, led to the designation of the Esc–E(z)–Su(z)12 complex as Polycomb Repressive Complex 2 (PRC2) (Czermin et al., 2002; Muller et al., 2002). Soon after its characterization in *Drosophila*, homologs of PRC2 proteins were identified across a wide array of eukaryotes, ranging from fungi to plants and mammals (Connolly et al., 2013; Grossniklaus et al., 1998; Kohler et al., 2003; O'Carroll et al., 2001; Ohad et al., 1999). These complexes have been shown to share a conserved catalytic function with *D. melanogaster* PRC2 (dPRC2), suggesting that PRC2-mediated repression emerged early on in eukaryotic evolution (Frapporti et al., 2019; Kuzmichev

et al., 2002; Muller et al., 2002; Sharaf et al., 2022). Since its discovery, the polycomb repression pathway has been extensively researched across many biological model systems, and these studies have provided greater context as to how epigenetic pathways contribute to gene repression and facultative heterochromatin formation (Blackledge & Klose, 2021; Di Croce & Helin, 2013; Margueron & Reinberg, 2011). However, there are fundamental questions about the mechanisms that underly PcG protein activity that remain unanswered.

Polycomb Function in Eukaryotes

Multicellular eukaryotes such as plants and vertebrates contain a largely conserved polycomb repression pathway compared to *D. melanogaster* (Kohler et al., 2003; O'Carroll et al., 2001; Ohad et al., 1999; Sharaf et al., 2022). This includes complete PRC1 and PRC2 complexes, in addition to accessory subunits that control where and how these complexes act (Blackledge & Klose, 2021; Gao et al., 2012; Kasinath et al., 2021; Laugesen et al., 2019). PRC1 and PRC2 are responsible for catalyzing histone H2A lysine 119 ubiquitination (H2AK119ub, or H2AK118ub in *Drosophila*) and histone H3 lysine 27 tri-methylation (H3K27me3) respectively, which are the two histone PTMs involved in polycomb repression (Cao et al., 2002; Czermin et al., 2002; de Napoles et al., 2004; Kuzmichev et al., 2002; Muller et al., 2002). These PTMs have been shown to function in a "positive feedback" loop, that recruits the proteins involved in the polycomb repression pathway to faithfully maintain gene repression and form heterochromatic domains at specific loci across the genome (Blackledge et al., 2020; Oksuz et al., 2018; Tamburri et al., 2020; Zhen et al., 2016).

This loop is established by transcription factor (TF) mediated recruitment of PcG complexes to their target sites, DNA sequences called polycomb response elements (PREs)

(Kahn et al., 2016; Kassis & Brown, 2013; Laprell et al., 2017; Oktaba et al., 2008; Okulski et al., 2011). PREs were initially discovered in *D. melanogaster*, where they are well-characterized and can be bound by TFs such as Pho, GAGA transcription factor (GAF), Zeste, etc. (Kahn et al., 2016; Kassis & Brown, 2013; Oktaba et al., 2008; Okulski et al., 2011). While evidence of PREs remains limited in mammals, TFs such as Ying Yang 1 (YY1) and RE1-Silencing Transcription Factor (REST) can recruit PcG proteins, and the KDM2B demethylase has been shown to recruit PRC1 to unmethylated CpG islands (CGIs) (Dietrich et al. 2012; Farcas et al., 2012; Li et al., 2017; Mendenhall et al., 2010; Perino et al., 2018; Srinivasan & Atchison, 2004). In plants, families of TFs such as VIVIPAROUS1/ABI3-LIKE (VAL) and EMBRYONIC FLOWER 1 (EMF1) work in unison with PcG proteins to regulate gene expression (Calonje et al., 2008; Xiao et al. 2017; Yuan et al., 2021; Zhou et al. 2018). Additionally, there is strong and emerging evidence for long non-coding RNAs (lncRNAs) playing a role in PRC2 recruitment, with the X-chromosome inactivation pathway (Xist) in mammals and FLOWERING LOCUS C pathway in plants representing some of the most well-studied systems (Bastow et al., 2004; Kim & Sung, 2017; Nielsen et al., 2024; Plath et al., 2003; Sarma et al., 2014; Zhao et al., 2008). While there is strong evidence for all these pathways in recruiting PcG proteins, no single one is universal to all facultative heterochromatin domains, suggesting that polycomb recruitment is dynamic and complex (Blackledge & Klose, 2021; Laugesen et al., 2019). Once recruited, PRC1 then deposits H2AK119ub, which has been shown to influence gene expression by restricting RNA polymerase II (RNAPII) engagement and limiting transcriptional initiation and early elongation (Blackledge et al., 2020; Dobrinic et al., 2021; Tamburri et al., 2020). Furthermore, there is evidence that PRC1 itself can contribute to chromatin compaction independent of its catalytic function (Eskeland et al., 2010; Francis et al., 2004; Grau et al., 2011). H2AK119ub

serves as a recruitment signal that is recognized by the PRC2 accessory subunits JARID2 and AEBP2, which bring PRC2 to these sites, allowing for establishment of H3K27me3 at what is referred to as a "nucleation site" (Kasinath et al., 2021; Oksuz et al., 2018). Once both PTMs are established, the CBX subunit of the PRC1 complex can then read H3K27me3 and recruit PRC1 back to these sites, completing the feedback loop that results in maintenance of both gene repression and the two modifications (Gao et al., 2012; Min et al., 2003; Zhen et al., 2016).

Once H2AK119ub and H3K27me3 are established, H3K27me3 must spread to adjacent nucleosomes to form a complete facultative heterochromatin domain (Fig. 1.1) (Laprell et al., 2017; Oksuz et al., 2018). This is largely achieved by recognition of existing H3K27me3 by PRC2 itself. Specifically, the EED subunit (dPRC2; Esc) binds H3K27me3 through its aromatic cage, which allosterically activates the complex to catalyze H3K27 methylation on the neighboring nucleosome (Lee et al., 2018; Margueron et al., 2009; Ueda et al., 2016). This mechanism allows for the continuous spread of H3K27me3 until PRC2 is met by a boundary element, such as insulator proteins, nascent RNA, or antagonistic modifications which inhibit the complex's activity (Dixon et al., 2012; Lavarone et al., 2019; Rhodes et al., 2020; Schmitges et al., 2011). CTCF and cohesion loops are insulator proteins, which can form DNA loop extrusions and exclude the activity of complexes such as PRC2 (Dixon et al., 2012; Rhodes et al., 2020; Rowley & Corces, 2018). Examples of antagonistic modifications include H3K36me3 and H3K4me2/3, which are hallmarks of active transcription, and H3K27 acetylation (H3K27ac), which typically marks active enhancers and promoters and is mutually exclusive with H3K27me3 (Creyghton et al., 2010; Pasini et al., 2010; Schmitges et al., 2011). Formation and maintenance of these complete facultative heterochromatin domains is critical for PcG repression (Blackledge & Klose, 2021; Margueron & Reinberg, 2011). These same mechanisms function to

maintain proper levels of H3K27me3 across the genome through mitotic cell division and during DNA replication, when parental histones marked by H3K27me3 are recycled evenly across both parent and daughter DNA strands, thereby diluting the mark—a process discussed in greater detail in a later section (Alabert et al., 2020; Jadhav et al., 2020; Petryk et al., 2018; Wenger et al., 2023; Yu et al., 2018).

A major distinction between facultative heterochromatin and constitutive heterochromatin is the ability to a create "dynamically repressive" environment, as previously described (Allshire & Madhani, 2018; Blackledge & Klose, 2021; Trojer & Reinberg, 2007). This requires the activity of mechanisms that serve to counteract the polycomb repression pathway. This includes demethylases such as KDM6A (dPRC2; Utx) and deubiquitinases such as PR-DUB (dPRC2; Calypso) that directly remove H3K27me3 and H2AK119ub respectively, and counteract the spread and maintenance of facultative heterochromatin domains (Agger et al., 2007; Lee et al., 2007; Scheuermann et al., 2010). This can make DNA within these regions more accessible, allowing transcriptional machinery to bind and promote gene expression (Bannister & Kouzarides, 2011; Buenrostro et al., 2013; Tie et al., 2009). Furthermore, this can allow for the deposition and propagation of PTMs that promote or are associated with active transcription (Creyghton et al., 2010; Pasini et al., 2010). There are some examples in which nucleosomes exhibit bivalency of H3K27me3 and H3K4me2/3, meaning that the same nucleosome is modified at both residues, but on opposite H3 histone proteins (Bernstein et al., 2006; Voigt et al., 2013). This creates a "primed" state, in which H3K27me3 can be removed, transcription can occur, and H3K4me2/3 and other PTMs can be propagated under specific conditions, creating a truly dynamic chromatin environment. This mechanism is highly prevalent in embryonic stem cells (ESCs), which require widespread and rapid transcriptional regulation

during differentiation to control cell fate (Bernstein et al., 2006; Boyer et al., 2006; Lee et al., 2006; Voigt et al., 2013). While PRC2-mediated repression is well conserved, many of the mechanisms that control its recruitment and activity are not, motivating research across diverse model systems to fully understand its origins and mechanistic determinants (Kassis & Brown, 2013; Li et al., 2017; Mendenhall et al., 2010; Yuan et al., 2021).

Polycomb Function in Fungi

Commonly studied eukaryotic fungi such as *Saccharomyces cerevisiae* (*S. cerevisiae*) and *Schizosaccharomyces pombe* (*S. pombe*) are devoid of known PRC2 homologs and H3K27me3, suggesting that polycomb repression was lost in some fungal lineages (Grewal, 2023; Ridenour et al., 2020; Sharaf et al., 2022). While the mechanisms behind heterochromatin formation are studied in these systems, studying facultative heterochromatin dynamics in the same way as other eukaryotes is impossible (Ridenour et al., 2020). In the early 2010s, H3K27me3 was mapped in the filamentous fungus *Neurospora crassa*, quickly followed by the characterization of its PRC2 protein homologs (Aramayo & Selker, 2013; Jamieson et al., 2013). *N. crassa* harbors a fully conserved core PRC2 complex, consisting of SUZ-12 (dPRC2; Su(z)12), EED (dPRC2; Esc), SET-7 (dPRC2; E(z)), and CAC-3 (dPRC2; NURF-55, also called NPF), but is devoid of known homologs for PRC1 or PRC2 accessory subunits (JARID2, AEBP2, etc.) (Jamieson et al., 2013; McNaught et al., 2020; Ridenour et al., 2020; Sharaf et al., 2022). Furthermore, it has been shown that knock-out (KO) deletions of PRC2 components resulting in H3K27me3 depletion are non-lethal in *N. crassa*, unlike what has been observed for mammals (Courtney et al., 2020; Jamieson et al., 2013; O'Carroll et al., 2001). This makes *N. crassa* an intriguing model to study the mechanisms that underly facultative heterochromatin, as

a simplified PRC2 complex is the only enzyme capable of establishing and maintaining H3K27me3 (Ridenour et al., 2020; Wiles et al., 2020). Since its discovery in *N. crassa*, homologs of PRC2 have been characterized in multiple fungal species, including the filamentous fungi *Zymoseptoria tritici* and *Fusarium graminearum*, and the pathogenic yeast *Cryptococcus neoformans* (Connolly et al., 2013; Dumesic et al., 2015; Moller et al., 2019). Genes within fungal facultative heterochromatin domains have been shown to be critical for specialized processes such as sexual development, effector gene expression, and secondary metabolite production (Collemare & Seidl, 2019; Connolly et al., 2013; Deaven et al., 2025; Fraser & Whitehall, 2022).

George Beadle and Edward Tatum's 1950s Nobel prize-winning research on the "one gene-one enzyme" hypothesis established *N. crassa* as a *bona fide* model for genetics research (Beadle & Tatum, 1941; Dunlap et al., 2007). This foundation has been critical for recent work studying chromatin formation and dynamics in this system (Aramayo & Selker, 2013). To date, studies of the PRC2 repression pathway in *N. crassa* have already implicated several chromatin-modifying complexes in the process of facultative heterochromatin formation. This includes PRC2's accessory proteins (CAC-3/NPF, EPR-1, and PAS), the IMITATION SWITCH (ISWI) chromatin remodeler, the histone variant H2A.Z, the histone deacetylase (HDAC) complexes HISTONE DEACETYLASE 1 (HDA-1) and RPD3L, and the H3K36 and H3K9 methyltransferases ASH-1 and DIM-5 respectively (Basenko et al., 2015; Bicocca et al., 2018; Courtney et al., 2020; Ebot-Ojong et al., 2025; Kamei et al., 2021; McNaught et al., 2020; Mumford et al., 2024; Wiles et al., 2022). Many of these proteins have homologous or orthologous counterparts in other eukaryotic species, allowing for translation of the research done in *N. crassa* to other model systems (Blackledge & Klose, 2021; Sharaf et al., 2022). My

work in this dissertation looks to build on the foundational knowledge of *N. crassa* PRC2 repression by identifying genes and mechanisms that play a role in maintaining gene repression and the facultative heterochromatin environment, with a particular focus on histone chaperones.

History of Histone Chaperones

Histone chaperones are a family of proteins that directly bind to histones, participate in their transport to the nucleus, and assist in the formation of nucleosomes (Gurard-Levin et al., 2014; Keck & Pemberton, 2012). These represent some of the key first steps that precede chromatin formation (Hammond et al., 2017). Histone chaperones were first discovered in experiments performed in *Xenopus laevis* egg extracts, a model system that provides a cell-free, "S-phase rich" environment to study DNA replication (Almouzni & Mechali, 1988). In the late 1980s, it was shown that the proteins present in these extracts were able to copy a single stranded DNA (ssDNA) template into double stranded DNA (dsDNA), perform DNA replication, and promote chromatin assembly *in vitro* (Blow & Laskey, 1986; Stillman, 1986). These experiments closely tied chromatin assembly to DNA replication and provided a model to identify the proteins required for both these processes. Nucleoplasmin and N1 were the first two proteins characterized as histone chaperones, binding to H2A/H2B and H3/H4 respectively (Dilworth et al., 1987). Depletion of either chaperone from *X. laevis* cell extracts resulted in defective nucleosome and chromatin assembly, a phenotype that was rescued upon their reintroduction, showing that these chaperones were necessary and sufficient to promote chromatin assembly (Dilworth et al., 1987).

Similar experiments in Human HeLa extracts showed that the proteins present were able to replicate and assemble SV40 virus DNA into chromatin, providing a mammalian model to

study chromatin assembly dynamics (Smith & Stillman, 1991; Stillman, 1986). These experiments identified multiple proteins required for these processes, including Chromatin Assembly Factor 1 (CAF-1) (Smith & Stillman, 1989). CAF-1 is a heterotrimeric histone chaperone complex (made up of subunits p150/CHAF1A, p60/CHAF1B, and p48/RbAp48 in humans) that binds to and tetramerizes H3/H4 dimers and deposits them specifically onto replicating DNA (Kaufman et al., 1995; Liu et al., 2023; Sauer et al., 2018; Shibahara & Stillman, 1999; Verreault et al., 1996). CAF-1 depletion in HeLa extracts prevented chromatin assembly of replicating SV40 DNA, much like what was observed for chaperone depletion experiments in *X. laevis* extracts (Dilworth et al., 1987; Smith & Stillman, 1989). The critical observation came when DNA replication was blocked in these extracts which showed that chromatin assembly was disrupted, even in the presence of CAF-1 (Smith & Stillman, 1991; Stillman, 1986). Follow-up experiments identified the DNA processivity factor, Proliferating Cell Nuclear Antigen (PCNA) as a direct interactor with the large subunit of CAF-1, which recruits the complex to sites of DNA replication and repair (Moggs et al., 2000; Shibahara & Stillman, 1999). These studies solidified CAF-1 as a “replication-dependent” histone chaperone (Hoek & Stillman, 2003).

Replication-dependent & Replication-independent Histone Chaperones

CAF-1's characterization led to a series of experiments that defined two distinct families of replication-dependent and replication-independent histone chaperones (Gurard-Levin et al., 2014; Shibahara & Stillman, 1999; Tagami et al., 2004). Replication-dependent chaperones are defined by their inability to assemble chromatin in the absence of DNA replication (Gurard-Levin et al., 2014; Hoek & Stillman, 2003; Smith & Stillman, 1991). Their production typically peaks during S-phase *in vivo*, along with their activity (Eriksson et al., 2012; Mendiratta et al., 2019). Experiments in *S. cerevisiae* and HeLa extracts defined anti-silencing function 1 (ASF-1) and nuclear autoantigenic sperm protein (NASP) as chaperones that function upstream of the CAF-1 pathway, due to defective chromatin assembly of replicating DNA upon their depletion, even in the presence of CAF-1 (Bao et al., 2022; Cook et al., 2011; Green et al., 2005; Le et al., 1997; Mello et al., 2002; Munakata et al., 2000; Richardson et al., 2006; Welch et al., 1990). The fungal-specific chaperone Regulator of Ty1 Transposition 106 (Rtt106) was also characterized in *S. cerevisiae* based on its association with CAF-1 and ASF-1 during S-phase (Clemente-Ruiz et al., 2011; Huang et al., 2007; Imbeault et al., 2008; Zunder et al., 2012). While these experiments clearly modeled a pathway of replication-dependent chromatin assembly, how this process occurs outside of S phase had yet to be clearly defined.

Replication-independent histone chaperones are defined by their ability to promote chromatin assembly independent of DNA replication. Their activity is typically independent of the cell cycle and is important for reassembling chromatin after transcription and DNA repair (Mello et al., 2002; Ray-Gallet et al., 2002; Tagami et al., 2004). Nucleoplasmin and N1 both fall into this category, as they contributed to assembly in the absence of DNA replication (Dilworth et al., 1987). Experiments in the 1990s in *S. cerevisiae* identified the Histone Regulatory (HIR)

protein complex as a regulator of histone protein expression that controls the supply of histone proteins throughout the cell cycle (Eriksson et al., 2012; Sherwood et al., 1993). Biochemical purification experiments revealed that this complex interacts with ASF-1 and deposits H3/H4 onto DNA when replication is blocked (Green et al., 2005). This revealed a replication-independent H3/H4 deposition pathway and identified ASF-1 as a general chaperone that hands off histones to multiple chaperone complexes (Green et al., 2005; Ransom et al., 2010). Later experiments identified human homologs of HIR complex proteins (HIRA) that exhibited H3/H4 deposition activity and interacted with human ASF-1 (Ray-Gallet et al., 2002; Ray-Gallet et al., 2018; Ricketts et al., 2015). Further experimentation led to the characterization of several other histone chaperones that function inside and outside of DNA replication, painting a more complete picture of the factors involved in chromatin formation and maintenance (Gurard-Levin et al., 2014; Hammond et al., 2017). However, there remained much that was unknown about how disruption of their function directly impacted chromatin dynamics *in vivo.*

Roles of Histone Chaperones in Chromatin Assembly

For a cell to assemble DNA into chromatin, there must be an adequate supply of histone proteins (Eriksson et al., 2012; Gurard-Levin et al., 2014; Mendiratta et al., 2019; Ransom et al., 2010). While some chaperones such as HIR can directly regulate the levels of histone proteins, others play roles in transporting newly synthesized histones to the nucleus, and ultimately to other chaperones that perform chromatin assembly (Eriksson et al., 2012; Green et al., 2005; Keck & Pemberton, 2012; Pardal et al., 2019; Sherwood et al., 1993). This process starts with chaperones in the NASP family, which bind to histones H3/H4 in the cytosol after they are translated and transport them across the nuclear membrane (Apta-Smith et al., 2018; Bao et al.,

2022; Cook et al., 2011; Pardal & Bowman, 2022; Richardson et al., 2006; Welch et al., 1990). During transport, histones are modified by histone acetyltransferase (HAT) complexes, which facilitates their hand off to other chaperones such as ASF-1 (Agudelo Garcia et al., 2017; Apta-Smith et al., 2018; Bao et al., 2022; Denu, 2019; Pardal & Bowman, 2022; Richardson et al., 2006; Welch et al., 1990; Zhang et al., 2012). ASF-1 acts as a central H3/H4 donor to other chaperone complexes that perform chromatin assembly, including CAF-1 and HIR (Green et al., 2005; Liu et al., 2012; Liu et al., 2016; Meijsing & Ehrenhofer-Murray, 2001; Mello et al., 2002). This pathway allows chromatin assembly to occur at any stage of the cell cycle through replication-independent processes (Gurard-Levin et al., 2014; Ray-Gallet et al., 2011; Tagami et al., 2004). However, replication-dependent assembly requires tighter spatiotemporal control, as it only occurs within S-phase (Alabert & Groth, 2012; Hoek & Stillman, 2003; MacAlpine & Almouzni, 2013; Shibahara & Stillman, 1999). ASF-1 remains a central player, delivering modified H3/H4 dimers to CAF-1 at replication forks (Alabert & Groth, 2012; Green et al., 2005; MacAlpine & Almouzni, 2013; Mello et al., 2002; Moggs et al., 2000; Shibahara & Stillman, 1999). Here, two CAF-1 complexes assemble and deposit a new H3/H4 tetramer onto either the leading or lagging DNA strands as the replication fork passes (Liu et al., 2023; Rouillon et al., 2023; Sauer et al., 2018). Once deposited, H2A/H2B chaperones such as the Facilitates Chromatin Transcription (FACT) and Nucleosome Assembly Protein (NAP1) complexes add 2 copies each of H2A/H2B to the H3/H4 tetramer to build a complete histone octamer that forms a nucleosome with DNA (Fig. 1.2) (Aguilar-Gurrieri et al., 2016; Liu et al., 2020).

Approximately half of the nucleosomes formed during replication-dependent chromatin assembly are comprised of newly synthesized histones (Jadhav et al., 2020; Petryk et al., 2018;

Veronezi & Ramachandran, 2024; Wenger et al., 2023; Yu et al., 2018). The other half is made up of parental histone proteins that were present on chromatin prior to replication and get recycled during DNA replication (Petryk et al., 2018; Wenger et al., 2023; Yu et al., 2018). When the replication fork passes, histones are evicted by DNA helicase allowing DNA polymerase to read DNA and synthesize a new strand (Alabert & Groth, 2012; MacAlpine & Almouzni, 2013; Ransom et al., 2010). Replication associated proteins including Mini-chromosome Maintenance Complex Component 2 (MCM2-7) complex and the DNA polymerase accessory subunits DPB3/4 bind these evicted histones and help transport them to DNA behind the replication fork, where they are reassembled into a full nucleosome (Fang et al., 2024; Huang et al., 2015; Petryk et al., 2018; Yu et al., 2018). ASF-1 and FACT are also known to help chaperone recycled histones H3/H4 and H2A/H2B respectively (Aguilar-Gurrieri et al., 2016; Huang et al., 2015; Liu et al., 2020). Recycling occurs evenly onto both leading and lagging strands, which leaves the gaps that chaperones such as CAF-1 function to fill (Fig. 1.2) (Petryk et al., 2018; Rouillon et al., 2023; Sauer et al., 2018; Verreault et al., 1996; Wenger et al., 2023).

A key distinction between newly synthesized and recycled histones are the histone PTMs that are present on their tails (Alabert & Groth, 2012; Alabert et al., 2020; Stewart-Morgan et al., 2019). Recycled parental histones exhibit a “mature” epigenetic profile, as they maintain the histone modifications that were established prior to DNA replication (Petryk et al., 2018; Veronezi & Ramachandran, 2024; Wenger et al., 2023). In contrast, newly synthesized histones are devoid of these modifications and are heavily acetylated, which facilitates the binding and transport activity of chaperone proteins(Agudelo Garcia et al., 2017; Tagami et al., 2004; Zhang et al., 2012). Upon deposition, these histones become rapidly deacetylated, and chromatin modifiers such as PRC2 re-establish the epigenetic environment present on the neighboring

histones in a process commonly referred to as chromatin "maturation" (Alabert et al., 2020; Clemente-Ruiz et al., 2011; Oksuz et al., 2018; Stewart-Morgan et al., 2019). This process is critical for maintaining a normal epigenetic and transcriptional profile throughout cellular division, yet the exact mechanisms are not fully understood.

CAF-1 and Heterochromatin

Prior research has shown that absence of CAF-1 histone deposition activity results in lower nucleosome occupancy during S-phase, leaving gaps of "naked" DNA after passage of the replication fork (Chen et al., 2023; Clemente-Ruiz et al., 2011; Ray-Gallet et al., 2011; Ye et al., 2003). These gaps become filled in by other histone chaperones, but the kinetics of chromatin assembly are altered, and DNA damage is accumulated at higher rates, resulting in longer S-phase in CAF-1-deficient cells (Hoek & Stillman, 2003; Linger & Tyler, 2005; Ray-Gallet et al., 2011; Ye et al., 2003). Although nucleosome occupancy can be fully restored in the absence of CAF-1 activity, the epigenetic environment experiences significant perturbations. Research across multiple eukaryotic model systems from fungi to mammals has shown that CAF-1 deficiency results defective gene silencing, which is associated with an altered heterochromatin environment (Cheloufi et al., 2015; Cheng et al., 2019; Dohke et al., 2008; Enomoto & Berman, 1998; Franklin et al., 2022; Houlard et al., 2006; Mozgova et al., 2015; Schonrock et al., 2006; Song et al., 2007).

In *S. cerevisiae*, gene silencing by CAF-1 and other replication-dependent histone chaperones is required for proper deacetylation by sirtuin (Sir) proteins, which ultimately facilitates the formation of a heterochromatic environment (Huang et al., 2007). CAF-1 deficiency in *S. pombe* and mouse embryonic stem cells (ESCs) has been linked to altered levels

of H3K9me3 at constitutive heterochromatin (Cheloufi et al., 2015; Dohke et al., 2008; Enomoto & Berman, 1998). These observations are consistent with the known interactions between CAF-1 and Heterochromatin Protein 1 (HP1), a reader of H3K9me3 (Huang et al., 2010; Quivy et al., 2008; Quivy et al., 2004; Roelens et al., 2017; Thiru et al., 2004). Studies in *D. melanogaster*, *Arabidopsis thaliana*, and CAF-1 deficient mouse embryonic stem cells (ESCs) have also implicated the complex in gene silencing and maintenance of H3K27me3 within facultative heterochromatin regions and have shown evidence of interaction between CAF-1 and the catalytic subunit of PRC2 (Cheng et al., 2019; Jiang & Berger, 2017; Yee et al., 2019). In ESCs, this results in aberrant expression of pluripotency genes during differentiation (Cheloufi et al., 2015; Cheng et al., 2019). Studying the importance of CAF-1 function in these systems has been difficult, due to KOs of the complex resulting in embryonic lethality in ESCs and severe developmental defects in plants and flies (Houlard et al., 2006; Jiang & Berger, 2017; Song et al., 2007). Furthermore, the absence of PRC2 components in *S. cerevisiae* and *S. pombe* makes it impossible to differentiate CAF-1's role in maintaining facultative heterochromatin versus constitutive heterochromatin (Allshire & Madhani, 2018; Sharaf et al., 2022). Due to these challenges, our understanding of how CAF-1 helps maintain heterochromatin remains incomplete.

N. crassa contains a conserved CAF-1 complex compared with these other model systems, and KOs of each of the three individual subunits of the complex have shown its activity to be non-essential for survival. Furthermore, the conservation of PRC2 in *N. crassa* makes it possible to study how CAF-1 directly contributes to its function. The third chapter of this dissertation will focus on my work in determining the role of the CAF-1 complex in maintaining gene repression and the epigenetic environment at facultative heterochromatin in *N. crassa*. My

findings will shed light on how proper chromatin assembly dynamics are critical for faithful transgenerational inheritance of histone PTMs in eukaryotic systems.

Dissertation Overview

This dissertation will focus on the work I've done to elucidate the mechanisms behind the establishment and maintenance of facultative heterochromatin by PRC2 in our model system *N. crassa*. The second chapter focuses on the development of an inducible PRC2 construct that I used to assay the kinetics of *de-novo* H3K27me3 establishment. I was able to successfully place the *suz-12* gene under control of a quinic acid-inducible promoter, providing the ability to control when PRC2 is active. Briefly, I observed a robust, but incomplete recovery of H3K27me3 at its normal sites across the genome, in addition to the emergence of numerous ectopic peaks. Furthermore, I identified specific sites at which H3K27me3 recovered rapidly after induction, suggesting that they directly recruit PRC2. Indeed, when a partial fragment of these sequences was ectopically inserted at a euchromatic locus, it was sufficient to recruit PRC2 and induce an ectopic facultative heterochromatin domain when H3K27me3 at normal loci was perturbed.

The third chapter will focus on a study performed to determine the role of CAF-1 in maintenance of facultative heterochromatin. Briefly, I found eliminating CAF-1 activity led to defective silencing of many genes within facultative heterochromatin regions, which was accompanied by a genome-wide rearrangement of H3K27me3. I also observed reduced ASH-1-mediated H3K36me and increased levels of histone PTMS associated with active transcription at these same loci. Lastly, by mutating both CAF-1 and PRC2 in the same strain background, I was able to show that these 2 complexes play unique roles in gene silencing and maintenance of the

heterochromatin environment. Collectively, the work performed in this dissertation makes significant contributions to our understanding of how facultative heterochromatin is established and maintained, and the chromatin modifying complexes that are involved in this process. These findings may also provide insights into how PRC2 activity is regulated in other eukaryotes and hold relevance in developing therapeutics that target PRC2 activity to treat human disease.

References

Agger, K., Cloos, P. A., Christensen, J., Pasini, D., Rose, S., Rappsilber, J., Issaeva, I., Canaani, E., Salcini, A. E., & Helin, K. (2007). UTX and JMJD3 are histone H3K27 demethylases involved in HOX gene regulation and development. *Nature*, *449*(7163), 731–734. https://doi.org/10.1038/nature06145

Agudelo Garcia, P. A., Hoover, M. E., Zhang, P., Nagarajan, P., Freitas, M. A., & Parthun, M. R. (2017). Identification of multiple roles for histone acetyltransferase 1 in replication-coupled chromatin assembly. *Nucleic Acids Res*, *45*(16), 9319–9335. https://doi.org/10.1093/nar/gkx545

Aguilar-Gurrieri, C., Larabi, A., Vinayachandran, V., Patel, N. A., Yen, K., Reja, R., Ebong, I. O., Schoehn, G., Robinson, C. V., Pugh, B. F., & Panne, D. (2016). Structural evidence for Nap1-dependent H2A-H2B deposition and nucleosome assembly. *EMBO J*, *35*(13), 1465–1482. https://doi.org/10.15252/embj.201694105

Alabert, C., & Groth, A. (2012). Chromatin replication and epigenome maintenance. *Nat Rev Mol Cell Biol*, *13*(3), 153–167. https://doi.org/10.1038/nrm3288

Alabert, C., Loos, C., Voelker-Albert, M., Graziano, S., Forne, I., Reveron-Gomez, N., Schuh, L., Hasenauer, J., Marr, C., Imhof, A., & Groth, A. (2020). Domain Model Explains Propagation Dynamics and Stability of Histone H3K27 and H3K36 Methylation Landscapes. *Cell Rep*, *30*(4), 1223–1234 e1228. https://doi.org/10.1016/j.celrep.2019.12.060

Allis, C. D., & Jenuwein, T. (2016). The molecular hallmarks of epigenetic control. *Nat Rev Genet*, *17*(8), 487–500. https://doi.org/10.1038/nrg.2016.59

Allshire, R. C., & Madhani, H. D. (2018). Ten principles of heterochromatin formation and function. *Nat Rev Mol Cell Biol*, *19*(4), 229–244. https://doi.org/10.1038/nrm.2017.119

Almouzni, G., & Mechali, M. (1988). Xenopus egg extracts: a model system for chromatin replication. *Biochim Biophys Acta*, *951*(2-3), 443–450. https://doi.org/10.1016/0167-4781(88)90118-2

Apta-Smith, M. J., Hernandez-Fernaud, J. R., & Bowman, A. J. (2018). Evidence for the nuclear import of histones H3.1 and H4 as monomers. *EMBO J*, *37*(19). https://doi.org/10.15252/embj.201798714

Aramayo, R., & Selker, E. U. (2013). Neurospora crassa, a model system for epigenetics research. *Cold Spring Harb Perspect Biol*, *5*(10), a017921. https://doi.org/10.1101/cshperspect.a017921

Bannister, A. J., & Kouzarides, T. (2011). Regulation of chromatin by histone modifications. *Cell Res*, *21*(3), 381–395. https://doi.org/10.1038/cr.2011.22

Bannister, A. J., Zegerman, P., Partridge, J. F., Miska, E. A., Thomas, J. O., Allshire, R. C., & Kouzarides, T. (2001). Selective recognition of methylated lysine 9 on histone H3 by the HP1 chromo domain. *Nature*, *410*(6824), 120–124. https://doi.org/10.1038/35065138

Bao, H., Carraro, M., Flury, V., Liu, Y., Luo, M., Chen, L., Groth, A., & Huang, H. (2022). NASP maintains histone H3-H4 homeostasis through two distinct H3 binding modes. *Nucleic Acids Res*, *50*(9), 5349–5368. https://doi.org/10.1093/nar/gkac303

Barnes, C. E., English, D. M., & Cowley, S. M. (2019). Acetylation & Co: an expanding repertoire of histone acylations regulates chromatin and transcription. *Essays Biochem*, *63*(1), 97–107. https://doi.org/10.1042/EBC20180061

Basenko, E. Y., Sasaki, T., Ji, L., Prybol, C. J., Burckhardt, R. M., Schmitz, R. J., & Lewis, Z. A. (2015). Genome-wide redistribution of H3K27me3 is linked to genotoxic stress and defective growth. *Proc Natl Acad Sci U S A*, *112*(46), E6339–6348. https://doi.org/10.1073/pnas.1511377112

Bastow, R., Mylne, J. S., Lister, C., Lippman, Z., Martienssen, R. A., & Dean, C. (2004). Vernalization requires epigenetic silencing of FLC by histone methylation. *Nature*, *427*(6970), 164–167. https://doi.org/10.1038/nature02269

Beadle, G. W., & Tatum, E. L. (1941). Genetic Control of Biochemical Reactions in Neurospora. *Proc Natl Acad Sci U S A*, *27*(11), 499–506. https://doi.org/10.1073/pnas.27.11.499

Berger, F. (2019). Emil Heitz, a true epigenetics pioneer. *Nat Rev Mol Cell Biol*, *20*(10), 572. https://doi.org/10.1038/s41580-019-0161-z

Bernstein, B. E., Mikkelsen, T. S., Xie, X., Kamal, M., Huebert, D. J., Cuff, J., Fry, B., Meissner, A., Wernig, M., Plath, K., Jaenisch, R., Wagschal, A., Feil, R., Schreiber, S. L., & Lander, E. S. (2006). A bivalent chromatin structure marks key developmental genes in embryonic stem cells. *Cell*, *125*(2), 315–326. https://doi.org/10.1016/j.cell.2006.02.041

Bicocca, V. T., Ormsby, T., Adhvaryu, K. K., Honda, S., & Selker, E. U. (2018). ASH1-catalyzed H3K36 methylation drives gene repression and marks H3K27me2/3-competent chromatin. *Elife*, *7*. https://doi.org/10.7554/eLife.41497

Bird, A. (2007). Perceptions of epigenetics. *Nature*, *447*(7143), 396–398. https://doi.org/10.1038/nature05913

Birve, A., Sengupta, A. K., Beuchle, D., Larsson, J., Kennison, J. A., Rasmuson-Lestander, A., & Muller, J. (2001). Su(z)12, a novel Drosophila Polycomb group gene that is conserved in vertebrates and plants. *Development*, *128*(17), 3371–3379. https://doi.org/10.1242/dev.128.17.3371

Blackledge, N. P., Fursova, N. A., Kelley, J. R., Huseyin, M. K., Feldmann, A., & Klose, R. J. (2020). PRC1 Catalytic Activity Is Central to Polycomb System Function. *Mol Cell*, *77*(4), 857–874 e859. https://doi.org/10.1016/j.molcel.2019.12.001

Blackledge, N. P., & Klose, R. J. (2021). The molecular principles of gene regulation by Polycomb repressive complexes. *Nat Rev Mol Cell Biol*, *22*(12), 815–833. https://doi.org/10.1038/s41580-021-00398-y

Blow, J. J., & Laskey, R. A. (1986). Initiation of DNA replication in nuclei and purified DNA by a cell-free extract of Xenopus eggs. *Cell*, *47*(4), 577–587. https://doi.org/10.1016/0092-8674(86)90622-7

Boyer, L. A., Plath, K., Zeitlinger, J., Brambrink, T., Medeiros, L. A., Lee, T. I., Levine, S. S., Wernig, M., Tajonar, A., Ray, M. K., Bell, G. W., Otte, A. P., Vidal, M., Gifford, D. K., Young, R. A., & Jaenisch, R. (2006). Polycomb complexes repress developmental regulators in murine embryonic stem cells. *Nature*, *441*(7091), 349–353. https://doi.org/10.1038/nature04733

Buenrostro, J. D., Giresi, P. G., Zaba, L. C., Chang, H. Y., & Greenleaf, W. J. (2013). Transposition of native chromatin for fast and sensitive epigenomic profiling of open chromatin, DNA-binding proteins and nucleosome position. *Nat Methods*, *10*(12), 1213–1218. https://doi.org/10.1038/nmeth.2688

Calonje, M., Sanchez, R., Chen, L., & Sung, Z. R. (2008). EMBRYONIC FLOWER1 participates in polycomb group-mediated AG gene silencing in Arabidopsis. *Plant Cell*, *20*(2), 277–291. https://doi.org/10.1105/tpc.106.049957

Cao, R., Wang, L., Wang, H., Xia, L., Erdjument-Bromage, H., Tempst, P., Jones, R. S., & Zhang, Y. (2002). Role of histone H3 lysine 27 methylation in Polycomb-group silencing. *Science*, *298*(5595), 1039–1043. https://doi.org/10.1126/science.1076997

Cheloufi, S., Elling, U., Hopfgartner, B., Jung, Y. L., Murn, J., Ninova, M., Hubmann, M., Badeaux, A. I., Euong Ang, C., Tenen, D., Wesche, D. J., Abazova, N., Hogue, M., Tasdemir, N., Brumbaugh, J., Rathert, P., Jude, J., Ferrari, F., Blanco, A.,…Hochedlinger, K. (2015). The histone chaperone CAF-1 safeguards somatic cell identity. *Nature*, *528*(7581), 218–224. https://doi.org/10.1038/nature15749

Chen, B., MacAlpine, H. K., Hartemink, A. J., & MacAlpine, D. M. (2023). Spatiotemporal kinetics of CAF-1-dependent chromatin maturation ensures transcription fidelity during S-phase. *bioRxiv*. https://doi.org/10.1101/2023.05.25.541209

Cheng, L., Zhang, X., Wang, Y., Gan, H., Xu, X., Lv, X., Hua, X., Que, J., Ordog, T., & Zhang, Z. (2019). Chromatin Assembly Factor 1 (CAF-1) facilitates the establishment of facultative heterochromatin during pluripotency exit. *Nucleic Acids Res*, *47*(21), 11114–11131. https://doi.org/10.1093/nar/gkz858

Clemente-Ruiz, M., Gonzalez-Prieto, R., & Prado, F. (2011). Histone H3K56 acetylation, CAF1, and Rtt106 coordinate nucleosome assembly and stability of advancing replication forks. *PLoS Genet*, *7*(11), e1002376. https://doi.org/10.1371/journal.pgen.1002376

Collemare, J., & Seidl, M. F. (2019). Chromatin-dependent regulation of secondary metabolite biosynthesis in fungi: is the picture complete? *FEMS Microbiol Rev*, *43*(6), 591–607. https://doi.org/10.1093/femsre/fuz018

Connolly, L. R., Smith, K. M., & Freitag, M. (2013). The Fusarium graminearum histone H3 K27 methyltransferase KMT6 regulates development and expression of secondary metabolite gene clusters. *PLoS Genet*, *9*(10), e1003916. https://doi.org/10.1371/journal.pgen.1003916

Cook, A. J., Gurard-Levin, Z. A., Vassias, I., & Almouzni, G. (2011). A specific function for the histone chaperone NASP to fine-tune a reservoir of soluble H3-H4 in the histone supply chain. *Mol Cell*, *44*(6), 918–927. https://doi.org/10.1016/j.molcel.2011.11.021

Courtney, A. J., Kamei, M., Ferraro, A. R., Gai, K., He, Q., Honda, S., & Lewis, Z. A. (2020). Normal Patterns of Histone H3K27 Methylation Require the Histone Variant H2A.Z in Neurospora crassa. *Genetics*, *216*(1), 51–66. https://doi.org/10.1534/genetics.120.303442

Creyghton, M. P., Cheng, A. W., Welstead, G. G., Kooistra, T., Carey, B. W., Steine, E. J., Hanna, J., Lodato, M. A., Frampton, G. M., Sharp, P. A., Boyer, L. A., Young, R. A., & Jaenisch, R. (2010). Histone H3K27ac separates active from poised enhancers and predicts developmental state. *Proc Natl Acad Sci U S A*, *107*(50), 21931–21936. https://doi.org/10.1073/pnas.1016071107

Czermin, B., Melfi, R., McCabe, D., Seitz, V., Imhof, A., & Pirrotta, V. (2002). Drosophila enhancer of Zeste/ESC complexes have a histone H3 methyltransferase activity that marks chromosomal Polycomb sites. *Cell*, *111*(2), 185–196. https://doi.org/10.1016/s0092-8674(02)00975-3

Davey, C. A., Sargent, D. F., Luger, K., Maeder, A. W., & Richmond, T. J. (2002). Solvent mediated interactions in the structure of the nucleosome core particle at 1.9 a resolution. *J Mol Biol*, *319*(5), 1097–1113. https://doi.org/10.1016/S0022-2836(02)00386-8

de Napoles, M., Mermoud, J. E., Wakao, R., Tang, Y. A., Endoh, M., Appanah, R., Nesterova, T. B., Silva, J., Otte, A. P., Vidal, M., Koseki, H., & Brockdorff, N. (2004). Polycomb group proteins Ring1A/B link ubiquitylation of histone H2A to heritable gene silencing and X inactivation. *Dev Cell*, *7*(5), 663–676. https://doi.org/10.1016/j.devcel.2004.10.005

Deaven, A. M., Ameri-Solanky, A. J., & Lewis, Z. A. (2025). Polycomb repressive complex 2 regulates sexual development in Neurospora crassa. *mBio*, e0150525. https://doi.org/10.1128/mbio.01505-25

DeCamillis, M., Cheng, N. S., Pierre, D., & Brock, H. W. (1992). The polyhomeotic gene of Drosophila encodes a chromatin protein that shares polytene chromosome-binding sites with Polycomb. *Genes Dev*, *6*(2), 223–232. https://doi.org/10.1101/gad.6.2.223

Denu, J. M. (2019). Histone Acetyltransferase 1 Links Metabolism and Transcription to Cell-Cycle Progression. *Mol Cell*, *75*(4), 664–665. https://doi.org/10.1016/j.molcel.2019.08.004

Dhalluin, C., Carlson, J. E., Zeng, L., He, C., Aggarwal, A. K., & Zhou, M. M. (1999). Structure and ligand of a histone acetyltransferase bromodomain. *Nature*, *399*(6735), 491–496. https://doi.org/10.1038/20974

Di Croce, L., & Helin, K. (2013). Transcriptional regulation by Polycomb group proteins. *Nat Struct Mol Biol*, *20*(10), 1147–1155. https://doi.org/10.1038/nsmb.2669

Dietrich, N., et al. (2012). "REST–Mediated Recruitment of Polycomb Repressor Complexes in Mammalian Cells." PLOS Genetics 8(3): e1002494.

Dilworth, S. M., Black, S. J., & Laskey, R. A. (1987). Two complexes that contain histones are required for nucleosome assembly in vitro: role of nucleoplasmin and N1 in Xenopus egg extracts. *Cell*, *51*(6), 1009–1018. https://doi.org/10.1016/0092-8674(87)90587-3

Dixon, J. R., Selvaraj, S., Yue, F., Kim, A., Li, Y., Shen, Y., Hu, M., Liu, J. S., & Ren, B. (2012). Topological domains in mammalian genomes identified by analysis of chromatin interactions. *Nature*, *485*(7398), 376–380. https://doi.org/10.1038/nature11082

Dobrinic, P., Szczurek, A. T., & Klose, R. J. (2021). PRC1 drives Polycomb-mediated gene repression by controlling transcription initiation and burst frequency. *Nat Struct Mol Biol*, *28*(10), 811–824. https://doi.org/10.1038/s41594-021-00661-y

Dohke, K., Miyazaki, S., Tanaka, K., Urano, T., Grewal, S. I., & Murakami, Y. (2008). Fission yeast chromatin assembly factor 1 assists in the replication-coupled maintenance of heterochromatin. *Genes Cells*, *13*(10), 1027–1043. https://doi.org/10.1111/j.1365-2443.2008.01225.x

Dumesic, P. A., Homer, C. M., Moresco, J. J., Pack, L. R., Shanle, E. K., Coyle, S. M., Strahl, B. D., Fujimori, D. G., Yates, J. R., 3rd, & Madhani, H. D. (2015). Product binding enforces the genomic specificity of a yeast polycomb repressive complex. *Cell*, *160*(1-2), 204–218. https://doi.org/10.1016/j.cell.2014.11.039

Duncan, I. M. (1982). POLYCOMBLIKE: A GENE THAT APPEARS TO BE REQUIRED FOR THE NORMAL EXPRESSION OF THE BITHORAX AND ANTENNAPEDIA GENE COMPLEXES OF DROSOPHILA MELANOGASTER. *Genetics*, *102*(1), 49–70. https://doi.org/10.1093/genetics/102.1.49

Dunlap, J. C., Borkovich, K. A., Henn, M. R., Turner, G. E., Sachs, M. S., Glass, N. L., McCluskey, K., Plamann, M., Galagan, J. E., Birren, B. W., Weiss, R. L., Townsend, J. P., Loros, J. J., Nelson, M. A., Lambreghts, R., Colot, H. V., Park, G., Collopy, P., Ringelberg, C.,…Xu, J. (2007). Enabling a community to dissect an organism: overview of the Neurospora functional genomics project. *Adv Genet*, *57*, 49–96. https://doi.org/10.1016/S0065-2660(06)57002-6

Ebot-Ojong, F., Ferraro, A. R., Yap, R. E., Kaddar, F., Hull-Crew, C., Scadden, A. W., Deaven, A. M., Klocko, A. D., & Lewis, Z. A. (2025). HISTONE DEACETYLASE-1 is required for epigenome stability in Neurospora crassa. *Proc Natl Acad Sci U S A*, *122*(40), e2503876122. https://doi.org/10.1073/pnas.2503876122

Elgin, S. C., & Reuter, G. (2013). Position-effect variegation, heterochromatin formation, and gene silencing in Drosophila. *Cold Spring Harb Perspect Biol*, *5*(8), a017780. https://doi.org/10.1101/cshperspect.a017780

Enomoto, S., & Berman, J. (1998). Chromatin assembly factor I contributes to the maintenance, but not the re-establishment, of silencing at the yeast silent mating loci. *Genes Dev*, *12*(2), 219–232. https://doi.org/10.1101/gad.12.2.219

Eriksson, P. R., Ganguli, D., Nagarajavel, V., & Clark, D. J. (2012). Regulation of histone gene expression in budding yeast. *Genetics*, *191*(1), 7–20. https://doi.org/10.1534/genetics.112.140145

Eskeland, R., Leeb, M., Grimes, G. R., Kress, C., Boyle, S., Sproul, D., Gilbert, N., Fan, Y., Skoultchi, A. I., Wutz, A., & Bickmore, W. A. (2010). Ring1B compacts chromatin structure and represses gene expression independent of histone ubiquitination. *Mol Cell*, *38*(3), 452–464. https://doi.org/10.1016/j.molcel.2010.02.032

Fang, Y., Hua, X., Shan, C. M., Toda, T., Qiao, F., Zhang, Z., & Jia, S. (2024). Coordination of histone chaperones for parental histone segregation and epigenetic inheritance. *Genes Dev*, *38*(3-4), 189–204. https://doi.org/10.1101/gad.351278.123

Farcas, A. M., Blackledge, N. P., Sudbery, I., Long, H. K., McGouran, J. F., Rose, N. R., Lee, S., Sims, D., Cerase, A., Sheahan, T. W., Koseki, H., Brockdorff, N., Ponting, C. P., Kessler, B. M., & Klose, R. J. (2012). KDM2B links the Polycomb Repressive Complex 1 (PRC1) to recognition of CpG islands. *Elife*, *1*, e00205. https://doi.org/10.7554/eLife.00205

Finch, J. T., & Klug, A. (1976). Solenoidal model for superstructure in chromatin. *Proc Natl Acad Sci U S A*, *73*(6), 1897–1901. https://doi.org/10.1073/pnas.73.6.1897

Francis, N. J., Kingston, R. E., & Woodcock, C. L. (2004). Chromatin compaction by a polycomb group protein complex. *Science*, *306*(5701), 1574–1577. https://doi.org/10.1126/science.1100576

Francis, N. J., Saurin, A. J., Shao, Z., & Kingston, R. E. (2001). Reconstitution of a functional core polycomb repressive complex. *Mol Cell*, *8*(3), 545–556. https://doi.org/10.1016/s1097-2765(01)00316-1

Franke, A., DeCamillis, M., Zink, D., Cheng, N., Brock, H. W., & Paro, R. (1992). Polycomb and polyhomeotic are constituents of a multimeric protein complex in chromatin of Drosophila melanogaster. *EMBO J*, *11*(8), 2941–2950. https://doi.org/10.1002/j.1460-2075.1992.tb05364.x

Franklin, R., Guo, Y., He, S., Chen, M., Ji, F., Zhou, X., Frankhouser, D., Do, B. T., Chiem, C., Jang, M., Blanco, M. A., Vander Heiden, M. G., Rockne, R. C., Ninova, M., Sykes, D. B., Hochedlinger, K., Lu, R., Sadreyev, R. I., Murn, J.,…Cheloufi, S. (2022). Regulation of chromatin accessibility by the histone chaperone CAF-1 sustains lineage fidelity. *Nat Commun*, *13*(1), 2350. https://doi.org/10.1038/s41467-022-29730-6

Frapporti, A., Miro Pina, C., Arnaiz, O., Holoch, D., Kawaguchi, T., Humbert, A., Eleftheriou, E., Lombard, B., Loew, D., Sperling, L., Guitot, K., Margueron, R., & Duharcourt, S. (2019). The Polycomb protein Ezl1 mediates H3K9 and H3K27 methylation to repress transposable elements in Paramecium. *Nat Commun*, *10*(1), 2710. https://doi.org/10.1038/s41467-019-10648-5

Fraser, C. J., & Whitehall, S. K. (2022). Heterochromatin in the fungal plant pathogen, Zymoseptoria tritici: Control of transposable elements, genome plasticity and virulence. *Front Genet*, *13*, 1058741. https://doi.org/10.3389/fgene.2022.1058741

Gao, Z., Zhang, J., Bonasio, R., Strino, F., Sawai, A., Parisi, F., Kluger, Y., & Reinberg, D. (2012). PCGF homologs, CBX proteins, and RYBP define functionally distinct PRC1 family complexes. *Mol Cell*, *45*(3), 344–356. https://doi.org/10.1016/j.molcel.2012.01.002

Gilbert, N., Boyle, S., Fiegler, H., Woodfine, K., Carter, N. P., & Bickmore, W. A. (2004). Chromatin architecture of the human genome: gene-rich domains are enriched in open chromatin fibers. *Cell*, *118*(5), 555–566. https://doi.org/10.1016/j.cell.2004.08.011

Grau, D. J., Chapman, B. A., Garlick, J. D., Borowsky, M., Francis, N. J., & Kingston, R. E. (2011). Compaction of chromatin by diverse Polycomb group proteins requires localized regions of high charge. *Genes Dev*, *25*(20), 2210–2221. https://doi.org/10.1101/gad.17288211

Green, E. M., Antczak, A. J., Bailey, A. O., Franco, A. A., Wu, K. J., Yates, J. R., 3rd, & Kaufman, P. D. (2005). Replication-independent histone deposition by the HIR complex and Asf1. *Curr Biol*, *15*(22), 2044–2049. https://doi.org/10.1016/j.cub.2005.10.053

Grewal, S. I. S. (2023). The molecular basis of heterochromatin assembly and epigenetic inheritance. *Mol Cell*, *83*(11), 1767–1785. https://doi.org/10.1016/j.molcel.2023.04.020

Grossniklaus, U., Vielle-Calzada, J.-P., Hoeppner, M. A., & Gagliano, W. B. (1998). Maternal Control of Embryogenesis by MEDEA, a Polycomb Group Gene in Arabidopsis. *Science*, *280*(5362), 446–450. https://doi.org/doi:10.1126/science.280.5362.446

Gurard-Levin, Z. A., Quivy, J. P., & Almouzni, G. (2014). Histone chaperones: assisting histone traffic and nucleosome dynamics. *Annu Rev Biochem*, *83*, 487–517. https://doi.org/10.1146/annurev-biochem-060713-035536

Hammond, C. M., Stromme, C. B., Huang, H., Patel, D. J., & Groth, A. (2017). Histone chaperone networks shaping chromatin function. *Nat Rev Mol Cell Biol*, *18*(3), 141–158. https://doi.org/10.1038/nrm.2016.159

Heitz, E. (1928). *"Das" Heterochromatin der Moose*. Bornträger.

Hoek, M., & Stillman, B. (2003). Chromatin assembly factor 1 is essential and couples chromatin assembly to DNA replication in vivo. *Proc Natl Acad Sci U S A*, *100*(21), 12183–12188. https://doi.org/10.1073/pnas.1635158100

Houlard, M., Berlivet, S., Probst, A. V., Quivy, J. P., Hery, P., Almouzni, G., & Gerard, M. (2006). CAF-1 is essential for heterochromatin organization in pluripotent embryonic cells. *PLoS Genet*, *2*(11), e181. https://doi.org/10.1371/journal.pgen.0020181

Huang, H., Stromme, C. B., Saredi, G., Hodl, M., Strandsby, A., Gonzalez-Aguilera, C., Chen, S., Groth, A., & Patel, D. J. (2015). A unique binding mode enables MCM2 to chaperone histones H3-H4 at replication forks. *Nat Struct Mol Biol*, *22*(8), 618–626. https://doi.org/10.1038/nsmb.3055

Huang, H., Yu, Z., Zhang, S., Liang, X., Chen, J., Li, C., Ma, J., & Jiao, R. (2010). Drosophila CAF-1 regulates HP1-mediated epigenetic silencing and pericentric heterochromatin stability. *J Cell Sci*, *123*(Pt 16), 2853–2861. https://doi.org/10.1242/jcs.063610

Huang, S., Zhou, H., Tarara, J., & Zhang, Z. (2007). A novel role for histone chaperones CAF-1 and Rtt106p in heterochromatin silencing. *EMBO J*, *26*(9), 2274–2283. https://doi.org/10.1038/sj.emboj.7601670

Imbeault, D., Gamar, L., Rufiange, A., Paquet, E., & Nourani, A. (2008). The Rtt106 histone chaperone is functionally linked to transcription elongation and is involved in the regulation of spurious transcription from cryptic promoters in yeast. *J Biol Chem*, *283*(41), 27350–27354. https://doi.org/10.1074/jbc.C800147200

Jadhav, U., Manieri, E., Nalapareddy, K., Madha, S., Chakrabarti, S., Wucherpfennig, K., Barefoot, M., & Shivdasani, R. A. (2020). Replicational Dilution of H3K27me3 in Mammalian Cells and the Role of Poised Promoters. *Mol Cell*, *78*(1), 141–151 e145. https://doi.org/10.1016/j.molcel.2020.01.017

Jamieson, K., Rountree, M. R., Lewis, Z. A., Stajich, J. E., & Selker, E. U. (2013). Regional control of histone H3 lysine 27 methylation in Neurospora. *Proc Natl Acad Sci U S A*, *110*(15), 6027–6032. https://doi.org/10.1073/pnas.1303750110

Janssen, A., Colmenares, S. U., & Karpen, G. H. (2018). Heterochromatin: Guardian of the Genome. *Annu Rev Cell Dev Biol*, *34*, 265–288. https://doi.org/10.1146/annurev-cellbio-100617-062653

Jiang, D., & Berger, F. (2017). DNA replication-coupled histone modification maintains Polycomb gene silencing in plants. *Science*, *357*(6356), 1146–1149. https://doi.org/10.1126/science.aan4965

Jones, P. A. (2012). Functions of DNA methylation: islands, start sites, gene bodies and beyond. *Nat Rev Genet*, *13*(7), 484–492. https://doi.org/10.1038/nrg3230

Kahn, T. G., Dorafshan, E., Schultheis, D., Zare, A., Stenberg, P., Reim, I., Pirrotta, V., & Schwartz, Y. B. (2016). Interdependence of PRC1 and PRC2 for recruitment to Polycomb Response Elements. *Nucleic Acids Res*, *44*(21), 10132–10149. https://doi.org/10.1093/nar/gkw701

Kamei, M., Ameri, A. J., Ferraro, A. R., Bar-Peled, Y., Zhao, F., Ethridge, C. L., Lail, K., Amirebrahimi, M., Lipzen, A., Ng, V., Grigoriev, I. V., Schmitz, R. J., Liu, Y., & Lewis, Z. A. (2021). IMITATION SWITCH is required for normal chromatin structure and gene repression in PRC2 target domains. *Proc Natl Acad Sci U S A*, *118*(4). https://doi.org/10.1073/pnas.2010003118

Kasinath, V., Beck, C., Sauer, P., Poepsel, S., Kosmatka, J., Faini, M., Toso, D., Aebersold, R., & Nogales, E. (2021). JARID2 and AEBP2 regulate PRC2 in the presence of H2AK119ub1 and other histone modifications. *Science*, *371*(6527). https://doi.org/10.1126/science.abc3393

Kassis, J. A. (2002). 14 - Pairing-Sensitive Silencing, Polycomb Group Response Elements, and Transposon Homing in Drosophila. In J. C. Dunlap & C. t. Wu (Eds.), *Advances in Genetics* (Vol. 46, pp. 421–438). Academic Press. https://doi.org/https://doi.org/10.1016/S0065-2660(02)46015-4

Kassis, J. A., & Brown, J. L. (2013). Polycomb group response elements in Drosophila and vertebrates. *Adv Genet*, *81*, 83–118. https://doi.org/10.1016/B978-0-12-407677-8.00003-8

Kassis, J. A., Kennison, J. A., & Tamkun, J. W. (2017). Polycomb and Trithorax Group Genes in Drosophila. *Genetics*, *206*(4), 1699–1725. https://doi.org/10.1534/genetics.115.185116

Kaufman, P. D., Kobayashi, R., Kessler, N., & Stillman, B. (1995). The p150 and p60 subunits of chromatin assembly factor I: a molecular link between newly synthesized histones and DNA replication. *Cell*, *81*(7), 1105–1114. https://doi.org/10.1016/s0092-8674(05)80015-7

Keck, K. M., & Pemberton, L. F. (2012). Histone chaperones link histone nuclear import and chromatin assembly. *Biochim Biophys Acta*, *1819*(3-4), 277–289. https://doi.org/10.1016/j.bbagrm.2011.09.007

Kim, D. H., & Sung, S. (2017). Vernalization-Triggered Intragenic Chromatin Loop Formation by Long Noncoding RNAs. *Dev Cell*, *40*(3), 302–312 e304. https://doi.org/10.1016/j.devcel.2016.12.021

Kim, K. H., & Roberts, C. W. (2016). Targeting EZH2 in cancer. *Nat Med*, *22*(2), 128–134. https://doi.org/10.1038/nm.4036

King, I. F. G., Francis, N. J., & Kingston, R. E. (2002). Native and Recombinant Polycomb Group Complexes Establish a Selective Block to Template Accessibility To Repress Transcription In Vitro. *Molecular and Cellular Biology*, *22*(22), 7919–7928. https://doi.org/10.1128/MCB.22.22.7919-7928.2002

Kohler, C., Hennig, L., Spillane, C., Pien, S., Gruissem, W., & Grossniklaus, U. (2003). The Polycomb-group protein MEDEA regulates seed development by controlling expression of the MADS-box gene PHERES1. *Genes Dev*, *17*(12), 1540–1553. https://doi.org/10.1101/gad.257403

Kornberg, R. D. (1974). Chromatin structure: a repeating unit of histones and DNA. *Science*, *184*(4139), 868–871. https://doi.org/10.1126/science.184.4139.868

Kornberg, R. D., & Lorch, Y. (1999). Twenty-five years of the nucleosome, fundamental particle of the eukaryote chromosome. *Cell*, *98*(3), 285–294. https://doi.org/10.1016/s0092-8674(00)81958-3

Kouzarides, T. (2007). Chromatin modifications and their function. *Cell*, *128*(4), 693–705. https://doi.org/10.1016/j.cell.2007.02.005

Kuzmichev, A., Nishioka, K., Erdjument-Bromage, H., Tempst, P., & Reinberg, D. (2002). Histone methyltransferase activity associated with a human multiprotein complex containing the Enhancer of Zeste protein. *Genes Dev*, *16*(22), 2893–2905. https://doi.org/10.1101/gad.1035902

Laprell, F., Finkl, K., & Muller, J. (2017). Propagation of Polycomb-repressed chromatin requires sequence-specific recruitment to DNA. *Science*, *356*(6333), 85–88. https://doi.org/10.1126/science.aai8266

Laugesen, A., Hojfeldt, J. W., & Helin, K. (2019). Molecular Mechanisms Directing PRC2 Recruitment and H3K27 Methylation. *Mol Cell*, *74*(1), 8–18. https://doi.org/10.1016/j.molcel.2019.03.011

Lavarone, E., Barbieri, C. M., & Pasini, D. (2019). Dissecting the role of H3K27 acetylation and methylation in PRC2 mediated control of cellular identity. *Nat Commun*, *10*(1), 1679. https://doi.org/10.1038/s41467-019-09624-w

Le, S., Davis, C., Konopka, J. B., & Sternglanz, R. (1997). Two New S-Phase-Specific Genes from Saccharomyces cerevisiae. *Yeast*, *13*(11), 1029–1042. https://doi.org/https://doi.org/10.1002/(SICI)1097-0061(19970915)13:11<1029::AID-YEA160>3.0.CO;2-1

Lee, C. H., Yu, J. R., Kumar, S., Jin, Y., LeRoy, G., Bhanu, N., Kaneko, S., Garcia, B. A., Hamilton, A. D., & Reinberg, D. (2018). Allosteric Activation Dictates PRC2 Activity Independent of Its Recruitment to Chromatin. *Mol Cell*, *70*(3), 422–434 e426. https://doi.org/10.1016/j.molcel.2018.03.020

Lee, M. G., Villa, R., Trojer, P., Norman, J., Yan, K. P., Reinberg, D., Di Croce, L., & Shiekhattar, R. (2007). Demethylation of H3K27 regulates polycomb recruitment and H2A ubiquitination. *Science*, *318*(5849), 447–450. https://doi.org/10.1126/science.1149042

Lee, T. I., Jenner, R. G., Boyer, L. A., Guenther, M. G., Levine, S. S., Kumar, R. M., Chevalier, B., Johnstone, S. E., Cole, M. F., Isono, K., Koseki, H., Fuchikami, T., Abe, K., Murray, H. L., Zucker, J. P., Yuan, B., Bell, G. W., Herbolsheimer, E., Hannett, N. M.,…Young, R. A. (2006). Control of developmental regulators by Polycomb in human embryonic stem cells. *Cell*, *125*(2), 301–313. https://doi.org/10.1016/j.cell.2006.02.043

Levine, S. S., Weiss, A., Erdjument-Bromage, H., Shao, Z., Tempst, P., & Kingston, R. E. (2002). The Core of the Polycomb Repressive Complex Is Compositionally and Functionally Conserved in Flies and Humans. *Molecular and Cellular Biology*, *22*(17), 6070–6078. https://doi.org/10.1128/MCB.22.17.6070-6078.2002

Lewis, P. (1947). Melanogaster-New mutants: Report of Pamela H. *Lewis. Dros. Inform. Serv*, *21*, 69.

Li, B., Carey, M., & Workman, J. L. (2007). The role of chromatin during transcription. *Cell*, *128*(4), 707–719. https://doi.org/10.1016/j.cell.2007.01.015

Li, H., Liefke, R., Jiang, J., Kurland, J. V., Tian, W., Deng, P., Zhang, W., He, Q., Patel, D. J., Bulyk, M. L., Shi, Y., & Wang, Z. (2017). Polycomb-like proteins link the PRC2 complex to CpG islands. *Nature*, *549*(7671), 287–291. https://doi.org/10.1038/nature23881

Lieberman-Aiden, E., van Berkum, N. L., Williams, L., Imakaev, M., Ragoczy, T., Telling, A., Amit, I., Lajoie, B. R., Sabo, P. J., Dorschner, M. O., Sandstrom, R., Bernstein, B., Bender, M. A., Groudine, M., Gnirke, A., Stamatoyannopoulos, J., Mirny, L. A., Lander, E. S., & Dekker, J. (2009). Comprehensive mapping of long-range interactions reveals folding principles of the human genome. *Science*, *326*(5950), 289–293. https://doi.org/10.1126/science.1181369

Linger, J., & Tyler, J. K. (2005). The yeast histone chaperone chromatin assembly factor 1 protects against double-strand DNA-damaging agents. *Genetics*, *171*(4), 1513–1522. https://doi.org/10.1534/genetics.105.043000

Liu, C. P., Yu, Z., Xiong, J., Hu, J., Song, A., Ding, D., Yu, C., Yang, N., Wang, M., Yu, J., Hou, P., Zeng, K., Li, Z., Zhang, Z., Zhang, X., Li, W., Zhang, Z., Zhu, B., Li, G., & Xu, R. M. (2023). Structural insights into histone binding and nucleosome assembly by chromatin assembly factor-1. *Science*, *381*(6660), eadd8673. https://doi.org/10.1126/science.add8673

Liu, W. H., Roemer, S. C., Port, A. M., & Churchill, M. E. (2012). CAF-1-induced oligomerization of histones H3/H4 and mutually exclusive interactions with Asf1 guide H3/H4 transitions among histone chaperones and DNA. *Nucleic Acids Res*, *40*(22), 11229–11239. https://doi.org/10.1093/nar/gks906

Liu, W. H., Roemer, S. C., Zhou, Y., Shen, Z. J., Dennehey, B. K., Balsbaugh, J. L., Liddle, J. C., Nemkov, T., Ahn, N. G., Hansen, K. C., Tyler, J. K., & Churchill, M. E. (2016). The Cac1 subunit of histone chaperone CAF-1 organizes CAF-1-H3/H4 architecture and tetramerizes histones. *Elife*, *5*. https://doi.org/10.7554/eLife.18023

Liu, Y., Zhou, K., Zhang, N., Wei, H., Tan, Y. Z., Zhang, Z., Carragher, B., Potter, C. S., D'Arcy, S., & Luger, K. (2020). FACT caught in the act of manipulating the nucleosome. *Nature*, *577*(7790), 426–431. https://doi.org/10.1038/s41586-019-1820-0

Lorch, Y., LaPointe, J. W., & Kornberg, R. D. (1987). Nucleosomes inhibit the initiation of transcription but allow chain elongation with the displacement of histones. *Cell*, *49*(2), 203–210. https://doi.org/10.1016/0092-8674(87)90561-7

Luger, K., Mader, A. W., Richmond, R. K., Sargent, D. F., & Richmond, T. J. (1997). Crystal structure of the nucleosome core particle at 2.8 A resolution. *Nature*, *389*(6648), 251–260. https://doi.org/10.1038/38444

MacAlpine, D. M., & Almouzni, G. (2013). Chromatin and DNA replication. *Cold Spring Harb Perspect Biol*, *5*(8), a010207. https://doi.org/10.1101/cshperspect.a010207

Mahy, N. L., Perry, P. E., & Bickmore, W. A. (2002). Gene density and transcription influence the localization of chromatin outside of chromosome territories detectable by FISH. *J Cell Biol*, *159*(5), 753–763. https://doi.org/10.1083/jcb.200207115

Margueron, R., Justin, N., Ohno, K., Sharpe, M. L., Son, J., Drury, W. J., 3rd, Voigt, P., Martin, S. R., Taylor, W. R., De Marco, V., Pirrotta, V., Reinberg, D., & Gamblin, S. J. (2009). Role of the polycomb protein EED in the propagation of repressive histone marks. *Nature*, *461*(7265), 762–767. https://doi.org/10.1038/nature08398

Margueron, R., & Reinberg, D. (2011). The Polycomb complex PRC2 and its mark in life. *Nature*, *469*(7330), 343–349. https://doi.org/10.1038/nature09784

McNaught, K. J., Wiles, E. T., & Selker, E. U. (2020). Identification of a PRC2 Accessory Subunit Required for Subtelomeric H3K27 Methylation in Neurospora crassa. *Mol Cell Biol*, *40*(11). https://doi.org/10.1128/MCB.00003-20

Meijsing, S. H., & Ehrenhofer-Murray, A. E. (2001). The silencing complex SAS-I links histone acetylation to the assembly of repressed chromatin by CAF-I and Asf1 in Saccharomyces cerevisiae. *Genes Dev*, *15*(23), 3169–3182. https://doi.org/10.1101/gad.929001

Mello, J. A., Sillje, H. H., Roche, D. M., Kirschner, D. B., Nigg, E. A., & Almouzni, G. (2002). Human Asf1 and CAF-1 interact and synergize in a repair-coupled nucleosome assembly pathway. *EMBO Rep*, *3*(4), 329–334. https://doi.org/10.1093/embo-reports/kvf068

Mendenhall, E. M., Koche, R. P., Truong, T., Zhou, V. W., Issac, B., Chi, A. S., Ku, M., & Bernstein, B. E. (2010). GC-rich sequence elements recruit PRC2 in mammalian ES cells. *PLoS Genet*, *6*(12), e1001244. https://doi.org/10.1371/journal.pgen.1001244

Mendiratta, S., Gatto, A., & Almouzni, G. (2019). Histone supply: Multitiered regulation ensures chromatin dynamics throughout the cell cycle. *J Cell Biol*, *218*(1), 39–54. https://doi.org/10.1083/jcb.201807179

Min, J., Zhang, Y., & Xu, R. M. (2003). Structural basis for specific binding of Polycomb chromodomain to histone H3 methylated at Lys 27. *Genes Dev*, *17*(15), 1823–1828. https://doi.org/10.1101/gad.269603

Moggs, J. G., Grandi, P., Quivy, J. P., Jonsson, Z. O., Hubscher, U., Becker, P. B., & Almouzni, G. (2000). A CAF-1-PCNA-mediated chromatin assembly pathway triggered by sensing DNA damage. *Mol Cell Biol*, *20*(4), 1206–1218. https://doi.org/10.1128/MCB.20.4.1206-1218.2000

Moller, M., Schotanus, K., Soyer, J. L., Haueisen, J., Happ, K., Stralucke, M., Happel, P., Smith, K. M., Connolly, L. R., Freitag, M., & Stukenbrock, E. H. (2019). Destabilization of chromosome structure by histone H3 lysine 27 methylation. *PLoS Genet*, *15*(4), e1008093. https://doi.org/10.1371/journal.pgen.1008093

Mozgova, I., Wildhaber, T., Liu, Q., Abou-Mansour, E., L'Haridon, F., Metraux, J. P., Gruissem, W., Hofius, D., & Hennig, L. (2015). Chromatin assembly factor CAF-1 represses priming of plant defence response genes. *Nat Plants*, *1*, 15127. https://doi.org/10.1038/nplants.2015.127

Muller, J., Hart, C. M., Francis, N. J., Vargas, M. L., Sengupta, A., Wild, B., Miller, E. L., O'Connor, M. B., Kingston, R. E., & Simon, J. A. (2002). Histone methyltransferase activity of a Drosophila Polycomb group repressor complex. *Cell*, *111*(2), 197–208. https://doi.org/10.1016/s0092-8674(02)00976-5

Mumford, C. C., Tanizawa, H., Wiles, E. T., McNaught, K. J., Jamieson, K., Tsukamoto, K., & Selker, E. U. (2024). The RPD3L deacetylation complex is required for facultative heterochromatin repression in Neurospora crassa. *Proc Natl Acad Sci U S A*, *121*(32), e2404770121. https://doi.org/10.1073/pnas.2404770121

Munakata, T., Adachi, N., Yokoyama, N., Kuzuhara, T., & Horikoshi, M. (2000). A human homologue of yeast anti-silencing factor has histone chaperone activity. *Genes to Cells*, *5*(3), 221–233. https://doi.org/https://doi.org/10.1046/j.1365-2443.2000.00319.x

Musselman, C. A., Lalonde, M. E., Cote, J., & Kutateladze, T. G. (2012). Perceiving the epigenetic landscape through histone readers. *Nat Struct Mol Biol*, *19*(12), 1218–1227. https://doi.org/10.1038/nsmb.2436

Ng, J., Hart, C. M., Morgan, K., & Simon, J. A. (2000). A Drosophila ESC-E(Z) protein complex is distinct from other polycomb group complexes and contains covalently modified ESC. *Mol Cell Biol*, *20*(9), 3069–3078. https://doi.org/10.1128/MCB.20.9.3069-3078.2000

Nielsen, M., Menon, G., Zhao, Y., Mateo-Bonmati, E., Wolff, P., Zhou, S., Howard, M., & Dean, C. (2024). COOLAIR and PRC2 function in parallel to silence FLC during vernalization. *Proc Natl Acad Sci U S A*, *121*(4), e2311474121. https://doi.org/10.1073/pnas.2311474121

O'Carroll, D., Erhardt, S., Pagani, M., Barton, S. C., Surani, M. A., & Jenuwein, T. (2001). The polycomb-group gene Ezh2 is required for early mouse development. *Mol Cell Biol*, *21*(13), 4330–4336. https://doi.org/10.1128/MCB.21.13.4330-4336.2001

Ohad, N., Yadegari, R., Margossian, L., Hannon, M., Michaeli, D., Harada, J. J., Goldberg, R. B., & Fischer, R. L. (1999). Mutations in FIE, a WD polycomb group gene, allow endosperm development without fertilization. *Plant Cell*, *11*(3), 407–416. https://doi.org/10.1105/tpc.11.3.407

Oksuz, O., Narendra, V., Lee, C. H., Descostes, N., LeRoy, G., Raviram, R., Blumenberg, L., Karch, K., Rocha, P. P., Garcia, B. A., Skok, J. A., & Reinberg, D. (2018). Capturing the Onset of PRC2-Mediated Repressive Domain Formation. *Mol Cell*, *70*(6), 1149–1162 e1145. https://doi.org/10.1016/j.molcel.2018.05.023

Oktaba, K., Gutierrez, L., Gagneur, J., Girardot, C., Sengupta, A. K., Furlong, E. E., & Muller, J. (2008). Dynamic regulation by polycomb group protein complexes controls pattern formation and the cell cycle in Drosophila. *Dev Cell*, *15*(6), 877–889. https://doi.org/10.1016/j.devcel.2008.10.005

Okulski, H., Druck, B., Bhalerao, S., & Ringrose, L. (2011). Quantitative analysis of polycomb response elements (PREs) at identical genomic locations distinguishes contributions of PRE sequence and genomic environment. *Epigenetics Chromatin*, *4*, 4. https://doi.org/10.1186/1756-8935-4-4

Oppikofer, M., Kueng, S., Martino, F., Soeroes, S., Hancock, S. M., Chin, J. W., Fischle, W., & Gasser, S. M. (2011). A dual role of H4K16 acetylation in the establishment of yeast silent chromatin. *EMBO J*, *30*(13), 2610–2621. https://doi.org/10.1038/emboj.2011.170

Oudet, P., Gross-Bellard, M., & Chambon, P. (1975). Electron microscopic and biochemical evidence that chromatin structure is a repeating unit. *Cell*, *4*(4), 281–300. https://doi.org/10.1016/0092-8674(75)90149-x

Pardal, A. J., & Bowman, A. J. (2022). A specific role for importin-5 and NASP in the import and nuclear hand-off of monomeric H3. *Elife*, *11*. https://doi.org/10.7554/eLife.81755

Pardal, A. J., Fernandes-Duarte, F., & Bowman, A. J. (2019). The histone chaperoning pathway: from ribosome to nucleosome. *Essays Biochem*, *63*(1), 29–43. https://doi.org/10.1042/EBC20180055

Pasini, D., Malatesta, M., Jung, H. R., Walfridsson, J., Willer, A., Olsson, L., Skotte, J., Wutz, A., Porse, B., Jensen, O. N., & Helin, K. (2010). Characterization of an antagonistic switch between histone H3 lysine 27 methylation and acetylation in the transcriptional regulation of Polycomb group target genes. *Nucleic Acids Res*, *38*(15), 4958–4969. https://doi.org/10.1093/nar/gkq244

Perino, M., van Mierlo, G., Karemaker, I. D., van Genesen, S., Vermeulen, M., Marks, H., van Heeringen, S. J., & Veenstra, G. J. C. (2018). MTF2 recruits Polycomb Repressive Complex 2 by helical-shape-selective DNA binding. *Nat Genet*, *50*(7), 1002–1010. https://doi.org/10.1038/s41588-018-0134-8

Petryk, N., Dalby, M., Wenger, A., Stromme, C. B., Strandsby, A., Andersson, R., & Groth, A. (2018). MCM2 promotes symmetric inheritance of modified histones during DNA replication. *Science*, *361*(6409), 1389–1392. https://doi.org/10.1126/science.aau0294

Plath, K., Fang, J., Mlynarczyk-Evans, S. K., Cao, R., Worringer, K. A., Wang, H., de la Cruz, C. C., Otte, A. P., Panning, B., & Zhang, Y. (2003). Role of histone H3 lysine 27 methylation in X inactivation. *Science*, *300*(5616), 131–135. https://doi.org/10.1126/science.1084274

Quivy, J. P., Gerard, A., Cook, A. J., Roche, D., & Almouzni, G. (2008). The HP1-p150/CAF-1 interaction is required for pericentric heterochromatin replication and S-phase progression in mouse cells. *Nat Struct Mol Biol*, *15*(9), 972–979. https://doi.org/10.1038/nsmb.1470

Quivy, J. P., Roche, D., Kirschner, D., Tagami, H., Nakatani, Y., & Almouzni, G. (2004). A CAF-1 dependent pool of HP1 during heterochromatin duplication. *EMBO J*, *23*(17), 3516–3526. https://doi.org/10.1038/sj.emboj.7600362

Ransom, M., Dennehey, B. K., & Tyler, J. K. (2010). Chaperoning histones during DNA replication and repair. *Cell*, *140*(2), 183–195. https://doi.org/10.1016/j.cell.2010.01.004

Ray-Gallet, D., Quivy, J. P., Scamps, C., Martini, E. M., Lipinski, M., & Almouzni, G. (2002). HIRA is critical for a nucleosome assembly pathway independent of DNA synthesis. *Mol Cell*, *9*(5), 1091–1100. https://doi.org/10.1016/s1097-2765(02)00526-9

Ray-Gallet, D., Ricketts, M. D., Sato, Y., Gupta, K., Boyarchuk, E., Senda, T., Marmorstein, R., & Almouzni, G. (2018). Functional activity of the H3.3 histone chaperone complex HIRA requires trimerization of the HIRA subunit. *Nat Commun*, *9*(1), 3103. https://doi.org/10.1038/s41467-018-05581-y

Ray-Gallet, D., Woolfe, A., Vassias, I., Pellentz, C., Lacoste, N., Puri, A., Schultz, D. C., Pchelintsev, N. A., Adams, P. D., Jansen, L. E., & Almouzni, G. (2011). Dynamics of histone H3 deposition in vivo reveal a nucleosome gap-filling mechanism for H3.3 to maintain chromatin integrity. *Mol Cell*, *44*(6), 928–941. https://doi.org/10.1016/j.molcel.2011.12.006

Rhodes, J. D. P., Feldmann, A., Hernandez-Rodriguez, B., Diaz, N., Brown, J. M., Fursova, N. A., Blackledge, N. P., Prathapan, P., Dobrinic, P., Huseyin, M. K., Szczurek, A., Kruse, K., Nasmyth, K. A., Buckle, V. J., Vaquerizas, J. M., & Klose, R. J. (2020). Cohesin Disrupts Polycomb-Dependent Chromosome Interactions in Embryonic Stem Cells. *Cell Rep*, *30*(3), 820–835 e810. https://doi.org/10.1016/j.celrep.2019.12.057

Richardson, R. T., Alekseev, O. M., Grossman, G., Widgren, E. E., Thresher, R., Wagner, E. J., Sullivan, K. D., Marzluff, W. F., & O'Rand, M. G. (2006). Nuclear autoantigenic sperm protein (NASP), a linker histone chaperone that is required for cell proliferation. *J Biol Chem*, *281*(30), 21526–21534. https://doi.org/10.1074/jbc.M603816200

Ricketts, M. D., Frederick, B., Hoff, H., Tang, Y., Schultz, D. C., Singh Rai, T., Grazia Vizioli, M., Adams, P. D., & Marmorstein, R. (2015). Ubinuclein-1 confers histone H3.3-specific-binding by the HIRA histone chaperone complex. *Nat Commun*, *6*, 7711. https://doi.org/10.1038/ncomms8711

Ridenour, J. B., Moller, M., & Freitag, M. (2020). Polycomb Repression without Bristles: Facultative Heterochromatin and Genome Stability in Fungi. *Genes (Basel)*, *11*(6). https://doi.org/10.3390/genes11060638

Robinson, P. J., Fairall, L., Huynh, V. A., & Rhodes, D. (2006). EM measurements define the dimensions of the "30-nm" chromatin fiber: evidence for a compact, interdigitated structure. *Proc Natl Acad Sci U S A*, *103*(17), 6506–6511. https://doi.org/10.1073/pnas.0601212103

Roelens, B., Clemot, M., Leroux-Coyau, M., Klapholz, B., & Dostatni, N. (2017). Maintenance of Heterochromatin by the Large Subunit of the CAF-1 Replication-Coupled Histone Chaperone Requires Its Interaction with HP1a Through a Conserved Motif. *Genetics*, *205*(1), 125–137. https://doi.org/10.1534/genetics.116.190785

Rouillon, C., Eckhardt, B. V., Kollenstart, L., Gruss, F., Verkennis, A. E. E., Rondeel, I., Krijger, P. H. L., Ricci, G., Biran, A., van Laar, T., Delvaux de Fenffe, C. M., Luppens, G., Albanese, P., Sato, K., Scheltema, R. A., de Laat, W., Knipscheer, P., Dekker, N. H., Groth, A., & Mattiroli, F. (2023). CAF-1 deposits newly synthesized histones during DNA replication using distinct mechanisms on the leading and lagging strands. *Nucleic Acids Res*, *51*(8), 3770–3792. https://doi.org/10.1093/nar/gkad171

Rowley, M. J., & Corces, V. G. (2018). Organizational principles of 3D genome architecture. *Nat Rev Genet*, *19*(12), 789–800. https://doi.org/10.1038/s41576-018-0060-8

Sarma, K., Cifuentes-Rojas, C., Ergun, A., Del Rosario, A., Jeon, Y., White, F., Sadreyev, R., & Lee, J. T. (2014). ATRX directs binding of PRC2 to Xist RNA and Polycomb targets. *Cell*, *159*(4), 869–883. https://doi.org/10.1016/j.cell.2014.10.019

Sauer, P. V., Gu, Y., Liu, W. H., Mattiroli, F., Panne, D., Luger, K., & Churchill, M. E. (2018). Mechanistic insights into histone deposition and nucleosome assembly by the chromatin assembly factor-1. *Nucleic Acids Res*, *46*(19), 9907–9917. https://doi.org/10.1093/nar/gky823

Scheuermann, J. C., de Ayala Alonso, A. G., Oktaba, K., Ly-Hartig, N., McGinty, R. K., Fraterman, S., Wilm, M., Muir, T. W., & Muller, J. (2010). Histone H2A deubiquitinase activity of the Polycomb repressive complex PR-DUB. *Nature*, *465*(7295), 243–247. https://doi.org/10.1038/nature08966

Schmitges, F. W., Prusty, A. B., Faty, M., Stutzer, A., Lingaraju, G. M., Aiwazian, J., Sack, R., Hess, D., Li, L., Zhou, S., Bunker, R. D., Wirth, U., Bouwmeester, T., Bauer, A., Ly-Hartig, N., Zhao, K., Chan, H., Gu, J., Gut, H.,…Thoma, N. H. (2011). Histone methylation by PRC2 is inhibited by active chromatin marks. *Mol Cell*, *42*(3), 330–341. https://doi.org/10.1016/j.molcel.2011.03.025

Schneuwly, S., Klemenz, R., & Gehring, W. J. (1987). Redesigning the body plan of Drosophila by ectopic expression of the homoeotic gene Antennapedia. *Nature*, *325*(6107), 816–818. https://doi.org/10.1038/325816a0

Schonrock, N., Exner, V., Probst, A., Gruissem, W., & Hennig, L. (2006). Functional genomic analysis of CAF-1 mutants in Arabidopsis thaliana. *J Biol Chem*, *281*(14), 9560–9568. https://doi.org/10.1074/jbc.M513426200

Schuettengruber, B., Bourbon, H. M., Di Croce, L., & Cavalli, G. (2017). Genome Regulation by Polycomb and Trithorax: 70 Years and Counting. *Cell*, *171*(1), 34–57. https://doi.org/10.1016/j.cell.2017.08.002

Shao, Z., Raible, F., Mollaaghababa, R., Guyon, J. R., Wu, C. T., Bender, W., & Kingston, R. E. (1999). Stabilization of chromatin structure by PRC1, a Polycomb complex. *Cell*, *98*(1), 37–46. https://doi.org/10.1016/S0092-8674(00)80604-2

Sharaf, A., Vijayanathan, M., Obornik, M., & Mozgova, I. (2022). Phylogenetic profiling resolves early emergence of PRC2 and illuminates its functional core. *Life Sci Alliance*, *5*(7). https://doi.org/10.26508/lsa.202101271

Sherwood, P. W., Tsang, S. V., & Osley, M. A. (1993). Characterization of HIR1 and HIR2, two genes required for regulation of histone gene transcription in Saccharomyces cerevisiae. *Mol Cell Biol*, *13*(1), 28–38. https://doi.org/10.1128/mcb.13.1.28-38.1993

Shibahara, K., & Stillman, B. (1999). Replication-dependent marking of DNA by PCNA facilitates CAF-1-coupled inheritance of chromatin. *Cell*, *96*(4), 575–585. https://doi.org/10.1016/s0092-8674(00)80661-3

Shogren-Knaak, M., Ishii, H., Sun, J. M., Pazin, M. J., Davie, J. R., & Peterson, C. L. (2006). Histone H4-K16 acetylation controls chromatin structure and protein interactions. *Science*, *311*(5762), 844–847. https://doi.org/10.1126/science.1124000

Simon, J. A., & Kingston, R. E. (2009). Mechanisms of polycomb gene silencing: knowns and unknowns. *Nat Rev Mol Cell Biol*, *10*(10), 697–708. https://doi.org/10.1038/nrm2763

Slifer, E. H. (1942). A mutant stock of Drosophila with extra sex-combs. *Journal of Experimental Zoology*, *90*(1), 31–40. https://doi.org/https://doi.org/10.1002/jez.1400900103

Smith, S., & Stillman, B. (1989). Purification and characterization of CAF-I, a human cell factor required for chromatin assembly during DNA replication in vitro. *Cell*, *58*(1), 15–25. https://doi.org/10.1016/0092-8674(89)90398-x

Smith, S., & Stillman, B. (1991). Stepwise assembly of chromatin during DNA replication in vitro. *EMBO J*, *10*(4), 971–980. https://doi.org/10.1002/j.1460-2075.1991.tb08031.x

Song, Y., He, F., Xie, G., Guo, X., Xu, Y., Chen, Y., Liang, X., Stagljar, I., Egli, D., Ma, J., & Jiao, R. (2007). CAF-1 is essential for Drosophila development and involved in the maintenance of epigenetic memory. *Dev Biol*, *311*(1), 213–222. https://doi.org/10.1016/j.ydbio.2007.08.039

Srinivasan, L. and M. L. Atchison (2004). "YY1 DNA binding and PcG recruitment requires CtBP." Genes Dev 18(21): 2596–2601.

Stewart-Morgan, K. R., Reveron-Gomez, N., & Groth, A. (2019). Transcription Restart Establishes Chromatin Accessibility after DNA Replication. *Mol Cell*, *75*(2), 284–297 e286. https://doi.org/10.1016/j.molcel.2019.04.033

Stillman, B. (1986). Chromatin assembly during SV40 DNA replication in vitro. *Cell*, *45*(4), 555–565. https://doi.org/10.1016/0092-8674(86)90287-4

Strahl, B. D., & Allis, C. D. (2000). The language of covalent histone modifications. *Nature*, *403*(6765), 41–45. https://doi.org/10.1038/47412

Tagami, H., Ray-Gallet, D., Almouzni, G., & Nakatani, Y. (2004). Histone H3.1 and H3.3 complexes mediate nucleosome assembly pathways dependent or independent of DNA synthesis. *Cell*, *116*(1), 51–61. https://doi.org/10.1016/s0092-8674(03)01064-x

Tamburri, S., Lavarone, E., Fernandez-Perez, D., Conway, E., Zanotti, M., Manganaro, D., & Pasini, D. (2020). Histone H2AK119 Mono-Ubiquitination Is Essential for Polycomb-Mediated Transcriptional Repression. *Mol Cell*, *77*(4), 840–856 e845. https://doi.org/10.1016/j.molcel.2019.11.021

Taverna, S. D., Li, H., Ruthenburg, A. J., Allis, C. D., & Patel, D. J. (2007). How chromatin-binding modules interpret histone modifications: lessons from professional pocket pickers. *Nat Struct Mol Biol*, *14*(11), 1025–1040. https://doi.org/10.1038/nsmb1338

Thiru, A., Nietlispach, D., Mott, H. R., Okuwaki, M., Lyon, D., Nielsen, P. R., Hirshberg, M., Verreault, A., Murzina, N. V., & Laue, E. D. (2004). Structural basis of HP1/PXVXL motif peptide interactions and HP1 localisation to heterochromatin. *EMBO J*, *23*(3), 489–499. https://doi.org/10.1038/sj.emboj.7600088

Tie, F., Banerjee, R., Stratton, C. A., Prasad-Sinha, J., Stepanik, V., Zlobin, A., Diaz, M. O., Scacheri, P. C., & Harte, P. J. (2009). CBP-mediated acetylation of histone H3 lysine 27 antagonizes Drosophila Polycomb silencing. *Development*, *136*(18), 3131–3141. https://doi.org/10.1242/dev.037127

Towbin, B. D., Gonzalez-Aguilera, C., Sack, R., Gaidatzis, D., Kalck, V., Meister, P., Askjaer, P., & Gasser, S. M. (2012). Step-wise methylation of histone H3K9 positions heterochromatin at the nuclear periphery. *Cell*, *150*(5), 934–947. https://doi.org/10.1016/j.cell.2012.06.051

Trojer, P., & Reinberg, D. (2007). Facultative heterochromatin: is there a distinctive molecular signature? *Mol Cell*, *28*(1), 1–13. https://doi.org/10.1016/j.molcel.2007.09.011

Ueda, T., Nakata, Y., Nagamachi, A., Yamasaki, N., Kanai, A., Sera, Y., Sasaki, M., Matsui, H., Honda, Z., Oda, H., Wolff, L., Inaba, T., & Honda, H. (2016). Propagation of trimethylated H3K27 regulated by polycomb protein EED is required for embryogenesis, hematopoietic maintenance, and tumor suppression. *Proc Natl Acad Sci U S A*, *113*(37), 10370–10375. https://doi.org/10.1073/pnas.1600070113

van Steensel, B., & Belmont, A. S. (2017). Lamina-Associated Domains: Links with Chromosome Architecture, Heterochromatin, and Gene Repression. *Cell*, *169*(5), 780–791. https://doi.org/10.1016/j.cell.2017.04.022

Veronezi, G. M. B., & Ramachandran, S. (2024). Nucleation and spreading maintain Polycomb domains every cell cycle. *Cell Rep*, *43*(4), 114090. https://doi.org/10.1016/j.celrep.2024.114090

Verreault, A., Kaufman, P. D., Kobayashi, R., & Stillman, B. (1996). Nucleosome assembly by a complex of CAF-1 and acetylated histones H3/H4. *Cell*, *87*(1), 95–104. https://doi.org/10.1016/s0092-8674(00)81326-4

Vertii, A., Ou, J., Yu, J., Yan, A., Pages, H., Liu, H., Zhu, L. J., & Kaufman, P. D. (2019). Two contrasting classes of nucleolus-associated domains in mouse fibroblast heterochromatin. *Genome Res*, *29*(8), 1235–1249. https://doi.org/10.1101/gr.247072.118

Voigt, P., Tee, W. W., & Reinberg, D. (2013). A double take on bivalent promoters. *Genes Dev*, *27*(12), 1318–1338. https://doi.org/10.1101/gad.219626.113

Waddington, C. H. (2012). The epigenotype. 1942. *Int J Epidemiol*, *41*(1), 10–13. https://doi.org/10.1093/ije/dyr184

Wakimoto, B. T. (1998). Beyond the nucleosome: epigenetic aspects of position-effect variegation in Drosophila. *Cell*, *93*(3), 321–324. https://doi.org/10.1016/s0092-8674(00)81159-9

Wallrath, L. L., & Elgin, S. C. (1995). Position effect variegation in Drosophila is associated with an altered chromatin structure. *Genes Dev*, *9*(10), 1263–1277. https://doi.org/10.1101/gad.9.10.1263

Weintraub, H. (1984). Histone-H1-dependent chromatin superstructures and the suppression of gene activity. *Cell*, *38*(1), 17–27. https://doi.org/10.1016/0092-8674(84)90522-1

Weintraub, H., & Groudine, M. (1976). Chromosomal subunits in active genes have an altered conformation. *Science*, *193*(4256), 848–856. https://doi.org/10.1126/science.948749

Welch, J. E., Zimmerman, L. J., Joseph, D. R., & O'Rand, M. G. (1990). Characterization of a sperm-specific nuclear autoantigenic protein. I. Complete sequence and homology with the Xenopus protein, N1/N2. *Biol Reprod*, *43*(4), 559–568. https://doi.org/10.1095/biolreprod43.4.559

Wenger, A., Biran, A., Alcaraz, N., Redo-Riveiro, A., Sell, A. C., Krautz, R., Flury, V., Reveron-Gomez, N., Solis-Mezarino, V., Volker-Albert, M., Imhof, A., Andersson, R., Brickman, J. M., & Groth, A. (2023). Symmetric inheritance of parental histones governs epigenome maintenance and embryonic stem cell identity. *Nat Genet*, *55*(9), 1567–1578. https://doi.org/10.1038/s41588-023-01476-x

Wiles, E. T., McNaught, K. J., Kaur, G., Selker, J. M. L., Ormsby, T., Aravind, L., & Selker, E. U. (2020). Evolutionarily ancient BAH-PHD protein mediates Polycomb silencing. *Proc Natl Acad Sci U S A*, *117*(21), 11614–11623. https://doi.org/10.1073/pnas.1918776117

Wiles, E. T., Mumford, C. C., McNaught, K. J., Tanizawa, H., & Selker, E. U. (2022). The ACF chromatin-remodeling complex is essential for Polycomb repression. *Elife*, *11*. https://doi.org/10.7554/eLife.77595

Woodcock, C. L., & Ghosh, R. P. (2010). Chromatin higher-order structure and dynamics. *Cold Spring Harb Perspect Biol*, *2*(5), a000596. https://doi.org/10.1101/cshperspect.a000596

Xiao, J., Jin, R., Yu, X., Shen, M., Wagner, J. D., Pai, A., Song, C., Zhuang, M., Klasfeld, S., He, C., Santos, A. M., Helliwell, C., Pruneda-Paz, J. L., Kay, S. A., Lin, X., Cui, S., Garcia, M. F., Clarenz, O., Goodrich, J.,…Wagner, D. (2017). Cis and trans determinants of epigenetic silencing by Polycomb repressive complex 2 in Arabidopsis. Nat Genet, 49(10), 1546–1552. https://doi.org/10.1038/ng.3937

Ye, X., Franco, A. A., Santos, H., Nelson, D. M., Kaufman, P. D., & Adams, P. D. (2003). Defective S phase chromatin assembly causes DNA damage, activation of the S phase checkpoint, and S phase arrest. *Mol Cell*, *11*(2), 341–351. https://doi.org/10.1016/s1097-2765(03)00037-6

Yee, W. B., Delaney, P. M., Vanderzalm, P. J., Ramachandran, S., & Fehon, R. G. (2019). The CAF-1 complex couples Hippo pathway target gene expression and DNA replication. *Mol Biol Cell*, *30*(23), 2929–2942. https://doi.org/10.1091/mbc.E19-07-0387

Yu, C., Gan, H., Serra-Cardona, A., Zhang, L., Gan, S., Sharma, S., Johansson, E., Chabes, A., Xu, R. M., & Zhang, Z. (2018). A mechanism for preventing asymmetric histone segregation onto replicating DNA strands. *Science*, *361*(6409), 1386–1389. https://doi.org/10.1126/science.aat8849

Yuan, L., Song, X., Zhang, L., Yu, Y., Liang, Z., Lei, Y., Ruan, J., Tan, B., Liu, J., & Li, C. (2021). The transcriptional repressors VAL1 and VAL2 recruit PRC2 for genome-wide Polycomb silencing in Arabidopsis. *Nucleic Acids Res*, *49*(1), 98–113. https://doi.org/10.1093/nar/gkaa1129

Zhang, H., Han, J., Kang, B., Burgess, R., & Zhang, Z. (2012). Human histone acetyltransferase 1 protein preferentially acetylates H4 histone molecules in H3.1-H4 over H3.3-H4. *J Biol Chem*, *287*(9), 6573–6581. https://doi.org/10.1074/jbc.M111.312637

Zhao, J., Sun, B. K., Erwin, J. A., Song, J. J., & Lee, J. T. (2008). Polycomb proteins targeted by a short repeat RNA to the mouse X chromosome. *Science*, *322*(5902), 750–756. https://doi.org/10.1126/science.1163045

Zhen, C. Y., Tatavosian, R., Huynh, T. N., Duc, H. N., Das, R., Kokotovic, M., Grimm, J. B., Lavis, L. D., Lee, J., Mejia, F. J., Li, Y., Yao, T., & Ren, X. (2016). Live-cell single-molecule tracking reveals co-recognition of H3K27me3 and DNA targets polycomb Cbx7-PRC1 to chromatin. *Elife*, *5*. https://doi.org/10.7554/eLife.17667

Zhou, Y., Wang, Y., Krause, K., Yang, T., Dongus, J. A., Zhang, Y., & Turck, F. (2018). Telobox motifs recruit CLF/SWN-PRC2 for H3K27me3 deposition via TRB factors in Arabidopsis. Nat Genet, 50(5), 638–644. https://doi.org/10.1038/s41588-018-0109-9

Zunder, R. M., Antczak, A. J., Berger, J. M., & Rine, J. (2012). Two surfaces on the histone chaperone Rtt106 mediate histone binding, replication, and silencing. *Proc Natl Acad Sci U S A*, *109*(3), E144–153. https://doi.org/10.1073/pnas.1119095109

Figures

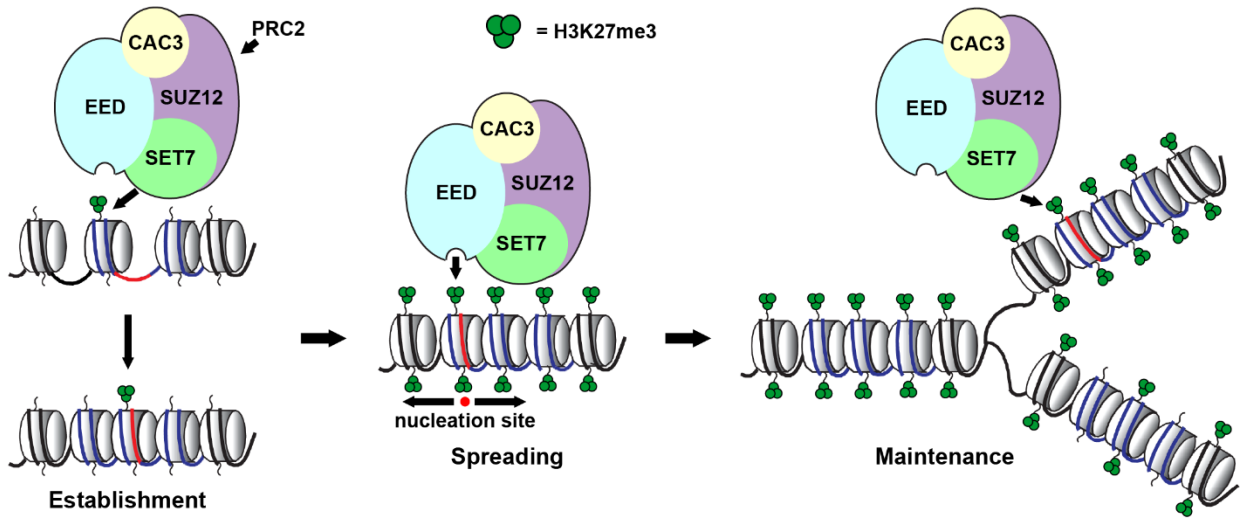

Figure 1.1: Model of the PRC2 repression pathway

PRC2 establishes H3K27me3 through recruitment to target loci. The complex then recognizes existing H3K27me3 to spread and maintain complete facultative heterochromatin domains.

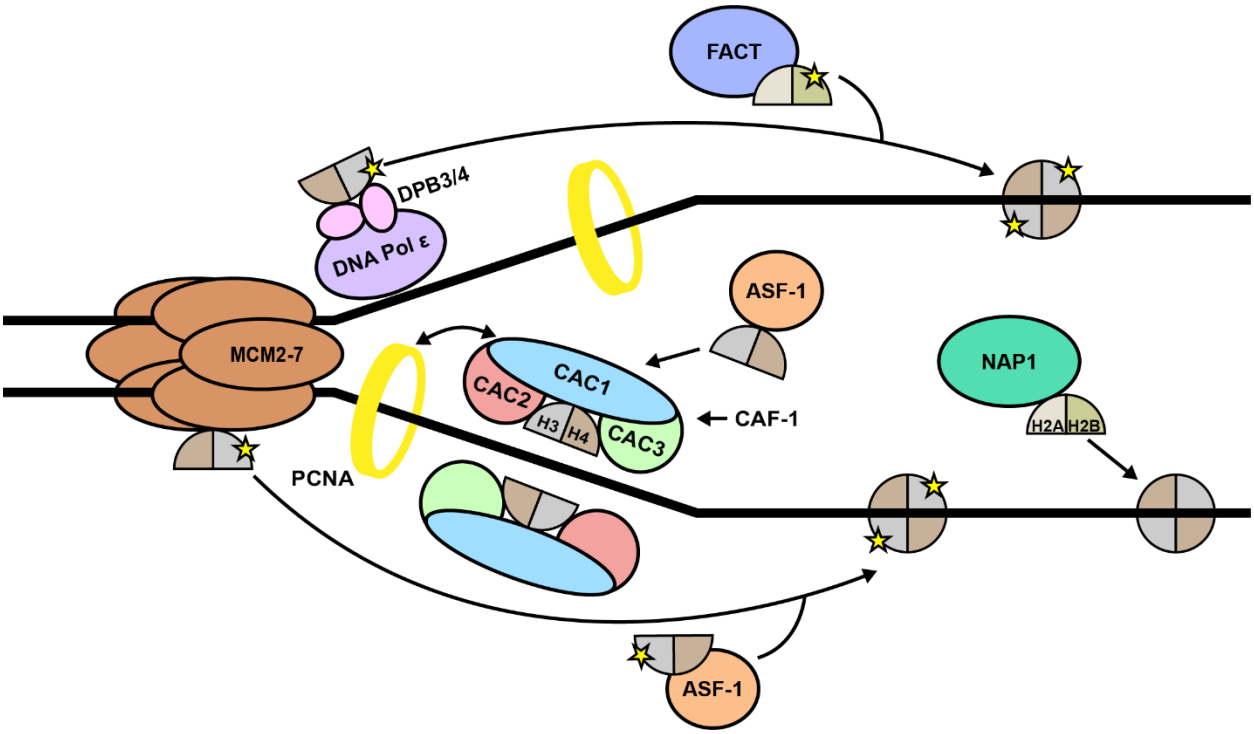

Figure 1.2: Model of CAF-1's activity at the replication fork

CAF-1 is recruited to DNA through its interaction with PCNA. Here 2 CAF-1 complexes await H3/H4 dimers from ASF-1 to form and deposit a H3/H4 tetramer onto DNA. Finally chaperones such as NAP1 add H2A/H2B to complete a newly synthesized histone octamer. This process fills in gaps left behind after histone recycling.

CHAPTER TWO

DEVELOPING AN INDUCIBLE POLYCOMB SYSTEM TO ASSAY *DE-NOVO* ESTABLISHMENT AND SPREADING OF FACULTATIVE HETEROCHROMATIN IN *NEUROSPORA CRASSA*[1]

[1] Torres, E.V., Steyer, J., Kamei M., Yap, R., and Lewis, Z.A., 2025, Developing an Inducible Polycomb System to Assay *de-novo* Establishment and Spreading of Facultative Heterochromatin in *Neurospora crassa*
To be submitted to a peer-reviewed journal

Abstract

Epigenetic regulation of gene expression during organismal development is a critical biological process that is conserved across eukaryotes. Post-translational modifications (PTMs) that repress transcription are deposited across the genome and faithfully inherited through mitotic divisions. Polycomb group (PcG) Proteins are a highly conserved family of proteins responsible for catalyzing Histone H3 lysine 27 tri-methylation (H3K27me3), a repressive histone modification that marks facultative heterochromatin. Here, we describe the development of a system harboring an inducible Polycomb repressive complex 2 (PRC2) in the model fungus *Neurospora crassa* (*N. crassa*). We placed the gene that encodes the SUZ-12 subunit of the PRC2 complex (*suz-12)* under control of the quinate dehydratase (*qa-2*) promoter to generate a *qaP-suz-12* construct. Cells lacking SUZ-12 are defective for catalytic activity of PRC2, resulting in H3K27me3 depletion. Upon introduction of quinic acid to growth medium, *qaP-suz-12* expression was induced, and H3K27me3 was re-established *de-novo* across the genome. Kinetics of H3K27me3 were variable across native loci, and we observed the emergence ectopic peaks genome-wide that were associated with downregulated transcription. Furthermore, we identified a *cis*-acting element capable of recruiting PRC2 when ectopically inserted at an euchromatic locus. This system provides a tool to uncover the molecular mechanisms that underly facultative heterochromatin formation in *N. crassa*, and determine the factors implicated in establishment and spreading of H3K27me3.

Introduction

Throughout organismal development, eukaryotes must be able to acutely regulate their gene expression (Allis & Jenuwein, 2016; Reik, 2007). This is primarily achieved via epigenetic

mechanisms that conditionally activate or repress genes in response to various biological stimuli such as cellular differentiation and environmental stress (Allis & Jenuwein, 2016; Bannister & Kouzarides, 2011; Bird, 2007; Strahl & Allis, 2000; Wilkinson et al., 2023). Post-translational modification (PTM) of histone proteins is one such mechanism that plays a significant role in this process (Bannister & Kouzarides, 2011; Kouzarides, 2007). These modifications serve as scaffolds for reader proteins that help reshape chromatin architecture and modulate transcriptional activity (Bannister et al., 2001; Musselman et al., 2012; Tang et al., 2021; Taverna et al., 2007; Wiles et al., 2020). Variation in the PTM landscape across the eukaryotic genome partitions chromatin into two distinct groups: euchromatin and heterochromatin (Allshire & Madhani, 2018; Bickmore & van Steensel, 2013; Bird, 2007; Saksouk et al., 2015; Woodcock & Ghosh, 2010). Euchromatin is relatively accessible and available to transcription factor binding and gene activation, whereas heterochromatin is more compact and limits access of regulatory proteins to DNA (Weintraub & Groudine, 1976; Woodcock & Ghosh, 2010). Heterochromatin can be further characterized into two groups, constitutive and facultative heterochromatin, which are marked by the repressive PTMs Histone H3 Lysine 9 tri-methylation (H3K9me3) and Histone H3 Lysine 27 tri-methylation (H3K27me3) (Kirmizis et al., 2004; Margueron & Reinberg, 2011; Nicetto & Zaret, 2019; Saksouk et al., 2015). While constitutive heterochromatin is typically gene poor and remains inaccessible throughout the cell cycle, accessibility of facultative heterochromatin can be altered in response to developmental or environmental cues (Allshire & Madhani, 2018; Blackledge & Klose, 2021; Nicetto & Zaret, 2019; Trojer & Reinberg, 2007). This is achieved through removal of H3K27me3, which allows genes located within facultative heterochromatin regions to be derepressed (Agger et al., 2007; Lavarone et al., 2019; Lee et al., 2007).

H3K27me3 is catalyzed by Polycomb Repressive Complex 2 (PRC2), a Polycomb Group (PcG) methyltransferase protein that is well conserved across eukaryotes (Di Croce & Helin, 2013; Margueron & Reinberg, 2011; Sharaf et al., 2022). PcG proteins were first characterized in *Drosophila melanogaster*, where their mutation results in various homeotic transformations (Kassis et al., 2017; Lewis, 1978; Schneuwly et al., 1987). PRC2 establishes H3K27me3 and spreads the PTM to build a complete, H3K27me3-marked facultative heterochromatin domain (Laprell et al., 2017; Laugesen et al., 2019; Oksuz et al., 2018). The complex can then maintain these domains through cellular divisions by recognizing existing H3K27me3 on parental histones post-DNA replication and re-establishing the mark on newly incorporated histones (Jadhav et al., 2020; Margueron et al., 2009; Ueda et al., 2016). Proper PcG function is crucial for numerous eukaryotic developmental processes, including vernalization and X chromosome inactivation in plants and mammals respectively (Bastow et al., 2004; Calonje et al., 2008; Plath et al., 2003; Zhao et al., 2008). Misregulation of PRC2 has also been implicated in human diseases such as Huntington's disease and various cancers (Blackledge & Klose, 2021; Kim & Roberts, 2016; Piunti & Shilatifard, 2021; Seong et al., 2010). In fungi PRC2 function has been linked to processes such as secondary metabolite production, effector gene expression, and sexual development (Connolly et al., 2013; Deaven et al., 2025; Ridenour et al., 2020). *N. crassa* possesses a minimal Polycomb repressive system, consisting of a core Polycomb Repressive Complex 2 (PRC2) and devoid of PRC1 homologs, making it an ideal system to study PRC2 function directly (Aramayo & Selker, 2013; Jamieson et al., 2013; Ridenour et al., 2020). Previous studies have shown that mutation of the genes encoding any of the three core *N. crassa* PRC2 subunits, EED, SET-7 (homolog of mammalian EZH2), or SUZ-12, results in complete depletion of H3K27me3 across the genome, leading to derepression of H3K27me3-marked genes

(Jamieson et al., 2013; Lewis, 2017; Ridenour et al., 2020). Furthermore, mutation of the CAC-3 (homolog of mammalian RbAp48/46) or PAS PRC2 accessory subunits results in a region-specific loss of H3K27me3 from sub-telomeric domains (Courtney et al., 2020; Jamieson et al., 2013; Klocko et al., 2016; McNaught et al., 2020). Furthermore, proteins such as the conserved H3K27me3 reader EPR-1 are known to be important for maintenance of gene repression within facultative heterochromatin (Tang et al., 2021; Wiles et al., 2020). Despite PRC2's importance in maintaining a normal heterochromatin environment, our understanding of how its activity is regulated on a molecular level remains incomplete.

In *Drosophila*, PRC2 can be recruited to target genes by a class of *cis*-regulatory elements called Polycomb Response Elements (PREs), which contain DNA motifs and repeat sequences that PcG proteins are able to recognize and bind (Kassis & Brown, 2013; Kassis et al., 2017; Laprell et al., 2017; Okulski et al., 2011). This recruitment can be influenced by the presence of other histone modifications or transcription factors at these loci, which can vary based on cell type or stage of development (Kasinath et al., 2021; Lavarone et al., 2019; Pasini et al., 2010; Schmitges et al., 2011). Evidence of PREs in mammals is limited, and PRC2 has been shown to preferentially occupy promoters and enhancers containing CpG Islands (CGIs) (Li et al., 2017; Mendenhall et al., 2010). Conversely, research in *Arabidopsis thaliana* has revealed the presence of *cis*-acting elements capable of recruiting PRC2 (Deng et al., 2013; Godwin & Farrona, 2022; Xiao et al., 2017; Zhou et al., 2018). Furthermore, long non-coding RNAs (lncRNAs) have been shown to directly recruit PRC2 to specific target regions in both plants and mammals (Kim & Sung, 2017; Plath et al., 2003; Zhao et al., 2008). Examples include *COOLAIR*, which regulates the expression of *FLOWERING LOCUS C* in *A. thaliana*, and *XIST*, which has been shown to recruit PRC2 to the inactive X chromosome in mammals (Kim & Sung,

2017; Nielsen et al., 2024; Sarma et al., 2014). Conversely, evidence of "PRE-like" sequences in fungi remains limited (Ferraro & Lewis, 2018; Lewis, 2017). Previous work in *N. crassa* has shown that insertion of a tandem telomere repeat array at the euchromatic *csr-1* locus results in ectopic nucleation and spreading of a H3K27me3 (Jamieson et al., 2018). Despite these findings, our general understanding of how PRC2 is recruited in fungi remains poorly understood.

In this study, we aimed to assay PRC2 recruitment and the kinetics of facultative heterochromatin formation in *N. crassa* through a *de-novo* histone methylation assay. We accomplished this by depleting H3K27me3 via knockout of the *suz-12* gene, then re-introducing the gene under control of the promoter for the quinate dehydratase (*qa-2*) gene, which is only activated in the presence of quinic acid. By changing media growth conditions, we show that we can tightly control PRC2 activity and directly assay H3K27me3 recovery in this system. We observed an incomplete recovery of H3K27me3 at native loci post-induction, accompanied by establishment at ectopic sites across the genome. We show that this rearrangement is associated with transcriptional changes caused by a switch to quinic acid containing media. Furthermore, we identify the existence of a *cis*-regulatory element that can ectopically recruit PRC2 when H3K27me3 maintenance is perturbed. Finally, we compare the H3K27me3 profile of our time course samples to those of previously studied mutants with H3K27me3 defects, allowing us to contextualize their role in establishment, spreading, and maintenance of facultative heterochromatin. Collectively, our data demonstrates the power of the *qaP-suz-12* system to uncover the mechanisms required for proper establishment and maintenance of facultative heterochromatin in *N. crassa*. Future experiments utilizing *qaP-suz-12* may provide insights into how PRC2 activity is regulated in other eukaryotes.

Results

Induction of qaP-suz-12 results in de-novo establishment and spread of H3K27me3

It is well known that PRC2 can faithfully maintain H3K27me3 domains after they are established, yet our understanding of how H3K27me3 is established *de-novo* remains incomplete (Alabert et al., 2020; Blackledge & Klose, 2021; Jadhav et al., 2020; Laugesen et al., 2019). We aimed to learn what molecular factors contribute to H3K27me3 establishment in *N. crassa* through development of an inducible PRC2 construct, *qaP-suz-12*. The *qaP-suz-12* strain was generated by transforming a copy of the *suz-12* gene tethered to a *qa-2* promoter into a *Δsuz-12/his-3(V661D)* double mutant strain, which complemented both mutations (Fig. 2.1A). Expression of *qaP-suz-12* remains off in normal growth conditions and is quickly activated upon introduction of quinic acid to the growth medium, producing a functional SUZ-12 (Fig. 2.1B). Concordantly, H3K27me3 is depleted in the *qaP-suz-12* background due to absence of the native *suz-12* gene, which renders the PRC2 complex inactive. Upon *qaP-suz-12* induction, SUZ-12 is produced and the PRC2 complex is reactivated, resulting in progressive recovery of H3K27me3 genome-wide (Fig. 2.1C-E). H3K27me3 was quickly recovered at the telomeres, consistent with the known recruitment activity of telomere repeats (Fig. 2.1C & D). Interestingly, time points collected before induction (0 hr) displayed H3K27me3 at telomere ends, suggesting leaky expression of the *qaP-suz-12* construct occurs in the absence of quinic acid (Fig. 2.1 D). In later timepoints, H3K27me3 enrichment is recovered at internal sites hundreds of kb away from chromosome ends, suggesting that PRC2 can re-establish the mark at normally methylated loci (Fig. 2.1D). However, analysis of all loci enriched for H3K27me3 in WT revealed that 143 peaks (encompassing ~14% of normally H3K27me3-marked DNA) were not enriched for H3K27me3, suggesting that recovery of H3K27me3 is incomplete by 24 hours post-induction (Fig. 2.1E &

1F). We hypothesized that 24 hours may not be a long enough growth period to observe complete re-establishment. Thus, we performed a 96-hour time course, which revealed a further, yet still incomplete rescue of H3K27me3 at native loci (Fig. S2.1). We categorized normally H3K27me3-marked loci into 3 groups based on their H3K27me3 enrichment profile during the *qaP-suz-12* time course: "rapid recovery" if they displayed significant enrichment by 4 hours post induction, "delayed recovery" if they displayed significant enrichment after 8 hours, and "unrecovered" if they did not display significant enrichment by 24 hours (Fig. 2.1C-D). Collectively, these results demonstrate the ability to precisely control the expression of SUZ-12 and subsequent PRC2 activity using the *qaP-suz-12* construct.

Gene repression is partially restored upon qaP-suz-12 induction

It is known that mutation of the PRC2 complex results in derepression of genes within facultative heterochromatin regions. Considering this, we asked if *de-novo* establishment of H3K27me3 was accompanied by a restoration of gene repression. Indeed, plotting expression levels of 528 H3K27me3-repressed genes revealed a significant increase of gene expression in *qaP-suz-12* that was rescued by 24 hours post-induction (Fig. 2.2A). 42 of the 45 H3K27me3-marked genes upregulated in the *qaP-suz-12* 0-hour timepoint are also upregulated in *Δsuz-12* suggesting PRC2 inhibition is responsible for changes in gene expression (Fig. S2.2A). Despite this, rescue of gene repression was incomplete, as the average expression level of H3K27me3-repressed genes remained significantly higher compared to 0-hour WT sample. Additionally, plotting relative expression levels for 386 differentially expressed, H3K27me3-marked genes revealed clusters of genes that remained expressed by 24 hours post-induction (Fig. 2.2B). Furthermore, 43 of the 70 upregulated H3K27me3-marked genes fell within late or unrecovered

H3K27me3 regions, which may explain the inability of PRC2 to re-establish H3K27me3 at these loci by 24 hours post-induction (Fig. 2.2C, S2.4A).

Indeed, genes within regions of delayed or unrecovered H3K27me3 displayed higher average expression levels in the 24-hour *qaP-suz-12* timepoint compared to either WT timepoint, whereas rapidly recovered genes did not (Fig. S2.2B). This suggests that maintained gene expression may antagonize PRC2 activity during the *qaP-suz-12* time course. Interestingly, 38 H3K27me3-marked genes upregulated in *qaP-suz-12* post-induction were not upregulated in the 0-hour timepoint, and 23 of these were also upregulated in WT strains grown in quinic acid (Fig. 2.2D). This suggests that quinic acid growth conditions may be altering gene expression patterns. Indeed, 34 H3K27me3-marked genes and 726 genes in total were upregulated in both WT and *qaP-suz-12* strains 24 hours post-induction (Fig. 2.2D & E). Collectively, these results suggest that induction of the *qaP-suz-12* construct results in a partial rescue of PRC2-mediated gene repression.

H3K27me3 is established at ectopic loci post-qaP-suz-12 induction

Our western blot data suggested that the SUZ-12 produced by the *qaP-suz-12* construct was abundant at levels comparable with the native protein (Fig. 2.1B). Despite this, we observed an incomplete rescue of H3K27me3, leading us to ask if PRC2 exhibited "off-target" activity at non-H3K27me3-marked regions when establishing H3K27me3 *de-novo* (Fig. 2.1C-F, Fig. S2.1A). Analysis of time course samples revealed the emergence of 155 ectopic peaks in *qaP-suz-12* by 24 hours post-induction (Fig. 2.3A). These peaks encompassed approximately 9% of methylated sites in the 24-hour *qaP-suz-12* timepoint (Fig. 2.3B, S2.5A). Only 8 of these peaks were significantly enriched in the WT 24-hour time point, suggesting that ectopic methylation

patterns are largely a result of *de-novo* H3K27me3 establishment. This observation motivated us to ask what factors may contribute to the altered pattern of methylation observed in this assay.

It is known that PRC2 is recruited to maintain gene repression in a cell type-specific context. We wondered if the adjusted growth conditions used may result in repression of non-H3K27me3-marked genes, thereby facilitating PRC2 recruitment during the *qaP-suz-12* time course. Analysis of 164 genes that fall within ectopic H3K27me3 peaks revealed a significant decrease in their average expression level in both WT and *qaP-suz-12* strains 24 hours post-induction relative to an uninduced strains (Fig. 2.3C). Furthermore, plotting relative expression levels of 161 differentially expressed, ectopically methylated genes revealed a large cluster that exhibited reduced expression post-induction in both WT and *qaP-suz-12* strains (Fig. 2.3D). This suggests that repression of these genes is independent of PRC2 activity, and that the complex may be recruited to these genes *de-novo*.

Indeed, differential expression analysis of 890 genes enriched for H3K27me3 across all time course conditions revealed that 63 genes were downregulated in *qaP-suz-12* 24 hours post-induction relative to an uninduced WT strain, including 28 of the 165 genes that fall within ectopic H3K27me3 peaks (Fig. 2.3E). In total, 26 H3K27me3-marked genes and 576 genes genome-wide were downregulated in both *qaP-suz-12* and WT 24 hours post-induction, further suggesting that quinic acid growth conditions result in widespread transcriptional changes (Fig. 2.3E, S2.5B). Collectively, these data suggest that H3K27me3 enrichment patterns are associated with altered gene expression caused by the growth conditions used in the *qaP-suz-12* time course, rather than re-activation of PRC2. Furthermore, the lack of ectopic methylation in a WT strain grown under identical conditions suggests that maintenance of native H3K27me3 may prevent a shift of the PTM to ectopic loci.

Putative nucleation sites emerge hours post-qaP-suz-12 induction

One of the primary motivations for developing an inducible Polycomb system was to determine the factors necessary for PRC2 recruitment. Specifically, we were interested to know if *N. crassa* possesses "PRE-like" DNA sequences that directly recruit PRC2, or if H3K27me3 establishment is largely dependent on chromatin context. To this end, we decided to more closely analyze the loci at which H3K27me3 was recovered early in the time course. We observed a robust recovery of H3K27me3 at subtelomeric sites 4 hours post-induction, an expected result due to the known recruitment activity of telomere repeats in *N. crassa* (Fig. 2.1C & D, 2.4A) (Jamieson et al., 2018). This methylation accounted for approximately 75% of all H3K27me3-marked loci in this timepoint (Fig. S2.5A). In addition, we observed the early emergence of multiple peaks at internal sites, suggesting that PRC2 may be directly recruited to these loci (Fig. 2.4B, S2.6A). We identified five of these sites and designated them as putative "nucleation" sites for downstream analysis.

We next wanted to determine if the DNA sequences at these putative nucleation sites are sufficient to recruit PRC2. We adapted the approach previously used in (Selker paper) and ectopically cloned 1-2 kb DNA fragments flanking peak summits for each nucleation site into the euchromatic *csr-1* locus (Fig. 2.4C). Surprisingly, ChIP-seq analysis revealed that none of the ectopically inserted putative nucleation sites were sufficient to induce a H3K27me3 domain at *csr-1* (Fig. S2.4B). We hypothesized that recruitment of PRC2 to native loci may sequester the complex, preventing establishment of an ectopic H3K27me3 domain. This hypothesis is supported by the observation that H3K27me3 established *de-novo* in *qaP-suz-12* exhibits a unique pattern compared to a WT strain cultured under identical conditions (Fig. 2.3A & B). We performed ChIP-seq on nucleation site insertion strains in an *Δepr-1* background and observed

the emergence of a novel H3K27me3 domain at *csr-1* for a putative nucleation site on the right arm of LGIII (Fig. 2.4D). The pattern of enrichment closely matched what was observed when a telomere repeat array was inserted at *csr-1* suggesting that these loci are particularly conducive to PRC2 activity (Fig. 2.4D). Collectively these data support the existence of *cis*-acting elements capable of directly recruiting PRC2 in *N. crassa*.

qaP-suz-12 time course delineates the roles of chromatin regulatory proteins in PRC2 activity

Extensive research using the *N. crassa* model system has revealed the importance of numerous chromatin regulatory proteins in establishing and maintaining a proper facultative heterochromatin environment (Basenko et al., 2015; Bicocca et al., 2018; Courtney et al., 2020; Ebot-Ojong et al., 2025; Jamieson et al., 2013; Jamieson et al., 2016; Kamei et al., 2021; Mumford et al., 2024; Wiles et al., 2020). However, it has remained challenging to determine the exact mechanisms by which these factors contribute to PRC2 activity. We compared the results of our *qaP-suz-12* time course to ChIP-seq data from other chromatin-related protein deficient mutants to further contextualize their defects in H3K27me2/3 occupancy. We first looked at sites of early recruitment, which revealed that mutants such as *Δisw*, *ΔhH2Az*, and *ash-1(Y888F)* exhibit fairly normal patterns of H3K27me2/3, displaying a profile similar to that of a 4-hour *qaP-suz-12* time point (Fig. 2.5A & B, S2.7A). Even an *Δhpo* mutant, in which most H3K27me2/3 is redirected to constitutive heterochromatin, exhibited a subtle enrichment at both sub-telomeric and putative nucleation sites (Fig. 2.5A). However, when looking at regions that experience late or no recovery during the *qaP-suz-12* time course, *ΔhH2Az* and *Δhpo* exhibited a nearly full depletion, while the defect in *Δisw* was partial (Fig. 2.5A & B, S2.7A). H3K27me2/3 enrichment in *ash-1(Y888F)* at these loci was more robust, suggesting that ASH-1 catalytic

activity is less critical for H3K27me2/3 at these sites (Fig. 2.5A & B, S2.7A). These data suggest that these mutants are more involved with the spreading and maintenance of H3K27me2/3 at native loci, while establishment remains relatively unaffected.

We also looked at enrichment in a *Δcac-3* mutant, which has previously been shown to display depletion of H3K27me2/3 at sub-telomeric regions. Indeed, this mutant exhibited a loss of H3K27me2/3 at a majority of loci that are recovered early in the *qaP-suz-12* time course (Fig. 2.5A & B, S2.5A & B). Interestingly, *Δcac-3* was the only mutant analyzed that exhibited depletion of H3K27me3 at putative nucleation sites (Fig. 2.5A). In contrast, regions that experience late or no recovery during the *qaP-suz-12* time course displayed robust H3K27me2/3 in *Δcac-3* (Fig. 2.5A & B, S2.5A & B). These results suggest that CAC-3 is more important for normal establishment of H3K27me2/3 at native loci, rather than spreading or maintenance. Interestingly, none of these mutants exhibited significant enrichment of H3K27me2/3 at loci with ectopic methylation in *qaP-suz-12*, suggesting that these sites gain methylation primarily due to time course growth conditions (Fig. 2.5B). Collectively, these comparisons shed greater light on the roles of chromatin-regulatory proteins in maintaining a proper facultative heterochromatin environment.

Discussion

The proper recruitment of PRC2 to establish and maintain facultative heterochromatin domains is crucial for transcriptional repression, organismal development, and safeguarding cellular identity, yet the mechanisms underlying this process remain incompletely understood. Previous work has identified a number *cis*- and *trans*-regulatory pathways that are able to direct PRC2 localization and activity by promoting or antagonizing PcG protein-histone interactions.

Here, we report the development of a system with which we can assay the kinetics of *de-novo* methylation by the PRC2 complex. By depleting H3K27me3 enrichment genome-wide through mutation of *suz-12*, we begin with a cellular context in which repression of genes within normal facultative heterochromatin domains cannot be maintained by PRC2. Through reintroduction of an inducible *qaP-suz-12* gene, we aimed to determine how PRC2 is recruited to establish and spread H3K27me3 across the genome.

Expression of qaP-suz-12 can induce facultative heterochromatin formation

We showed that we can successfully induce expression of the *qaP-suz-12* construct by using quinic acid as a carbon source, resulting in widespread recovery of H3K27me3 across the genome (Fig. 2.1A & B). H3K27me3 recovery at native loci was incomplete and PRC2 established methylation at ectopic sites during the 24-hour time course (Fig. 2.1C-F, Fig. 2.3A & B). We sought to understand what contributes to this altered pattern of methylation when H3K27me3 is established *de-novo*. Interestingly, comparing our data to H3K27me3 enrichment in complemented *Δeed* strain revealed that it did not exhibit the same ectopic methylation patterns, even though this strain must also recover H3K27me3 *de-novo* (Fig. S2.3C) (Courtney et al., 2020). This suggests that the ectopic H3K27me3 phenotype in *qaP-suz-12* is specific to the time course conditions, rather than a general phenotype that occurs upon PRC2 complementation. Furthermore, our western blot data suggests that expression of *qaP-suz-12* results in production of SUZ-12 at levels similar to WT (Fig. 2.1B). This likely rules out the possibility that *qaP-suz-12* is not expressed at high enough levels to achieve complete recovery. Collectively, our data supports a model in which PRC2 quickly establishes H3K27me3 *de-novo* and reaches an equilibrium at which H3K27me3 is maintained at both native and ectopic loci.

This would necessitate the presence of other factors that differentially recruit PRC2 in this time course compared to WT conditions.

Changes in gene expression influence de-novo methylation patterns

To maintain expression of the *qaP-suz-12* construct, strains needed to be cultured in low glucose containing media as described in (Campbell et al., 1994; Giles et al., 1985; Lamb et al., 2013). We observed that these adjusted growth conditions resulted in an altered transcriptional profile, and we asked if this may be influencing PRC2 recruitment (Fig. 2.2E, S2.5B). Indeed, we observed a rearrangement of H3K27me3 from normally H3K27me3-marked genes that remained upregulated in *qaP-suz-12* 24 hours post-induction, to downregulated genes outside of facultative heterochromatin regions (Fig. 2.3, Fig. S2.2). This result, in addition to the inconsistencies in H3K27me3 enrichment compared to a PRC2 complementation under normal conditions, provides strong evidence that quinic acid media promotes an altered pattern of PRC2 recruitment. While not all genes that are ectopically methylated are downregulated, it is possible the genes that are may serve as the initial recruitment sites for PRC2 *de-novo*, facilitating spread of H3K27me3 to neighboring genes.

In contrast with this hypothesis a WT strain grown under identical conditions does not experience a similar rearrangement of H3K27me3, despite sharing a similar gene expression profile (Fig. 2.3). We hypothesize that this is due to existing H3K27me3 at native loci maintaining the PTM at native loci. Conversely, completely stripping H3K27me3 prior to quinic acid induction may be what facilitates ectopic methylation, as there is no H3K27me3 present to recruit PRC2. Future experiments performed under quinic acid conditions in a mutant background that perturbs maintenance could be used to test this hypothesis. Future experiments

that aim to connect altered gene expression with off-target H3K27me3 could potentially provide insights into how altered PRC2 activity may contribute to specific disease states in humans. Collectively, these data suggest that the altered H3K27me3 pattern observed in *qaP-suz-12* is closely associated with altered gene expression, although further work is needed to determine the exact mechanism behind H3K27me3 rearrangement.

qaP-suz-12 time course reveals putative PRC2 recruitment sequences

We were interested in using our *qaP-suz-12* strain to identify sites at which H3K27me3 is quickly recovered to determine where PRC2 is recruited in *N. crassa*. While most H3K27me3 was located at subtelomeric regions, we were able to identify internal sites at which PRC2 is able to establish H3K27me3 as soon as 4 hours post induction (Fig. 2.4A & B, S2.6A). These results suggested that these internal sites are capable of directly recruiting PRC2, although inserting them into the *csr-1* locus did not result in ectopic H3K27me3 like what is observed for telomere repeats (Fig. S2.66B) (Jamieson et al., 2018). We hypothesized that telomere repeat arrays may represent a stronger recruitment motif, which allows for establishment of an ectopic H3K27me3 domain in an otherwise WT background. Considering this, we decided to perturb normal PRC2 activity in a strain harboring an ectopically inserted nucleation site.

We introduced an *Δepr-1* mutation into strains with nucleation sites at *csr-1* and observed that the site located on the right arm of LGIII was capable of inducing an ectopic H3K27me3 domain (Fig. 2.4D). *epr-1* is a reader of H3K27me3 that is conserved in many eukaryotes and has been shown to be important for H3K27me3-marked gene repression (Wiles et al., 2020). While deficiency of *epr-1* has mild effects on H3K27me3 enrichment, it has been shown to be important for formation of nuclear foci, suggesting that its deletion may be important for

maintaining specific chromatin interactions. This may also prevent PRC2 from being sequestered to native loci, which ultimately facilitates formation of the ectopic H3K27me3 domain. Further experimentation should look at the effect of *Δepr-1* on H3K27me3 in other mutants and growth conditions and employ the mutant for testing the recruitment activity of other putative nucleation sites. By the same logic, *Δepr-1* is a potential candidate to test the effect of quinic acid-containing media on H3K27me3 patterns.

Chromatin regulators are uniquely involved in establishment and maintenance of facultative heterochromatin

Prior Research in our lab and others has revealed that mutation of various chromatin regulators results in defective facultative heterochromatin formation in *N. crassa*, including histone variants, PTM writers and readers, and chromatin remodelers (Basenko et al., 2015; Bicocca et al., 2018; Courtney et al., 2020; Jamieson et al., 2016; Kamei et al., 2021; Wiles et al., 2020; Wiles et al., 2022). We compared the pattern of H3K27me3 in these mutants to regions of early, late, and unrecovered H3K27me3 during the *qaP-suz-12* time course, which revealed unique characteristics of each phenotype. Mutants such as *ΔhH2Az* and *Δisw* were defective for H3K27me3 at regions of later recovery, while mutants such as *Δcac-3* are unable to methylate early recovered regions (Fig. 2.5A & B). This analysis provides insights into how these proteins specifically contribute to the establishment and maintenance of facultative heterochromatin. Interestingly, every mutant except *Δcac-3* was able to efficiently methylate the putative nucleation sites identified on LGIII and LGVI. This, in addition to the inability of *Δcac-3* to methylate subtelomeric regions, suggests that the mutant may be defective for establishment of H3K27me3 at normal PRC2 target regions. It is possible that CAC-3 allows PRC2 to properly

bind to *cis*-regulatory elements that directly recruit PRC2. Future experimentation should focus on conducting *qaP-suz-12* time courses in strains with mutations of chromatin regulators, to see how their deficiency impacts *de-novo* facultative heterochromatin formation. We hypothesize that strains such as *Δisw* and *ΔhH2Az* may struggle to recover methylation outside of early recovered regions, while *Δcac-3* may struggle to methylate at most loci if it is truly required for DNA binding of PRC2.

In summary, development of an inducible PRC2 complex provides a tool to visualize H3K27me3 recovery and *de-novo* recruitment patterns in *N. crassa*. This system provides a tractable platform to dissect the role of various chromatin regulators in establishing and maintaining a proper facultative heterochromatin environment. Findings from these studies will improve our understanding of how PRC2 activity is regulated in fungi and may potentially hold relevance for Polycomb function across metazoans.

Materials and Methods

Media conditions

Strains for ChIP and RNA-seq experiments were grown overnight in Vogel's minimal media (VMM) containing 2.0% glucose as previously described (Davis & de Serres, 1970). Uninduced samples were harvested after overnight growth. To induce expression of *qaP-suz-12*, strains cultured overnight were transferred to VMM containing 0.1% glucose and 12.5 mM quinic acid, as previously described (Campbell et al., 1994; Giles et al., 1985; Lamb et al., 2013). Strains grown longer than 24 hours were reinduced in fresh quinic acid media every 24 hours.

Cloning and strain construction

Knockout (KO) strains were obtained from the FGSC KO collection (Dunlap et al., 2007). To generate the *qaP-suz-12* construct, A copy of the native *suz-12* gene was fused to the *qa-2* gene promoter and inserted into a plasmid containing DNA flanks homologous to the *his-3* gene locus via Gibson cloning. The construct was then linearized and transformed into the *his-3* locus of a *Δsuz-12/his-3-V661D* strain via homologous recombination. To generate the nucleation site strain for LGVI 1, a ~2.5 kb DNA fragment containing the sequence of the nucleation site was amplified by PCR and inserted into a plasmid containing DNA flanks homologous to the *csr-1* gene via Gibson cloning. This construct was linearized and transformed into the *csr-1* locus via homologous recombination. Fragments used to generate other sites were ordered from twist biosciences, amplified by PCR, and transformed into the *csr-1* locus via homologous recombination. All cloned fragment sequences can be found in Appendix 2.1. Nucleation site insertion strains were crossed to KO strains to generate double mutants. Crosses were performed on low-nitrogen synthetic cross (SC) media as previously described (Davis & de Serres, 1970). Spores were collected 14 days post-fertilization, germinated on SC plates, and picked to selective media slants. All strains were genotyped by PCR, western blotting, or growth on selective media.

Neurospora transformation

DNA transformations were performed as previously described in (Margolin et al., 1997). Transformants were picked to selective media slants and genotyped by PCR or western blotting.

Protein extraction & western blotting

Cultures were grown in a shaking incubator overnight (~18-22 hours) in liquid VMM + 2.0% glucose at 32 °C and 180 rpm, then transferred to liquid VMM + 0.1% glucose + 12.5 mM quinic acid for 4-24 hours at 32 °C and 180 rpm. Cultures were harvested and washed with 1x PBS, and protein was extracted by sonication on ice for 1 min. (60 sec. on, 60 sec. off; 30 µm Amplitude) in protein extraction buffer (50 mM HEPES pH 7.5, 150 mM NaCl, 1 mM EDTA, 0.02% IGEPAL, 1 mM PMSF, 1x Protease Inhibitor Cocktail; Cat #: HY-K0011). Cell lysates were centrifuged at 17,000 g (~13,300 rpm) at 4 °C, and the supernatant containing protein extract was mixed 3:1 with 4x Laemmli sample buffer, boiled at 95 °C for 3 minutes, and run on 7% SDS-PAGE gels at 185 V for ~45 minutes. Protein was transferred to 0.45 µm PVDF membranes (Sigma; Cat #: IPVH00010; activated using supplier recommendations) via wet transfer in 1x Towbin's Buffer with SDS (25 mM Tris, 192 mM glycine, 20% methanol, 0.01% SDS) for 1.5 hours at 100 V and 4 °C. Blots to assay SUZ-12 expression were incubated with a primary antibody targeted to 3x-FLAG (Sigma; Cat #:F1804-200UG) in 3% milk in 1x TBST overnight. Blots were then washed 3x with 1x TBST for 5 minutes each, then incubated with an anti-mouse secondary antibody (Thermo Fisher; Cat #: 31430) in 3% milk in 1x TBST for 30 minutes. Blots were then washed 3x with 1x TBST for 5 minutes each, then developed for 5 minutes using a west femto chemiluminescent substrate developer kit (Thermo Fisher, Cat #: 34096).

ChIP-seq & ChIP-qPCR

ChIP experiments were performed as previously described (Ferraro & Lewis, 2018), using antibodies recognizing present in Table S2.3. ChIP samples were analyzed by Illumina sequencing.

RNA Isolation

RNA extraction was performed as previously described (Zhou et al., 2018). Briefly, total RNA was extracted using TRIzol reagent (Thermo Fisher; Cat #:15596026) and then purified with 7.5 M LiCl. RNA purity was analyzed on agarose gels prior to library preparation.

Library preparation

ChIP Libraries were constructed as previously described (Courtney et al., 2020; Ferraro & Lewis, 2018). Size selection with magnetic beads was performed after the adapter ligation and PCR steps with Sera-Mag SpeedBeads (65152105050250) suspended in a solution of 20 mM PEG 8000, 1 mM NaCl, 10 mM Tris-HCl, 1 mM EDTA (Rohland & Reich, 2012). RNA Libraries were prepared using a NEBNext Ultra II Directional RNA Library Prep Kit according to manufacturer specifications (E7760S).

Bioinformatic analyses

Peaks were called for all ChIP-seq samples using MACS3 (v3.0.1). ChIP-seq enrichment was quantified using the csaw package in R (v1.42.0) and normalizing to input samples. H3K27me3 enrichment was calculated from 500 bp upstream to 300 bp downstream of the TSS. Genes were considered enriched for H3K27me3 if they exhibited > 1 log2FC over input, and

their gene bodies and promoters fell within MACS3 peak calls. Genes were considered differently enriched for H3K27me3 if they exhibited ± 1 log2FC enrichment compared to uninduced WT samples. Peak coverage was calculated by summing the number of bp within each respective category. RNA-seq data was analyzed using the DEseq package in R (v1.48.2). Genes were considered "repressed" if they exhibited < 10 TPM on average across WT samples. Genes were considered differentially expressed if they exhibited ± 1 log2FC (2-fold change) in expression compared to WT and an adjusted p-value of < 0.05.

Data availability

Prior to publication, sequencing data generated at the University of Georgia will be deposited to the National Center for Biotechnology Information's Gene Expression Omnibus database (https://www.ncbi.nlm.nih.gov/geo). A summary list of Sequence Read Archive (https://www.ncbi.nlm.nih.gov/sra) accession numbers and associated strain information for samples generated at the Joint Genome Institute and other previously published datasets analyzed in this study are included in Supplementary Table S2.4. All scripts used are publicly available on GitHub at https://github.com/eddietorres24/Research.

References

Agger, K., Cloos, P. A., Christensen, J., Pasini, D., Rose, S., Rappsilber, J., Issaeva, I., Canaani, E., Salcini, A. E., & Helin, K. (2007). UTX and JMJD3 are histone H3K27 demethylases involved in HOX gene regulation and development. *Nature*, *449*(7163), 731–734. https://doi.org/10.1038/nature06145

Alabert, C., Loos, C., Voelker-Albert, M., Graziano, S., Forne, I., Reveron-Gomez, N., Schuh, L., Hasenauer, J., Marr, C., Imhof, A., & Groth, A. (2020). Domain Model Explains Propagation Dynamics and Stability of Histone H3K27 and H3K36 Methylation Landscapes. *Cell Rep*, *30*(4), 1223–1234 e1228. https://doi.org/10.1016/j.celrep.2019.12.060

Allis, C. D., & Jenuwein, T. (2016). The molecular hallmarks of epigenetic control. *Nat Rev Genet*, *17*(8), 487–500. https://doi.org/10.1038/nrg.2016.59

Allshire, R. C., & Madhani, H. D. (2018). Ten principles of heterochromatin formation and function. *Nat Rev Mol Cell Biol*, *19*(4), 229–244. https://doi.org/10.1038/nrm.2017.119

Aramayo, R., & Selker, E. U. (2013). Neurospora crassa, a model system for epigenetics research. *Cold Spring Harb Perspect Biol*, *5*(10), a017921. https://doi.org/10.1101/cshperspect.a017921

Bannister, A. J., & Kouzarides, T. (2011). Regulation of chromatin by histone modifications. *Cell Res*, *21*(3), 381–395. https://doi.org/10.1038/cr.2011.22

Bannister, A. J., Zegerman, P., Partridge, J. F., Miska, E. A., Thomas, J. O., Allshire, R. C., & Kouzarides, T. (2001). Selective recognition of methylated lysine 9 on histone H3 by the HP1 chromo domain. *Nature*, *410*(6824), 120–124. https://doi.org/10.1038/35065138

Basenko, E. Y., Sasaki, T., Ji, L., Prybol, C. J., Burckhardt, R. M., Schmitz, R. J., & Lewis, Z. A. (2015). Genome-wide redistribution of H3K27me3 is linked to genotoxic stress and defective growth. *Proc Natl Acad Sci U S A*, *112*(46), E6339–6348. https://doi.org/10.1073/pnas.1511377112

Bastow, R., Mylne, J. S., Lister, C., Lippman, Z., Martienssen, R. A., & Dean, C. (2004). Vernalization requires epigenetic silencing of FLC by histone methylation. *Nature*, *427*(6970), 164–167. https://doi.org/10.1038/nature02269

Bickmore, W. A., & van Steensel, B. (2013). Genome architecture: domain organization of interphase chromosomes. *Cell*, *152*(6), 1270–1284. https://doi.org/10.1016/j.cell.2013.02.001

Bicocca, V. T., Ormsby, T., Adhvaryu, K. K., Honda, S., & Selker, E. U. (2018). ASH1-catalyzed H3K36 methylation drives gene repression and marks H3K27me2/3-competent chromatin. *Elife*, *7*. https://doi.org/10.7554/eLife.41497

Bird, A. (2007). Perceptions of epigenetics. *Nature*, *447*(7143), 396–398. https://doi.org/10.1038/nature05913

Blackledge, N. P., & Klose, R. J. (2021). The molecular principles of gene regulation by Polycomb repressive complexes. *Nat Rev Mol Cell Biol*, *22*(12), 815–833. https://doi.org/10.1038/s41580-021-00398-y

Calonje, M., Sanchez, R., Chen, L., & Sung, Z. R. (2008). EMBRYONIC FLOWER1 participates in polycomb group-mediated AG gene silencing in Arabidopsis. *Plant Cell*, *20*(2), 277–291. https://doi.org/10.1105/tpc.106.049957

Campbell, J. W., Enderlin, C. S., & Selitrennikoff, C. P. (1994). Vectors for expression and modification of cDNA sequences in Neurospora crassa. *Fungal Genetics Reports*, *41*(1), 20–21. https://doi.org/10.4148/1941-4765.1366

Connolly, L. R., Smith, K. M., & Freitag, M. (2013). The Fusarium graminearum histone H3 K27 methyltransferase KMT6 regulates development and expression of secondary metabolite gene clusters. *PLoS Genet*, *9*(10), e1003916. https://doi.org/10.1371/journal.pgen.1003916

Courtney, A. J., Kamei, M., Ferraro, A. R., Gai, K., He, Q., Honda, S., & Lewis, Z. A. (2020). Normal Patterns of Histone H3K27 Methylation Require the Histone Variant H2A.Z in Neurospora crassa. *Genetics*, *216*(1), 51–66. https://doi.org/10.1534/genetics.120.303442

Davis, R. H., & de Serres, F. J. (1970). [4] Genetic and microbiological research techniques for Neurospora crassa. In *Methods in Enzymology* (Vol. 17, pp. 79–143). Academic Press. https://doi.org/https://doi.org/10.1016/0076-6879(71)17168-6

Deaven, A. M., Ameri-Solanky, A. J., & Lewis, Z. A. (2025). Polycomb repressive complex 2 regulates sexual development in Neurospora crassa. *mBio*, e0150525. https://doi.org/10.1128/mbio.01505-25

Deng, W., Buzas, D. M., Ying, H., Robertson, M., Taylor, J., Peacock, W. J., Dennis, E. S., & Helliwell, C. (2013). Arabidopsis Polycomb Repressive Complex 2 binding sites contain putative GAGA factor binding motifs within coding regions of genes. *BMC Genomics*, *14*, 593. https://doi.org/10.1186/1471-2164-14-593

Di Croce, L., & Helin, K. (2013). Transcriptional regulation by Polycomb group proteins. *Nat Struct Mol Biol*, *20*(10), 1147–1155. https://doi.org/10.1038/nsmb.2669

Dunlap, J. C., Borkovich, K. A., Henn, M. R., Turner, G. E., Sachs, M. S., Glass, N. L., McCluskey, K., Plamann, M., Galagan, J. E., Birren, B. W., Weiss, R. L., Townsend, J. P., Loros, J. J., Nelson, M. A., Lambreghts, R., Colot, H. V., Park, G., Collopy, P., Ringelberg, C.,…Xu, J. (2007). Enabling a community to dissect an organism: overview of the Neurospora functional genomics project. *Adv Genet*, *57*, 49–96. https://doi.org/10.1016/S0065-2660(06)57002-6

Ebot-Ojong, F., Ferraro, A. R., Yap, R. E., Kaddar, F., Hull-Crew, C., Scadden, A. W., Deaven, A. M., Klocko, A. D., & Lewis, Z. A. (2025). HISTONE DEACETYLASE-1 is required for epigenome stability in Neurospora crassa. *Proc Natl Acad Sci U S A*, *122*(40), e2503876122. https://doi.org/10.1073/pnas.2503876122

Ferraro, A. R., & Lewis, Z. A. (2018). ChIP-Seq Analysis in Neurospora crassa. In R. P. de Vries, A. Tsang, & I. V. Grigoriev (Eds.), *Fungal Genomics: Methods and Protocols* (pp. 241–250). Springer New York. https://doi.org/10.1007/978-1-4939-7804-5_19

Giles, N. H., Case, M. E., Baum, J., Geever, R., Huiet, L., Patel, V., & Tyler, B. (1985). Gene organization and regulation in the qa (quinic acid) gene cluster of Neurospora crassa. *Microbiol Rev*, *49*(3), 338–358. https://doi.org/10.1128/mr.49.3.338-358.1985

Godwin, J., & Farrona, S. (2022). The Importance of Networking: Plant Polycomb Repressive Complex 2 and Its Interactors. *Epigenomes*, *6*(1). https://doi.org/10.3390/epigenomes6010008

Jadhav, U., Manieri, E., Nalapareddy, K., Madha, S., Chakrabarti, S., Wucherpfennig, K., Barefoot, M., & Shivdasani, R. A. (2020). Replicational Dilution of H3K27me3 in Mammalian Cells and the Role of Poised Promoters. *Mol Cell*, *78*(1), 141–151 e145. https://doi.org/10.1016/j.molcel.2020.01.017

Jamieson, K., McNaught, K. J., Ormsby, T., Leggett, N. A., Honda, S., & Selker, E. U. (2018). Telomere repeats induce domains of H3K27 methylation in Neurospora. *Elife*, *7*. https://doi.org/10.7554/eLife.31216

Jamieson, K., Rountree, M. R., Lewis, Z. A., Stajich, J. E., & Selker, E. U. (2013). Regional control of histone H3 lysine 27 methylation in Neurospora. *Proc Natl Acad Sci U S A*, *110*(15), 6027–6032. https://doi.org/10.1073/pnas.1303750110

Jamieson, K., Wiles, E. T., McNaught, K. J., Sidoli, S., Leggett, N., Shao, Y., Garcia, B. A., & Selker, E. U. (2016). Loss of HP1 causes depletion of H3K27me3 from facultative heterochromatin and gain of H3K27me2 at constitutive heterochromatin. *Genome Res*, *26*(1), 97–107. https://doi.org/10.1101/gr.194555.115

Kamei, M., Ameri, A. J., Ferraro, A. R., Bar-Peled, Y., Zhao, F., Ethridge, C. L., Lail, K., Amirebrahimi, M., Lipzen, A., Ng, V., Grigoriev, I. V., Schmitz, R. J., Liu, Y., & Lewis, Z. A. (2021). IMITATION SWITCH is required for normal chromatin structure and gene repression in PRC2 target domains. *Proc Natl Acad Sci U S A*, *118*(4). https://doi.org/10.1073/pnas.2010003118

Kasinath, V., Beck, C., Sauer, P., Poepsel, S., Kosmatka, J., Faini, M., Toso, D., Aebersold, R., & Nogales, E. (2021). JARID2 and AEBP2 regulate PRC2 in the presence of H2AK119ub1 and other histone modifications. *Science*, *371*(6527). https://doi.org/10.1126/science.abc3393

Kassis, J. A., & Brown, J. L. (2013). Polycomb group response elements in Drosophila and vertebrates. *Adv Genet*, *81*, 83–118. https://doi.org/10.1016/B978-0-12-407677-8.00003-8

Kassis, J. A., Kennison, J. A., & Tamkun, J. W. (2017). Polycomb and Trithorax Group Genes in Drosophila. *Genetics*, *206*(4), 1699–1725. https://doi.org/10.1534/genetics.115.185116

Kim, D. H., & Sung, S. (2017). Vernalization-Triggered Intragenic Chromatin Loop Formation by Long Noncoding RNAs. *Dev Cell*, *40*(3), 302–312 e304. https://doi.org/10.1016/j.devcel.2016.12.021

Kim, K. H., & Roberts, C. W. (2016). Targeting EZH2 in cancer. *Nat Med*, *22*(2), 128–134. https://doi.org/10.1038/nm.4036

Kirmizis, A., Bartley, S. M., Kuzmichev, A., Margueron, R., Reinberg, D., Green, R., & Farnham, P. J. (2004). Silencing of human polycomb target genes is associated with methylation of histone H3 Lys 27. *Genes Dev*, *18*(13), 1592–1605. https://doi.org/10.1101/gad.1200204

Klocko, A. D., Ormsby, T., Galazka, J. M., Leggett, N. A., Uesaka, M., Honda, S., Freitag, M., & Selker, E. U. (2016). Normal chromosome conformation depends on subtelomeric facultative heterochromatin in Neurospora crassa. *Proc Natl Acad Sci U S A*, *113*(52), 15048–15053. https://doi.org/10.1073/pnas.1615546113

Kouzarides, T. (2007). Chromatin modifications and their function. *Cell*, *128*(4), 693–705. https://doi.org/10.1016/j.cell.2007.02.005

Lamb, T. M., Vickery, J., & Bell-Pedersen, D. (2013). Regulation of gene expression in Neurospora crassa with a copper responsive promoter. *G3 (Bethesda)*, *3*(12), 2273–2280. https://doi.org/10.1534/g3.113.008821

Laprell, F., Finkl, K., & Muller, J. (2017). Propagation of Polycomb-repressed chromatin requires sequence-specific recruitment to DNA. *Science*, *356*(6333), 85–88. https://doi.org/10.1126/science.aai8266

Laugesen, A., Hojfeldt, J. W., & Helin, K. (2019). Molecular Mechanisms Directing PRC2 Recruitment and H3K27 Methylation. *Mol Cell*, *74*(1), 8–18. https://doi.org/10.1016/j.molcel.2019.03.011

Lavarone, E., Barbieri, C. M., & Pasini, D. (2019). Dissecting the role of H3K27 acetylation and methylation in PRC2 mediated control of cellular identity. *Nat Commun*, *10*(1), 1679. https://doi.org/10.1038/s41467-019-09624-w

Lee, M. G., Villa, R., Trojer, P., Norman, J., Yan, K. P., Reinberg, D., Di Croce, L., & Shiekhattar, R. (2007). Demethylation of H3K27 regulates polycomb recruitment and H2A ubiquitination. *Science*, *318*(5849), 447–450. https://doi.org/10.1126/science.1149042

Lewis, E. B. (1978). A gene complex controlling segmentation in Drosophila. *Nature*, *276*(5688), 565–570. https://doi.org/10.1038/276565a0

Lewis, Z. A. (2017). Polycomb Group Systems in Fungi: New Models for Understanding Polycomb Repressive Complex 2. *Trends Genet*, *33*(3), 220–231. https://doi.org/10.1016/j.tig.2017.01.006

Li, H., Liefke, R., Jiang, J., Kurland, J. V., Tian, W., Deng, P., Zhang, W., He, Q., Patel, D. J., Bulyk, M. L., Shi, Y., & Wang, Z. (2017). Polycomb-like proteins link the PRC2 complex to CpG islands. *Nature*, *549*(7671), 287–291. https://doi.org/10.1038/nature23881

Margolin, B. S., Freitag, M., & Selker, E. U. (1997). Improved plasmids for gene targeting at the his-3 locus of Neurospora crassa by electroporation. *Fungal Genetics Reports*, *44*(1), 34–36. https://doi.org/10.4148/1941-4765.1281

Margueron, R., Justin, N., Ohno, K., Sharpe, M. L., Son, J., Drury, W. J., 3rd, Voigt, P., Martin, S. R., Taylor, W. R., De Marco, V., Pirrotta, V., Reinberg, D., & Gamblin, S. J. (2009). Role of the polycomb protein EED in the propagation of repressive histone marks. *Nature*, *461*(7265), 762–767. https://doi.org/10.1038/nature08398

Margueron, R., & Reinberg, D. (2011). The Polycomb complex PRC2 and its mark in life. *Nature*, *469*(7330), 343–349. https://doi.org/10.1038/nature09784

McNaught, K. J., Wiles, E. T., & Selker, E. U. (2020). Identification of a PRC2 Accessory Subunit Required for Subtelomeric H3K27 Methylation in Neurospora crassa. *Mol Cell Biol*, *40*(11). https://doi.org/10.1128/MCB.00003-20

Mendenhall, E. M., Koche, R. P., Truong, T., Zhou, V. W., Issac, B., Chi, A. S., Ku, M., & Bernstein, B. E. (2010). GC-rich sequence elements recruit PRC2 in mammalian ES cells. *PLoS Genet*, *6*(12), e1001244. https://doi.org/10.1371/journal.pgen.1001244

Mumford, C. C., Tanizawa, H., Wiles, E. T., McNaught, K. J., Jamieson, K., Tsukamoto, K., & Selker, E. U. (2024). The RPD3L deacetylation complex is required for facultative heterochromatin repression in Neurospora crassa. *Proc Natl Acad Sci U S A*, *121*(32), e2404770121. https://doi.org/10.1073/pnas.2404770121

Musselman, C. A., Lalonde, M. E., Cote, J., & Kutateladze, T. G. (2012). Perceiving the epigenetic landscape through histone readers. *Nat Struct Mol Biol*, *19*(12), 1218–1227. https://doi.org/10.1038/nsmb.2436

Nicetto, D., & Zaret, K. S. (2019). Role of H3K9me3 heterochromatin in cell identity establishment and maintenance. *Curr Opin Genet Dev*, *55*, 1–10. https://doi.org/10.1016/j.gde.2019.04.013

Nielsen, M., Menon, G., Zhao, Y., Mateo-Bonmati, E., Wolff, P., Zhou, S., Howard, M., & Dean, C. (2024). COOLAIR and PRC2 function in parallel to silence FLC during vernalization. *Proc Natl Acad Sci U S A*, *121*(4), e2311474121. https://doi.org/10.1073/pnas.2311474121

Oksuz, O., Narendra, V., Lee, C. H., Descostes, N., LeRoy, G., Raviram, R., Blumenberg, L., Karch, K., Rocha, P. P., Garcia, B. A., Skok, J. A., & Reinberg, D. (2018). Capturing the Onset of PRC2-Mediated Repressive Domain Formation. *Mol Cell*, *70*(6), 1149–1162 e1145. https://doi.org/10.1016/j.molcel.2018.05.023

Okulski, H., Druck, B., Bhalerao, S., & Ringrose, L. (2011). Quantitative analysis of polycomb response elements (PREs) at identical genomic locations distinguishes contributions of PRE sequence and genomic environment. *Epigenetics Chromatin*, *4*, 4. https://doi.org/10.1186/1756-8935-4-4

Pasini, D., Malatesta, M., Jung, H. R., Walfridsson, J., Willer, A., Olsson, L., Skotte, J., Wutz, A., Porse, B., Jensen, O. N., & Helin, K. (2010). Characterization of an antagonistic switch between histone H3 lysine 27 methylation and acetylation in the transcriptional regulation of Polycomb group target genes. *Nucleic Acids Res*, *38*(15), 4958–4969. https://doi.org/10.1093/nar/gkq244

Piunti, A., & Shilatifard, A. (2021). The roles of Polycomb repressive complexes in mammalian development and cancer. *Nat Rev Mol Cell Biol*, *22*(5), 326–345. https://doi.org/10.1038/s41580-021-00341-1

Plath, K., Fang, J., Mlynarczyk-Evans, S. K., Cao, R., Worringer, K. A., Wang, H., de la Cruz, C. C., Otte, A. P., Panning, B., & Zhang, Y. (2003). Role of histone H3 lysine 27 methylation in X inactivation. *Science*, *300*(5616), 131–135. https://doi.org/10.1126/science.1084274

Reik, W. (2007). Stability and flexibility of epigenetic gene regulation in mammalian development. *Nature*, *447*(7143), 425–432. https://doi.org/10.1038/nature05918

Ridenour, J. B., Moller, M., & Freitag, M. (2020). Polycomb Repression without Bristles: Facultative Heterochromatin and Genome Stability in Fungi. *Genes (Basel)*, *11*(6). https://doi.org/10.3390/genes11060638

Rohland, N., & Reich, D. (2012). Cost-effective, high-throughput DNA sequencing libraries for multiplexed target capture. *Genome Res*, *22*(5), 939–946. https://doi.org/10.1101/gr.128124.111

Saksouk, N., Simboeck, E., & Dejardin, J. (2015). Constitutive heterochromatin formation and transcription in mammals. *Epigenetics Chromatin*, *8*, 3. https://doi.org/10.1186/1756-8935-8-3

Sarma, K., Cifuentes-Rojas, C., Ergun, A., Del Rosario, A., Jeon, Y., White, F., Sadreyev, R., & Lee, J. T. (2014). ATRX directs binding of PRC2 to Xist RNA and Polycomb targets. *Cell*, *159*(4), 869–883. https://doi.org/10.1016/j.cell.2014.10.019

Schmitges, F. W., Prusty, A. B., Faty, M., Stutzer, A., Lingaraju, G. M., Aiwazian, J., Sack, R., Hess, D., Li, L., Zhou, S., Bunker, R. D., Wirth, U., Bouwmeester, T., Bauer, A., Ly-Hartig, N., Zhao, K., Chan, H., Gu, J., Gut, H.,…Thoma, N. H. (2011). Histone methylation by PRC2 is inhibited by active chromatin marks. *Mol Cell*, *42*(3), 330–341. https://doi.org/10.1016/j.molcel.2011.03.025

Schneuwly, S., Klemenz, R., & Gehring, W. J. (1987). Redesigning the body plan of Drosophila by ectopic expression of the homoeotic gene Antennapedia. *Nature*, *325*(6107), 816–818. https://doi.org/10.1038/325816a0

Seong, I. S., Woda, J. M., Song, J. J., Lloret, A., Abeyrathne, P. D., Woo, C. J., Gregory, G., Lee, J. M., Wheeler, V. C., Walz, T., Kingston, R. E., Gusella, J. F., Conlon, R. A., & MacDonald, M. E. (2010). Huntingtin facilitates polycomb repressive complex 2. *Hum Mol Genet*, *19*(4), 573–583. https://doi.org/10.1093/hmg/ddp524

Sharaf, A., Vijayanathan, M., Obornik, M., & Mozgova, I. (2022). Phylogenetic profiling resolves early emergence of PRC2 and illuminates its functional core. *Life Sci Alliance*, *5*(7). https://doi.org/10.26508/lsa.202101271

Strahl, B. D., & Allis, C. D. (2000). The language of covalent histone modifications. *Nature*, *403*(6765), 41–45. https://doi.org/10.1038/47412

Tang, G., Yuan, J., Wang, J., Zhang, Y. Z., Xie, S. S., Wang, H., Tao, Z., Liu, H., Kistler, H. C., Zhao, Y., Duan, C. G., Liu, W., Ma, Z., & Chen, Y. (2021). Fusarium BP1 is a reader of H3K27 methylation. *Nucleic Acids Res*, *49*(18), 10448–10464. https://doi.org/10.1093/nar/gkab844

Taverna, S. D., Li, H., Ruthenburg, A. J., Allis, C. D., & Patel, D. J. (2007). How chromatin-binding modules interpret histone modifications: lessons from professional pocket pickers. *Nat Struct Mol Biol*, *14*(11), 1025–1040. https://doi.org/10.1038/nsmb1338

Trojer, P., & Reinberg, D. (2007). Facultative heterochromatin: is there a distinctive molecular signature? *Mol Cell*, *28*(1), 1–13. https://doi.org/10.1016/j.molcel.2007.09.011

Ueda, T., Nakata, Y., Nagamachi, A., Yamasaki, N., Kanai, A., Sera, Y., Sasaki, M., Matsui, H., Honda, Z., Oda, H., Wolff, L., Inaba, T., & Honda, H. (2016). Propagation of trimethylated H3K27 regulated by polycomb protein EED is required for embryogenesis, hematopoietic maintenance, and tumor suppression. *Proc Natl Acad Sci U S A*, *113*(37), 10370–10375. https://doi.org/10.1073/pnas.1600070113

Weintraub, H., & Groudine, M. (1976). Chromosomal subunits in active genes have an altered conformation. *Science*, *193*(4256), 848–856. https://doi.org/10.1126/science.948749

Wiles, E. T., McNaught, K. J., Kaur, G., Selker, J. M. L., Ormsby, T., Aravind, L., & Selker, E. U. (2020). Evolutionarily ancient BAH-PHD protein mediates Polycomb silencing. *Proc Natl Acad Sci U S A*, *117*(21), 11614–11623. https://doi.org/10.1073/pnas.1918776117

Wiles, E. T., Mumford, C. C., McNaught, K. J., Tanizawa, H., & Selker, E. U. (2022). The ACF chromatin-remodeling complex is essential for Polycomb repression. *Elife*, *11*. https://doi.org/10.7554/eLife.77595

Wilkinson, A. L., Zorzan, I., & Rugg-Gunn, P. J. (2023). Epigenetic regulation of early human embryo development. *Cell Stem Cell*, *30*(12), 1569–1584. https://doi.org/10.1016/j.stem.2023.09.010

Woodcock, C. L., & Ghosh, R. P. (2010). Chromatin higher-order structure and dynamics. *Cold Spring Harb Perspect Biol*, *2*(5), a000596. https://doi.org/10.1101/cshperspect.a000596

Xiao, J., Jin, R., Yu, X., Shen, M., Wagner, J. D., Pai, A., Song, C., Zhuang, M., Klasfeld, S., He, C., Santos, A. M., Helliwell, C., Pruneda-Paz, J. L., Kay, S. A., Lin, X., Cui, S., Garcia, M. F., Clarenz, O., Goodrich, J.,…Wagner, D. (2017). Cis and trans determinants of epigenetic silencing by Polycomb repressive complex 2 in Arabidopsis. *Nat Genet*, *49*(10), 1546–1552. https://doi.org/10.1038/ng.3937

Zhao, J., Sun, B. K., Erwin, J. A., Song, J. J., & Lee, J. T. (2008). Polycomb proteins targeted by a short repeat RNA to the mouse X chromosome. *Science*, *322*(5902), 750–756. https://doi.org/10.1126/science.1163045

Zhou, Y., Wang, Y., Krause, K., Yang, T., Dongus, J. A., Zhang, Y., & Turck, F. (2018). Telobox motifs recruit CLF/SWN-PRC2 for H3K27me3 deposition via TRB factors in Arabidopsis. *Nat Genet*, *50*(5), 638–644. https://doi.org/10.1038/s41588-018-0109-9

Zhou, Z., et al. (2018). "Codon usage biases co-evolve with transcription termination machinery to suppress premature cleavage and polyadenylation." Elife 7

Figures

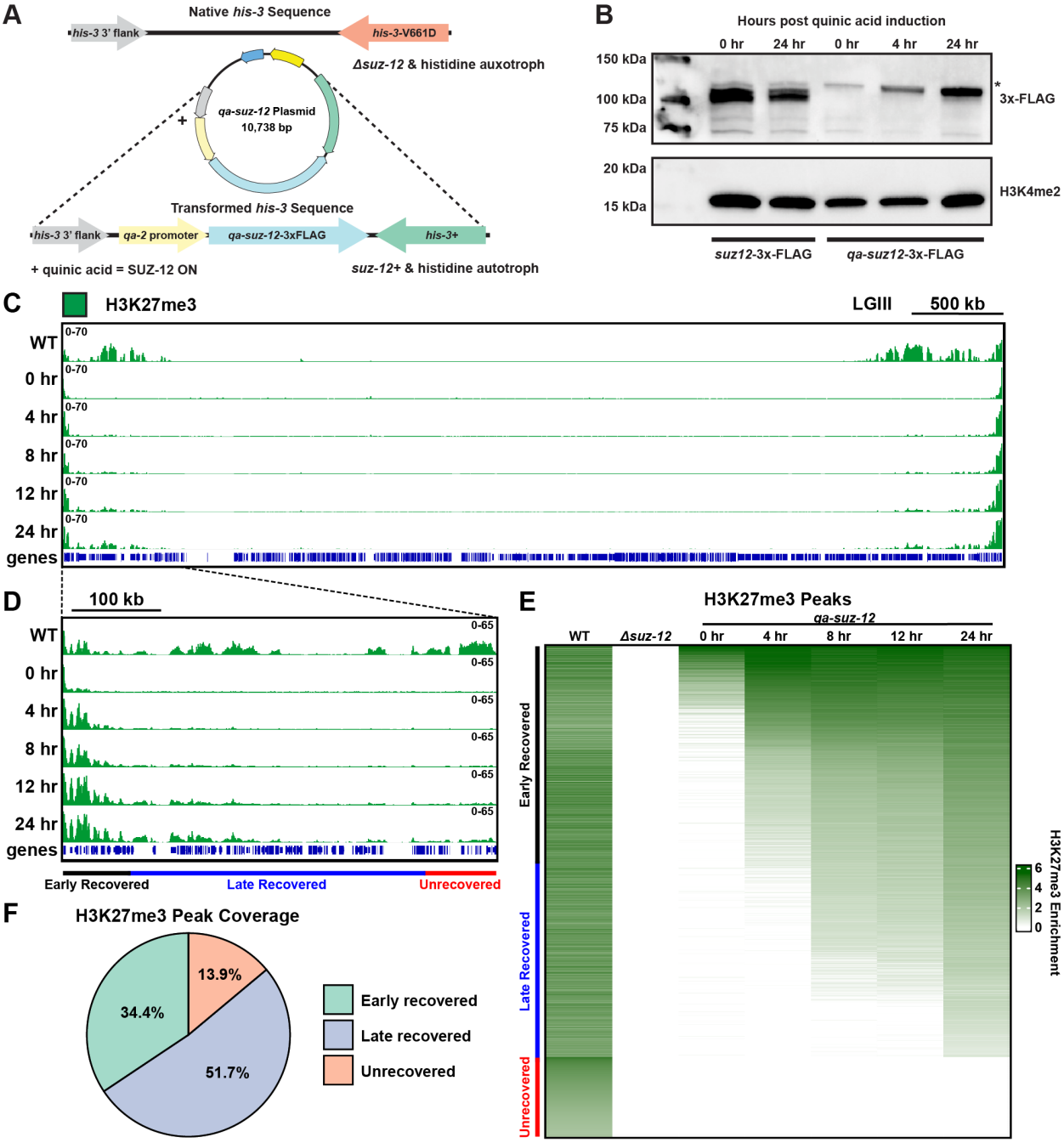
A
Native his-3 Sequence
his-3 3' flank
his-3-V661D
Δsuz-12 & histidine auxotroph
qa-suz-12 Plasmid
10,738 bp
Transformed his-3 Sequence
his-3 3' flank
qa-2 promoter
qa-suz-12-3xFLAG
his-3+
+ quinic acid = SUZ-12 ON
suz-12+ & histidine autotroph
B
Hours post quinic acid induction
0 hr
24 hr
0 hr
4 hr
24 hr
150 kDa
100 kDa
75 kDa
3x-FLAG
20 kDa
15 kDa
H3K4me2
suz12-3x-FLAG
qa-suz12-3x-FLAG
C
H3K27me3
LGIII
500 kb
WT
0 hr
4 hr
8 hr
12 hr
24 hr
genes
0-70
D
100 kb
0-65
Early Recovered
Late Recovered
Unrecovered
E
H3K27me3 Peaks
qa-suz-12
WT
Δsuz-12
0 hr
4 hr
8 hr
12 hr
24 hr
Early Recovered
Late Recovered
Unrecovered
H3K27me3 Enrichment
6
4
2
0
F
H3K27me3 Peak Coverage
13.9%
34.4%
51.7%
Early recovered
Late recovered
Unrecovered

Figure 2.1: *qaP-suz-12*-3x-FLAG is functional and produces H3K27me3 recovery by 24 hours

(A) Diagram displaying how the *qa-suz12*-3xFLAG strain was generated. **(B)** Western blot displaying levels of *suz-12*-3xFLAG enrichment. *qa-suz12*-3xFLAG samples were collected at 0, 6, and 24 hours post-induction. A *suz12*-3x-FLAG strain was used as a positive control. H3K4me2 was used as a loading control. * denotes a background band observed in samples incubated with the M2-FLAG primary antibody. **(C)** Whole-chromosome view of H3K27me3 enrichment in WT and *qaP-suz-12* samples from 0 to 24 hours post-quinic acid induction on LGIII **(D)** Zoom-in view of H3K27me3 enrichment in WT and *qaP-suz-12* samples from 0 to 24 hours post-quinic acid induction on the left arm of LGIII. Colored lines denote early recovering (black) late recovering (blue) and unrecovered (red) peaks **(E)** Heatmap displaying H3K27me3 enrichment across all H3K27me3 peaks called in WT in 300 bp windows across WT, *Δsuz-12*, and induced or uninduced *qaP-suz-12* strains. All values with < 1 log2FC vs. input and an FDR > 0.05 were set to 0. Recovered and unrecovered peaks were clustered separately. Recovered peaks were sorted by enrichment across *qaP-suz-12* samples. Unrecovered peaks were sorted by enrichment in WT **(F)** Pie chart displaying % of total bp that fall into each of the three recovery categories.

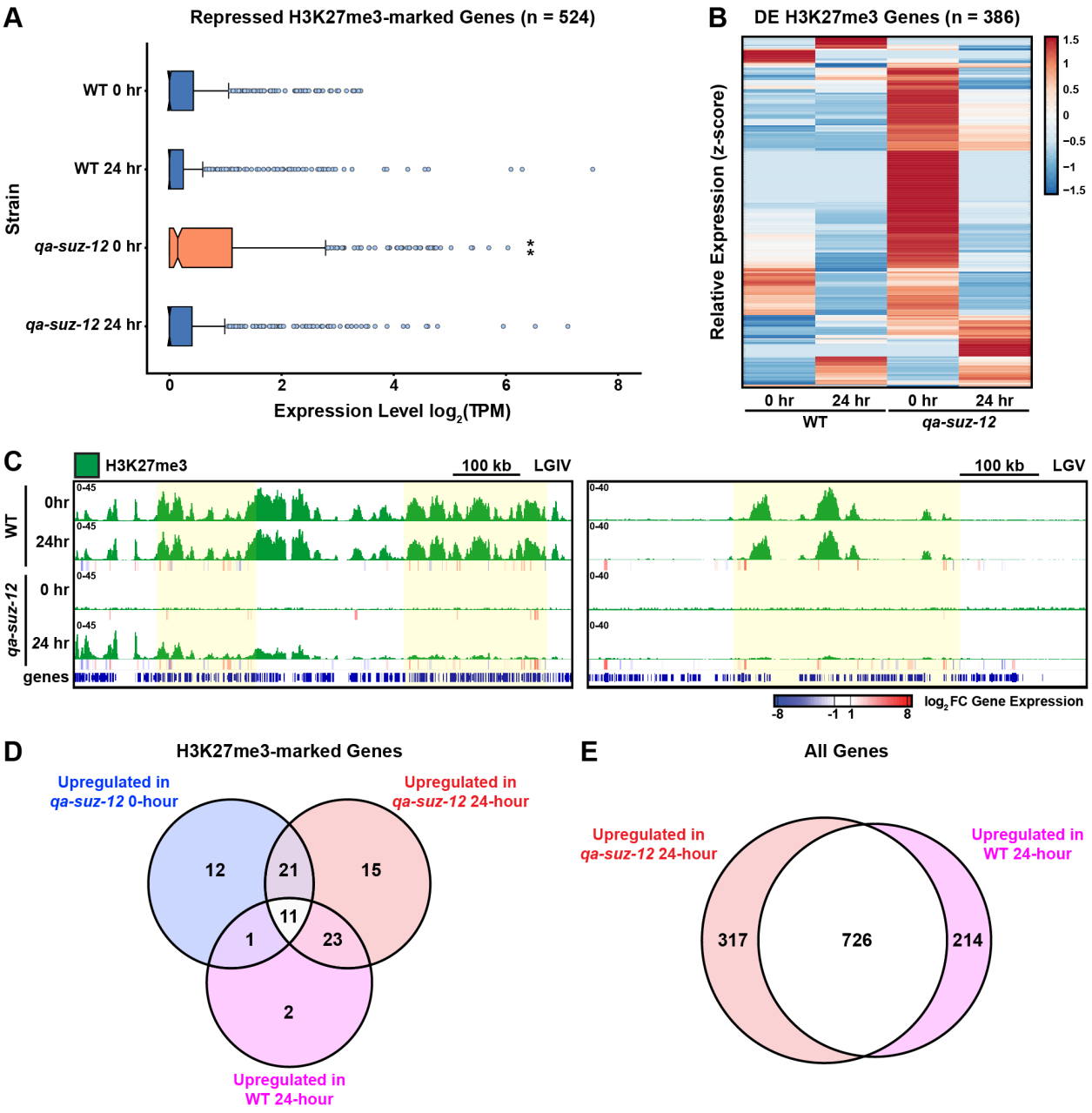
A
Repressed H3K27me3-marked Genes (n = 524)
WT 0 hr
WT 24 hr
qa-suz-12 0 hr
qa-suz-12 24 hr
Strain
0
2
4
6
8
Expression Level log2(TPM)
B
DE H3K27me3 Genes (n = 386)
Relative Expression (z-score)
1.5
1
0.5
0
−0.5
−1
−1.5
0 hr
24 hr
0 hr
24 hr
WT
qa-suz-12
C
H3K27me3
100 kb
LGIV
100 kb
LGV
WT
0hr
24hr
qa-suz-12
0 hr
24 hr
genes
log2FC Gene Expression
-8
-1 1
8
D
H3K27me3-marked Genes
Upregulated in qa-suz-12 0-hour
Upregulated in qa-suz-12 24-hour
Upregulated in WT 24-hour
12
21
15
11
1
23
2
E
All Genes
Upregulated in qa-suz-12 24-hour
Upregulated in WT 24-hour
317
726
214

Figure 2.2: *qaP-suz-12* induction restores gene repression.

(A) Box plot displaying expression levels of 528 H3K27me3-repressed genes (log_2(Transcripts per Million)). ** ($p < 0.01$) represents significant difference in average expression level relative to WT 0hr based on Wilcoxon test. **(B)** Heatmap displaying relative expression level of 386 differentially expressed, H3K27me3-repressed genes in induced and uninduced WT and *qaP-suz-12* strains. Data is row-normalized, and genes (rows) are hierarchically clustered by expression similarity across strains (columns). **(C)** Browser shots displaying ChIP-seq data for H3K27me3 enrichment at two loci on LGVI (left) and LGV (right) in WT and *qaP-suz-12* strains uninduced or induced for 24 hours in quinic acid. **(D)** Venn diagram displaying overlap H3K27me3-marked genes upregulated in uninduced *qaP-suz-12*, induced *qaP-suz-12*, and induced WT strains **(E)** Venn diagram displaying all genes upregulated in induced *qaP-suz-12* and WT strains.

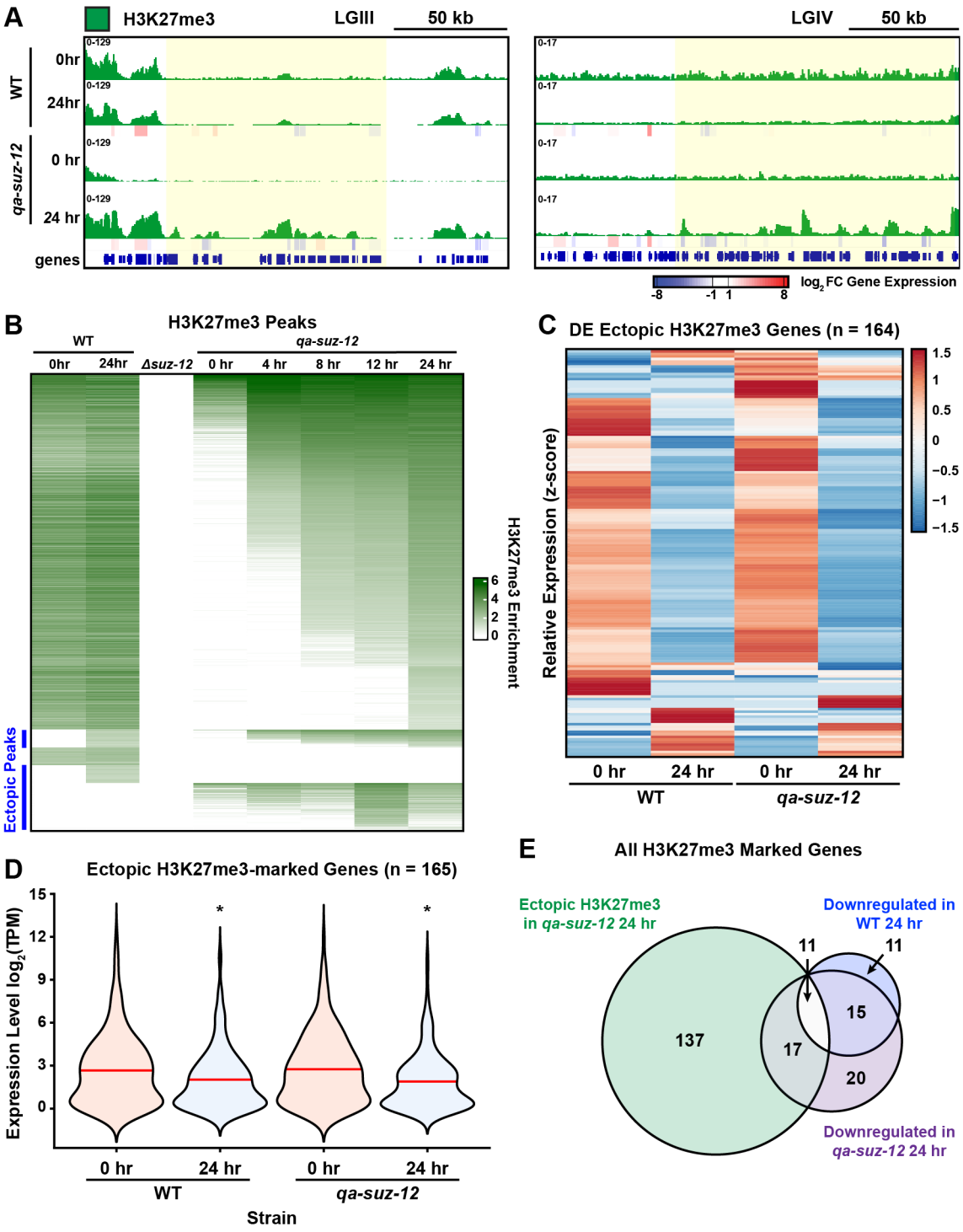
A
H3K27me3
LGIII
50 kb
LGIV
50 kb
WT
0hr
24hr
qa-suz-12
0 hr
24 hr
genes
log2 FC Gene Expression
B
H3K27me3 Peaks
WT
qa-suz-12
0hr
24hr
Δsuz-12
0 hr
4 hr
8 hr
12 hr
24 hr
Ectopic Peaks
H3K27me3 Enrichment
C
DE Ectopic H3K27me3 Genes (n = 164)
Relative Expression (z-score)
0 hr
24 hr
WT
qa-suz-12
D
Ectopic H3K27me3-marked Genes (n = 165)
Expression Level log2(TPM)
Strain
E
All H3K27me3 Marked Genes
Ectopic H3K27me3 in qa-suz-12 24 hr
Downregulated in WT 24 hr
Downregulated in qa-suz-12 24 hr
137
17
11
11
15
20

Figure 2.3: *qaP-suz-12* induction results in ectopic H3K27me3

(A) Browser shots displaying ChIP-seq data for H3K27me3 enrichment at two loci on LGIII (left) and LGIV (right) in WT and *qaP-suz-12* strains uninduced or induced for 24 hours in quinic acid. **(B)** Heatmap displaying H3K27me3 enrichment across all H3K27me3 peaks called in WT or *qaP-suz-12* in 300 bp windows across *Δsuz-12* and induced or uninduced WT and *qaP-suz-12* strains. All values with < 1 log2FC vs. input and an FDR > 0.05 were set to 0. Ectopic peaks are denoted by blue bars. Recovered, unrecovered, and ectopic peaks were clustered separately. Recovered and ectopic peaks were sorted by enrichment across *qaP-suz-12* samples. Unrecovered peaks were sorted by enrichment in WT **(C)** Heatmap displaying relative expression level of 164 differentially expressed, ectopically H3K27me3-marked genes in induced and uninduced WT and *qaP-suz-12* strains. Data is row-normalized, and genes (rows) are hierarchically clustered by expression similarity across strains (columns). **(D)** Box plot displaying expression levels of 165 ectopically H3K27me3-marked genes (log_2(Transcripts per Million)). * represents significant difference in average expression level relative to WT 0hr based on Wilcoxon test. **(E)** Venn diagram displaying overlap of H3K27me3-marked genes that are ectopically enriched for H3K27me3 *qaP-suz-12*, and downregulated in induced *qaP-suz-12* or WT strains

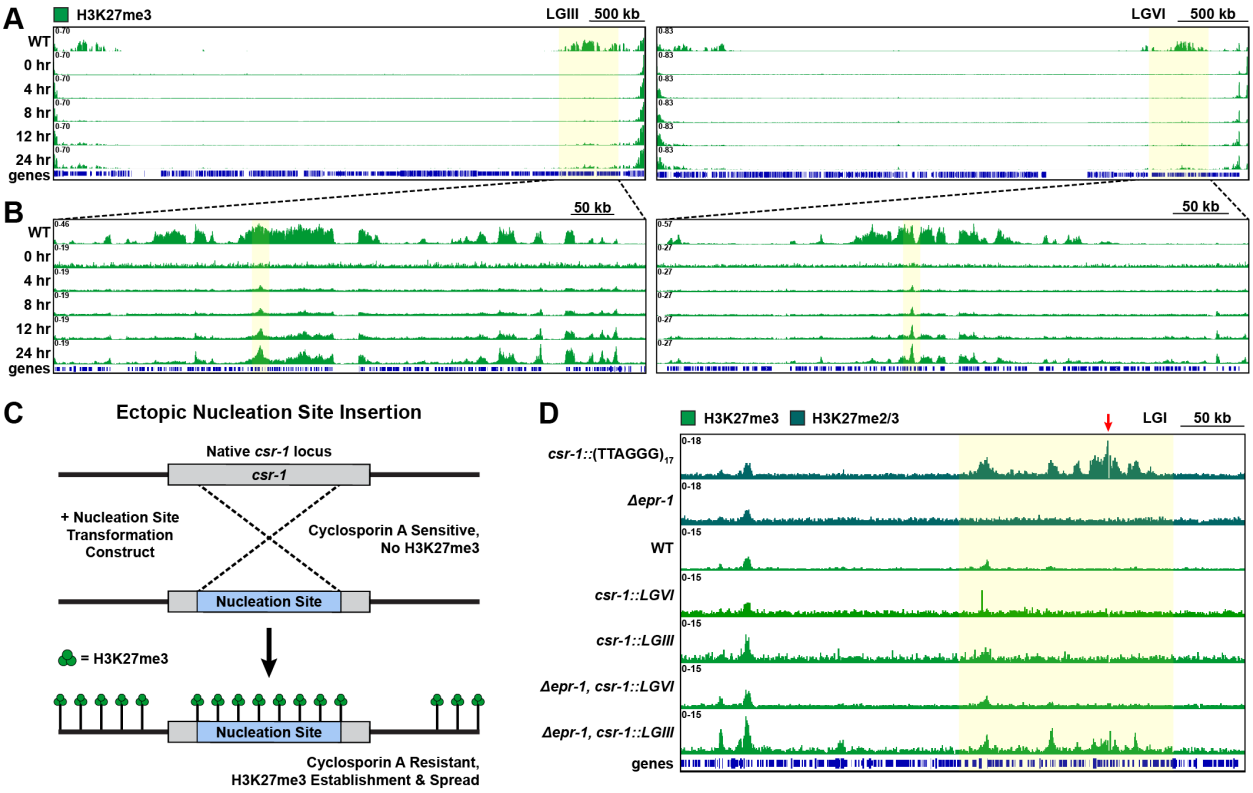

Figure 2.4: *qaP-suz-12* time course reveals putative nucleation sites

(A) Browser shots displaying ChIP-seq data for H3K27me3 enrichment at two loci on LGIII (left) and LGIV (right) in WT and *qaP-suz-12* time course strains. **(B)** Zoom-in view of H3K27me3 enrichment at putative nucleation sites of LGIII and LGVI **(C)** Diagram explaining integration of ectopic nucleation sites into *csr-1* **(D)** Zoom-in browser shot displaying H3K27me3 enrichment at the *csr-1* locus in putative nucleation site strains compared with controls. Red arrow represents location of ectopic fragment insertion.

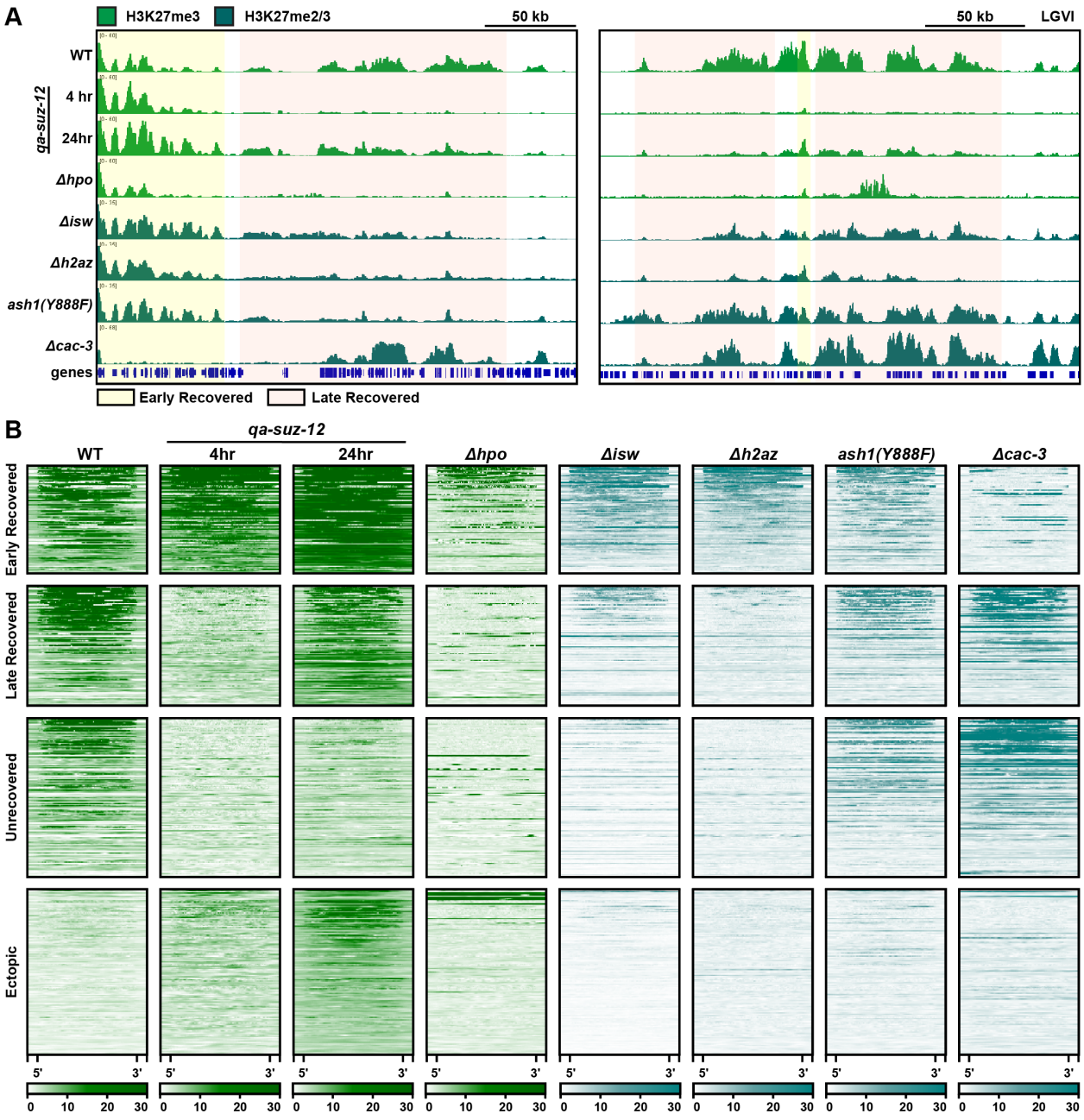
A
H3K27me3
H3K27me2/3
50 kb
50 kb
LGVI
qa-suz-12
WT
4 hr
24hr
Δhpo
Δisw
Δh2az
ash1(Y888F)
Δcac-3
genes
Early Recovered
Late Recovered
B
qa-suz-12
WT
4hr
24hr
Δhpo
Δisw
Δh2az
ash1(Y888F)
Δcac-3
Early Recovered
Late Recovered
Unrecovered
Ectopic
5'
3'
0
10
20
30

Figure 2.5: *qaP-suz-12* H3K27me3 profile resembles mutants of other chromatin regulators

(A) Browser shots displaying ChIP-seq data for H3K27me3 enrichment at two loci on LGVI in WT, induced *qaP-suz-12* time course strains, and mutants of various chromatin regulators **(B)** Heatmap displaying H3K27me3 enrichment at called peaks in WT and *qaP-suz-12* strains across WT, induced *qaP-suz-12* time course strains, and strains with mutations of various chromatin regulators. Peaks (rows) are clustered into 4 groups: early recovered, late recovered, unrecovered, and ectopically methylated during the *qaP-suz-12* time course.

Supplemental Figures and Tables

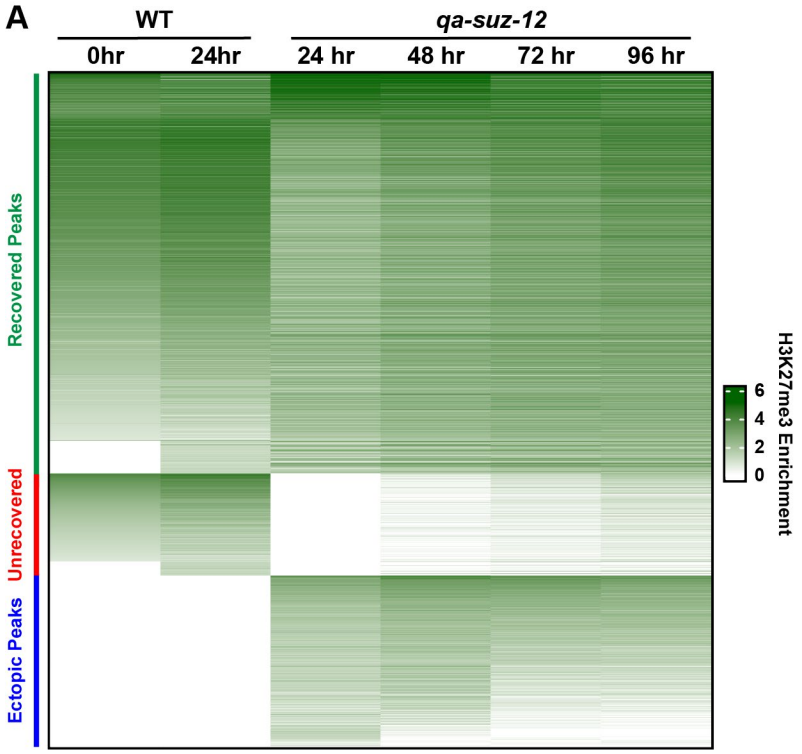

Figure S2.1: 96-hour *qaP-suz-12* time course reveals incomplete recovery of H3K27me3

(A) Heatmap displaying H3K27me3 enrichment at all peaks called in WT and *qaP-suz-12* ChIP-seq samples across induced and uninduced WT strains and induced *qaP-suz-12* strains. Clusters were made based on enrichment in *qaP-suz-12* 24 hours post-induction. Recovered and ectopic clusters are sorted based on enrichment across all strains. The unrecovered cluster is sorted based on enrichment in uninduced WT strains.

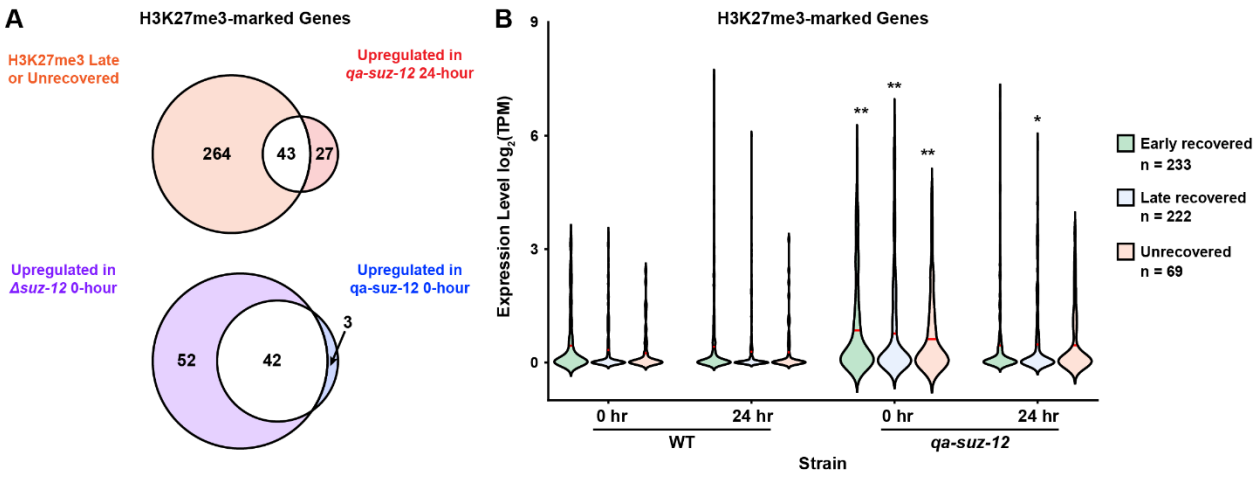

Figure S2.2: Upregulation of gene expression is associated with H3K27me3 recovery

(A) Venn diagrams displaying overlap of H3K27me3-marked genes within late recovering or unrecovered H3K27me3 regions that are upregulated in induced *qaP-suz-12* strains, or H3K27me3-marked genes that are upregulated in *Δsuz-12* and uninduced *qaP-suz-12* strains **(B)** Violin plot displaying expression levels of 524 ectopically H3K27me3-marked genes (log2(Transcripts per Million)). * ($p < 0.05$) & ** ($p < 0.01$) represents significant difference in average expression level relative to WT 0hr based on Wilcoxon test.

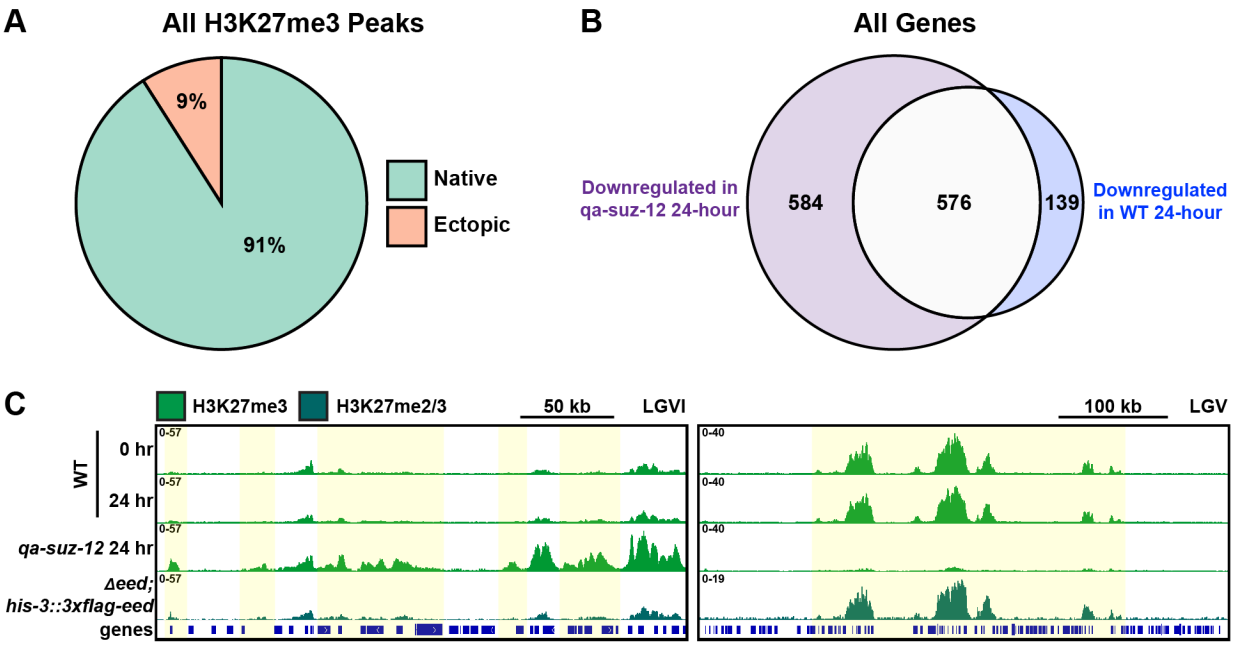

Figure S2.3: Ectopic methylation is associated with *qaP-suz-12* time course growth conditions

(A) Pie chart displaying percentage of H3K27me3 enrichment within Native and ectopic domains in induced *qaP-suz-12* strains. **(B)** Venn diagrams displaying overlap of genes downregulated in induced WT and *qaP-suz-12* strains. **(C)** Zoom-in browser shots displaying H3K27me3-enrichment at two loci on LGVI and LGV for induced and uninduced WT, induced *qaP-suz-12*, and *eed* complementation strains.

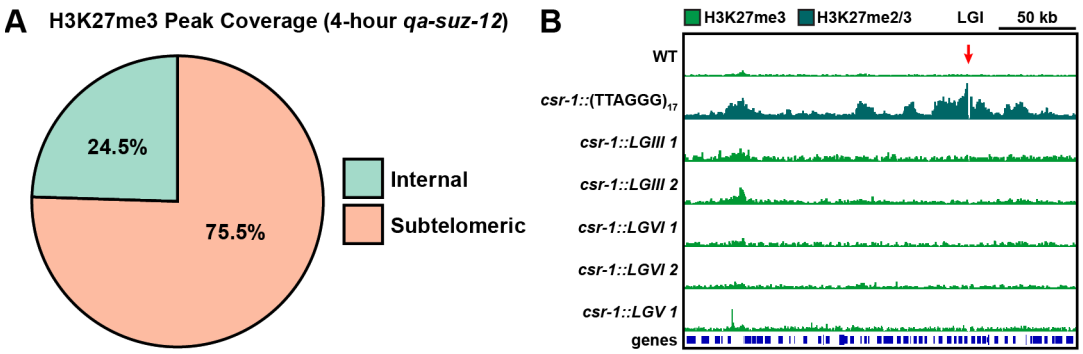

Figure S2.4: Putative nucleation sites cannot recruit PRC2 to *csr-1* in a WT background

(A) Pie chart displaying percentage of H3K27me3 enrichment within subtelomeric and internal domains in *qaP-suz-12* strains 4 hours post-induction. **(B)** Zoom-in browser shot displaying H3K27me3-enrichment at the csr-1 locus in WT, ectopic telomere insertion, and ectopic nucleation site insertion strains. Red arrow represents location of ectopic fragment insertion.

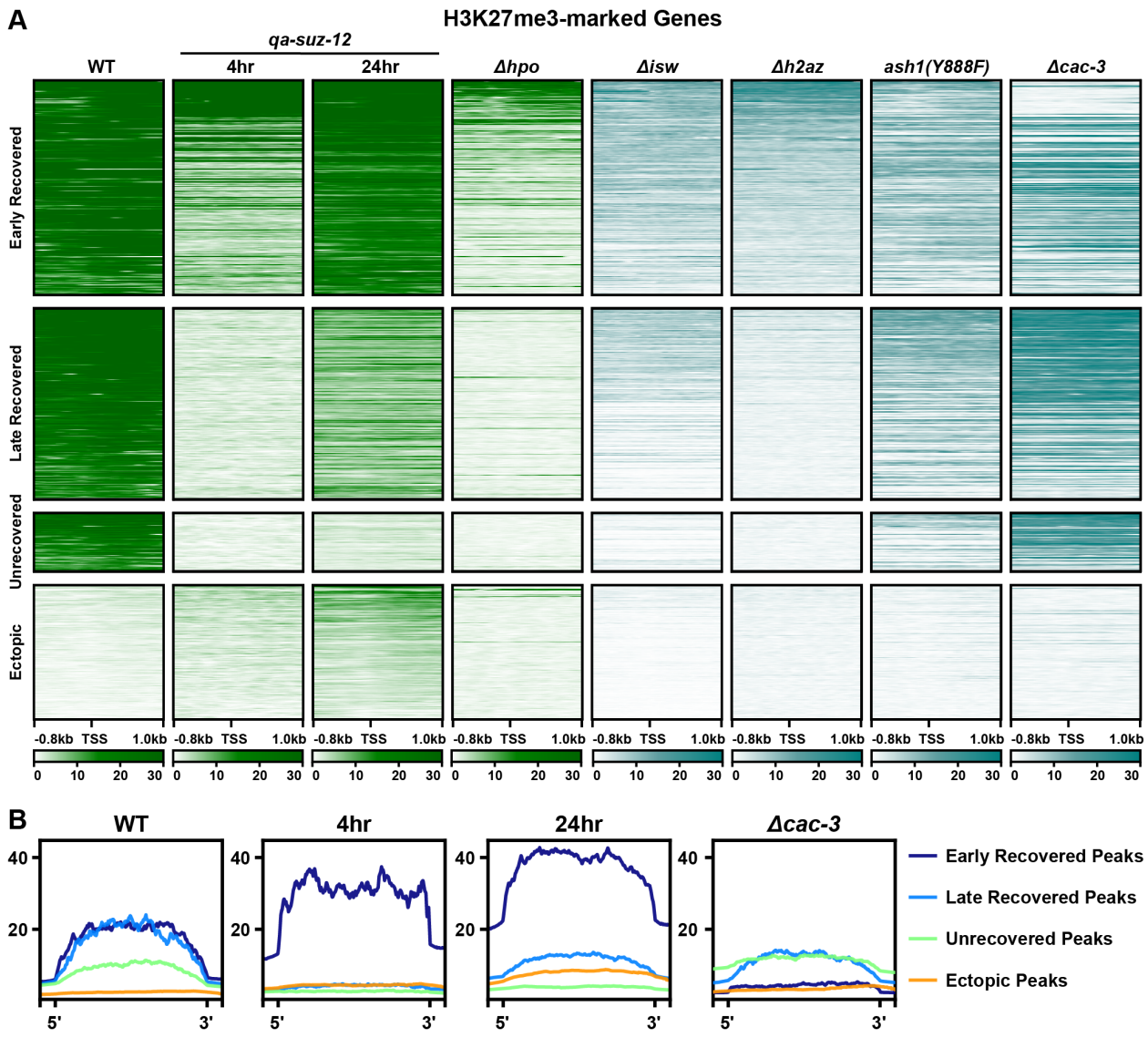

Figure S2.5: Deficiency of chromatin-associated proteins perturbs H3K27me3 establishment and maintenance

(A) Heatmap displaying H3K27me3 enrichment at genes within called peaks in WT and *qaP-suz-12* strains across WT, induced *qaP-suz-12* time course strains, and strains with mutations of various chromatin regulators. Genes (rows) are clustered into 4 groups: early recovered, late recovered, unrecovered, and ectopically methylated during the *qaP-suz-12* time course. **(B)** Metaplots displaying H3K27me3 enrichment at called peaks in WT and *qaP-suz-12* strains across WT, induced *qaP-suz-12* time course, and Δcac-3 strains. Peaks are clustered into 4 groups: early recovered, late recovered, unrecovered, and ectopically methylated during the *qaP-suz-12* time course.

Table S2.1: Strains used in this study

Strain	Genotype	Source
S2	WT	FGSC
S375	*suz-12::hph*	FGSC
S898	*epr-1::hph*	FGSC
ETT111-3	*suz-12::hph, his-3*$^{-}$::*qaP-suz-12*-3xFLAG::*his-3*$^{+}$	This Study
ETT180-4	*suz-12::hph, his-3*$^{-}$::*qaP-suz-12*-3xFLAG::*his-3*$^{+}$	This Study
ETT156-5	*csr-1::LGIII nucleation site 1*	This Study
ETT157-2	*csr-1::LGIII nucleation site 2*	This Study
ETT158-1	*csr-1::LGV nucleation site 1*	This Study
ETT161-4	*csr-1::LGVI nucleation site 1*	This Study
ETT159-1	*csr-1::LGVI nucleation site 2*	This Study
ETX121-1	*epr-1::hph csr-1::LGIII nucleation site 1*	This Study
ETX121-3	*epr-1::hph csr-1::LGIII nucleation site 1*	This Study
ETX123-1	*epr-1::hph csr-1::LGVI nucleation site 1*	This Study

Table S2.2: Primers used in this study

Primer Name	Sequence	Description	Designed
csr-1-geno-F	TCCCGGGATTTCTTGGCATC	*csr-1* genotyping primer	This Study
csr-1-geno-R	AGCATTCAATGTGTTGGCGA	*csr-1* genotyping primer	This Study
suz12_geno_F	TCCGTCTTTTGGGTAGCTAGAT	suz-12 genotyping primer	This Study
suz12_geno_R	GGGTTGTGCGAGGTGTGG	suz-12 genotyping primer	This Study
HPH_300_Universal	TAAAGGGAGGAAGGGCGAAC	*hph* genotyping primer	This Study
Gibson Primer 1 pEAG249G	TAAGAATTCGATATCAAGCTTATC	Gibson Cloning Primer for plasmid backbone	This Study
Gibson Primer 2 pEAG249G	CGGCCGCTCTAGAACTAGTG	Gibson Cloning Primer for plasmid backbone	This Study
LGVI_nuc_3_F	CACTAGTTCTAGAGCGGCCGCAGCAGCTGCAAGGAGCAAA	LGVI 1 nucleation site Gibson Cloning Primer	This Study
LGVI_nuc_3_R	GATAAGCTTGATATCGAATTCTTACCAAGTTCAACAAGTCTGTT	LGVI 1 nucleation site Gibson Cloning Primer	This Study
Universal_Flanking_seq_F	CAATCCGCCCTCACTACAACCG	Universal primers for twist fragments	This Study
Universal_Flanking_seq_R	TCCCTCATCGACGCCAGAGTAG	Universal primers for twist fragments	This Study

Table S2.3: Antibodies used in this study

Antigen	Supplier	Catalog #
H3K27me3	Abcam	ab6002
H3K27me2/3	Active Motif	39535
FLAG	Sigma-Aldrich	F1804

Table S2.4: Sequencing samples used in this study

Title	Type	SRA
Δsuz-12 rep 1	RNA	SRR9027658
Δsuz-12 rep 2	RNA	SRR9027759
Δsuz-12 rep 3	RNA	SRR9027689
Δepr-1 H3K27me2/3 rep 1	ChIP	SRR8730376
csr-1::$(TTAGGG)_{17}$ H3K27me2/3	ChIP	SRR6051552
Δeed; *his-3::eed*-3xFLAG*::his-3*$^{+}$ H3K27me2/3	ChIP	SRR11266651
Δhpo H3K27me3	ChIP	SRR2026380
Δisw H3K27me2/3	ChIP	SRR11806697
ΔhH2Az H3K27me2/3	ChIP	SRR11266618
ash-1(Y888F) H3K27me2/3	ChIP	SRR7690295

Appendix

Appendix 2.1: DNA sequences cloned in this study

LGIII 1 nucleation site:

TCCATTGCCAAGTCTGGTCGTGAATGGCTGCTGGTGGAGATAGTATCCGAAACACAC
CGGGTTAAGTAAATGCTAAATAGGGATTCGGATGAATTCATGGGGTTGAACTCCACT
TCTTCAACCTTGTTCCCGAGTCCATCCTAAAGTCAACCTGAATCTCCTTTGGTCGAGA
TAAAGCGATGTGCAATGAATGGAATTTGAGACATGATATAGAAAAAACTGAAGAGA
TGAAGCTTGAAAAAGTGAGAAATCATGAAATTTGCCGGAAGTAGGGACGTCCAACA
ATTGTGCGGGCAATGAAACTGGGAGCGTCCCTGGCCAGAAACATTCGGGAGCCCGT
ATGCTATCGCCGTGGGCCGCGAGAATACCTTAAGCTCGAGTGGAGGGATCTTGGTA
AGGTTGAGACGTATTGAAGATGGGGCAGACGTGTGCCGATCCGTTTGTCCTGCGTCG
CTTCAGTGTGATCGGATTGCGCACAGATCATGTCCGAGAAGCTTTGACTTAAGGTTT
AGTAGTATGATCTGAATGGAAAGCGATGAGCAGACGAGAAACCCGGAGGAGTGTA
AAAAGATCATGAAGCGGCAGTGAGGCTCAGATATCGGTATACTGGCAAATGGCAGT
TCAAATACAGGGGCACGTAGACAACAATGAGCACACTGAAAATTTAGAAGAACTCC
AGAAACCTTCAACTCATGCTGGATGACGTATCGTGCGTTGTCATCCCGAGGGCCAAA
TCCAAAACTGAGCCGGTGGTGAATGCAAGAGCGGATGAGAACAATAAGGGCAACCT
TCAGTGGAACGGCTGGAAGTGTGAGAAATCCGCGAAAATCAAACGGAAAGAGCTCA
AATATATCGGTCCCGATGAGACATCTGCTGCACTTGAATAGCTCCCGTCTATGTACA
TAGCCATTATCTTGGACAAGAAACAGTCGCACCGCATCTTCGAGTGCAACTCCGTCC
TGCCTTCCGGCTAACGGTCCCCACAGACGAGGAAGATCAGGGGTGCAGTTTCCGTTC
CGCTGGTCATTGTTAGATCTGCGACTTCCATTGCATGGATTTGGCCGAGCCTTTGTGC
CAAGACCAGAGGCAGACAAGATAAGATCTGTGGACGGGCCGTTTTAGCGTATCCGG
TAAACATTTTCTGTAGAAACCTTGGCAATCGGCGGAAACCGTTAGCGACTGCAATGC
CACATGGATTCAAGAGTGTTCTCGCGAAAAGGTTCCTTTTCTCAGTCAATGCGATGA
TTTCGATTTTCTTTGCCTTCCTTCGCAAATCCTCCTTTGTTCCTACCCTCTCGAATGAT
TTCGTCGTTACCGAGTTGTGTCTGTCCCCTCGACGTTTAGGATCCATCTTTATGAGTA
GGGCACCCCTGTCAGTGAGTGGAAATACGGCCAATGAGATAGAATCAACCTGACAG
AAAGGGAAGGTGTGACAGGGTTCTTGCCGAAACCAAAACGCCGAGCCTCCATGGTG
CCTTCCCCACTGTAGACGACGTGCCATGGGTGACATCAATTGACCCTGAAAGGTCAT
GTTTGTCGGACCGGAGGACGATTATCGGTGATCGAAGTAACGGAGTAGACACAGTT
TCTGGGGGATAATGGGATCGTTAATGCATACCTGTTTAGAGGTACTCGCCGTATTTC
CCTCCAAGTTGACATGATATCCGGCTGTCAAGTCGTGCGCAATCGGTACAAACAGAA
GTTGCGACTCTCCAGAGGCCATCGCACCGGAACTTGGCGTTGTATCAAATACCCTTC
ATCGTACTTTCCAAATGCCAGAGTGAAATGGTGATGTTCCCACTGCATGATTGTTAC
TTCCTTACTCGCTATCACCTTCTCCTACTGTTTCCCCCGCTCGCAGCGAGGGGTTCCT
GCTCGCCGCTTTGCTTCGGTAATGCTGCCAGAATCGCCGAGGCAGCCGAATGAGCCG
TCATGCACATGTGCTTGGCAGATATTTGACAGAAAGAGGATCGTGAGCAGCCTCGG
CGAGAAGAGGGAAAGCCCACATACGTGTACGGTGCAGCTGACACCTAAATGCATGC
GTGGTAAATCGAGCTCGTCCTTGGCAGTTGAAACGGACTGCACCGGGACATGTTCCT
CCAGTCCAACTGGGACCATTGCCATTGCCCAGAATCCACGCGCATGGGTTGGCTCAG
TTATGTGCCCGCTCTCCCTCTTCTTCCAAATATCCTTCGATATCGTCAGGGGAATCAT
TTGCTTCCGTCACCTCCTTGCTCCTGCCTTTGGCCCCCATCGTGGACGAAAGTGTCGT

AGCCTATTCCCATCGTCCATTTTCGCAACTGCCCCTTATACTGTTGATGGCAACAACG
CGTCCCGTCCTCGCGCCTTCCACCTGCCACCTGCAATGTTGACCCTGACCCACTCTGC
TTCAGCGCCCTATCATTTGCGAGCTCTCGTGTTGTTCTGTGACGGCTCGCTGACTTTG
CTGTCATGTACCGGTCCTCATTTCCATCTCTTGGCCTTTGATGCGATATCGACAGACT
CGACCCGTTTCAGAGATAACCTGAGAAGATTTCGCGCCGGTGATCTCTGGCGGACCT
ACTTCCCACACGGACCCAAAATTTCCTACGCCCCCCTCTTTCTGTATCGGCAACGTTT
TGTACATCAACCCGTGCTTCCAGATGGCCCAAAAGCCTCCACCAGGAGCTTGTAGTT
GGCGACCTGGAGAGCTGTATCCTTCGATGGGGGAAAGTACTCCAGTTTGATCTAT

LGIII 2 nucleation site:

CATTGTGTCTTGGGTATACCCAATATGCCACGATTGCAAGCGACTTTATTTTACCTCT
GAACTTGATTTCAATGTACCTGATTTCCGATTAGAAATATTGAAAGGGGACTCGTAC
TGCGTTTACTCTCTATTGGAATCATCAACCGGTTCATCCTTCACTTCATGACAAAAAG
CCCACCAGTTACTTCAGGTCCTTCCACTCAGGAGTCTTCTTGATGAACTCCTCCCATG
TAGTCAACTTGTCCTCGACCAACGAATGTGTCCAGTCCAGACTCTCGCCGCCGTAGT
ACCCAAAGGTACCCAGAAGCAAAAAGTTCTCTAGCAGCTCTTGGGCCACATAGTCC
GGCATGCCAGCGCCCTTGAGATTGTCAAGATAAACATCTCCTGGAACCTGGTAGTAC
GAGGCCGTCGCCCCGGCCTCGGGAAACACCTTCTTGAAGCCTTCAACCACCTGGTCG
CCCGTCAAGTACTCGGTTGCACCGAGGAGTCTCTTGCCGAGGGTTTCCTCGCGGTGG
AGGACGGCCGCCTTGACGAACTTGCCTGTGTCTGCCGTGTCGAAAAGGGGGAAGAT
TGACGAGCTCGCGGGGGTGGGCAGGGCAAATGTCCACTTGCCGGTGTTGGTGTCGT
GGTGGGTTAGACCGAGAGCCGGGCCGGAAAAGTTGGACATGTAGAAACCTGGGAG
GAAGAAGGTGGAGGGGAGACTGGTGGCGATGGAGCGGGCGTACTCTTCTACCTCGG
CTTTGCTGTCGAAGTGGTAGAGGTGGGGCAGTTTGCCTTTGCTCACTGTTTGGGTTTT
TGTTGTTAGAGGATTGTTACCTAACATGTACCTTTACAGGCAGGTACAATAGGTATA
TATGCCTGGTGGACAAGATTGAAGGCAGAGATGAGAACAAACAAACATTTGTTAAT
ATTCAAAACAGAACTCCAAATAAAGTGCTGCACGCCCGCCTCGGCAGCTGCATCCA
CCAGGTTCTTGCCCTGCTGCACCTCGACGTCCTTGTCCATCTTCTCCCAGTAGTTGGT
CACGGCGAAAACGGCATACGCGCCGTCGACTGCTGCCCGGAGACTCGACTTGTCGT
TCAGATCGGCGGC

LGV 1 nucleation site:

TGCCCTTACAGCTTCTCTGGTACAGGAATTGGTATGAAGACCGTGATACTAGGTCTT
ACGACGAATACATAGCTCCAAGCTGGTCTTATGCCTCCATCCCTAGCGCAATAAATC
CGCCCAGAATTCTAGACGGGTGCGATCGATATAAGGAACAGGAATACCGACCTATT
ATTCAGATTCTAGACGCGACCATCGCCCTGGTGGATGAGAACAATCCATTTGGAGCA
GTATCAGGGGGAGCATTGCGTATAGAAGGCCCTTTGGCGAATAGCTCCCTGATTAAA
CATTATGGGGTTTCCAGAATTTTTCCGACCTACGAAATTAATATTACGTATCAGGAT
GGACCGACTCGAGTAGGAATGTGCTACATGGATAGAATGCGCTATTACGGACAGAT
GGCGACCAAGCAAAAGCCGATTTACTTGCTTCCTGTTATGCTGAACATGTCCATTTTT
TATGGATACTATAACGAGAAGACTGTTAGTGGGTTGATACTACAAGAGACGAGTGA
CGAAAATACGTTTCGAAGAGTTGGGGTGTTTGTGGTTGAAAGGCCTAGGCAGAAGG
AAAATGCATGTGGCGTTCGGATGTTACAAGAAGCTTGTCGCTCTCAAAATGGGCTGG
ATGAGGATGGTGCATTCCCTGAATGGGGGAAGTTTCGGACTATTACTCTCGTCTAAC
TTTCACTCTTTCTTTGTTTTGTGCTTTCATTTTCTAGTATTCTTCGTTCTCCTTTTGTGT
GTTCTCTCCTTGGTACAGCTCAACGTCAAGTACGCTTCAAGCGTTCATATTCCTTCCT
TTGTACCTAGAACAACCAACTGACCCAGACTTCAAACACCATGTCCCGACTTTCAGC
TGTTATTGACTGACATCTGCTAGACATCTAACTTCAAGATACCTCAGCAGAGCTCTC
GAGATGCCAGCTTCGCCATACCTTTCTAACTCTTAGTACCGTGCCTAGCTATTAAACC
TCCAACTCGTCTTTTGCCCTCTTATGTCATTACCTAGCTATCTGAATATCCTTGCACG
AATTGCATTACACAGACCCCCTTCTCTGTAACGTAGCCGAAGACACTCTACAATAGC
TCGAAGCTCACAGTTACGTGCTTGACAGAACTTGAACACGAGGGGTACCGACACAG
TTGAGATGAAAACTACCTCCATGCCTCTCTCTGCCAAGGCAAAAAAACTTTCACTTT
CGACGCAACGCGTATTTCGATGATTTTGTTTATCGTCTGGCCTCATCTCTTCTACCTC
TACAGGTTCAGATAACGAAACTAGTGGTCATCCGTAGCTCTTCTCGTGCCTAGCTAG
AGGTATAAATCAGTGTGGTCGCCCTCGGAGAAGCCAAAACCTCTTCCTTCTTTCTTC
ATGTGCACTAGCACACAACCAACATCACTCACTTGACAGTTACCACAGCACCAACA
GCGCGGTTACTACCTCCCCATTTCCAACTCACTTCCCCCCCTGTCTGTCCTTCAGCAT
CATCCAGATCACAGGTATCCTTCGCCTGCTCTCGCCATCGAACCAGCGGGCAGTCAC
TTACTCCTACCTTACCTCTACTCCTTGCCCGTGATCACCATCACCTTGCCCTCAGCTG
ACTGAAACCTCAAGAGGTACCTAAGATGGCCCCAACCAAAGAAGAACTCGACCGCG
CCCTCAACGAAATCCAAGCCACCTTCCTCTCCAGGGAAACCAAGCTCGCCAAAGCCT
ACGCCGAGCACCCCGATCCGGACGCGTGGTACTTGAACTTTATTAGCTGCCTTGCTA
AAGTCGCTGCTGGACCGCCGCCGTTGCCCTCTACCACCACTGGTCACAAGCAGCCAG
CAGCTGGGGTTGGAGTTGGAGTTGGGGTTGAAGCTGAAGTTGAACCTGAGGCGGCA
AAGGATAGTGGCGGTTGTGATGTGATTGCGGGGGTGGGTACCACCTCTAGAGGTAT
GAAGAGACCTAGTGTTGAGGAGATGGATGGTGGTAGTGGTAACGGCAGAGGCACCG
GCACAGGCAAGAAAGTGAGGGTTGAGCATTCTATGTCGACTGGGGACACCGAGTAC
CGGACAGCCGAAGGTGTTCTGGTTAGTACTACGATGACTGGTAAGTTGTTGTTGCTT
TGCACTTCCAGACTCGTCCGTCCGTGTCTTGTGGATCGAGCTAATTGACTGACCTCTA
TGGACAAGTTAGGAACAGGCACCCGTTGGATAGTCCCGGCTTGACCACAGCGACTG
GTGATGTGAAGGTGGAGGTAAAAAGGGAGGAATAGGAGATGGAGAGGACGAACGA
AACAGCACTGGTGGTTCAAGAA

LGVI 1 nucleation site:

TCAAACTCAACTCCGACATCGCAAAGAAGACCGCCGCCTGGAGGAGACGTATCAGC
TTGCGTAGCGCCGCTTTAGGGACCACCAGCGGAACCAGAGGCACCACCGCCAGCAG
CGGCACCTCCCTTTGAAGCACCACCCTTAGCAGAACCACCAGCGGCACCACCACCA
GATGCGGCACCTCCCTTCGAAGCACCTCCCTTAGCAGAACCTCCACCAGCAGCGGA
AGCACCTCCACCAGCAGTAGCACCACCAGCTGCGGCACCGCCTCCACCAGCAGCGG
CACCACCCTTAGAAGCACCGCCTTTGGAATCACCTCCCTTCGAAGCGCCTCCCTTCG
AAGCACCACCCTTAGCAGCACCACCTCCACCAGCAGTAGCACCACCAGCTGCGGCA
CCTCCCTTCGAAGCACCACCCTTAGCAGAACTATCACCACCACCTCCACCAGCAGCG
GCACCACCAGAGGCACCTCCCTTACCGGAAGCGGCGCCGGCGGCGGCACCTCCCTT
CGAAGCACCTCCTTTAGCAGAACCTCCACCAGCAGCGGAAGCACCTCCACCAGCAG
TAGCACCACCAGCTGCGGCACCGCCTCCACCAGCAGCGGCACCACCCTTAGAAGCA
CCACCCTTGGAAGCACCACCCTTAGCAGCACCTCCGCCAGCAGCGGCACCACCAGC
TGCAGCACCTCCACCAGCAGTAGCACCACCAGCTGCAGCCCCTCCACCCGCAGCGG
CACCACCCTTAGAAGCACCACCCTTGGAAGCAGCACCTCCACCAGCAGTAGCACCA
CCAGCTGCGGCACCACCTCCACCAGCAGCGGCACCACCCTTAGAAGCACCACCCTT
GGAAGCACCACCTCCACCAGCAGTAGCACCACCAGCTGCGGCACCACCTCCACCAG
CAGCGGCACCACCCTTAGAAGCACCGCCCTTGGAAGCACCTCCTTTAGCAGCACCGC
CCTTAGAAGCACCTCCCTTATCAGCTCCCTTAGAAGCACCTCCCTTGGTAGCACCAC
CAGCCGTAGCACCACCAGCTGTAGTACCACTGCTAGCGGTACTTCCACTACTACTAG
CAGTAGTACTAGCGGCAGTGGCACTGCTAGCGGCACTGCCACGATGTTTTCTCTTGC
CGATTACACTCGGCTCGAGATTGCTACCATCATCAAAGACCACGGCCCTAGGATCAC
GACGGACGGGAACGGAGCGGCGAGCGCCGGCCCGGATGGTGGGTGAAGGAGAAGC
GATGACGCCGGGGGAGTCAGGGTGGCGGGCGGCCAGAGAACCGGAGTCGCCGGGG
GCAAAGCCAGTCGGGGCCGCGTAGGCGGAGAGAGCCGAGGTAAGGAGGAAGAACG
AAGAGAGCTTCATGTCGACGTTGAAGTGGGTGTTGTTGGGTTGTTGTGTAGATCAGT
TGTAAGAGTGAAATGGGTAAGGTAAGTTTGGGTCTTTGAAAGTATTGGTGTCAAAAC
ACAAGTTGTGAAGTTACTGGCCGGCAGATGAGAGCGTGGGAGGTAAGGTTGAAATG
GGTACACGATAGAAGGTGGTAAGTGAAGAAGCTGATGACCGGCAGCGGGAGAAGA
AAAGAAGTCAAGGAGTACCAGACTCGACTCTGTTGGTGTTCGAAGGAAGTCGAACG
GAGACAAGACAAATGTGTCCTTGTTGTTGTTGCTGCTGATGCTGCTACAGATGAGAA
GAGATTCCCCCTCCAAATCAGAGAGTAAACGATAGTTATATACGCCAAGACTCGTGC
GCGTTGTGGGTGCCCATCCGGCATTCGGTATCCAGAGTCCAGAGAACTGGTGTCTGA
CATCTGTGGGTCCGTGAGGGGCTGTGAAGGAGGCGCGAAACGGAATGGTCGGTTAC
CCAGTAGGGCAGGACCTGCTACCACGATGGCCGAATCTCCACGTCTCGAACCATGA
CAGTTTCGAAGCAGCTCGAAGGGAGCTGTCAGATGTCAGTTGGTGTTAGGTTGTGAA
ACCATCCAGGGAAATGTTTCGGTTGAAAGATGTTTTCGATACAAAACTCCTAGAATC
ATGGCTGTCCTGTTGGTTGTGTCATGGCTGTGTTTTCGAAGTGGTGTCGGATCGACGT
TAGCCACTAGTATGGAAAACCTTTTTCTTTCGTGGTCGCTTGTAACTGCTAGATCACC
CGGCGGTTCGTGTTTCTTTCGGTTCCCTCCTTTCGTCTAGTGGTCTTCTGGTCCTTCTC
CGATGAAGAAGAGACTGGGACAGGCCGGGATGAACTCGAAATTCTGACGACGAGAT
GGCTTTGCGTCAAGGGGTCTGGAGACAGAACATTGGTCTGTCTGTGTTAGGGGAAG
AAAACAGGGAAGTTCGTAGTTGTTCGTGTCAGGAGTACGGAGAAAGTTGAGACGGG
TGGCGAGTTCAGCGTTCGGATGGGCAGGACTCCGGAGGGGGTAAAGCAAGTCTGAG

CTCAGGATTCTGGAAGAGTTTGTCGAGGACAGCGTGATGGACGATGGCTGGCTTGTG
TTGTGAAACTCTAAGGATAA

LGVI 2 nucleation site:

CTCCAGCGATCGCAAGATGCAAGTCCCAATTCGTTAATGAAAAACATTTGCACACAA
CTTCTGAAAAGACCTTGTAAAGCTGGATGTTTGAACCATGTTTCTACCTTATAGTAA
AGTCCTCGGTCCAGATTCATTACCATCCCCTATCCCTTGGATGGAAGGGAATTCACA
TGTCGGCGCTTGCCAAAGCGAGAACCAACCTCAACCTTTCCAACCGCATCTCAAAAT
GTCAAATAGGAAAAATGTGGCAGCACCGATGCCGATGCAGACATATCAAGAGCACC
ACGACATGGCACTTTGCAACCTGTTTTCAGTCATGCGATCCCGTGAAGTCTTCGCGC
CAACCCGTCTCTTGCCTGTCATTTGGTAACCGCAAGCTCGCAAATCTCGATCTTGCC
AGAACCATGGGCAACACTCCGATCAGACTGACCGGATGCAAACCCCTTCCTGCCGT
GGGAGATCTCTTGATATTGGCTTTTAGATCCTGATAACTGCCTGTCTTCTCTTACCAG
TCTTGACTATGCCTGCTGATGCAACTGAATCCCTCCCACTGGTGCCGCTCAATACAG
GAGAAAGCGGGACCGTTGCCTCCGCAGATGCTTCTACAGCCTGTACAGCTCGACTTC
CACAGTTTGATGGCCATTGCATTTTCCTTCTCTCTTTCGCTAGCCACGGTTTGCGACT
GAGACTTCATCCAGACTTTGGTCGAGTGTTGGTGCAACTCCCGTCGGGTCGCACAAC
TTTCCCGTGCTCTCCCATGCCGCAGAGCGTAGGGCACATAGAGGGGCAAGAAAGAA
AGCGAAAACAAGAAAAGCAACGGCAGGAAACTTGAGCTTGGCGATATGTGCTCATG
ATTTGTTTTGAGTGAGTTTTGTACCCATGTCTGACCTAACGCGCCTGCGTCCCGCTTC
AGCAACCAAGTTAAAAATCTCTCGTAGCAAAGCACACA

CHAPTER THREE

CHROMATIN ASSEMBLY FACTOR 1 IS REQUIRED FOR NORMAL GENE REPRESSION AND FACULTATIVE HETEROCHROMATIN FORMATION IN *NEUROSPORA CRASSA*[1]

1 Torres, E.V., Link, C., Yap, R., Ferraro, A.R., Pelham, J.F., and Lewis, Z.A., 2025, Chromatin Assembly Factor 1 is Required for Normal Gene Repression and Facultative Heterochromatin Formation in *Neurospora crassa*

To be submitted to PLOS Genetics

Abstract

Formation of facultative heterochromatin by Polycomb Repressive Complex 2 (PRC2) is a well conserved epigenetic mechanism that functions to control transcriptional dynamics across eukaryotes. PRC2 catalyzes histone H3 lysine 27 tri-methylation (H3K27me3), a dynamic histone post-translational modification (PTM) that helps maintain gene repression in specific cellular contexts. PRC2 repression has been implicated in numerous developmental processes and human ailments, including Huntington's disease and various cancers. In this study, we reveal the replication-dependent histone chaperone, Chromatin Assembly Factor 1 (CAF-1), is required for normal PRC2 activity in model fungus *N. crassa*. CAF-1 deficiency results in widespread misregulation of gene expression, particularly within facultative heterochromatin domains, which is accompanied by a rearrangement of H3K27me3 patterns. We show that PRC2 activity remains intact in the absence of CAF-1 activity, and that regional losses of H3K27me3 are associated with reduced levels of ASH-1 catalyzed H3K36 methylation, and gains of histone PTMs associated with active transcription. Furthermore, analysis of a double mutant deficient for both CAF-1 and PRC2 revealed that these complexes play distinct roles in maintaining gene repression and facultative heterochromatin. Collectively, these results shed light on CAF-1's role in maintaining a repressive chromatin environment in eukaryotes.

Introduction

Eukaryotic organisms regulate gene expression in response to environmental and developmental stimuli. This is accomplished through a variety of epigenetic mechanisms including histone post-translational modification (PTMs) (Allis & Jenuwein, 2016). Certain histone PTMs can activate or repress gene expression by regulating genome accessibility to

transcription factors, RNA polymerases, and various chromatin modifying enzymes (Allis & Jenuwein, 2016; Kouzarides, 2007; Li et al., 2007). Regions of the genome marked by repressive histone PTMs are referred to as heterochromatin, which is characterized by its compact structure that is generally inaccessible to DNA-interacting proteins (Allshire & Madhani, 2018; Janssen et al., 2018). Heterochromatin can be further categorized into constitutive and facultative heterochromatin. Constitutive heterochromatin is characterized by repeat rich, gene poor regions of the genome, while facultative heterochromatin is gene rich and dynamically repressive, meaning genes in these regions can be expressed under specific cellular contexts or environmental conditions (Grewal, 2023; Saksouk et al., 2015; Trojer & Reinberg, 2007).

Facultative heterochromatin is established and maintained by Polycomb Group (PcG) proteins, which deposit repressive histone PTMs that contribute to chromatin compaction. This includes histone H3 lysine 27 trimethylation (H3K27me3), which is catalyzed by Polycomb Repressive Complex 2 (PRC2) (Cao et al., 2002; Muller et al., 2002). Proper formation of facultative heterochromatin is critical for maintaining gene repression and contributes to several biological processes across eukaryotes, including X-chromosome inactivation in mammals and vernalization in plants (Bastow et al., 2004; Di Croce & Helin, 2013; Plath et al., 2003). These systems also possess Polycomb Repressive Complex 1 (PRC1), another PcG complex that works in parallel with PRC2. The activity of both these complexes is required for proper formation of facultative heterochromatin in these systems (Blackledge & Klose, 2021; Di Croce & Helin, 2013; Francis et al., 2004). Defects in the PcG gene repression pathway have been shown to cause numerous developmental defects, and are associated with several human diseases, including Huntington's disease and various cancers (Kim & Roberts, 2016; Margueron & Reinberg, 2011; Seong et al., 2010).

While many commonly studied fungi such as S*accharomyces cerevisiae* and *Schizosaccharomyces pombe* lack PcG complexes, many fungal lineages have retained PRC2-catalyzed H3K27me3, which has been shown to contribute to biological processes such as regulation of sexual development, secondary metabolite biosynthetic gene clusters, and effector gene expression (Collemare & Seidl, 2019; Connolly et al., 2013; Deaven et al., 2025; Fraser & Whitehall, 2022; Ridenour et al., 2020). The filamentous fungus *Neurospora crassa* contains a conserved core PRC2 complex made up of subunits EED, SUZ-12, and SET-7, but is devoid of homologs for most other PcG proteins (Aramayo & Selker, 2013; Jamieson et al., 2013). This simplified system makes *N. crassa* an attractive model to directly probe the roles of other chromatin modifying complexes in the PRC2 repression pathway. To date, studies in *N. crassa* and other fungi have implicated a range of factors in proper PRC2 activity, including its accessory proteins (CAC-3/NPF, EPR-1, and PAS), the IMITATION SWITCH (ISWI) chromatin remodeler, the histone variant H2A.Z , the histone deacetylase (HDAC) complexes HISTONE DEACETYLASE 1 (HDA-1) and RPD3L, and the H3K36 and H3K9 methyltransferases ASH-1 and DIM-5 respectively (Basenko et al., 2015; Bicocca et al., 2018; Courtney et al., 2020; Ebot-Ojong et al., 2025; Kamei et al., 2021; McNaught et al., 2020; Mumford et al., 2024; Wiles et al., 2020). In contrast to mammalian systems, in which H3K36me3 is typically antagonistic to PRC2 activity (Alabert et al., 2020), ASH-1 catalyzed H3K36me has been shown to localize at the promoters and gene bodies of H3K27me3-marked genes in *N. crassa* and other fungi (Bicocca et al., 2018; Janevska et al., 2018; Moller et al., 2023; Xu et al., 2024). Furthermore, a catalytic point mutant of *N. crassa* ASH-1 *(ash1(Y888F))* was previously shown to experience a near complete loss of H3K36me3 at H3K27me3-marked

genes, which resulted in altered H3K27me patterns (Bicocca et al., 2018). In contrast, SET-2 is responsible for methylating the gene bodies of actively transcribed genes.

Despite major advances in our understanding of facultative heterochromatin formation in filamentous fungi, the role of histone chaperones remains underexplored. Histone chaperones are a group of chromatin modifying complexes that are responsible for transporting newly synthesized or recycled histones to DNA and assembling them into nucleosomes (Gurard-Levin et al., 2014; Hammond et al., 2017). Histone chaperones are generally categorized into two groups, replication-dependent or replication-independent, based on their activity inside or outside of S-phase (Ransom et al., 2010; Tagami et al., 2004). Proper function of replication-dependent chaperones has been shown to be critical for maintenance of epigenetic modifications across cellular divisions (Alabert & Groth, 2012; Dreyer et al., 2024; Hammond et al., 2017). Chromatin Assembly Factor 1 (CAF-1) is a highly conserved, heterotrimeric, replication-dependent histone chaperone complex, whose canonical role is tetramerizing and depositing newly synthesized histone H3/H4 dimers onto DNA behind the replication fork (Smith & Stillman, 1989). CAF-1 is recruited to replication fork and sites of DNA double-strand breaks (DSBs) through the interaction of its large subunit (*N. crassa*; CAC-1) with the DNA processivity factor Proliferating Cell Nuclear Antigen (PCNA) (Moggs et al., 2000; Ransom et al., 2010; Shibahara & Stillman, 1999; Zhang et al., 2000). Here, 2 CAF-1 complexes await H3/H4 dimers from other chaperone proteins to form and deposit a new H3/H4 tetramer onto naked DNA (Liu et al., 2023; Rouillon et al., 2023; Sauer et al., 2018; Smith & Stillman, 1989, 1991). Previous work in *S. cerevisiae* and *S. pombe* has implicated CAF-1 and other replication-dependent chaperones in gene silencing and heterochromatin maintenance (Dohke et al., 2008; Enomoto & Berman, 1998; Franklin et al., 2025; Huang et al., 2007). Studies in *Drosophila*,

Arabidopsis thaliana, and CAF-1 deficient ESCs have implicated activity of the complex in proper gene silencing, H3K27me3 maintenance, and cellular plasticity (Cheloufi et al., 2015; Cheng et al., 2019; Dreyer et al., 2024; Franklin et al., 2022; Houlard et al., 2006; Huang et al., 2010; Ishiuchi et al., 2015; Jiang & Berger, 2017; Mozgova et al., 2015; Roelens et al., 2017; Schonrock et al., 2006; Song et al., 2007). However, CAF-1 knockouts exhibit severe developmental defects in these systems, and are embryonic lethal in mammals, making it difficult to study its role in facultative heterochromatin formation (Hoek & Stillman, 2003; Schonrock et al., 2006; Song et al., 2007). Much like PRC2, *N. crassa* has a fully conserved CAF-1 complex, which we show is non-essential for survival.

Here, we report that mutation of individual CAF-1 subunits results in derepression of H3K27me3-marked genes in *N. crassa*. This is accompanied by widespread changes to the chromatin environment, including loss of H3K27me3 at genes within facultative heterochromatin domains. Comparing the phenotypes of CAF-1 and PRC2-deficient mutants revealed that many of the observed changes in the chromatin environment were a result of CAF-1-deficiency rather than H3K27me3 depletion. Lastly, double mutants deficient for both CAF-1 and PRC2 activity displayed a more severe silencing defect for H3K27me3-marked genes than either single mutant and resulted in additive defects to the chromatin environment, suggesting that CAF-1 acts in parallel with PRC2 to maintain facultative heterochromatin. Collectively, these results reveal that CAF-1 plays a role in safeguarding the chromatin environment by maintaining gene repression within heterochromatic loci in *N. crassa*.

Results

The CAF-1 complex is required for normal repression of genes within facultative heterochromatin

Based on previous research in other model systems, we hypothesized that one or more histone chaperones would be required for proper establishment or maintenance of facultative heterochromatin in *N. crassa* (Hammond et al., 2017). To test this, we obtained mutant strains lacking individual histone chaperone-coding genes available from the *N. crassa* gene deletion collection and performed RNA-seq (Dunlap et al., 2007). Plotting average transcription levels of 506 H3K27me3-marked genes normally repressed in WT mycelia (H3K27me3-repressed) revealed that mutations in any of the three genes encoding the individual subunits of the CAF-1 complex (Δ*cac-1*, Δ*cac-2*, Δ*cac-3*) displayed significantly elevated expression levels on average, comparable with that of Δ*set-7*, which lacks the catalytic subunit of PRC2 (Fig. 3.1A). Other histone H3/H4 histone chaperone-deficient mutants tested exhibited no significant induction H3K27me3-marked genes (Δ*asf-1*, Δ*naf-1*, Δ*naf-2*, Δ*atrx*), suggesting CAF-1 activity is required for PRC2-mediated gene repression.

To examine expression of H3K27me3-marked genes at the individual gene level, we constructed a heatmap plotting relative transcript levels for H3K27me3-repressed genes that are differentially expressed in one or more of the histone chaperone-deficient mutants. These data revealed clusters of H3K27me3-repressed genes that were most highly expressed in CAF-1-deficient mutants relative to other histone chaperone-deficient mutants or Δ*set-7* (Fig. 3.1B). The pattern of gene induction was similar for Δ*cac-1* and Δ*cac-2*, which displayed overlap for ~75% of genes upregulated across both mutants (Fig. 3.1D). This concordance likely reflects the fact that disrupting any interactions between the CAF-1 subunits severely diminishes the complex's

H3–H4 binding activity (Kaufman et al., 1995; Liu et al., 2016; Sauer et al., 2018). The gene expression pattern of Δ*cac*-3 was distinct, likely because CAC-3 and its homologs are present in multiple chromatin modifying complexes, including the SIN3 and RPD3S/L histone deacetylase (HDAC) complexes and PRC2 itself (Fig. 3.1B & D) (Jamieson et al., 2013; Lin et al., 2022; Martinez-Balbas et al., 1998; Tang et al., 2021; Zhang et al., 1997). CAF-1–deficient mutants exhibited widespread transcriptional changes, with 2,973 genes being differentially expressed across all three mutants relative to WT (~28% of the genome), and H3K27me3-marked genes being among the most highly upregulated (Fig. 3.1C & D). Despite this, neither Δ*cac-1* nor Δ*cac-2* exhibited any obvious growth defects, but were sensitive to DNA damage, which is consistent with CAF-1's known role in DNA repair in other systems (Fig. S3.3). Furthermore, CAF-1 mutants displayed substantial overlap of upregulated H3K27me3-marked genes, with 202 of the 369 genes upregulated across all three mutants held in common, suggesting a direct role of the CAF-1 complex in silencing these genes (Fig. 3.1E). Collectively, these data suggest that CAF-1-deficiency results in widespread misregulation of gene expression, particularly within facultative heterochromatin domains.

CAF-1 is required for normal H3K27me3 patterns at facultative heterochromatin

Interestingly, 104 of the 315 H3K27me3-marked genes upregulated in Δ*set-7* remained repressed in Δ*cac-1* and Δ*cac-2*, while 81 genes upregulated in Δ*cac-1* or Δ*cac-2* remained repressed in Δ*set-7* (Fig. 3.1E). This observation suggests that the derepression of H3K27me3-marked genes in CAF-1 deficient mutants is not a direct result of H3K27me3 depletion. We next asked if CAF-1-deficiency leads to defects in normal H3K27me3 occupancy. Indeed, we observed that some clusters of upregulated genes experienced a loss of H3K27me3, with a total

of 200 genes displaying a significant loss of H3K27me3 compared to WT (Fig. 3.2A & B, left panel). Analyzing genome-wide H3K27me3 levels revealed a significant rearrangement of the PTM in all three mutants, including both regional losses and ectopic gains at novel loci (Fig 2C). The Δ*cac-3* strain displayed a sub-telomeric loss and internal ectopic gain of H3K27me3 as previously reported (Courtney et al., 2020; Jamieson et al., 2013), but the enrichment pattern in the Δ*cac-1* and Δ*cac-2* strains was distinct from Δ*cac-3,* consistent with their gene expression profiles (Fig. 3.2A-C). The Δ*cac-1* and Δ*cac-2* profiles were highly similar, suggesting that inhibition of CAF-1 activity is responsible for the observed H3K27me3 defect. Independent validation of select regions by ChIP-qPCR supported ChIP-seq observations, and replicate experiments using an alternative H3K27me3 antibody produced identical results (Fig. S3.4). Furthermore, complementing either mutation resulted in a full recovery of the H3K27me3 phenotype (Fig. S3.10). Interestingly, measuring H3K27me3 levels by western blot revealed that CAF-1 deficiency did not result in a significant global decrease of H3K27me3 (Fig. 3.2D).

We next asked if these losses of H3K27me3 were correlated with increased transcription of H3K27me3-marked genes. Indeed, 147 of the 190 protein-coding genes that lose H3K27me3 in Δ*cac-1* or Δ*cac-2* were also upregulated in either strain (Fig. 3.2E). Additionally, 90 protein-coding genes were located at sites of ectopically gained H3K27me3, 10 of which were significantly downregulated (Fig. 3.2B, right panel). Furthermore, plotting relative H3K27me3 enrichment against relative expression levels for these genes between WT and Δ*cac-1* (log2FC[Δcac-1/WT]) revealed a weak correlation between loss of H3K27me3 and upregulated gene expression (Fig. 3.2F). Δ*cac-2* displayed a similarly weak correlation between H3K27me3 levels and gene expression, while Δ*cac-3* showed little correlation (Fig. S3.5A). However, an additional 145 H3K27me3-marked genes upregulated in Δ*cac-1* or Δ*cac-2* did not lose

H3K27me3, suggesting that increased expression alone is not causing the observed H3K27me3 defect (Fig. 3.1E, Fig. S3.3B). Collectively, these data suggest that the silencing defects of CAF-1 mutants are associated with an altered facultative heterochromatin environment, but that perturbing the complex does not prevent genome-wide PRC2 activity. Furthermore, considering the alternative roles and distinct methylation profile of CAC-3, we decided to focus our downstream analysis on the Δ*cac-1* and Δ*cac-2* mutants to specifically determine the role of CAF-1 in facultative heterochromatin formation.

CAF-1 deficiency impacts ASH1 Mediated H3K36me within facultative heterochromatin regions

Considering the partial defect of H3K27me3 in CAF-1-deficienct mutants, we next asked if altered levels of other repressive histone modifications might explain the silencing defect observed in Δ*cac-1* and Δ*cac-2*. We first looked at H4K20me3, a mark that colocalizes with H3K27me3 and contributes to gene repression in *Zymoseptoria tritici* (Moller et al., 2023). ChIP-seq analysis of H4K20me3 revealed that the PTM is widespread, largely colocalizing with H3K36me3 (Fig. S3.6). No obvious defects in H4K20me3 patterns were observed in Δ*cac-1*, Δ*cac*-2, or Δ*set-7* compared to WT (Fig. S3.6C & E). Previous work in *S. pombe* and ESCs found that CAF-1-deficiency results in altered H3K9me3 at constitutive heterochromatin and revealed a direct interaction between CAF-1 and Heterochromatin Protein 1 (HP1), a H3K9me3 reader protein (Cheloufi et al., 2015; Dohke et al., 2008; Houlard et al., 2006; Murzina et al., 1999; Thiru et al., 2004). However, ChIP-seq experiments in CAF-1-deficient mutants revealed no significant loss or rearrangement of H3K9me3, suggesting that constitutive heterochromatin remains intact in the absence of *N. crassa* CAF-1 activity (Fig. S3.6A-C & D). Finally, we

assayed levels of H3K36me3 to determine if CAF-1 activity is important for ASH-1 catalytic function at facultative heterochromatin.

ChIP-seq analysis revealed that CAF-1-deficient mutants displayed a mild reduction of H3K36me3 at promoters and gene bodies of 83 H3K27me3-marked genes (Fig. 3.3A-C). The Δ*set-7* mutant displayed a loss of H3K36me3 at only 33 of these 83 promoters, while gene bodies remained relatively unaffected (Fig. 3.3A & C). 63 of the 76 protein-coding, H3K27me3-marked genes that lost H3K36me3 were upregulated in Δ*cac-1* or Δ*cac-2* (Fig. 3.3D). However, plotting log2FC of H3K36me3 against log2FC of gene expression in CAF-1-deficient mutants relative to WT revealed a weaker correlation than what was observed when plotting against log2FC of H3K27me3, while Δ*set-7* displayed no obvious correlation (Fig. S3.8A-C). Reductions of H3K36me3 and H3K27me3 displayed a synergy, with 51 of 76 the protein-coding genes that lose H3K36me3 in Δ*cac-1* or Δ*cac-2* also exhibiting a loss of H3K27me3 (Fig. S3.7A & S3.7B). Previously published H3K27me2/3 data for *ash-1(Y888F)* displayed an appreciable overlap with the altered H3K27me3 pattern in CAF-1-deficient mutants, with 152 of the 200 genes that lose H3K27me3 in Δ*cac-1* or Δ*cac-2* also losing H3K27me2/3 in *ash1(Y888F)* (Fig. 3.3E, Fig. S3.7D) (Bicocca et al., 2018). Furthermore, 256 of the 292 H3K27me3-marked genes upregulated in Δ*cac-1* or Δ*cac-2* are also upregulated in *ash-1(Y888F*) (Fig. 3.3D). This represents a higher percentage of overlap than genes that display upregulation in Δ*cac-1* or Δ*cac-2* and Δ*set-7* (~67%), or Δ*set-7* and *ash1(Y888F)* (~74%) (Fig. 3.1E, S3.7D). *ash-1(Y888F)* also exhibits depletion of H3K36me2/3 at 985 non-H3K27me3-marked genes, 47 of which exhibited loss of H3K36me3 in CAF-1-deficient mutants, while Δset-7 remained unaffected (Fig. S3.7C). H3K36me3 at genes within other euchromatic regions was not lost in any of the mutants (Fig.

3.3A). Collectively, these data support a PRC2-independent effect of CAF-1-deficiency on ASH-1 catalytic activity, while SET2 activity remains unaffected.

CAF-1 Deficiency Leads to Gain of Active PTMs Within Facultative Heterochromatin Regions

Considering the transcriptional misregulation and defects in heterochromatin formation observed in CAF-1 mutants, we next asked if CAF-1 deficiency results in an increase of histone PTMs associated with active transcription at H3K27me3-marked genes. We decided to look at H3K4me and pan-lysine acetylation (Kac), PTMs that are known to antagonize PRC2 activity (Creyghton et al., 2010; Pasini et al., 2010; Schmitges et al., 2011; Tie et al., 2009). ChIP-seq analysis of H3K4me2 revealed gains in 24 H3K27me3-marked genes in Δ*cac-1* or Δ*cac-2* (Fig. 3.4B, Fig. S3.9A). 22 of these 24 genes, in addition to 26 other H3K27me3-marked genes gained H3K4me2 in Δ*set-7*, suggesting that this phenotype arises due to H3K27me3 loss (Fig. 3.4B & C, Fig. S3.9A). Gains in Kac were more widespread, with 104 genes exhibiting elevated levels in Δ*cac-1* or Δ*cac-2* (Fig. 3.4A & B). Interestingly, Kac patterns were distinct between CAF-1 and PRC2-deficient mutants, with only ~11.5% of genes with increased Kac in Δ*cac-1* or Δ*cac-2* exhibiting gains in Δ*set-7*, which also displayed elevated Kac at 37 unique genes (Fig. 3.4A & C). Conversely, Δ*cac-1* and Δ*cac-2* displayed significant overlap in enrichment of both H3K4me2 and Kac, with 60 of the 62 genes that gain either modification in Δ*cac-1* also exhibiting gains in Δ*cac-2*, supporting a CAF-1-centric role in regulation of these modifications within facultative heterochromatin (Fig. S3.9C). Surprisingly, Δ*cac-2* displayed gains of H3K4me2 or Kac at an additional 60 genes compared to Δ*cac-1*, suggesting CAC-2 may play an alternative role in regulating these modifications outside of the CAF-1 complex (Fig. S3.9C).

Approximately 77% of H3K27me3-marked genes with gains in these H3K4me2 or Kac were upregulated in Δ*cac-1* or Δ*cac-2*, and changes in gene expression exhibited a weak positive correlation with enrichment of Kac in both Δ*cac-1* and Δ*cac-2*, while Δ*set-7* displayed little correlation (Fig. 3.4D, Fig. S3.9C & F). Plotting log2FC of H3K27me3 or H3K36me3 against log2FC of Kac in CAF-1-deficient mutants relative to WT revealed a weak negative correlation, while Δ*set-7* displayed no obvious correlation (Fig. 3.4D, Fig. S3.8D-F, Fig. S3.9E). Furthermore, clustering analysis revealed that genes that gain Kac experience the largest depletions of H3K27me3 in CAF-1-deficient mutants (Fig. 3.4A, Fig. S3.9B & S3.9D). Conversely, genes that only gained Kac in Δ*set-7* experienced no depletion of H3K27me3 in Δ*cac-1* or Δ*cac-2*, suggesting that elevated Kac is closely associated with local depletion of H3K27me3 in CAF-1-deficient mutants (Fig. 3.4A, Fig. S3.9B). Expectedly, genes that gained Kac in CAF-1-deficient mutants also experienced the largest increases in gene expression relative to WT, whereas the same was true for genes that gained Kac in Δ*set-7* (Fig. 3.4A). Collectively, these data suggest that upregulation of gene expression in CAF-1-deficient mutants is closely associated with changes in the chromatin environment that perturb PRC2 activity.

CAF-1 and PRC2 play distinct roles in gene repression

Genome-wide analysis of the epigenetic landscape in CAF-1-deficient mutants revealed significant impacts to the integrity of the facultative heterochromatin environment. Previous research from our lab has shown that genes within facultative heterochromatin regions are important for sexual development in *N. crassa*, and are not expressed during asexual growth unless H3K27me3 is perturbed (Courtney et al., 2020; Deaven et al., 2025; Ebot-Ojong et al., 2025; Kamei et al., 2021). H3K27me3-marked genes becoming upregulated in CAF-1-deficient

mutants despite persistence of PRC2 activity led us to ask if CAF-1 is directly involved in the PRC2 gene repression pathway. To address this question, we generated a double mutant for *cac-1* and the PRC2 subunit *suz-12* (Δ*cac-1*Δ*suz-12*), which allowed us to determine the impact of CAF-1 on gene silencing in the absence of H3K27me3. Δ*cac-1*Δ*suz-12* exhibited a striking silencing defect, with 500 of the 545 protein-coding H3K27me3-marked genes (~92%) exhibiting significant upregulation compared to WT (Fig. 3.5A-D). Notably, Δ*cac-1*Δ*suz-12* displayed upregulation of nearly every H3K27me3-marked gene upregulated in Δ*cac-1* or Δ*suz-12*, in addition to 146 genes that were not upregulated in either single mutant, suggesting that CAF-1 and PRC2 work in parallel to maintain proper gene repression at facultative heterochromatin (Fig. 3.5B & C). Plotting relative expression levels for individual genes across these 3 mutants revealed distinct clusters of genes upregulated in either Δ*cac-1* or Δ*suz-12*, further supporting this hypothesis. Interestingly, 4,577 genes were differentially expressed in Δ*cac-1*Δ*suz-12* (~47% of the genome), 2,699 of which were upregulated, suggesting that combined CAF-1 and PRC2-deficiency results in a genome-wide misregulation of gene expression (Fig. 3.5D). Collectively, these data suggest that CAF-1 and PRC2 play unique roles in maintaining gene repression and independently contribute to silencing of H3K27me3-marked genes.

CAF-1 and PRC2 work together to maintain the facultative heterochromatin environment

The observation of widespread gene misregulation in Δ*cac-1*Δ*suz-12* led us to ask this strain exhibited additional defects in the epigenetic environment when compared with the single mutants, particularly within facultative heterochromatin. ChIP-seq analysis in Δ*cac-1*Δ*suz-12* revealed an additive gain of H3K4me2 at 62 H3K27me3-marked genes (Fig. 3.6A, B, & D). This

included every gene that gained H3K4me2 in either Δ*cac-1 or* Δ*suz-12*, supporting the hypothesis that gains H3K4me2 are a result of H3K27me3 depletion (Fig. 3.6B & D). Interestingly, gains of Kac in Δ*cac-1*Δ*suz-12* were not additive but rather displayed a profile that was distinct from either single mutant. 33 genes gained acetylation in Δ*cac-1*Δ*suz-12* that were not differentially acetylated in either Δ*cac-1* or Δ*suz-12*, and the double mutant displayed partial overlap in acetylation profiles with both single mutants (Fig. 3.6C & D, Fig. S3.12A & B). This suggests that the acetylation pattern observed in Δ*cac-1* is redistributed upon depletion of H3K27me3. Interestingly, genes that gained Kac in Δ*cac-1* exhibited similar gene expression profiles in Δ*cac-1*Δ*suz-12*, suggesting that upregulation of these genes may occur upstream of Kac deposition (Fig. S3.12A & SB). Indeed, plotting log2FC of Kac against log2FC of gene expression for Δ*cac-1*Δ*suz-12* relative to WT revealed no obvious correlation.

We also decided to assay levels of H3K36me3 in the Δ*cac-1*Δ*suz-12* to see how ASH-1 catalytic activity was impacted. ChIP-seq analysis revealed a more severe loss of H3K36me3 at H3K27me3-marked genes in Δ*cac-1*Δ*suz-12* than either Δ*cac-1* or Δ*suz-12*, particularly within gene bodies (Fig. 3.6E & F). Genes outside of facultative heterochromatin regions that lose H3K36me2/3 in *ash-1(Y888F)* exhibited no further defect in H3K36me3 compared with Δ*cac-1* (Fig. S3.12D). Interestingly, H3K36me3 at SET-2-methylated genes was reduced in all 3 ChIP-seq experiments performed on Δ*cac-1*Δ*suz-12*, unlike what was observed for either single mutant (Fig. 3.6E, Fig. S3.12D). Collectively, these data suggest that CAF-1 and PRC2 work in parallel to properly maintain the facultative heterochromatin environment.

Discussion

The mechanisms that underly facultative heterochromatin formation and maintenance have remained a topic of extensive research. Leveraging the *N. crassa* model system, we show that the CAF-1 histone chaperone complex is required for repression of H3K27me3-marked genes and maintenance of the facultative heterochromatin environment, and that its role in these processes is independent of PRC2 activity.

CAF-1 is important for gene silencing genome-wide

We identified CAF-1 as the only H3/H4 histone chaperone whose mutation resulted in derepression of H3K27me3-marked genes, and genome-wide analysis revealed that this silencing defect was not limited to genes within facultative heterochromatin (Fig. 3.1). These results are consistent with previous work that implicates CAF-1 in gene silencing across many model systems, although the exact mechanisms remain unclear. Previous work suggests that CAF-1-deficiency results in lower nucleosome occupancy and altered assembly kinetics, specifically during S phase, which may provide a window of opportunity for transcription factors, RNA polymerase, and other transcriptional machinery to bind to promoters before chromatin is ultimately reassembled by other factors (Barrientos-Moreno et al., 2023; Chen et al., 2023; Cheng et al., 2019; Fennessy & Owen-Hughes, 2016; Munoz-Viana et al., 2017). This could explain the upregulation of genes within heterochromatin regions in particular, as heterochromatic DNA has been shown to be packaged quickly and efficiently after passage of the replication fork. Alternatively other H3/H4 chaperones that fill in gaps left by CAF-1's absence could incorporate other histone variants or directly contribute to recruitment of transcriptional machinery to these sites. Indeed, prior studies using HeLa cells have shown that

the H3/H4 chaperone HIRA incorporates histone H3.3 variants at gaps left behind when CAF-1 activity is impaired during replication, and that H3.3 signal was highly correlated with enrichment of RNA pol II (Ray-Gallet et al., 2011). To try and determine the driving force behind the silencing defects in CAF-1-deficient mutants, we decided to profile the chromatin environment to determine if changes in gene expression were associated with changes to the epigenome.

CAF-1 deficiency leads to defects in the heterochromatin environment

The observation that many H3K27me3-marked genes were upregulated in response to CAF-1 deficiency prompted us to begin our epigenetic analyses by assaying H3K27me3 enrichment, which unsurprisingly revealed a significant defect in normal H3K27me3 occupancy (Fig. 3.2). Interestingly, we did not observe a significant global loss of H3K27me3, but rather a rearrangement of H3K27me3 patterns genome-wide, suggesting that overall PRC2 activity was not reduced in the absence of CAF-1 (Fig. 3.2B-D). What causes this rearrangement is unknown, but we hypothesize that displacement from upregulated genes "frees up" more PRC2 to methylate other regions of the genome. This is in line with a "source-sink" hypothesis, in which WT conditions would normally isolate PRC2 activity (the source) to a specific set of loci that most strongly recruit the complex (the sink) (Murphy & Berger, 2023). However, many upregulated genes fell within loci that did not exhibit H3K27me3 depletion, suggesting that other factors contribute to the observed H3K27me3 defect.

This observation motivated us to assay levels of other histone PTMs in the CAF-1 mutants, starting with H3K36me3 as a logical next step considering its known roles in transcriptional regulation, and its co-localization with H3K27me3 in fungi (Bicocca et al., 2018;

Carrozza et al., 2005; Keogh et al., 2005; Moller et al., 2023; Xu et al., 2024). We observed that CAF-1-deficiency resulted in a subtle decrease of H3K36me3 at genes that lose the PTM in the absence of ASH-1 catalytic activity (Fig. 3.3, Fig. S3.7). Based on these data, we hypothesize that CAF-1 deficiency may reduce the efficiency at which the ASH-1 complex is able to perform its catalytic function. One possibility is that reduced histone occupancy at ASH-1-methylated genes during S phase could eliminate the availability of a substrate for ASH-1 to act on, which may contribute to the observed silencing defect. Alternatively, increased transcription of ASH-1-methylated genes might recruit SET-2 in place of ASH-1, which could explain the greater loss of H3K36me3 at promoters versus gene bodies in both CAF-1- and PRC2-deficient mutants (Fig. 3.3B & C). By the same logic, it is possible that decreased ASH-1 activity at H3K27me3-marked genes results in a larger proportion of ASH-1 complexes acting outside of facultative heterochromatin. This may be consistent with the observed redistribution of H3K27me3 to genes that are downregulated in CAF-1-deficient and ASH-1 catalytic mutants.

Future work should include biochemical experiments to determine if CAF-1 directly interacts with ASH-1, or if CAF-1-deficiency alters ASH-1's association with chromatin. Furthermore, determining what stages of the cell cycle ASH-1 is most highly expressed could provide more context as to when H3K36 methylation is re-established at promoters post-DNA replication. Collectively, these observations shed light on the relationship between H3K27me3, H3K36me3, and gene expression in eukaryotic fungi, and agrees with recent studies which suggest that H3K27me3 and H3K36me3 exhibit crosstalk activity in these systems.

CAF-1 inhibition Results in a more active chromatin environment

Our observations of elevated expression and loss of H3K27me3 and H3K36me3 at genes within facultative heterochromatin led us to ask if these changes were accompanied by gains in PTMs associated with active transcription. Indeed, ChIP-seq experiments for H3K4me2 and Kac revealed elevated levels of both PTMs at sites of H3K27me3 depletion (Fig. 3.4, Fig. S3.9). Gains of H3K4me2 within facultative heterochromatin in CAF-1-deficient mutants largely coincided with the observed gains in PRC2-deficient mutants, which suggests that H3K4me2 is deposited as a result of H3K27me3 depletion at these genes as opposed to elevated levels of gene expression (Fig. 3.4C, Fig. S3.9A). Conversely, gains in Kac were distinct between CAF-1 and PRC2-deficient mutants and overlapped closely with both elevated gene expression and H3K27me3 depletion in CAF-1 deficient mutants (Fig. 3.4A & C, Fig. S3.9B). This observation, in addition to the fact that PRC2-deficient mutants did not display elevated Kac levels at the same genes, supports a model in which elevated lysine acetylation precedes loss of H3K27me3 in CAF-1-deficient mutants. This would be in line with the observations made for repressive modifications in CAF-1-deficient mutants, as acetylation, particularly on H3K27, is known to antagonize PRC2 activity, and efficient deacetylation is required for H3K36me3 deposition during transcription (Carrozza et al., 2005; Creyghton et al., 2010; Keogh et al., 2005; Pasini et al., 2010; Tie et al., 2009; Venkatesh & Workman, 2013).

While it is unsurprising that gains in Kac are correlated with increased expression of H3K27me3-marked genes, it is still unclear which occurs first. A model in which CAF-1 deficiency results in reduced nucleosome occupancy and increased gene expression during S-phase may create a more accessible chromatin environment that allows histone acetyltransferases (HATs) to deposit acetylation co-transcriptionally. This would explain both the observed defects

in gene silencing and H3K27me3 patterning at facultative heterochromatin in CAF-1-deficient mutants. Alternatively, it is possible that CAF-1-deficiency leads to defective recruitment of HDAC complexes, which may result in hyper-acetylation at facultative heterochromatin. This could then promote transcription, ultimately resulting in reduced H3K27me3 and ASH-1-catalyzed H3K36me3. Indeed, CAF-1 is necessary for normal activity of Sir deacetylase proteins in *S. cerevisiae* (Huang et al., 2007; Sharp et al., 2003; Tamburini et al., 2006). Furthermore, it is known that the CAC-3 subunit of CAF-1 also a member of HDAC complexes, in addition to both PRC2 and ASH-1 across multiple model systems (Lin et al., 2022; Martinez-Balbas et al., 1998; Zhang et al., 1997). It is possible that this protein helps coordinate the activity of all these complexes at heterochromatin, and perturbing any part of this pathway leads to altered activity or association of CAC-3 with the other complexes. Indeed, CAC-3 mutation leads to severe defects in silencing and heterochromatin formation that are distinct from either CAF-1 or PRC2-deficient mutants, suggesting that the activity of all these complexes is altered (Fig. S3.13). Further experimentation will be needed to elucidate the mechanism behind the gains in Kac and determine if they are directly responsible for the H3K27me3 defects observed in CAF-1-deficient mutants.

CAF-1 and PRC2 play unique roles in gene repression and heterochromatin maintenance

We observed that a unique set of H3K27me3-marked genes were upregulated between CAF-1 and PRC2-deficient mutants, leading us to ask what the consequences of dual CAF-1 and PRC2-deficiency would be on gene repression and heterochromatin environment. (Fig. 3.1B & E, Fig. 3.6B). RNA-seq experiments revealed a widespread, robust upregulation of almost all H3K27me3-marked genes in a Δcac-1Δsuz-12 mutant (Fig 3.5A-C). This suggests that while

CAF-1-deficiency results in upregulation of a subset of H3K27me3-marked genes, PRC2 activity is still able to maintain repression of others and vice versa. Additionally, nearly half the genome was differentially expressed in this mutant, representing a much higher ratio than what is observed for either single mutant (Fig. 3.5D). The split between upregulated and downregulated genes was approximately 60-40, which likely suggests that induction of hundreds of genes that are usually repressed in WT mycelia results in downregulation of genes that are normally highly expressed due to limited availability of transcriptional machinery.

These results motivated us to assay levels of H3K4me2 and Kac in Δ*cac-1*Δ*suz-12*, which revealed a unique profile in each modification compared with either single mutant. While gains of H3K4me2 at H3K27me3-marked genes were additive, Kac displayed a "hybrid" enrichment pattern, displaying partial overlaps with both Δ*cac-1 and* Δ*suz-12,* in addition to emergence of novel peaks (Fig 3.6B-D). These data also support a source-sink-like model, in which HATs are ectopically recruited the regions of H3K27me3 depletion, which would explain why Kac is redirected when a H3K27me3 is depleted compared to a Δ*cac-1* background. Furthermore, the observation that expression of these genes is induced in Δ*cac-1*Δ*suz*-12, even in the absence of elevated Kac, suggests that transcription may precede Kac deposition at these genes, although whether or not this induction would occur in a Δ*cac-1* mutant in the absence of increased Kac remains unclear.

In agreement with the increased levels of gene expression and active chromatin modifications, Δ*cac-1*Δ*suz-12* also displayed an additive loss of H3K36me3 at H3K27me3-marked genes (Fig. 3.6E). This suggests that ASH-1 methyltransferase activity at these genes is closely tied to transcriptional repression by CAF-1 and PRC2. Interestingly SET-2 methylated genes also displayed reduced H3K36me3 at gene bodies in Δ*cac-1*Δ*suz-12*, a phenotype more

consistent with an *ash-1(Y888F)* mutation than that of either single mutant (Fig. 3.6E, Fig. S3.12D). This observation may agree with the hypothesis that SET-2 is being pulled away from its normal targets, due to many normally repressed genes being transcribed in this mutant. In summary, we hypothesize that Δ*cac-1*Δ*suz-12* experiences a major shift from a repressive to permissive chromatin environment, particularly within facultative heterochromatin regions, resulting in widespread transcriptional upregulation of otherwise silenced genes.

In conclusion, this study elucidates a clear role for the replication-dependent histone chaperone CAF-1 in PRC2 gene repression and facultative heterochromatin formation. We show that CAF-1 inhibition leads to a significant defect in H3K27me3-marked gene repression, accompanied by a loss of H3K27me3 and H3K36me3 at promoters and gene bodies. This results in a more permissive chromatin environment, characterized by gains in H3K4me2 and Kac, PTMs associated with active transcription and accessible chromatin. These phenotypes are not fully recapitulated in PRC2-deficient mutants, suggesting that the CAF-1 complex plays a unique role in maintaining facultative heterochromatin independent of PRC2.

Further experimentation will be needed to determine the exact mechanism behind the H3K27me3 defect in CAF-1-deficient mutants. While the catalytic activity of PRC2 does not seem to be significantly reduced, our data show a clear mislocalization of the complex across the genome. Whether this is a result of elevated transcription levels, inhibition of PRC2 by other PTMs, changes in chromatin accessibility, a combination of these factors, or an alternative pathway remains unclear. Our results support the conclusions from prior studies, which have shown that CAF-1 perturbations lead to significant defects in chromatin structure and gene silencing within heterochromatic regions across many eukaryotes. It will be interesting to further study the mechanisms that underly CAF-1's repressive activity, as these studies may shed light

on the importance of proper chromatin assembly kinetics post-DNA replication in faithfully maintaining transcriptional repression and the epigenetic environment.

Materials and Methods

Strains generation and growth conditions

Knockout strains not obtained from the KO collection were generated by transforming a hygromycin resistant construct at the gene of interest and plating on selective media. Heterokaryotic strains were backcrossed to WT to obtain homokaryotic mutants. Crosses were performed on low-nitrogen synthetic cross (SC) media as previously described (Davis & de Serres, 1970). Spores were collected 14 days post-fertilization, germinated on SC plates, and picked to selective media slants. Strains were genotyped by PCR or western blotting. Strains for ChIP and RNA-seq experiments were grown overnight in Vogel's minimal media as described in (Davis & de Serres, 1970). Complementation strains were generated by transforming 3xFLAG-tagged, full length gene constructs into the his-3 locus of strains harboring a mutation for the complemented genes. The *cac-1-3xFLAG::his-3*$^{+}$ complement was generated by crossing a strain with the complement construct into a *cac-1* mutant, as this strain was unable to be transformed, likely due to known defects in homologous recombination and DNA repair (Linger & Tyler, 2005; Park et al., 2011).

RNA isolation:

RNA extraction was performed as previously described (Zhou et al., 2018). Briefly, total RNA was extracted using TRIzol reagent (Thermo Fisher; Cat #:15596026) and then purified with 7.5 M LiCl. RNA purity was analyzed on agarose gels prior to library preparation.

ChIP-seq and ChIP-qPCR:

ChIP experiments were performed as previously described (Ferraro & Lewis, 2018), using antibodies in Table S3. ChIP samples were analyzed by Illumina sequencing and qPCR (SYBR Green Universal Master Mix, Bio-Rad, 4309155)

ChIP and RNA library preparation

ChIP Libraries were constructed as previously described (Courtney et al., 2020; Ferraro & Lewis, 2018). Size selection with magnetic beads was performed after the adapter ligation and PCR steps with Sera-Mag SpeedBeads (65152105050250) suspended in a solution of 20 mM PEG 8000, 1 mM NaCl, 10 mM Tris-HCl, 1 mM EDTA (Rohland & Reich, 2012). RNA Libraries were prepared using a NEBNext Ultra II Directional RNA Library Prep Kit according to manufacturer specifications (E7760S).

DNA transformation:

DNA transformations were performed as previously described in (Margolin et al., 1997). Transformants were picked to selective media slants and genotyped by PCR or western blotting.

Protein extraction & western blotting:

Cultures were grown in a shaking incubator overnight (~18-22 hours) in liquid VMM + 1.5% sucrose at 32 °C and 180 rpm. Cultures were harvested and washed with 1x PBS, and protein was extracted by sonicating tissue on ice for 1 min. (60 sec. on, 60 sec. off; 30 µm Amplitude) in protein extraction buffer (50 mM HEPES pH 7.5, 150 mM NaCl, 1 mM EDTA, 0.02% IGEPAL, 1 mM PMSF, 1x Protease Inhibitor Cocktail; Cat #: HY-K0011). Cell lysates

were centrifuged at 17,000 g (~13,300 rpm) at 4 °C, and the supernatant containing protein extract was mixed 3:1 with 4x Laemmli sample buffer (Bio-Rad, 1610747), boiled at 95 °C for 3 minutes, and run on SDS-PAGE gels at 185 V for ~45 minutes. Western blots probing for 3xFLAG-tagged constructs were transferred to 0.45 um membranes (1.5 hours wet transfer in Towbin's buffer) and blocked for 1 hour in 5% milk in TBST, then incubated at 4 C overnight with an anti-M2-FLAG antibody (Sigma-Aldrich, F1804) in 5% milk in TBST. Western blots probing for H3K27me3 constructs were transferred to 0.45 um membranes (7-minute Trans-Blot Turbo Transfer, 1704150) and blocked for 1 hour in 5% BSA in TBST, then incubated at 4 C overnight with an anti-H3K27me3 antibody (diagenode, NBP2-59295) in in 5% BSA in TBST. Anti-mouse and anti-rabbit primary antibodies were probed with Goat anti-Mouse IgG (H+L), HRP (Fisher, 31430) and Goat anti-Rabbit IgG (H+L), HRP (Fisher, 31460) secondary antibodies respectively. Membranes were developed using West-Femto Maximum Sensitivity Substrate (34094) for 5 minutes and imaged on a Bio-Rad chemidoc imaging system (12003153).

Bioinformatic analyses

Peaks were called for all ChIP-seq samples using MACS3 (v3.0.1). ChIP-seq enrichment was quantified using the csaw package in R (v1.42.0) and normalizing to input samples. H3K27me3 and H3K36me3 enrichment was calculated from 500 bp upstream to 300 bp downstream of the TSS. Kac was calculated from 1000 bp upstream to 800 bp downstream of the TSS. H3K4me2 enrichment was calculated over the whole gene body (TSS to TES). Genes were considered enriched for H3K27me3 if they exhibited > 1 log2FC, and their gene bodies and promoters fell within H3K27me3 MACS3 peak calls. Genes were considered enriched for

H3K36me3, H3K4me2, or Kac if they exhibited > 0 log2FC over input. Genes were considered differently enriched if they exhibited ± 0.75 log2FC (~1.7-fold change) enrichment compared to WT for H3K27me3, H3K36me3 and H3K4me2, and ± 0.585 log2FC (~1.5-fold change) enrichment compared to WT for Kac. RNA-seq data was analyzed using the DEseq package in R (v1.48.2). Genes were considered "repressed" if they exhibited < 10 TPM on average across WT samples. Genes were considered differentially expressed if they exhibited ± 1 log2FC (2-fold change) in expression compared to WT and an adjusted p-value of < 0.05.

Data availability:

Prior to publication, sequencing data generated at the University of Georgia will be deposited to the National Center for Biotechnology Information's Gene Expression Omnibus database (https://www.ncbi.nlm.nih.gov/geo). A summary list of Sequence Read Archive (https://www.ncbi.nlm.nih.gov/sra) accession numbers and associated strain information for samples generated at the Joint Genome Institute and other previously published datasets analyzed in this study are included in Supplementary Table S3.4. All scripts used are publicly available on GitHub at https://github.com/eddietorres24/Research.

References

Alabert, C., & Groth, A. (2012). Chromatin replication and epigenome maintenance. *Nat Rev Mol Cell Biol*, *13*(3), 153–167. https://doi.org/10.1038/nrm3288

Alabert, C., Loos, C., Voelker-Albert, M., Graziano, S., Forne, I., Reveron-Gomez, N., Schuh, L., Hasenauer, J., Marr, C., Imhof, A., & Groth, A. (2020). Domain Model Explains Propagation Dynamics and Stability of Histone H3K27 and H3K36 Methylation Landscapes. *Cell Rep*, *30*(4), 1223–1234 e1228. https://doi.org/10.1016/j.celrep.2019.12.060

Allis, C. D., & Jenuwein, T. (2016). The molecular hallmarks of epigenetic control. *Nat Rev Genet*, *17*(8), 487–500. https://doi.org/10.1038/nrg.2016.59

Allshire, R. C., & Madhani, H. D. (2018). Ten principles of heterochromatin formation and function. *Nat Rev Mol Cell Biol*, *19*(4), 229–244. https://doi.org/10.1038/nrm.2017.119

Aramayo, R., & Selker, E. U. (2013). Neurospora crassa, a model system for epigenetics research. *Cold Spring Harb Perspect Biol*, *5*(10), a017921. https://doi.org/10.1101/cshperspect.a017921

Barrientos-Moreno, M., Maya-Miles, D., Murillo-Pineda, M., Fontalva, S., Perez-Alegre, M., Andujar, E., & Prado, F. (2023). Transcription and FACT facilitate the restoration of replication-coupled chromatin assembly defects. *Sci Rep*, *13*(1), 11397. https://doi.org/10.1038/s41598-023-38280-w

Basenko, E. Y., Sasaki, T., Ji, L., Prybol, C. J., Burckhardt, R. M., Schmitz, R. J., & Lewis, Z. A. (2015). Genome-wide redistribution of H3K27me3 is linked to genotoxic stress and defective growth. *Proc Natl Acad Sci U S A*, *112*(46), E6339–6348. https://doi.org/10.1073/pnas.1511377112

Bastow, R., Mylne, J. S., Lister, C., Lippman, Z., Martienssen, R. A., & Dean, C. (2004). Vernalization requires epigenetic silencing of FLC by histone methylation. *Nature*, *427*(6970), 164–167. https://doi.org/10.1038/nature02269

Bernstein, B. E., Mikkelsen, T. S., Xie, X., Kamal, M., Huebert, D. J., Cuff, J., Fry, B., Meissner, A., Wernig, M., Plath, K., Jaenisch, R., Wagschal, A., Feil, R., Schreiber, S. L., & Lander, E. S. (2006). A bivalent chromatin structure marks key developmental genes in embryonic stem cells. *Cell*, *125*(2), 315–326. https://doi.org/10.1016/j.cell.2006.02.041

Bicocca, V. T., Ormsby, T., Adhvaryu, K. K., Honda, S., & Selker, E. U. (2018). ASH1-catalyzed H3K36 methylation drives gene repression and marks H3K27me2/3-competent chromatin. *Elife*, *7*. https://doi.org/10.7554/eLife.41497

Blackledge, N. P., & Klose, R. J. (2021). The molecular principles of gene regulation by Polycomb repressive complexes. *Nat Rev Mol Cell Biol*, *22*(12), 815–833. https://doi.org/10.1038/s41580-021-00398-y

Cao, R., Wang, L., Wang, H., Xia, L., Erdjument-Bromage, H., Tempst, P., Jones, R. S., & Zhang, Y. (2002). Role of histone H3 lysine 27 methylation in Polycomb-group silencing. *Science*, *298*(5595), 1039–1043. https://doi.org/10.1126/science.1076997

Carrozza, M. J., Li, B., Florens, L., Suganuma, T., Swanson, S. K., Lee, K. K., Shia, W. J., Anderson, S., Yates, J., Washburn, M. P., & Workman, J. L. (2005). Histone H3 methylation by Set2 directs deacetylation of coding regions by Rpd3S to suppress spurious intragenic transcription. *Cell*, *123*(4), 581–592. https://doi.org/10.1016/j.cell.2005.10.023

Cheloufi, S., Elling, U., Hopfgartner, B., Jung, Y. L., Murn, J., Ninova, M., Hubmann, M., Badeaux, A. I., Euong Ang, C., Tenen, D., Wesche, D. J., Abazova, N., Hogue, M., Tasdemir, N., Brumbaugh, J., Rathert, P., Jude, J., Ferrari, F., Blanco, A.,…Hochedlinger, K. (2015). The histone chaperone CAF-1 safeguards somatic cell identity. *Nature*, *528*(7581), 218–224. https://doi.org/10.1038/nature15749

Chen, B., MacAlpine, H. K., Hartemink, A. J., & MacAlpine, D. M. (2023). Spatiotemporal kinetics of CAF-1-dependent chromatin maturation ensures transcription fidelity during S-phase. *bioRxiv*. https://doi.org/10.1101/2023.05.25.541209

Cheng, L., Zhang, X., Wang, Y., Gan, H., Xu, X., Lv, X., Hua, X., Que, J., Ordog, T., & Zhang, Z. (2019). Chromatin Assembly Factor 1 (CAF-1) facilitates the establishment of facultative heterochromatin during pluripotency exit. *Nucleic Acids Res*, *47*(21), 11114–11131. https://doi.org/10.1093/nar/gkz858

Collemare, J., & Seidl, M. F. (2019). Chromatin-dependent regulation of secondary metabolite biosynthesis in fungi: is the picture complete? *FEMS Microbiol Rev*, *43*(6), 591–607. https://doi.org/10.1093/femsre/fuz018

Connolly, L. R., Smith, K. M., & Freitag, M. (2013). The Fusarium graminearum histone H3 K27 methyltransferase KMT6 regulates development and expression of secondary metabolite gene clusters. *PLoS Genet*, *9*(10), e1003916. https://doi.org/10.1371/journal.pgen.1003916

Courtney, A. J., Kamei, M., Ferraro, A. R., Gai, K., He, Q., Honda, S., & Lewis, Z. A. (2020). Normal Patterns of Histone H3K27 Methylation Require the Histone Variant H2A.Z in Neurospora crassa. *Genetics*, *216*(1), 51–66. https://doi.org/10.1534/genetics.120.303442

Creyghton, M. P., Cheng, A. W., Welstead, G. G., Kooistra, T., Carey, B. W., Steine, E. J., Hanna, J., Lodato, M. A., Frampton, G. M., Sharp, P. A., Boyer, L. A., Young, R. A., & Jaenisch, R. (2010). Histone H3K27ac separates active from poised enhancers and predicts developmental state. *Proc Natl Acad Sci U S A*, *107*(50), 21931–21936. https://doi.org/10.1073/pnas.1016071107

Davis, R. H., & de Serres, F. J. (1970). [4] Genetic and microbiological research techniques for Neurospora crassa. In *Methods in Enzymology* (Vol. 17, pp. 79–143). Academic Press. https://doi.org/https://doi.org/10.1016/0076-6879(71)17168-6

Deaven, A. M., Ameri-Solanky, A. J., & Lewis, Z. A. (2025). Polycomb repressive complex 2 regulates sexual development in Neurospora crassa. *mBio*, e0150525. https://doi.org/10.1128/mbio.01505-25

Di Croce, L., & Helin, K. (2013). Transcriptional regulation by Polycomb group proteins. *Nat Struct Mol Biol*, *20*(10), 1147–1155. https://doi.org/10.1038/nsmb.2669

Dohke, K., Miyazaki, S., Tanaka, K., Urano, T., Grewal, S. I., & Murakami, Y. (2008). Fission yeast chromatin assembly factor 1 assists in the replication-coupled maintenance of heterochromatin. *Genes Cells*, *13*(10), 1027–1043. https://doi.org/10.1111/j.1365-2443.2008.01225.x

Dreyer, J., Ricci, G., van den Berg, J., Bhardwaj, V., Funk, J., Armstrong, C., van Batenburg, V., Sine, C., VanInsberghe, M. A., Marsman, R., Mandemaker, I. K., di Sanzo, S., Costantini, J., Manzo, S. G., Biran, A., Burny, C., Volker-Albert, M., Groth, A., Spencer, S. L.,…Mattiroli, F. (2024). Acute multi-level response to defective de novo chromatin assembly in S-phase. *bioRxiv*. https://doi.org/10.1101/2024.03.22.586291

Dunlap, J. C., Borkovich, K. A., Henn, M. R., Turner, G. E., Sachs, M. S., Glass, N. L., McCluskey, K., Plamann, M., Galagan, J. E., Birren, B. W., Weiss, R. L., Townsend, J. P., Loros, J. J., Nelson, M. A., Lambreghts, R., Colot, H. V., Park, G., Collopy, P., Ringelberg, C.,…Xu, J. (2007). Enabling a community to dissect an organism: overview of the Neurospora functional genomics project. *Adv Genet*, *57*, 49–96. https://doi.org/10.1016/S0065-2660(06)57002-6

Ebot-Ojong, F., Ferraro, A. R., Yap, R. E., Kaddar, F., Hull-Crew, C., Scadden, A. W., Deaven, A. M., Klocko, A. D., & Lewis, Z. A. (2025). HISTONE DEACETYLASE-1 is required for epigenome stability in Neurospora crassa. *Proc Natl Acad Sci U S A*, *122*(40), e2503876122. https://doi.org/10.1073/pnas.2503876122

Enomoto, S., & Berman, J. (1998). Chromatin assembly factor I contributes to the maintenance, but not the re-establishment, of silencing at the yeast silent mating loci. *Genes Dev*, *12*(2), 219–232. https://doi.org/10.1101/gad.12.2.219

Fennessy, R. T., & Owen-Hughes, T. (2016). Establishment of a promoter-based chromatin architecture on recently replicated DNA can accommodate variable inter-nucleosome spacing. *Nucleic Acids Res*, *44*(15), 7189–7203. https://doi.org/10.1093/nar/gkw331

Ferraro, A. R., & Lewis, Z. A. (2018). ChIP-Seq Analysis in Neurospora crassa. In R. P. de Vries, A. Tsang, & I. V. Grigoriev (Eds.), *Fungal Genomics: Methods and Protocols* (pp. 241–250). Springer New York. https://doi.org/10.1007/978-1-4939-7804-5_19

Francis, N. J., Kingston, R. E., & Woodcock, C. L. (2004). Chromatin compaction by a polycomb group protein complex. *Science*, *306*(5701), 1574–1577. https://doi.org/10.1126/science.1100576

Franklin, R., Guo, Y., He, S., Chen, M., Ji, F., Zhou, X., Frankhouser, D., Do, B. T., Chiem, C., Jang, M., Blanco, M. A., Vander Heiden, M. G., Rockne, R. C., Ninova, M., Sykes, D. B., Hochedlinger, K., Lu, R., Sadreyev, R. I., Murn, J.,…Cheloufi, S. (2022). Regulation of chromatin accessibility by the histone chaperone CAF-1 sustains lineage fidelity. *Nat Commun*, *13*(1), 2350. https://doi.org/10.1038/s41467-022-29730-6

Franklin, R., Zhang, B., Frazier, J., Chen, M., Do, B. T., Padayao, S., Wu, K., Vander Heiden, M. G., Vakoc, C. R., Roe, J. S., Ninova, M., Murn, J., Sykes, D. B., & Cheloufi, S. (2025). Histone chaperones coupled to DNA replication and transcription control divergent chromatin elements to maintain cell fate. *Genes Dev*, *39*(9-10), 652–675. https://doi.org/10.1101/gad.352316.124

Fraser, C. J., & Whitehall, S. K. (2022). Heterochromatin in the fungal plant pathogen, Zymoseptoria tritici: Control of transposable elements, genome plasticity and virulence. *Front Genet*, *13*, 1058741. https://doi.org/10.3389/fgene.2022.1058741

Grewal, S. I. S. (2023). The molecular basis of heterochromatin assembly and epigenetic inheritance. *Mol Cell*, *83*(11), 1767–1785. https://doi.org/10.1016/j.molcel.2023.04.020

Gurard-Levin, Z. A., Quivy, J. P., & Almouzni, G. (2014). Histone chaperones: assisting histone traffic and nucleosome dynamics. *Annu Rev Biochem*, *83*, 487–517. https://doi.org/10.1146/annurev-biochem-060713-035536

Hammond, C. M., Stromme, C. B., Huang, H., Patel, D. J., & Groth, A. (2017). Histone chaperone networks shaping chromatin function. *Nat Rev Mol Cell Biol*, *18*(3), 141–158. https://doi.org/10.1038/nrm.2016.159

Hoek, M., & Stillman, B. (2003). Chromatin assembly factor 1 is essential and couples chromatin assembly to DNA replication in vivo. *Proc Natl Acad Sci U S A*, *100*(21), 12183–12188. https://doi.org/10.1073/pnas.1635158100

Houlard, M., Berlivet, S., Probst, A. V., Quivy, J. P., Hery, P., Almouzni, G., & Gerard, M. (2006). CAF-1 is essential for heterochromatin organization in pluripotent embryonic cells. *PLoS Genet*, *2*(11), e181. https://doi.org/10.1371/journal.pgen.0020181

Huang, H., Yu, Z., Zhang, S., Liang, X., Chen, J., Li, C., Ma, J., & Jiao, R. (2010). Drosophila CAF-1 regulates HP1-mediated epigenetic silencing and pericentric heterochromatin stability. *J Cell Sci*, *123*(Pt 16), 2853–2861. https://doi.org/10.1242/jcs.063610

Huang, S., Zhou, H., Tarara, J., & Zhang, Z. (2007). A novel role for histone chaperones CAF-1 and Rtt106p in heterochromatin silencing. *EMBO J*, *26*(9), 2274–2283. https://doi.org/10.1038/sj.emboj.7601670

Ishiuchi, T., Enriquez-Gasca, R., Mizutani, E., Boskovic, A., Ziegler-Birling, C., Rodriguez-Terrones, D., Wakayama, T., Vaquerizas, J. M., & Torres-Padilla, M. E. (2015). Early embryonic-like cells are induced by downregulating replication-dependent chromatin assembly. *Nat Struct Mol Biol*, *22*(9), 662–671. https://doi.org/10.1038/nsmb.3066

Jamieson, K., Rountree, M. R., Lewis, Z. A., Stajich, J. E., & Selker, E. U. (2013). Regional control of histone H3 lysine 27 methylation in Neurospora. *Proc Natl Acad Sci U S A*, *110*(15), 6027–6032. https://doi.org/10.1073/pnas.1303750110

Janevska, S., Baumann, L., Sieber, C. M. K., Munsterkotter, M., Ulrich, J., Kamper, J., Guldener, U., & Tudzynski, B. (2018). Elucidation of the Two H3K36me3 Histone Methyltransferases Set2 and Ash1 in Fusarium fujikuroi Unravels Their Different Chromosomal Targets and a Major Impact of Ash1 on Genome Stability. *Genetics*, *208*(1), 153–171. https://doi.org/10.1534/genetics.117.1119

Janssen, A., Colmenares, S. U., & Karpen, G. H. (2018). Heterochromatin: Guardian of the Genome. *Annu Rev Cell Dev Biol*, *34*, 265–288. https://doi.org/10.1146/annurev-cellbio-100617-062653

Jiang, D., & Berger, F. (2017). DNA replication-coupled histone modification maintains Polycomb gene silencing in plants. *Science*, *357*(6356), 1146–1149. https://doi.org/10.1126/science.aan4965

Kamei, M., Ameri, A. J., Ferraro, A. R., Bar-Peled, Y., Zhao, F., Ethridge, C. L., Lail, K., Amirebrahimi, M., Lipzen, A., Ng, V., Grigoriev, I. V., Schmitz, R. J., Liu, Y., & Lewis, Z. A. (2021). IMITATION SWITCH is required for normal chromatin structure and gene repression in PRC2 target domains. *Proc Natl Acad Sci U S A*, *118*(4). https://doi.org/10.1073/pnas.2010003118

Kaufman, P. D., Kobayashi, R., Kessler, N., & Stillman, B. (1995). The p150 and p60 subunits of chromatin assembly factor I: a molecular link between newly synthesized histones and DNA replication. *Cell*, *81*(7), 1105–1114. https://doi.org/10.1016/s0092-8674(05)80015-7

Keogh, M. C., Kurdistani, S. K., Morris, S. A., Ahn, S. H., Podolny, V., Collins, S. R., Schuldiner, M., Chin, K., Punna, T., Thompson, N. J., Boone, C., Emili, A., Weissman, J. S., Hughes, T. R., Strahl, B. D., Grunstein, M., Greenblatt, J. F., Buratowski, S., & Krogan, N. J. (2005). Cotranscriptional set2 methylation of histone H3 lysine 36 recruits a repressive Rpd3 complex. *Cell*, *123*(4), 593–605. https://doi.org/10.1016/j.cell.2005.10.025

Kim, K. H., & Roberts, C. W. (2016). Targeting EZH2 in cancer. *Nat Med*, *22*(2), 128–134. https://doi.org/10.1038/nm.4036

Kouzarides, T. (2007). Chromatin modifications and their function. *Cell*, *128*(4), 693–705. https://doi.org/10.1016/j.cell.2007.02.005

Li, B., Carey, M., & Workman, J. L. (2007). The role of chromatin during transcription. *Cell*, *128*(4), 707–719. https://doi.org/10.1016/j.cell.2007.01.015

Lin, C., Wu, Z., Shi, H., Yu, J., Xu, M., Lin, F., Kou, Y., & Tao, Z. (2022). The additional PRC2 subunit and Sin3 histone deacetylase complex are required for the normal distribution of H3K27me3 occupancy and transcriptional silencing in Magnaporthe oryzae. *New Phytol*, *236*(2), 576–589. https://doi.org/10.1111/nph.18383

Linger, J., & Tyler, J. K. (2005). The yeast histone chaperone chromatin assembly factor 1 protects against double-strand DNA-damaging agents. *Genetics*, *171*(4), 1513–1522. https://doi.org/10.1534/genetics.105.043000

Liu, C. P., Yu, Z., Xiong, J., Hu, J., Song, A., Ding, D., Yu, C., Yang, N., Wang, M., Yu, J., Hou, P., Zeng, K., Li, Z., Zhang, Z., Zhang, X., Li, W., Zhang, Z., Zhu, B., Li, G., & Xu, R. M. (2023). Structural insights into histone binding and nucleosome assembly by chromatin assembly factor-1. *Science*, *381*(6660), eadd8673. https://doi.org/10.1126/science.add8673

Liu, W. H., Roemer, S. C., Zhou, Y., Shen, Z. J., Dennehey, B. K., Balsbaugh, J. L., Liddle, J. C., Nemkov, T., Ahn, N. G., Hansen, K. C., Tyler, J. K., & Churchill, M. E. (2016). The Cac1 subunit of histone chaperone CAF-1 organizes CAF-1-H3/H4 architecture and tetramerizes histones. *Elife*, *5*. https://doi.org/10.7554/eLife.18023

Margolin, B. S., Freitag, M., & Selker, E. U. (1997). Improved plasmids for gene targeting at the his-3 locus of Neurospora crassa by electroporation. *Fungal Genetics Reports*, *44*(1), 34–36. https://doi.org/10.4148/1941-4765.1281

Margueron, R., & Reinberg, D. (2011). The Polycomb complex PRC2 and its mark in life. *Nature*, *469*(7330), 343–349. https://doi.org/10.1038/nature09784

Martinez-Balbas, M. A., Tsukiyama, T., Gdula, D., & Wu, C. (1998). Drosophila NURF-55, a WD repeat protein involved in histone metabolism. *Proc Natl Acad Sci U S A*, *95*(1), 132–137. https://doi.org/10.1073/pnas.95.1.132

McNaught, K. J., Wiles, E. T., & Selker, E. U. (2020). Identification of a PRC2 Accessory Subunit Required for Subtelomeric H3K27 Methylation in Neurospora crassa. *Mol Cell Biol*, *40*(11). https://doi.org/10.1128/MCB.00003-20

Moggs, J. G., Grandi, P., Quivy, J. P., Jonsson, Z. O., Hubscher, U., Becker, P. B., & Almouzni, G. (2000). A CAF-1-PCNA-mediated chromatin assembly pathway triggered by sensing DNA damage. *Mol Cell Biol*, *20*(4), 1206–1218. https://doi.org/10.1128/MCB.20.4.1206-1218.2000

Moller, M., Ridenour, J. B., Wright, D. F., Martin, F. A., & Freitag, M. (2023). H4K20me3 is important for Ash1-mediated H3K36me3 and transcriptional silencing in facultative heterochromatin in a fungal pathogen. *PLoS Genet*, *19*(9), e1010945. https://doi.org/10.1371/journal.pgen.1010945

Mozgova, I., Wildhaber, T., Liu, Q., Abou-Mansour, E., L'Haridon, F., Metraux, J. P., Gruissem, W., Hofius, D., & Hennig, L. (2015). Chromatin assembly factor CAF-1 represses priming of plant defence response genes. *Nat Plants*, *1*, 15127. https://doi.org/10.1038/nplants.2015.127

Muller, J., Hart, C. M., Francis, N. J., Vargas, M. L., Sengupta, A., Wild, B., Miller, E. L., O'Connor, M. B., Kingston, R. E., & Simon, J. A. (2002). Histone methyltransferase activity of a Drosophila Polycomb group repressor complex. *Cell*, *111*(2), 197–208. https://doi.org/10.1016/s0092-8674(02)00976-5

Mumford, C. C., Tanizawa, H., Wiles, E. T., McNaught, K. J., Jamieson, K., Tsukamoto, K., & Selker, E. U. (2024). The RPD3L deacetylation complex is required for facultative heterochromatin repression in Neurospora crassa. *Proc Natl Acad Sci U S A*, *121*(32), e2404770121. https://doi.org/10.1073/pnas.2404770121

Munoz-Viana, R., Wildhaber, T., Trejo-Arellano, M. S., Mozgova, I., & Hennig, L. (2017). Arabidopsis Chromatin Assembly Factor 1 is required for occupancy and position of a subset of nucleosomes. *Plant J*, *92*(3), 363–374. https://doi.org/10.1111/tpj.13658

Murphy, P. J., & Berger, F. (2023). The chromatin source-sink hypothesis: a shared mode of chromatin-mediated regulations. *Development*, *150*(21). https://doi.org/10.1242/dev.201989

Murzina, N., Verreault, A., Laue, E., & Stillman, B. (1999). Heterochromatin dynamics in mouse cells: interaction between chromatin assembly factor 1 and HP1 proteins. *Mol Cell*, *4*(4), 529–540. https://doi.org/10.1016/s1097-2765(00)80204-x

Park, G., Colot, H. V., Collopy, P. D., Krystofova, S., Crew, C., Ringelberg, C., Litvinkova, L., Altamirano, L., Li, L., Curilla, S., Wang, W., Gorrochotegui-Escalante, N., Dunlap, J. C., & Borkovich, K. A. (2011). High-throughput production of gene replacement mutants in Neurospora crassa. *Methods Mol Biol*, *722*, 179–189. https://doi.org/10.1007/978-1-61779-040-9_13

Pasini, D., Malatesta, M., Jung, H. R., Walfridsson, J., Willer, A., Olsson, L., Skotte, J., Wutz, A., Porse, B., Jensen, O. N., & Helin, K. (2010). Characterization of an antagonistic switch between histone H3 lysine 27 methylation and acetylation in the transcriptional regulation of Polycomb group target genes. *Nucleic Acids Res*, *38*(15), 4958–4969. https://doi.org/10.1093/nar/gkq244

Plath, K., Fang, J., Mlynarczyk-Evans, S. K., Cao, R., Worringer, K. A., Wang, H., de la Cruz, C. C., Otte, A. P., Panning, B., & Zhang, Y. (2003). Role of histone H3 lysine 27 methylation in X inactivation. *Science*, *300*(5616), 131–135. https://doi.org/10.1126/science.1084274

Ransom, M., Dennehey, B. K., & Tyler, J. K. (2010). Chaperoning histones during DNA replication and repair. *Cell*, *140*(2), 183–195. https://doi.org/10.1016/j.cell.2010.01.004

Ray-Gallet, D., Woolfe, A., Vassias, I., Pellentz, C., Lacoste, N., Puri, A., Schultz, D. C., Pchelintsev, N. A., Adams, P. D., Jansen, L. E., & Almouzni, G. (2011). Dynamics of histone H3 deposition in vivo reveal a nucleosome gap-filling mechanism for H3.3 to maintain chromatin integrity. *Mol Cell*, *44*(6), 928–941. https://doi.org/10.1016/j.molcel.2011.12.006

Ridenour, J. B., Moller, M., & Freitag, M. (2020). Polycomb Repression without Bristles: Facultative Heterochromatin and Genome Stability in Fungi. *Genes (Basel)*, *11*(6). https://doi.org/10.3390/genes11060638

Roelens, B., Clemot, M., Leroux-Coyau, M., Klapholz, B., & Dostatni, N. (2017). Maintenance of Heterochromatin by the Large Subunit of the CAF-1 Replication-Coupled Histone Chaperone Requires Its Interaction with HP1a Through a Conserved Motif. *Genetics*, *205*(1), 125–137. https://doi.org/10.1534/genetics.116.190785

Rohland, N., & Reich, D. (2012). Cost-effective, high-throughput DNA sequencing libraries for multiplexed target capture. *Genome Res*, *22*(5), 939–946. https://doi.org/10.1101/gr.128124.111

Rouillon, C., Eckhardt, B. V., Kollenstart, L., Gruss, F., Verkennis, A. E. E., Rondeel, I., Krijger, P. H. L., Ricci, G., Biran, A., van Laar, T., Delvaux de Fenffe, C. M., Luppens, G., Albanese, P., Sato, K., Scheltema, R. A., de Laat, W., Knipscheer, P., Dekker, N. H., Groth, A., & Mattiroli, F. (2023). CAF-1 deposits newly synthesized histones during DNA replication using distinct mechanisms on the leading and lagging strands. *Nucleic Acids Res*, *51*(8), 3770–3792. https://doi.org/10.1093/nar/gkad171

Saksouk, N., Simboeck, E., & Dejardin, J. (2015). Constitutive heterochromatin formation and transcription in mammals. *Epigenetics Chromatin*, *8*, 3. https://doi.org/10.1186/1756-8935-8-3

Sauer, P. V., Gu, Y., Liu, W. H., Mattiroli, F., Panne, D., Luger, K., & Churchill, M. E. (2018). Mechanistic insights into histone deposition and nucleosome assembly by the chromatin assembly factor-1. *Nucleic Acids Res*, *46*(19), 9907–9917. https://doi.org/10.1093/nar/gky823

Schmitges, F. W., Prusty, A. B., Faty, M., Stutzer, A., Lingaraju, G. M., Aiwazian, J., Sack, R., Hess, D., Li, L., Zhou, S., Bunker, R. D., Wirth, U., Bouwmeester, T., Bauer, A., Ly-Hartig, N., Zhao, K., Chan, H., Gu, J., Gut, H.,…Thoma, N. H. (2011). Histone methylation by PRC2 is inhibited by active chromatin marks. *Mol Cell*, *42*(3), 330–341. https://doi.org/10.1016/j.molcel.2011.03.025

Schonrock, N., Exner, V., Probst, A., Gruissem, W., & Hennig, L. (2006). Functional genomic analysis of CAF-1 mutants in Arabidopsis thaliana. *J Biol Chem*, *281*(14), 9560–9568. https://doi.org/10.1074/jbc.M513426200

Seong, I. S., Woda, J. M., Song, J. J., Lloret, A., Abeyrathne, P. D., Woo, C. J., Gregory, G., Lee, J. M., Wheeler, V. C., Walz, T., Kingston, R. E., Gusella, J. F., Conlon, R. A., & MacDonald, M. E. (2010). Huntingtin facilitates polycomb repressive complex 2. *Hum Mol Genet*, *19*(4), 573–583. https://doi.org/10.1093/hmg/ddp524

Sharp, J. A., Krawitz, D. C., Gardner, K. A., Fox, C. A., & Kaufman, P. D. (2003). The budding yeast silencing protein Sir1 is a functional component of centromeric chromatin. *Genes Dev*, *17*(19), 2356–2361. https://doi.org/10.1101/gad.1131103

Shibahara, K., & Stillman, B. (1999). Replication-dependent marking of DNA by PCNA facilitates CAF-1-coupled inheritance of chromatin. *Cell*, *96*(4), 575–585. https://doi.org/10.1016/s0092-8674(00)80661-3

Smith, S., & Stillman, B. (1989). Purification and characterization of CAF-I, a human cell factor required for chromatin assembly during DNA replication in vitro. *Cell*, *58*(1), 15–25. https://doi.org/10.1016/0092-8674(89)90398-x

Smith, S., & Stillman, B. (1991). Stepwise assembly of chromatin during DNA replication in vitro. *EMBO J*, *10*(4), 971–980. https://doi.org/10.1002/j.1460-2075.1991.tb08031.x

Song, Y., He, F., Xie, G., Guo, X., Xu, Y., Chen, Y., Liang, X., Stagljar, I., Egli, D., Ma, J., & Jiao, R. (2007). CAF-1 is essential for Drosophila development and involved in the maintenance of epigenetic memory. *Dev Biol*, *311*(1), 213–222. https://doi.org/10.1016/j.ydbio.2007.08.039

Tagami, H., Ray-Gallet, D., Almouzni, G., & Nakatani, Y. (2004). Histone H3.1 and H3.3 complexes mediate nucleosome assembly pathways dependent or independent of DNA synthesis. *Cell*, *116*(1), 51–61. https://doi.org/10.1016/s0092-8674(03)01064-x

Tamburini, B. A., Carson, J. J., Linger, J. G., & Tyler, J. K. (2006). Dominant mutants of the Saccharomyces cerevisiae ASF1 histone chaperone bypass the need for CAF-1 in transcriptional silencing by altering histone and Sir protein recruitment. *Genetics*, *173*(2), 599–610. https://doi.org/10.1534/genetics.105.054783

Tang, G., Yuan, J., Wang, J., Zhang, Y. Z., Xie, S. S., Wang, H., Tao, Z., Liu, H., Kistler, H. C., Zhao, Y., Duan, C. G., Liu, W., Ma, Z., & Chen, Y. (2021). Fusarium BP1 is a reader of H3K27 methylation. *Nucleic Acids Res*, *49*(18), 10448–10464. https://doi.org/10.1093/nar/gkab844

Thiru, A., Nietlispach, D., Mott, H. R., Okuwaki, M., Lyon, D., Nielsen, P. R., Hirshberg, M., Verreault, A., Murzina, N. V., & Laue, E. D. (2004). Structural basis of HP1/PXVXL motif peptide interactions and HP1 localisation to heterochromatin. *EMBO J*, *23*(3), 489–499. https://doi.org/10.1038/sj.emboj.7600088

Tie, F., Banerjee, R., Stratton, C. A., Prasad-Sinha, J., Stepanik, V., Zlobin, A., Diaz, M. O., Scacheri, P. C., & Harte, P. J. (2009). CBP-mediated acetylation of histone H3 lysine 27 antagonizes Drosophila Polycomb silencing. *Development*, *136*(18), 3131–3141. https://doi.org/10.1242/dev.037127

Trojer, P., & Reinberg, D. (2007). Facultative heterochromatin: is there a distinctive molecular signature? *Mol Cell*, *28*(1), 1–13. https://doi.org/10.1016/j.molcel.2007.09.011

Venkatesh, S., & Workman, J. L. (2013). Set2 mediated H3 lysine 36 methylation: regulation of transcription elongation and implications in organismal development. *Wiley Interdiscip Rev Dev Biol*, *2*(5), 685–700. https://doi.org/10.1002/wdev.109

Voigt, P., Tee, W. W., & Reinberg, D. (2013). A double take on bivalent promoters. *Genes Dev*, *27*(12), 1318–1338. https://doi.org/10.1101/gad.219626.113

Wiles, E. T., McNaught, K. J., Kaur, G., Selker, J. M. L., Ormsby, T., Aravind, L., & Selker, E. U. (2020). Evolutionarily ancient BAH-PHD protein mediates Polycomb silencing. *Proc Natl Acad Sci U S A*, *117*(21), 11614–11623. https://doi.org/10.1073/pnas.1918776117

Xu, M., Sun, Z., Shi, H., Yue, J., Xiong, X., Wu, Z., Kou, Y., & Tao, Z. (2024). Two H3K36 methyltransferases differentially associate with transcriptional activity and enrichment of facultative heterochromatin in rice blast fungus. *aBIOTECH*, *5*(1), 1–16. https://doi.org/10.1007/s42994-023-00127-3

Zhang, Y., Iratni, R., Erdjument-Bromage, H., Tempst, P., & Reinberg, D. (1997). Histone deacetylases and SAP18, a novel polypeptide, are components of a human Sin3 complex. *Cell*, *89*(3), 357–364. https://doi.org/10.1016/s0092-8674(00)80216-0

Zhang, Z., Shibahara, K., & Stillman, B. (2000). PCNA connects DNA replication to epigenetic inheritance in yeast. *Nature*, *408*(6809), 221–225. https://doi.org/10.1038/35041601

Zhou, Z., et al. (2018). "Codon usage biases co-evolve with transcription termination machinery to suppress premature cleavage and polyadenylation." Elife 7.

Figures

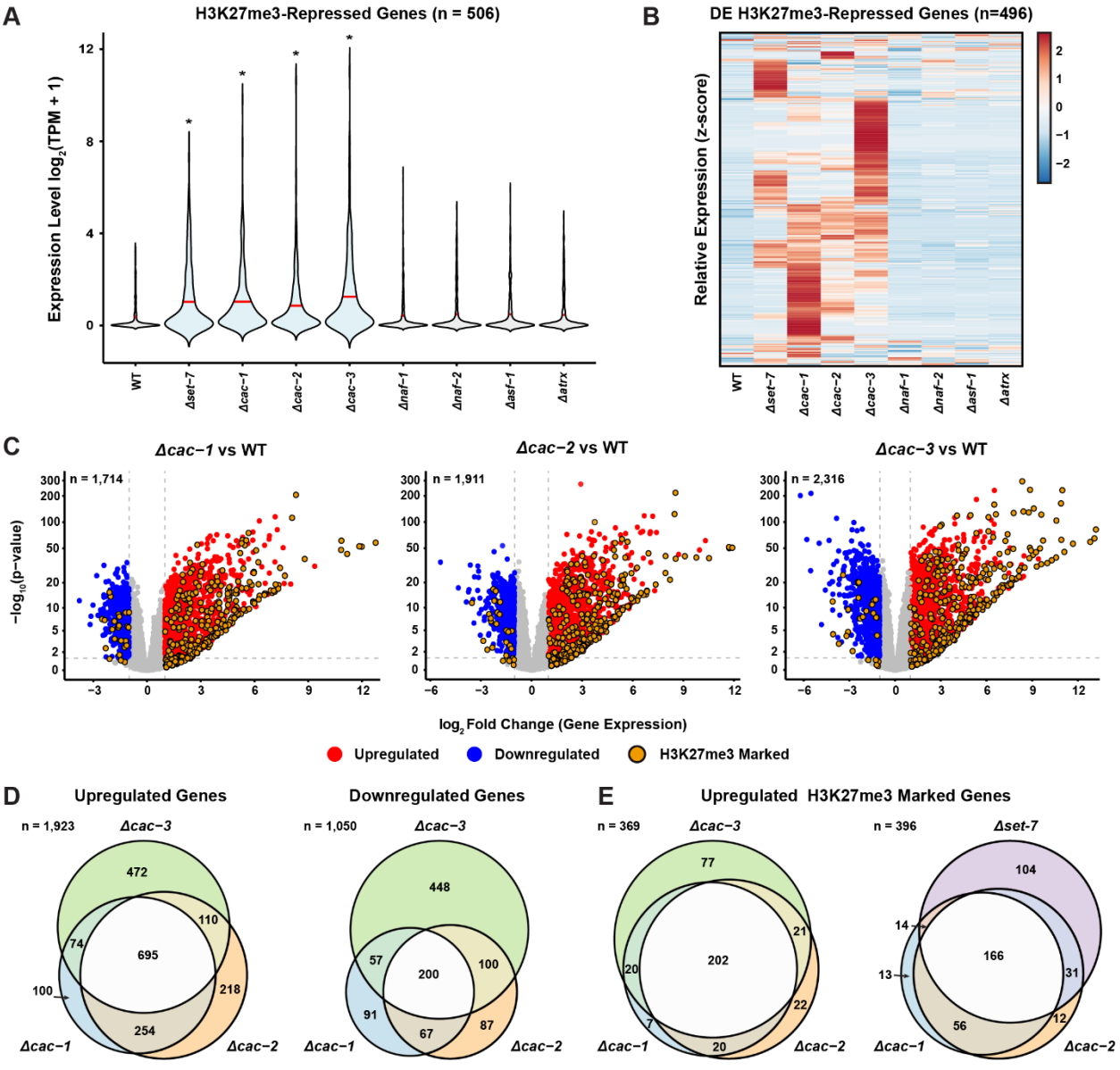
A
H3K27me3-Repressed Genes (n = 506)
Expression Level log2(TPM + 1)
WT
Δset-7
Δcac-1
Δcac-2
Δcac-3
Δnaf-1
Δnaf-2
Δasf-1
Δatrx
B
DE H3K27me3-Repressed Genes (n=496)
Relative Expression (z-score)
C
Δcac-1 vs WT
Δcac-2 vs WT
Δcac-3 vs WT
n = 1,714
n = 1,911
n = 2,316
−log10(p-value)
log2 Fold Change (Gene Expression)
Upregulated
Downregulated
H3K27me3 Marked
D
Upregulated Genes
Downregulated Genes
n = 1,923
n = 1,050
Δcac-3
Δcac-1
Δcac-2
472
110
74
695
100
218
254
448
57
200
100
91
67
87
E
Upregulated H3K27me3 Marked Genes
n = 369
n = 396
Δset-7
77
21
20
202
1
22
20
104
14
166
13
31
56
12

Figure 3.1: CAF-1 deficiency results in derepression of H3K27me3-marked genes

(A) Violin plot displaying expression level of H3K27me3-repressed genes (n= 506) in WT and histone chaperone-deficient mutants. * indicates significant difference in average expression level across all plotted genes compared to WT based on Wilcoxon test. **(B)** Heatmap displaying relative expression level of 496 differentially expressed, H3K27me3-repressed genes in WT and histone chaperone-deficient mutants. Data is row-normalized, and genes (rows) are hierarchically clustered by expression similarity across strains (columns). **(C)** Volcano plots displaying log_2FC in gene expression (x-axis) against $-log_{10}$(adjusted p-value) (y-axis) for all *N. crassa* genes in CAF-1-deficient mutants compared to WT. "n" represents total number of differentially expressed genes. Non-differentially expressed and non-H3K27me3-marked genes are colored gray. **(D)** Venn Diagrams displaying overlap of genes significantly upregulated or downregulated in CAF-1-deficient mutants ("n" represents total) **(E)** Venn Diagrams displaying overlap of H3K27me3-marked genes significantly upregulated in CAF-1-deficient and PRC2-deficient ("n" represents total).

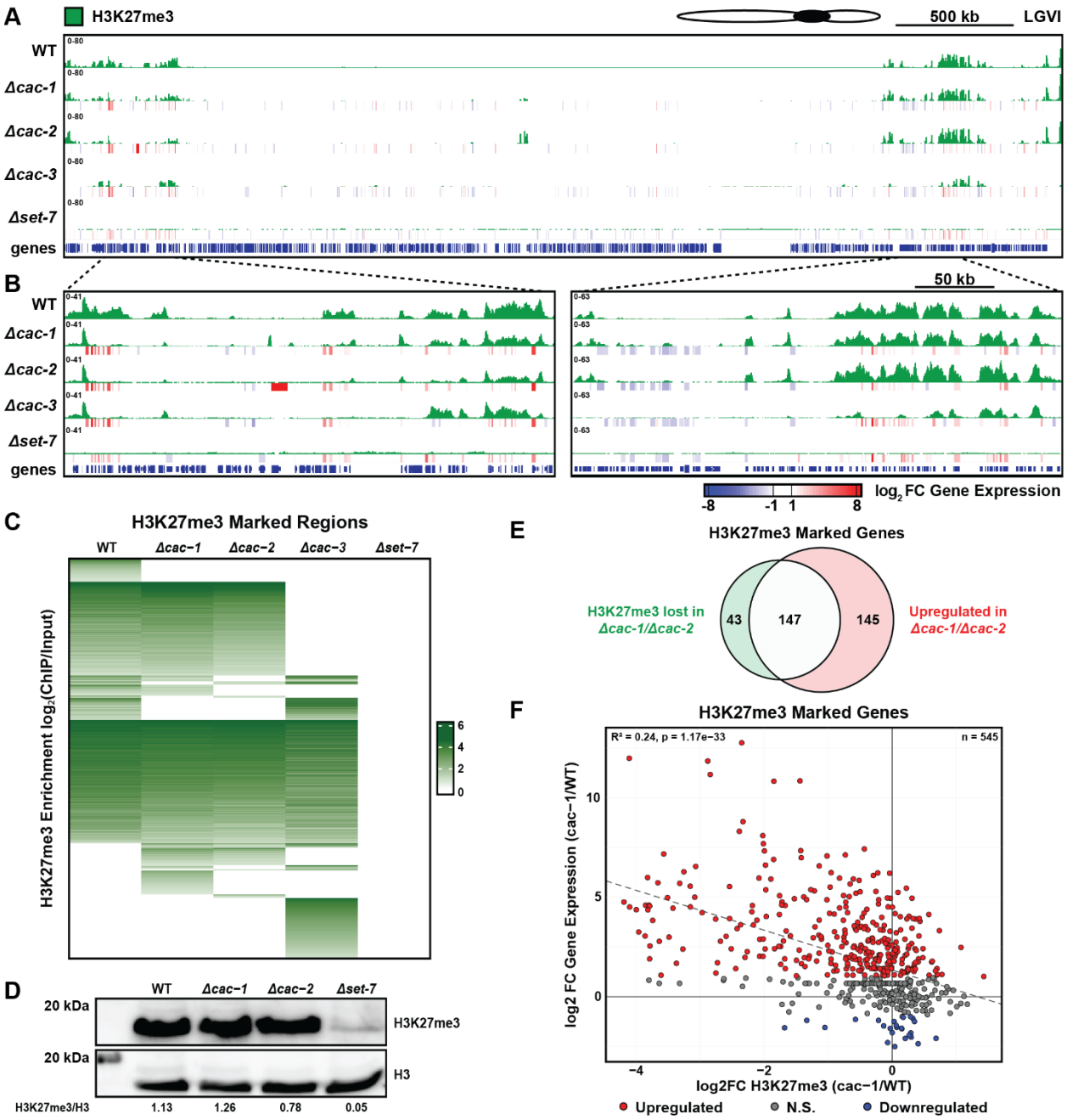
A
H3K27me3
500 kb
LGVI
WT
Δcac-1
Δcac-2
Δcac-3
Δset-7
genes
B
50 kb
log2 FC Gene Expression
C
H3K27me3 Marked Regions
H3K27me3 Enrichment log2(ChIP/Input)
D
20 kDa
H3K27me3
H3
H3K27me3/H3
1.13
1.26
0.78
0.05
E
H3K27me3 Marked Genes
H3K27me3 lost in Δcac-1/Δcac-2
Upregulated in Δcac-1/Δcac-2
43
147
145
F
H3K27me3 Marked Genes
R² = 0.24, p = 1.17e−33
n = 545
log2 FC Gene Expression (cac−1/WT)
log2FC H3K27me3 (cac−1/WT)
Upregulated
N.S.
Downregulated

Figure 3.2: CAF-1 deficiency results in aberrant H3K27me3 patterns

(A) Whole chromosome view of H3K27me3 enrichment and log_2FC of gene expression on linkage group VI. **(B)** Zoom-in views of H3K27me3 enrichment and log_2FC of gene expression at two facultative heterochromatin domains on linkage group VI. **(C)** Heatmap displaying H3K27me3 enrichment (log_2[ChIP/Input]) in WT, CAF-1 deficient mutants, and *Δset-7* across H3K27me3-methylated regions. Values with an FDR > 0.05 were set to 0. Rows correspond to 300-bp bins within H3K27me3-marked loci, clustered and sorted by enrichment in WT and mutant strains. **(D)** Western blots performed on whole-cell extract displaying global levels of H3K27me3 and total histone H3 in WT CAF-1 deficient mutants, and *Δset-7*. Numbers represent H3K27me3 band intensities quantified by densitometry and normalized to total H3 **(E)** Venn diagram displaying overlap of H3K27me3-marked genes that lose H3K37me3 or are upregulated in *Δcac-1* or *Δcac-2*. **(F)** Scatter plot displaying log_2FC of H3K27me3 enrichment (x-axis) against log_2FC of gene expression (y-axis) for H3K27me3-marked genes in *Δcac-1* vs. WT.

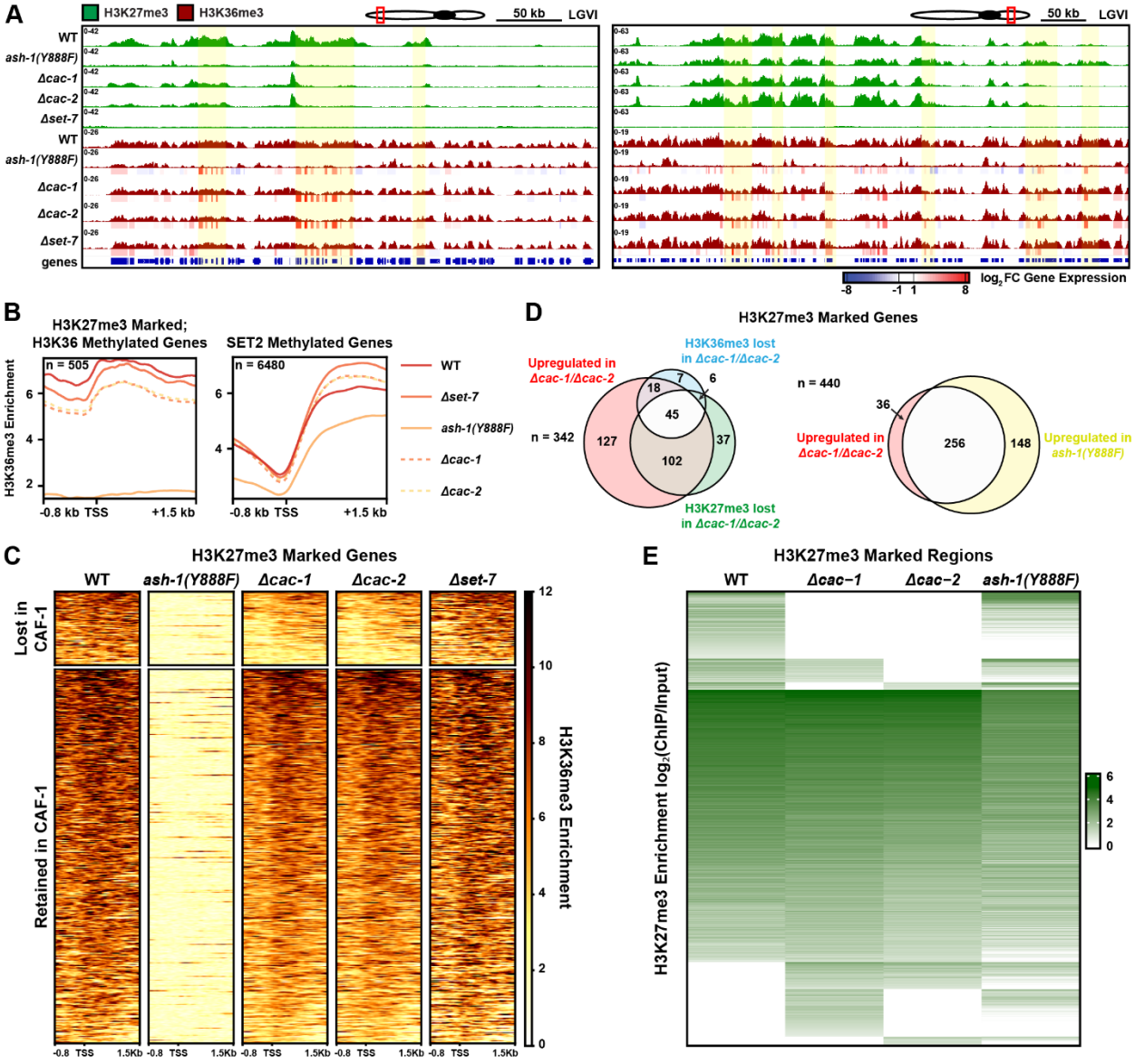
A
H3K27me3
H3K36me3
50 kb
LGVI
WT
ash-1(Y888F)
Δcac-1
Δcac-2
Δset-7
genes
log2 FC Gene Expression
B
H3K27me3 Marked;
H3K36 Methylated Genes
SET2 Methylated Genes
n = 505
n = 6480
H3K36me3 Enrichment
-0.8 kb TSS
+1.5 kb
C
H3K27me3 Marked Genes
Lost in CAF-1
Retained in CAF-1
H3K36me3 Enrichment
D
H3K27me3 Marked Genes
Upregulated in Δcac-1/Δcac-2
H3K36me3 lost in Δcac-1/Δcac-2
H3K27me3 lost in Δcac-1/Δcac-2
n = 342
n = 440
Upregulated in ash-1(Y888F)
E
H3K27me3 Marked Regions
H3K27me3 Enrichment log2(ChIP/Input)

Figure 3.3: CAF-1 deficiency impacts ASH-1-catalyzed H3K36me3

(A) Metaplots displaying mean H3K36me3 enrichment from −0.8 kb to +1.5 kb relative to the TSS for three gene sets: H3K27me3-marked, ASH-1–dependent; H3K27me3-depleted, and SET-2–methylated genes ("n" = total for each category). CAF-1–deficient mutants (*Δcac-1*, *Δcac-2*) are represented by dashed lines and controls (WT, *Δset-7*, *ash-1(Y888F)*) are represented by solid lines. **(B)** Zoomed in browser shots displaying enrichment of loss of H3K36me3 and $\log_2$FC of gene expression at 2 facultative heterochromatin domains on linkage group VI. *ash-1(Y888F)* data represents H3K27me2/3 enrichment **(C)** Heatmaps displaying H3K36me3 enrichment from −0.8 kb to +1.5 kb relative to the TSS for H3K36me3-enriched, H3K27me3-marked genes (n = XX). Clusters represent genes that lose or retain H3K36me3 in *Δcac-1* and *Δcac-2* (n = 505) **(D)** Venn diagrams displaying overlap of genes that lose H3K36me3, lose H3K27me3, or are upregulated in *Δcac-1* and *Δcac-2* (n = 342) and genes that are upregulated in *Δcac-1* and *Δcac-2* or upregulated in *ash-1(Y888F)* (n = 440) **(E)** Heatmap displaying H3K27me3 enrichment for WT and CAF-1-deficient mutants, and H3K27me2/3 enrichment for *ash-1(Y888F)* ($\log_2$[ChIP/Input]) across H3K27me3 methylated regions. Values with an FDR > 0.05 were set to 0. Rows correspond to 300-bp bins within H3K27me3-marked loci, clustered and sorted by enrichment in WT and *Δcac-1*, *Δcac-2*.

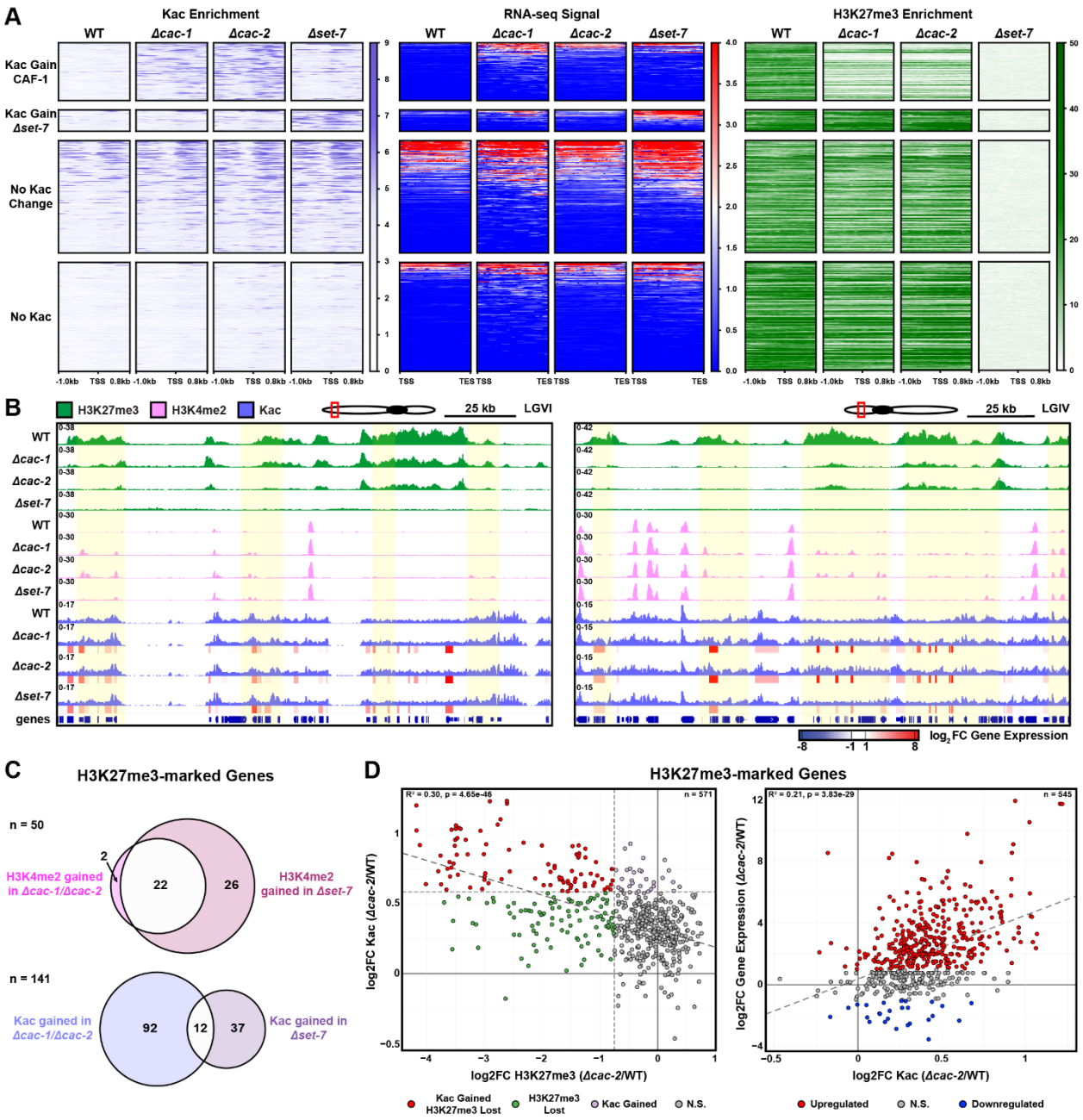
A
Kac Enrichment
RNA-seq Signal
H3K27me3 Enrichment
WT
Δcac-1
Δcac-2
Δset-7
Kac Gain CAF-1
Kac Gain Δset-7
No Kac Change
No Kac
-1.0kb TSS 0.8kb
TSS TES
B
H3K27me3
H3K4me2
Kac
25 kb
LGVI
LGIV
genes
log2FC Gene Expression
C
H3K27me3-marked Genes
n = 50
H3K4me2 gained in Δcac-1/Δcac-2
H3K4me2 gained in Δset-7
2
22
26
n = 141
Kac gained in Δcac-1/Δcac-2
Kac gained in Δset-7
92
12
37
D
H3K27me3-marked Genes
log2FC Kac (Δcac-2/WT)
log2FC H3K27me3 (Δcac-2/WT)
log2FC Gene Expression (Δcac-2/WT)
Kac Gained H3K27me3 Lost
H3K27me3 Lost
Kac Gained
N.S.
Upregulated
Downregulated

Figure 3.4: CAF-1 deficiency results in an euchromatin-like environment at H3K27me3-marked genes

(A) Heatmaps displaying: Kac from −1 kb to +0.8 kb relative to the TSS (Left), RNA-seq signal across gene bodies (Center), and H3K27me3 from −1 kb to +0.8 kb relative to the TSS (Right) at H3K27me3-marked genes (n= 571). Genes (rows) are split into four clusters (top to bottom): Kac gained in CAF-1–deficient mutants (1), Kac gained in *Δset-7* but not in CAF-1-deficient mutants (2) , no change in Kac vs WT (3), and unacetylated in all strains (4). Clusters are individually sorted by RNA-seq signal across all strains. **(B)** Browser shots displaying gains of H3K4me2 and Kac, log_2FC of gene expression at 2 facultative heterochromatin domains on linkage groups IV and VI. **(C)** Venn diagrams displaying overlap in H3K27me3-marked genes that gain H3K4me2 or gain Kac in Δcac-1/Δcac-2 or *Δset-7*. **(D)** Scatter plots displaying log_2FC of H3K27me3 enrichment (x-axis) against log_2FC of Kac enrichment (y-axis) for H3K27me3-marked genes in *Δcac-2* vs. WT, and log_2FC of Kac enrichment (x-axis) against log_2FC of gene expression (y-axis) for H3K27me3-marked genes in *Δcac-2* vs. WT

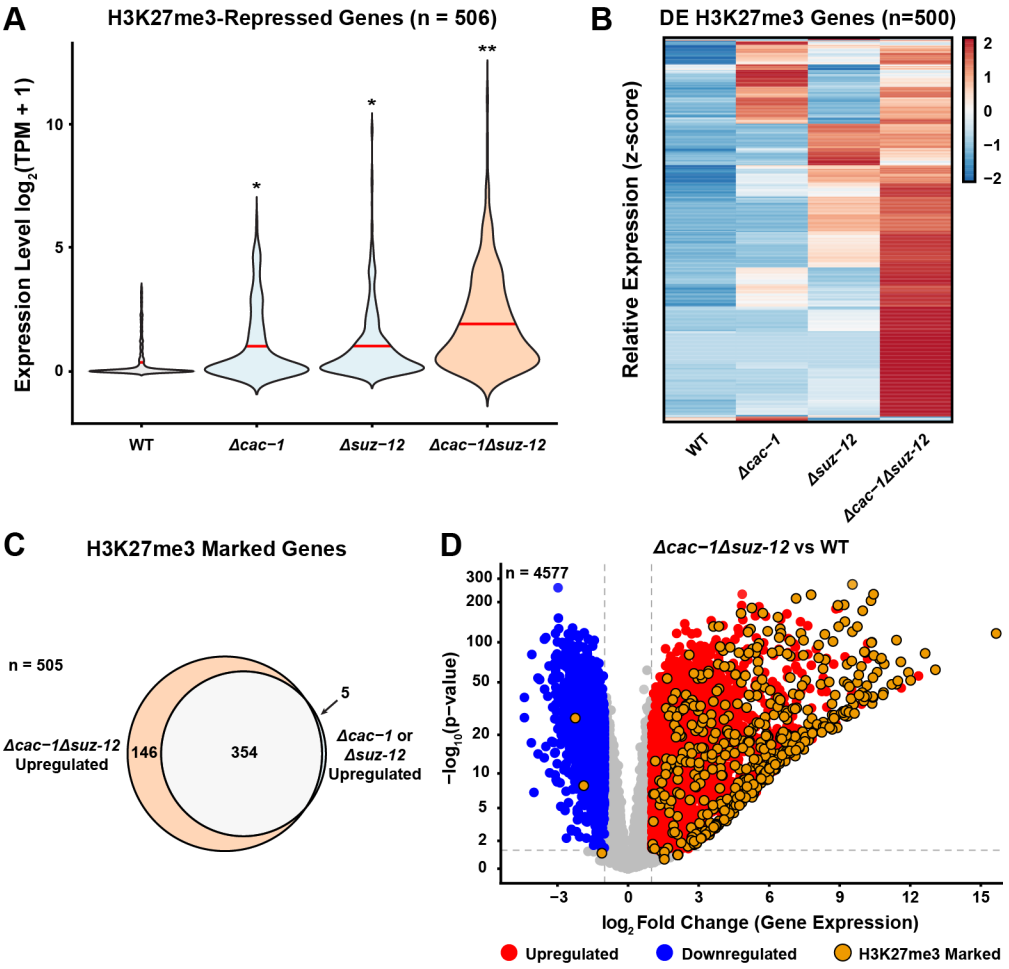

Figure 3.5: CAF-1 and PRC2 play distinct roles in H3K27me3-marked gene repression

(A) Violin plot displaying expression level of H3K27me3-repressed genes (n = 506) in *Δcac-1*, *Δsuz-12*, and *Δcac-1Δsuz-12*. * and ** indicates significant difference in average expression level across all plotted genes compared to WT based on Wilcoxon test (* = p-value < 1.5e-14 , ** = p-value < 1.04e-88) **(B)** Heatmap displaying relative expression level of 496 differentially expressed, H3K27me3-repressed genes in WT, *Δcac-1*, *Δsuz-12*, and *Δcac-1Δsuz-12*. Data is row-normalized, and genes (rows) are hierarchically clustered by expression similarity across strains (columns). **(C)** Venn diagram displaying overlap of H3K27me3-marked genes upregulated in *Δcac-1* or *Δsuz-12* and *Δcac-1Δsuz-12* **(D)** Volcano plots displaying $\log_2$FC in gene expression (x-axis) against $-\log_{10}$(adjusted p-value) (y-axis) for all *N. crassa* genes in *Δcac-1Δsuz-12* compared to WT. "n" represents total number of differentially expressed genes. Non-differentially expressed and non-H3K27me3-marked genes are colored gray.

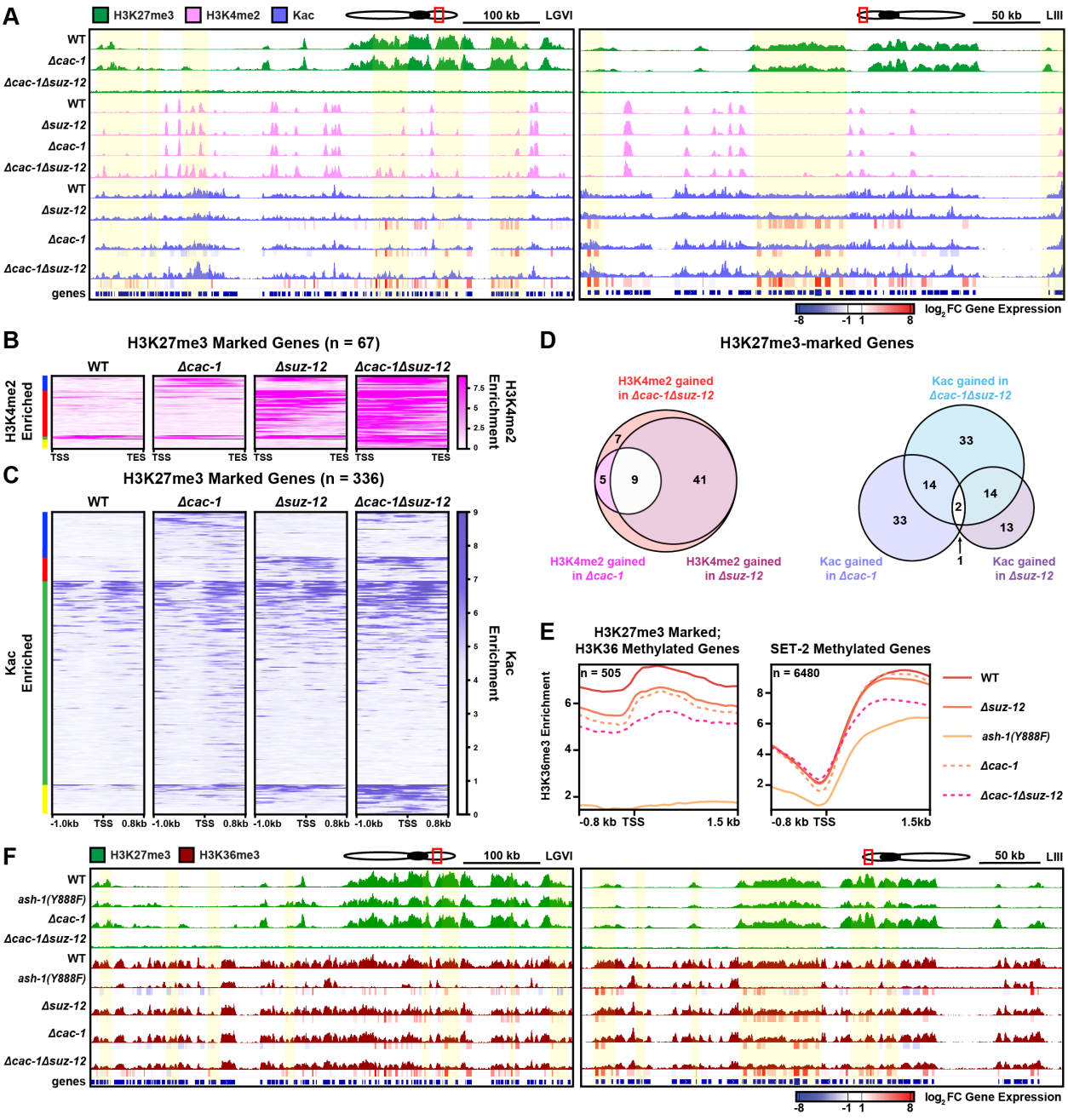
A
H3K27me3
H3K4me2
Kac
100 kb
LGVI
50 kb
LIII
WT
Δcac-1
Δcac-1Δsuz-12
WT
Δsuz-12
Δcac-1
Δcac-1Δsuz-12
WT
Δsuz-12
Δcac-1
Δcac-1Δsuz-12
genes
log2 FC Gene Expression
-8
-1
1
8
B
H3K27me3 Marked Genes (n = 67)
WT
Δcac-1
Δsuz-12
Δcac-1Δsuz-12
H3K4me2 Enriched
H3K4me2 Enrichment
TSS
TES
C
H3K27me3 Marked Genes (n = 336)
Kac Enriched
Kac Enrichment
-1.0kb
TSS
0.8kb
D
H3K27me3-marked Genes
H3K4me2 gained in Δcac-1Δsuz-12
7
5
9
41
H3K4me2 gained in Δcac-1
H3K4me2 gained in Δsuz-12
Kac gained in Δcac-1Δsuz-12
33
14
14
2
33
13
1
Kac gained in Δcac-1
Kac gained in Δsuz-12
E
H3K27me3 Marked; H3K36 Methylated Genes
SET-2 Methylated Genes
n = 505
n = 6480
H3K36me3 Enrichment
-0.8 kb
TSS
1.5 kb
1.5kb
WT
Δsuz-12
ash-1(Y888F)
Δcac-1
Δcac-1Δsuz-12
F
H3K27me3
H3K36me3
100 kb
LGVI
50 kb
LIII
WT
ash-1(Y888F)
Δcac-1
Δcac-1Δsuz-12
WT
ash-1(Y888F)
Δsuz-12
Δcac-1
Δcac-1Δsuz-12
genes
log2 FC Gene Expression
-8
-1
1
8

Figure 3.6: CAF-1 and PRC2 work in parallel to maintain facultative heterochromatin

(A) Browser shots displaying gains of H3K4me2 and Kac, log_2FC of gene expression at 2 facultative heterochromatin domains on linkage groups III and VI. **(B)** Heatmap displaying H3K4me2 enrichment across gene bodies at H3K27me3-marked genes enriched for H3K4me2 in WT, *Δcac-1*, *Δsuz-12*, or *Δcac-1Δsuz-12*. Genes (rows) are split into four clusters denoted by colored bars (top to bottom): H3K4me2 gained in CAF-1–deficient mutants (blue) , H3K4me2 gained in *Δsuz-12* but not in CAF-1-deficient mutants (red) , no change in H3K4me2 vs WT (green), and H3K4me2 gained only in *Δcac-1Δsuz-12* (yellow). Clusters are individually sorted by H3K4me2 enrichment across all strains. **(C)** Heatmap displaying Kac enrichment from −1 kb to +0.8 kb relative to the TSS at H3K27me3-marked genes enriched for Kac in WT, *Δcac-1*, *Δsuz-12*, or *Δcac-1Δsuz-12*. Genes (rows) are split into four clusters denoted by colored bars (top to bottom): Kac gained in CAF-1–deficient mutants (blue), Kac gained in *Δsuz-12* but not in CAF-1-deficient mutants (red) , no change in Kac vs WT (green), and Kac gained only in *Δcac-1Δsuz-12* (yellow). Clusters are individually sorted by Kac enrichment across all strains. **(D)** Venn diagrams displaying overlap in genes that gain H3K4me2 or Kac in *Δcac-1*, *Δsuz-12*, and *Δcac-1Δsuz-12* **(E)** Metaplots displaying mean H3K36me3 enrichment from −0.8 kb to +1.5 kb relative to the TSS for two gene sets: H3K27me3-marked and ASH-1–dependent; H3K27me3-depleted ("n" = total for each category). CAF-1–deficient mutants (*Δcac-1*, *Δcac-1Δsuz-12*) are represented by dashed lines and controls (WT, *Δsuz-12*, *ash-1(Y888F)*) are represented by solid lines. **(F)** Browser shots displaying loss of H3K36me3 and log_2FC of gene expression at 2 facultative heterochromatin domains on linkage groups III and VI.

Supplemental Figures and Tables

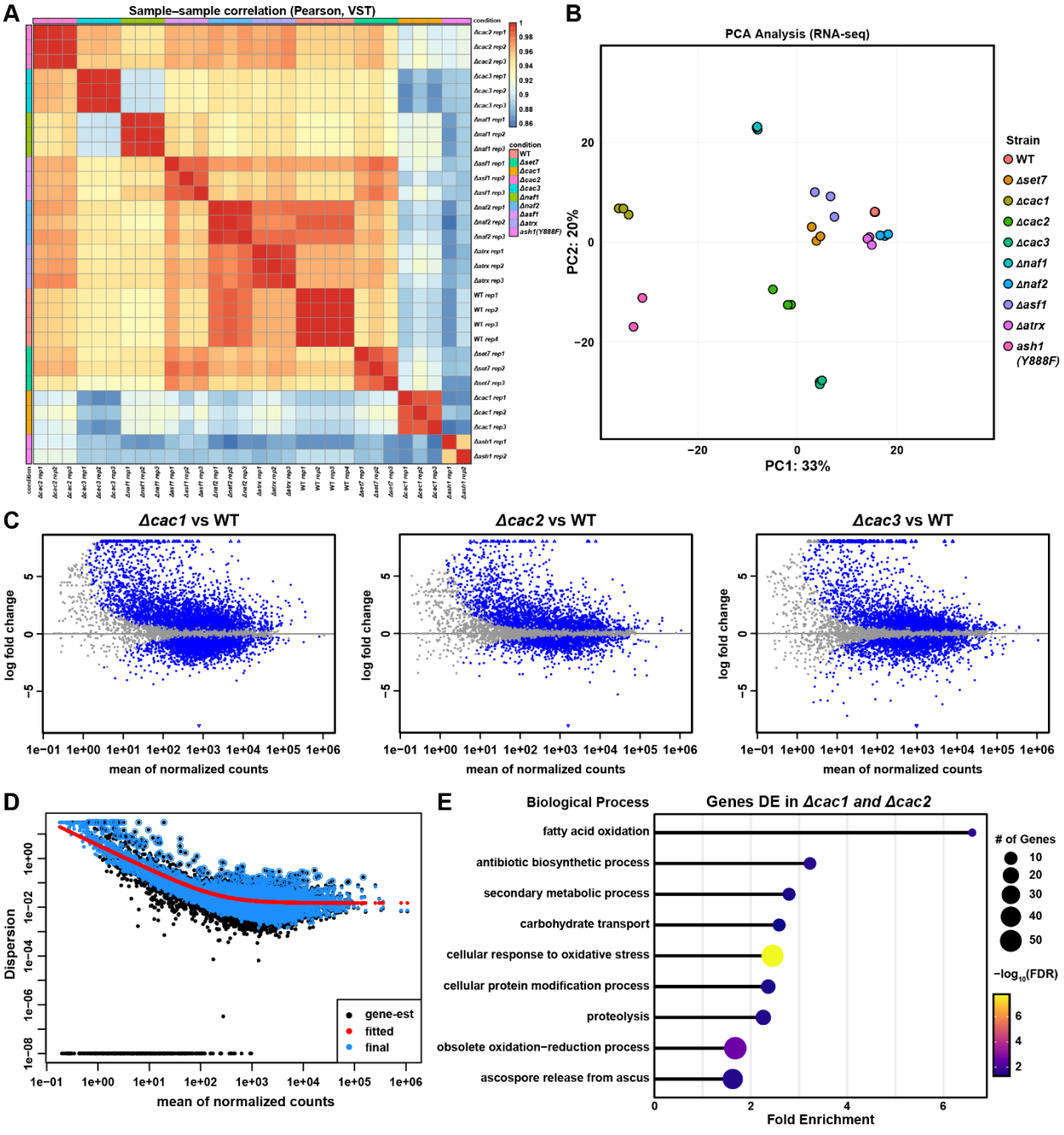

Figure S3.1: QC analysis of RNA-seq samples for histone chaperone-deficient mutants

(A) Correlation plot displaying similarity of expression profiles across RNA-seq samples for histone chaperone mutants and *ash-1(Y888F)*. **(B)** PCA Plot displaying likeness of expression profiles of RNA-seq samples for histone chaperone mutants and *ash-1(Y888F)*. **(C)** MA plots displaying mean normalized counts (x-axis) against log2FC in gene expression for CAF-1 deficient mutants vs WT. **(D)** GO analysis for genes that are upregulated in both *Δcac-1* and *Δcac-2*. **(E)** GO analysis for genes that are downregulated in both *Δcac-1* and *Δcac-2*.

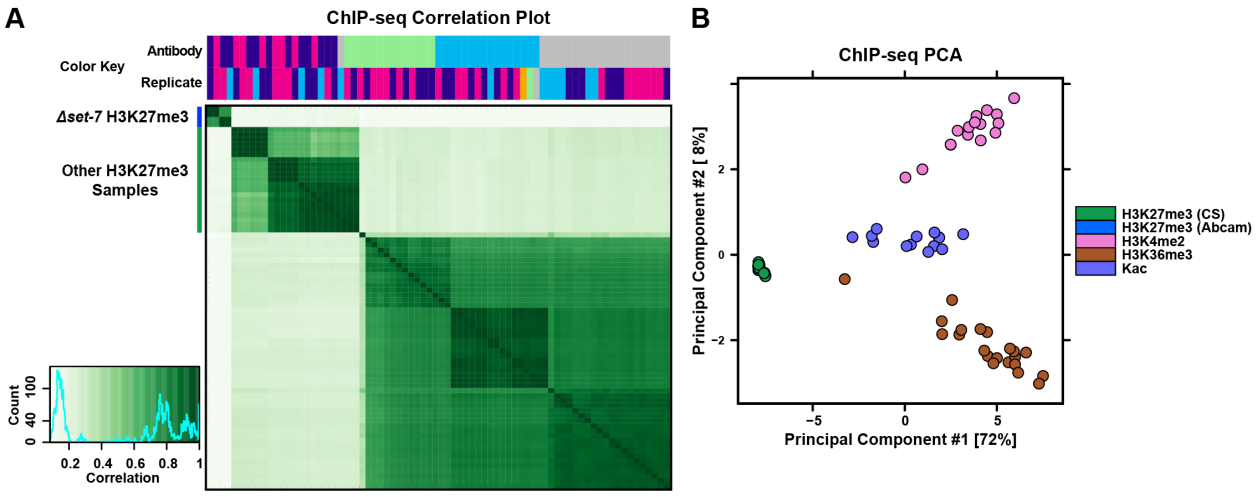

Figure S3.2: QC analysis of ChIP-seq samples

(A) Correlation plot displaying similarity of ChIP-seq enrichment across all samples used in analysis. H3K27me3 samples are annotated at the top left. Full results with sample labels can be found in Dataset S1G. **(B)** PCA plot displaying likeness of enrichment profiles for all ChIP-seq samples used in analysis. Circles represent individual replicates and are colored by antibody.

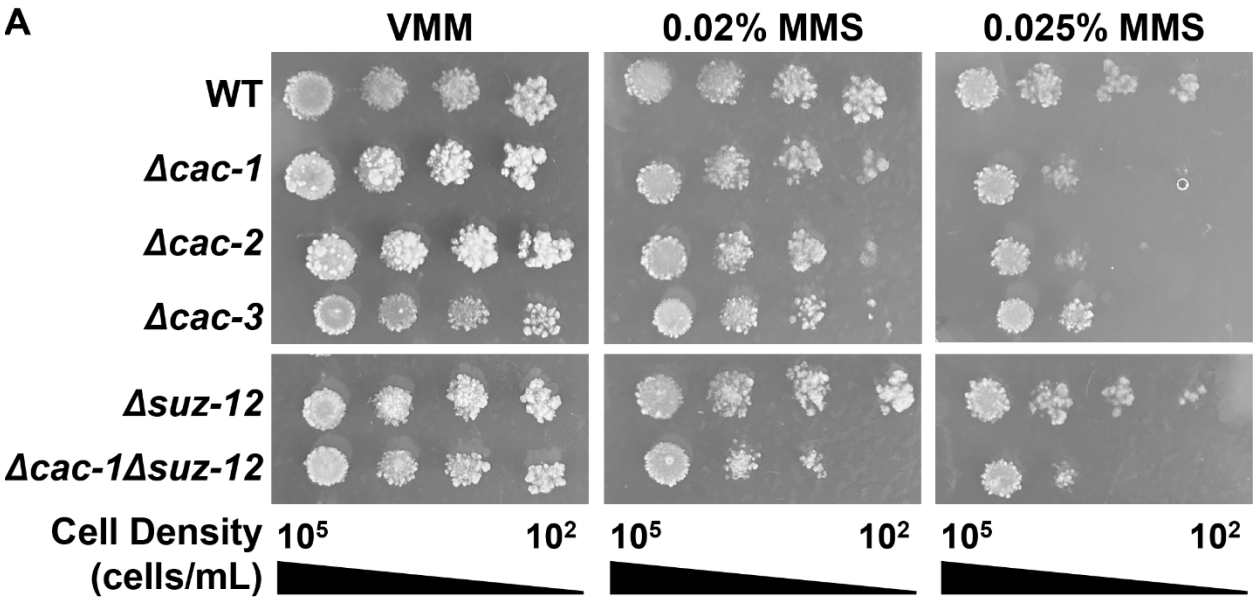

Figure S3.3: CAF-1 deficiency results in DNA damage sensitivity

(A) Spot test displaying MMS sensitivity (0.02 and 0.025% v/v) of CAF-1 and PRC2-deficient mutants. VMM plate was used as a negative control.

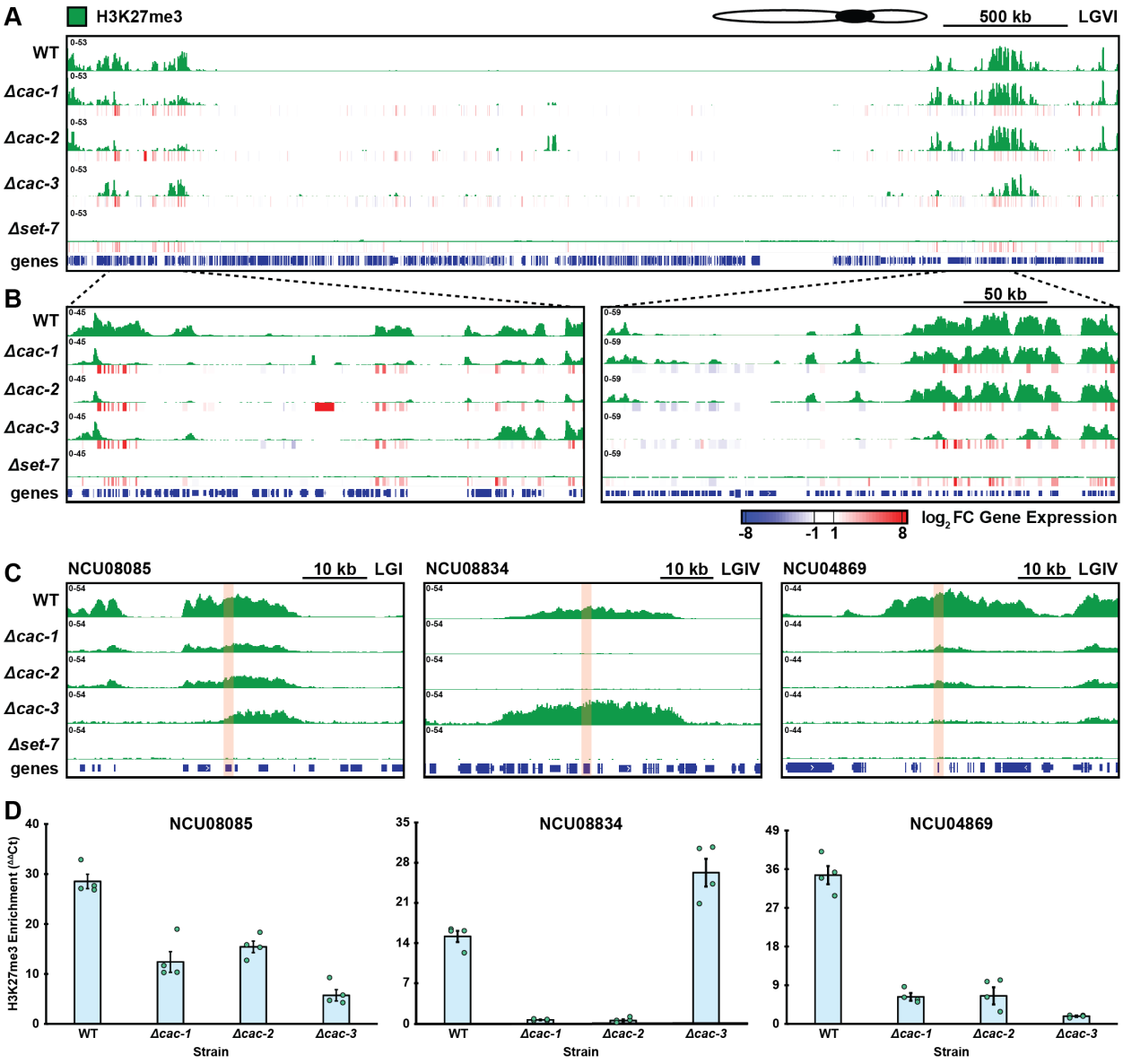

Figure S3.4: Abcam antibody replicates the H3K27me3 profile

(A) Whole-chromosome view of H3K27me3 enrichment in WT, CAF-1-deficient mutants, and *Δset-7* on LGVI. The Abcam antibody displays a highly similar profile compared to the Cell Signaling antibody. **(B)** Zoom-in views of H3K27me3 enrichment in WT, CAF-1-deficient mutants, and *Δset-7* at two facultative heterochromatin regions on LGVI. **(C)** Zoom-in views of three facultative heterochromatin regions analyzed by ChIP-qPCR. Red lines denote genes that were targeted by qPCR primers. **(D)** Bar graph displaying H3K27me3 enrichment ($^{\Delta\Delta}$Ct) at three H3K27me3-marked genes in WT and CAF-1-deficient mutants.

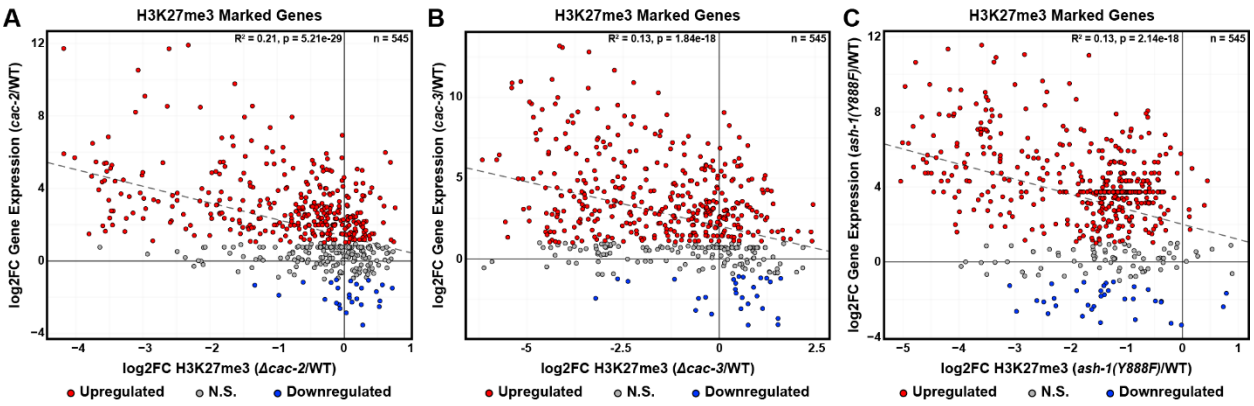

Figure S3.5: Loss of H3K27me3 is weakly correlated with transcriptional changes in *Δcac-2*

(A) Scatter plot displaying log2FC of H3K27me3 enrichment vs. log2FC of gene expression in *Δcac-2* vs WT. **(B)** Scatter plot displaying log2FC of H3K27me3 enrichment vs. log2FC of gene expression in *Δcac-3* vs WT. **(C)** Scatter plot displaying log2FC of H3K27me3 enrichment vs. log2FC of gene expression in *ash1(Y888F)* vs WT.

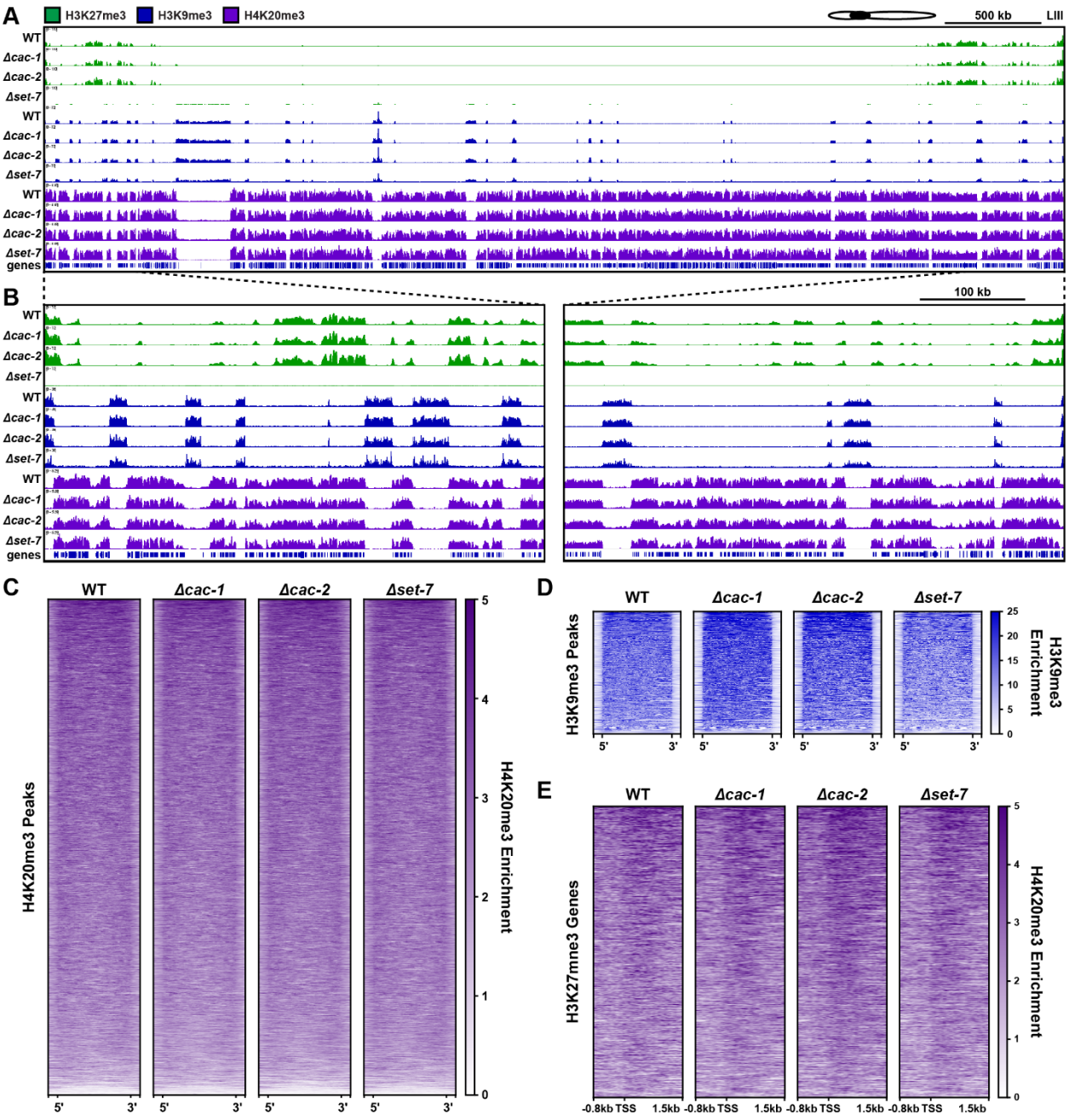
A
H3K27me3
H3K9me3
H4K20me3
500 kb
WT
Δcac-1
Δcac-2
Δset-7
genes
B
100 kb
C
H4K20me3 Peaks
H4K20me3 Enrichment
5'
3'
D
H3K9me3 Peaks
H3K9me3 Enrichment
E
H3K27mne3 Genes
-0.8kb TSS
1.5kb

Figure S3.6: CAF-1 deficiency does not impact H3K9me3 or H4K20me3

(A) Whole-chromosome view of H3K27me3, H3K9me3, and H4K20me3 enrichment in WT, CAF-1-deficient mutants, and *Δset-7* on LGIII. **(B)** Zoom-in views of H3K27me3, H3K9me3, and H4K20me3 enrichment in WT, CAF-1-deficient mutants, and *Δset-7* at two facultative heterochromatin regions on LGIII. **(C)** Heatmaps displaying H4K20me3 enrichment across all called H4K20me3 peaks in WT, CAF-1-deficient mutants, and *Δset-7*. **(D)** Heatmaps displaying H3K9me3 enrichment across all called H3K9me3 peaks in WT, CAF-1-deficient mutants, and *Δset-7*. **(E)** Heatmaps displaying H4K20me3 enrichment across H3K27me3-marked genes in WT, CAF-1-deficient mutants, and *Δset-7*.

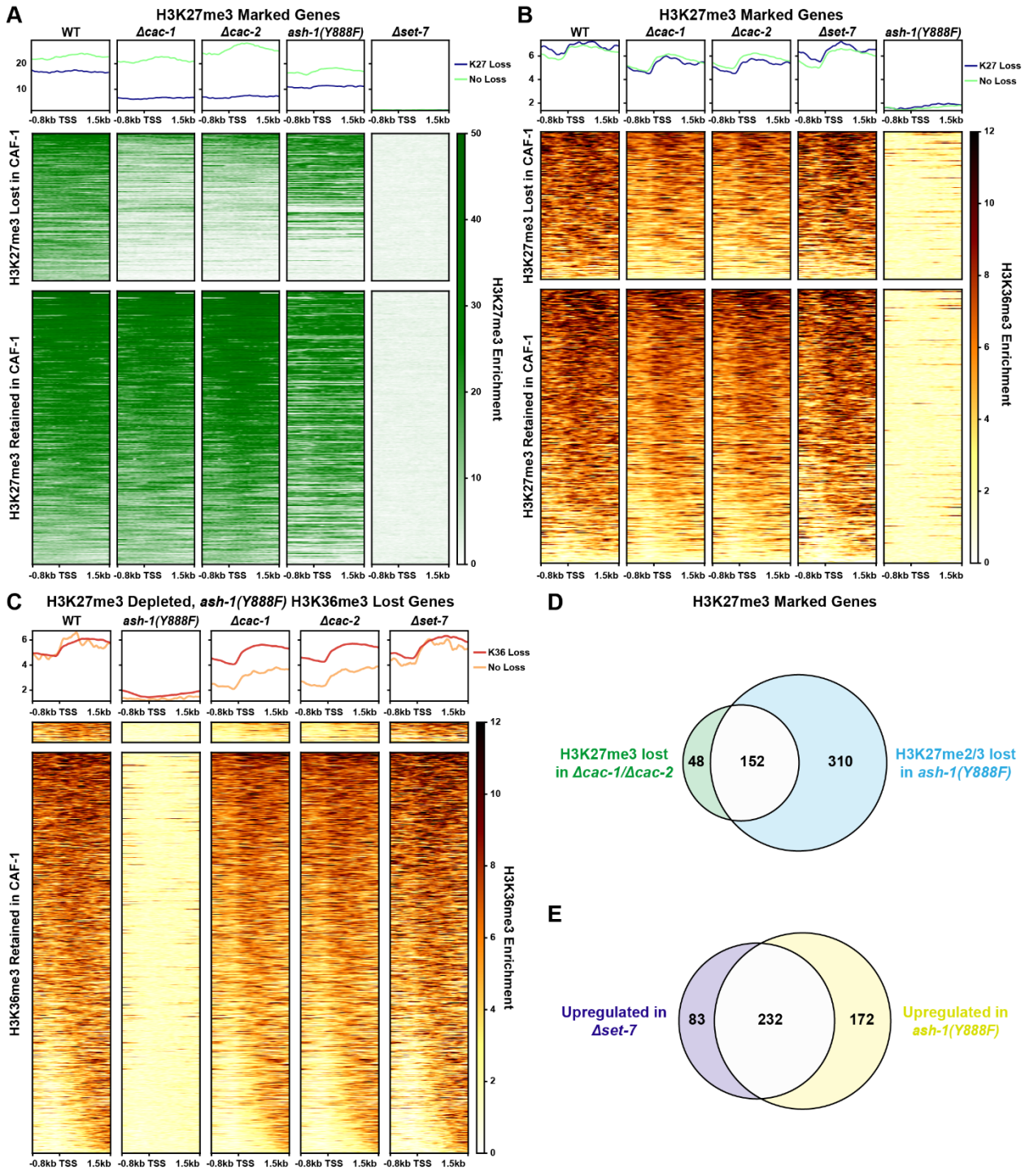
A
H3K27me3 Marked Genes
WT
Δcac-1
Δcac-2
ash-1(Y888F)
Δset-7
K27 Loss
No Loss
H3K27me3 Lost in CAF-1
H3K27me3 Retained in CAF-1
H3K27me3 Enrichment
-0.8kb TSS
1.5kb
B
H3K27me3 Marked Genes
H3K36me3 Enrichment
C
H3K27me3 Depleted, ash-1(Y888F) H3K36me3 Lost Genes
K36 Loss
No Loss
H3K36me3 Retained in CAF-1
D
H3K27me3 Marked Genes
H3K27me3 lost in Δcac-1/Δcac-2
48
152
310
H3K27me2/3 lost in ash-1(Y888F)
E
Upregulated in Δset-7
83
232
172
Upregulated in ash-1(Y888F)

Figure S3.7: CAF-1 deficiency impacts ASH-1 activity independent of PRC2

(A) Heatmaps and metaplots displaying H2K27me3 enrichment across H3K27me3-marked genes in WT, CAF-1-deficient mutants, and *Δset-7*. genes are clustered by loss of H3K27me3 in CAF-1-deficient mutants. Clusters are individually sorted by H3K27me3 enrichment **(B)** Heatmaps and metaplots displaying H3K36me3 enrichment across H3K27me3-marked genes in WT, CAF-1-deficient mutants, and *Δset-7*. genes are clustered by loss of H3K27me3 in CAF-1-deficient mutants. Clusters are individually sorted by H3K36me3 enrichment **(B)** Heatmaps and metaplots displaying H3K36me3 enrichment across H3K27me3-depleted genes that lose H3K36me3 in *ash-1(Y888F)* for WT, *ash-1(Y888F)*, CAF-1-deficient mutants, and *Δset-7*. genes are clustered by loss of H3K36me3 in CAF-1-deficient mutants **(D)** Venn Diagram displaying overlap between genes that lose H3K27me3 in *Δcac-1* or *Δcac-2* and lose H3K27me2/3 in *ash-1(Y888F)* **(E)** Venn Diagram displaying overlap between genes that are upregulated in *Δset-7* and upregulated in and *ash-1(Y888F)*

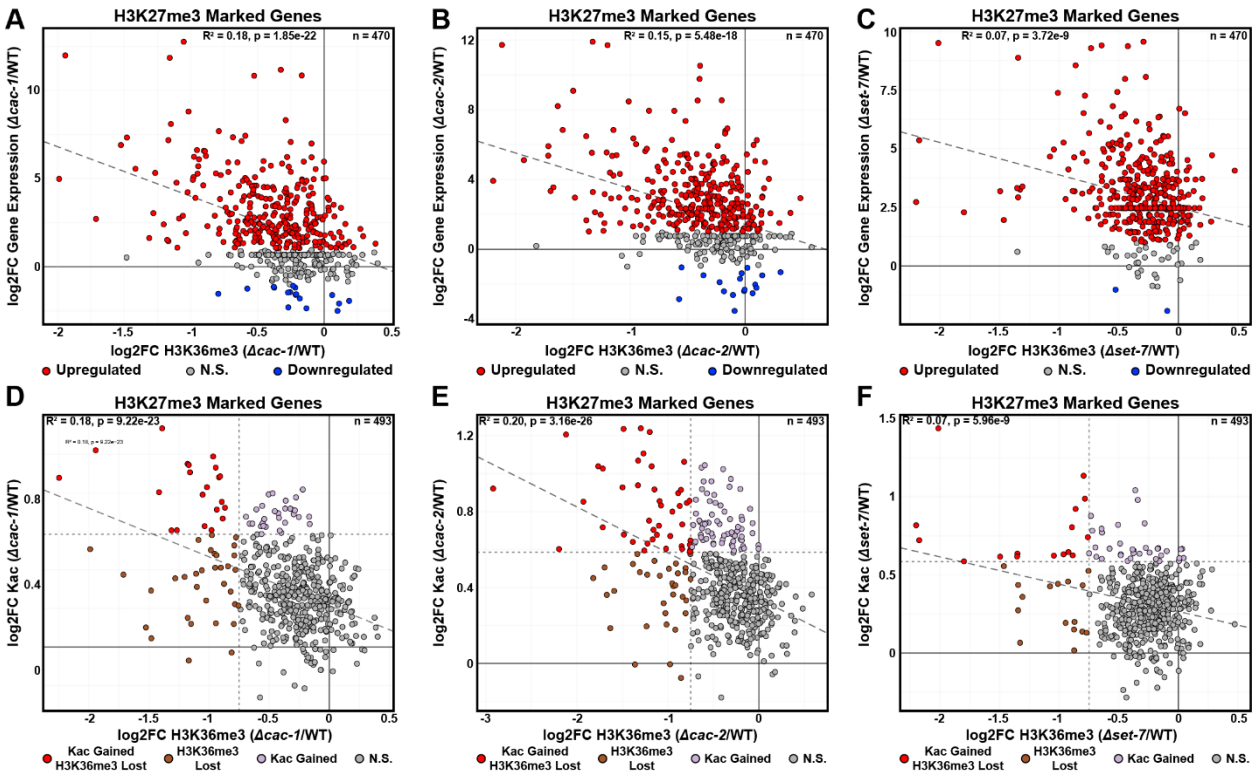

Figure S3.8: Loss of H3K36me3 is correlated with gene expression and lysine acetylation in CAF-1-deficient mutants

(A) Scatter plot displaying log2FC of H3K36me3 enrichment vs. log2FC of gene expression in *Δcac-1* vs WT. **(B)** Scatter plot displaying log2FC of H3K36me3 enrichment vs. log2FC of gene expression in *Δcac-2* vs WT. **(C)** Scatter plot displaying log2FC of H3K36me3 enrichment vs. log2FC of gene expression in *Δset-7* vs WT. **(D)** Scatter plot displaying log2FC of H3K36me3 enrichment vs. log2FC of Kac enrichment in *Δcac-1* vs WT. **(E)** Scatter plot displaying log2FC of H3K36me3 enrichment vs. log2FC of Kac enrichment in *Δcac-2* vs WT. **(F)** Scatter plot displaying log2FC of H3K36me3 enrichment vs. log2FC of Kac enrichment in *Δset-7* vs WT.

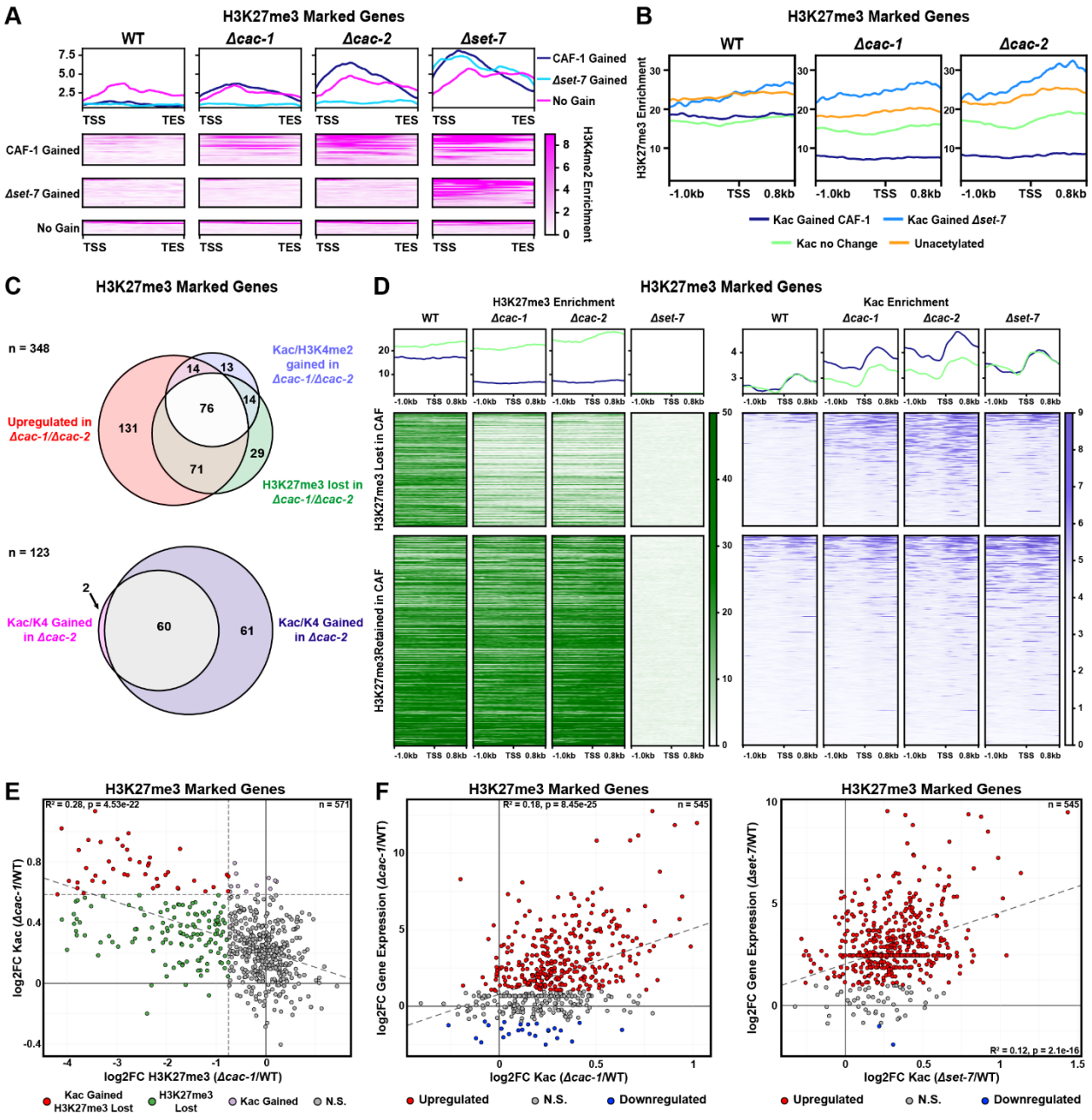
A
H3K27me3 Marked Genes
WT
Δcac-1
Δcac-2
Δset-7
CAF-1 Gained
Δset-7 Gained
No Gain
TSS
TES
H3K4me2 Enrichment
B
H3K27me3 Marked Genes
H3K27me3 Enrichment
-1.0kb
TSS
0.8kb
Kac Gained CAF-1
Kac Gained Δset-7
Kac no Change
Unacetylated
C
H3K27me3 Marked Genes
n = 348
Kac/H3K4me2 gained in Δcac-1/Δcac-2
Upregulated in Δcac-1/Δcac-2
H3K27me3 lost in Δcac-1/Δcac-2
14
13
14
76
131
29
71
n = 123
2
Kac/K4 Gained in Δcac-2
60
61
Kac/K4 Gained in Δcac-2
D
H3K27me3 Marked Genes
H3K27me3 Enrichment
Kac Enrichment
H3K27me3 Lost in CAF
H3K27me3Retained in CAF
E
H3K27me3 Marked Genes
R² = 0.28, p = 4.53e-22
n = 571
log2FC Kac (Δcac-1/WT)
log2FC H3K27me3 (Δcac-1/WT)
Kac Gained H3K27me3 Lost
H3K27me3 Lost
Kac Gained
N.S.
F
H3K27me3 Marked Genes
R² = 0.18, p = 8.45e-25
n = 545
log2FC Gene Expression (Δcac-1/WT)
log2FC Kac (Δcac-1/WT)
Upregulated
N.S.
Downregulated
H3K27me3 Marked Genes
n = 545
log2FC Gene Expression (Δset-7/WT)
R² = 0.12, p = 2.1e-16
log2FC Kac (Δset-7/WT)
Upregulated
N.S.
Downregulated

Figure S3.9: Loss of H3K27me3 in CAF-1-deficient mutants is correlated with gains in H3K4me2 and acetylation

(A) Heatmaps displaying H3K4me2 enrichment at H3K27me3-marked genes enriched for H3K4me2 in WT, CAF-1-deficient mutants, and *Δset-7*. Genes (rows) are split into three clusters (top to bottom): H3K4me2 gained in CAF-1–deficient mutants (1), H3K4me2 gained in *Δset-7* but not in CAF-1-deficient mutants (2), and no change in H3K4me2 vs WT (3). **(B)** Metaplots displaying H3K27me3 enrichment in 4 clusters of genes: Kac gained in CAF-1–deficient mutants (1, dark blue) , Kac gained in *Δset-7* but not in CAF-1-deficient mutants (2, light blue) , no change in Kac vs WT (3, green), and unacetylated in all strains (4, orange). **(C)** Venn diagrams displaying overlap of genes that lose H3K27me3 in *Δcac-1* or *Δcac-2*, gain Kac or H3K4me2 in *Δcac-1* or *Δcac-2* and are upregulated in *Δcac-1* or *Δcac-2* (Top) and genes that gain Kac in *Δcac-1* or gain Kac in *Δcac-2* (Bottom). **(D)** Heatmaps displaying H3K27me3 enrichment (left) and Kac enrichment (right) at H3K27me3-marked genes in WT, CAF-1-deficient mutants, and *Δset-7*. Genes are clustered by loss of H3K27me3 in CAF-1-deficient mutants. Clusters are individually sorted by Kac enrichment **(E)** Scatter plots displaying log2FC of H3K27me3 enrichment vs. log2FC of Kac enrichment in *Δcac-1* vs WT (left) and log2FC of Kac enrichment vs. log2FC of gene expression in *Δcac-1* vs WT **(E)** Scatter plot displaying log2FC of Kac enrichment vs. log2FC of gene expression in *Δset-7* vs WT.

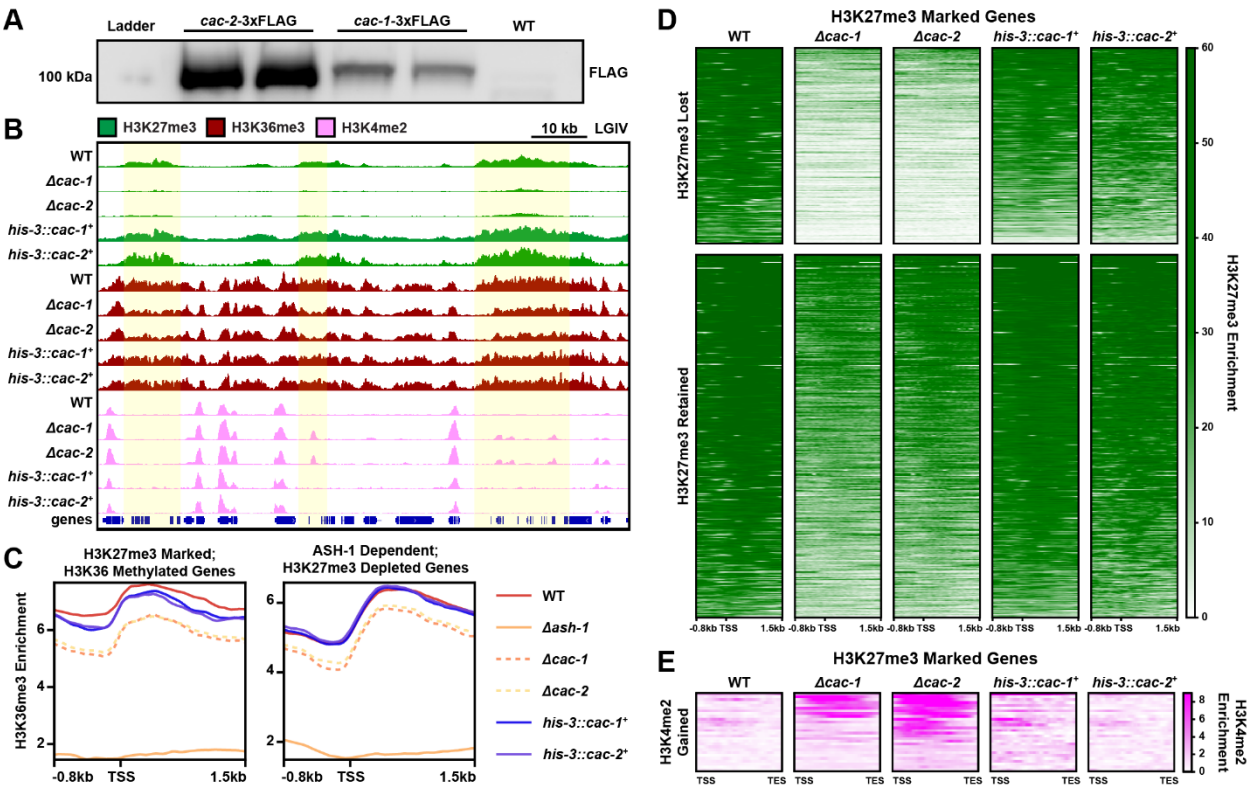

Figure S3.10: CAF-1 complementation restores the facultative heterochromatin environment

(A) Western blot displaying protein expression of the *cac-1-3xFLAG::his-3*$^{+}$ and *cac-2-3xFLAG::his-3*$^{+}$ complementation constructs **(B)** Browser shots displaying H3K27me3, H3K4me2, and H3K36me3 enrichment in WT, CAF-1-deficient mutants, and CAF-1 complements at a facultative heterochromatin region on LGIV **(C)** Metaplots displaying H3K36me3 enrichment at H3K27me3-marked genes and H3K27me3-depleted genes that lose H3K36me3 in *ash-1(Y888F)* for WT, *ash-1(Y888F)*, CAF-1-deficient mutants, and CAF-1 complements **(D)** Heatmaps displaying H3K27me3 enrichment at H3K27me3-marked genes in WT, CAF-1-deficient mutants, and CAF-1 complements. Genes are clustered by loss of H3K27me3 in CAF-1-deficient mutants. Clusters are individually sorted by H3K27me3 enrichment **(E)** Heatmaps displaying H3K4me2 enrichment at H3K4me2-enriched, H3K27me3-marked genes in WT, CAF-1-deficient mutants, and CAF-1 complements.

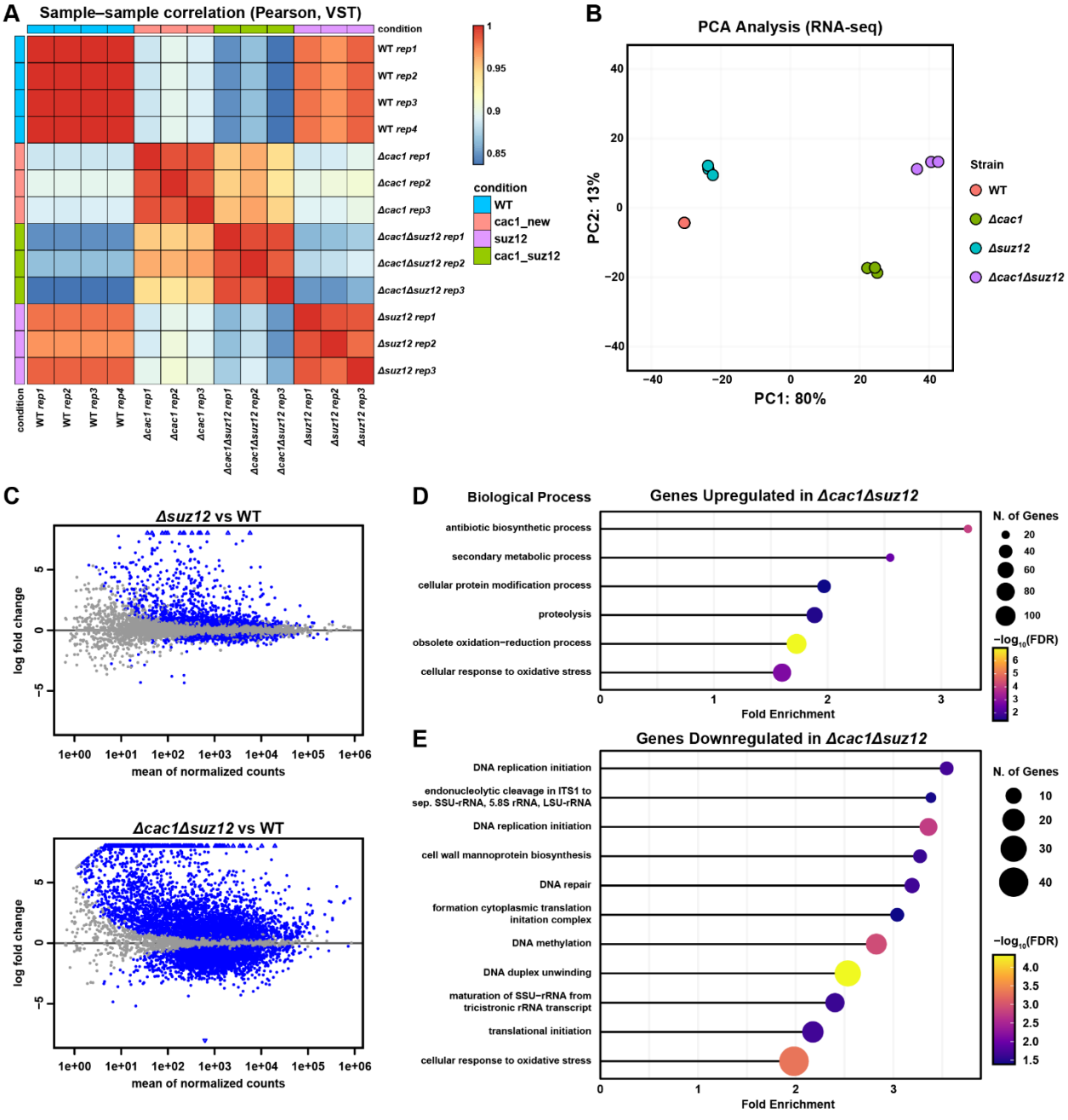
A
Sample–sample correlation (Pearson, VST)
condition
WT rep1
WT rep2
WT rep3
WT rep4
Δcac1 rep1
Δcac1 rep2
Δcac1 rep3
Δcac1Δsuz12 rep1
Δcac1Δsuz12 rep2
Δcac1Δsuz12 rep3
Δsuz12 rep1
Δsuz12 rep2
Δsuz12 rep3
1
0.95
0.9
0.85
condition
WT
cac1_new
suz12
cac1_suz12
B
PCA Analysis (RNA-seq)
PC2: 13%
PC1: 80%
Strain
WT
Δcac1
Δsuz12
Δcac1Δsuz12
C
Δsuz12 vs WT
log fold change
mean of normalized counts
Δcac1Δsuz12 vs WT
log fold change
mean of normalized counts
D
Biological Process
Genes Upregulated in Δcac1Δsuz12
antibiotic biosynthetic process
secondary metabolic process
cellular protein modification process
proteolysis
obsolete oxidation−reduction process
cellular response to oxidative stress
Fold Enrichment
N. of Genes
−log10(FDR)
E
Genes Downregulated in Δcac1Δsuz12
DNA replication initiation
endonucleolytic cleavage in ITS1 to sep. SSU-rRNA, 5.8S rRNA, LSU-rRNA
DNA replication initiation
cell wall mannoprotein biosynthesis
DNA repair
formation cytoplasmic translation initation complex
DNA methylation
DNA duplex unwinding
maturation of SSU−rRNA from tricistronic rRNA transcript
translational initiation
cellular response to oxidative stress
Fold Enrichment
N. of Genes
−log10(FDR)

Figure S3.11: QC analysis of RNA-seq for *Δcac-1Δsuz-12*

(A) Correlation plot displaying similarity of expression profiles across RNA-seq samples for *Δcac-1*, *Δsuz-12*, and *Δcac-1Δsuz-12.* **(B)** PCA Plot displaying likeness of expression profiles of RNA-seq samples for *Δcac-1*, *Δsuz-12*, and *Δcac-1Δsuz-12.* **(C)** MA plots displaying mean normalized counts (x-axis) against log2FC in gene expression for *Δsuz-12* (Top) and *Δcac-1Δsuz-12* (Bottom) vs WT. **(D)** GO analysis for genes that are upregulated in *Δcac-1Δsuz-12*. **(E)** GO analysis for genes that are downregulated in *Δcac-1Δsuz-12.*

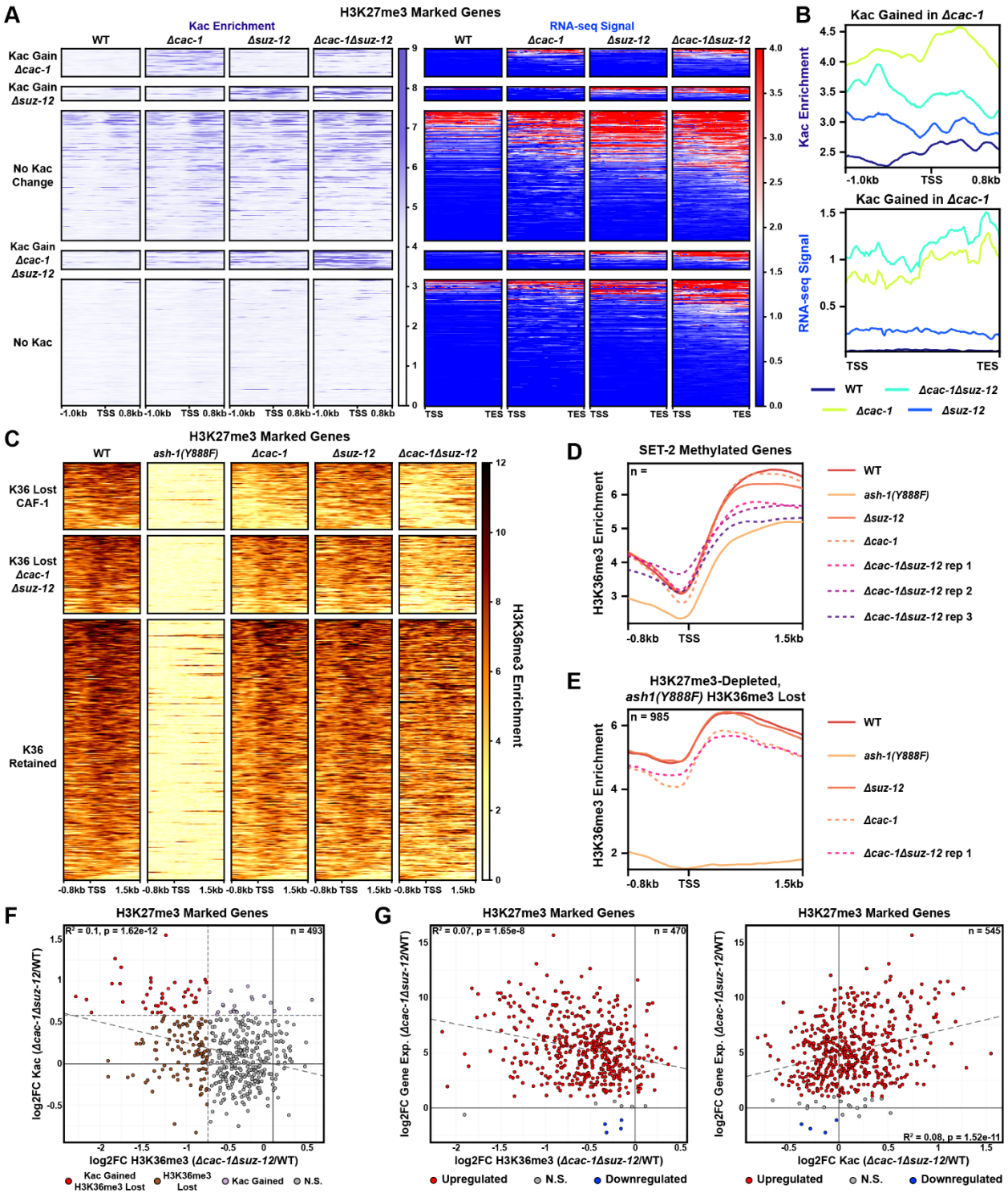
A
H3K27me3 Marked Genes
Kac Enrichment
RNA-seq Signal
WT
Δcac-1
Δsuz-12
Δcac-1Δsuz-12
Kac Gain Δcac-1
Kac Gain Δsuz-12
No Kac Change
Kac Gain Δcac-1 Δsuz-12
No Kac
-1.0kb TSS 0.8kb
TSS TES
B
Kac Gained in Δcac-1
Kac Enrichment
RNA-seq Signal
TSS
TES
WT
Δcac-1Δsuz-12
Δcac-1
Δsuz-12
C
H3K27me3 Marked Genes
ash-1(Y888F)
K36 Lost CAF-1
K36 Lost Δcac-1 Δsuz-12
K36 Retained
-0.8kb TSS 1.5kb
H3K36me3 Enrichment
D
SET-2 Methylated Genes
n =
H3K36me3 Enrichment
-0.8kb TSS 1.5kb
WT
ash-1(Y888F)
Δsuz-12
Δcac-1
Δcac-1Δsuz-12 rep 1
Δcac-1Δsuz-12 rep 2
Δcac-1Δsuz-12 rep 3
E
H3K27me3-Depleted, ash1(Y888F) H3K36me3 Lost
n = 985
H3K36me3 Enrichment
-0.8kb TSS 1.5kb
WT
ash-1(Y888F)
Δsuz-12
Δcac-1
Δcac-1Δsuz-12 rep 1
F
H3K27me3 Marked Genes
R² = 0.1, p = 1.62e-12
n = 493
log2FC Kac (Δcac-1Δsuz-12/WT)
log2FC H3K36me3 (Δcac-1Δsuz-12/WT)
Kac Gained H3K36me3 Lost
H3K36me3 Lost
Kac Gained
N.S.
G
H3K27me3 Marked Genes
R² = 0.07, p = 1.65e-8
n = 470
log2FC Gene Exp. (Δcac-1Δsuz-12/WT)
log2FC H3K36me3 (Δcac-1Δsuz-12/WT)
Upregulated
N.S.
Downregulated
H3K27me3 Marked Genes
n = 545
R² = 0.08, p = 1.52e-11
log2FC Gene Exp. (Δcac-1Δsuz-12/WT)
log2FC Kac (Δcac-1Δsuz-12/WT)
Upregulated
N.S.
Downregulated

Figure S3.12: *Δcac-1Δsuz-12* experiences additive defects in the heterochromatin environment

(A) Heatmaps displaying Kac enrichment (Left) and RNA-seq signal (Right) at H3K27me3-marked genes in WT, *Δcac-1*, *Δsuz-12*, and *Δcac-1Δsuz-12*. Genes (rows) are split into five clusters (top to bottom): Kac gained in CAF-1–deficient mutants (1) , Kac gained in *Δset-7* but not in CAF-1-deficient mutants (2) , no change in Kac vs WT (3), Kac gained only in *Δcac-1Δsuz-12* (4), and unacetylated in all strains (5). Clusters are individually sorted by RNA-seq signal **(B)** Metaplots displaying enrichment of Kac (Top) and RNA-seq signal (Bottom) at H3K27me3-marked genes that gain Kac in CAF-1 for WT (dark blue), *Δcac-1* (green), *Δsuz-12* (light blue), and *Δcac-1Δsuz-12* (aqua) **(C)** Heatmap displaying H3K36me3 enrichment at H3K36me3-enriched, H3K27me3-marked genes for WT, *ash-1(Y888F), Δcac-1*, *Δsuz-12*, and *Δcac-1Δsuz-12*. Genes (rows) are split into three clusters (top to bottom): H3K36me3 lost in CAF-1-deficient mutants (1), H3K36me3 lost only in *Δcac-1Δsuz-12* (2), and no H3K36me3 lost (3). **(D)** Metaplot displaying H3K36me3 enrichment at SET-2 methylated genes for WT, *Δcac-1*, *Δsuz-12*, and all 3 replicates of *Δcac-1Δsuz-12*. **(E)** Metaplot displaying H3K36me3 enrichment at H3K27me3-depleted genes that lose H3K36me3 in *ash-1(Y888F)* for WT, *ash-1(Y888F), Δcac-1*, *Δsuz-12*, and *Δcac-1Δsuz-12*. **(F)** Scatter plot displaying log2FC of H3K36me3 enrichment vs. log2FC of Kac enrichment in *Δcac-1Δsuz-12* vs WT. **(G)** Scatter plots displaying log2FC of H3K36me3 enrichment vs. log2FC of gene expression (left) and log2FC of Kac enrichment vs. log2FC of gene expression (right) in *Δcac-1Δsuz-12* vs WT.

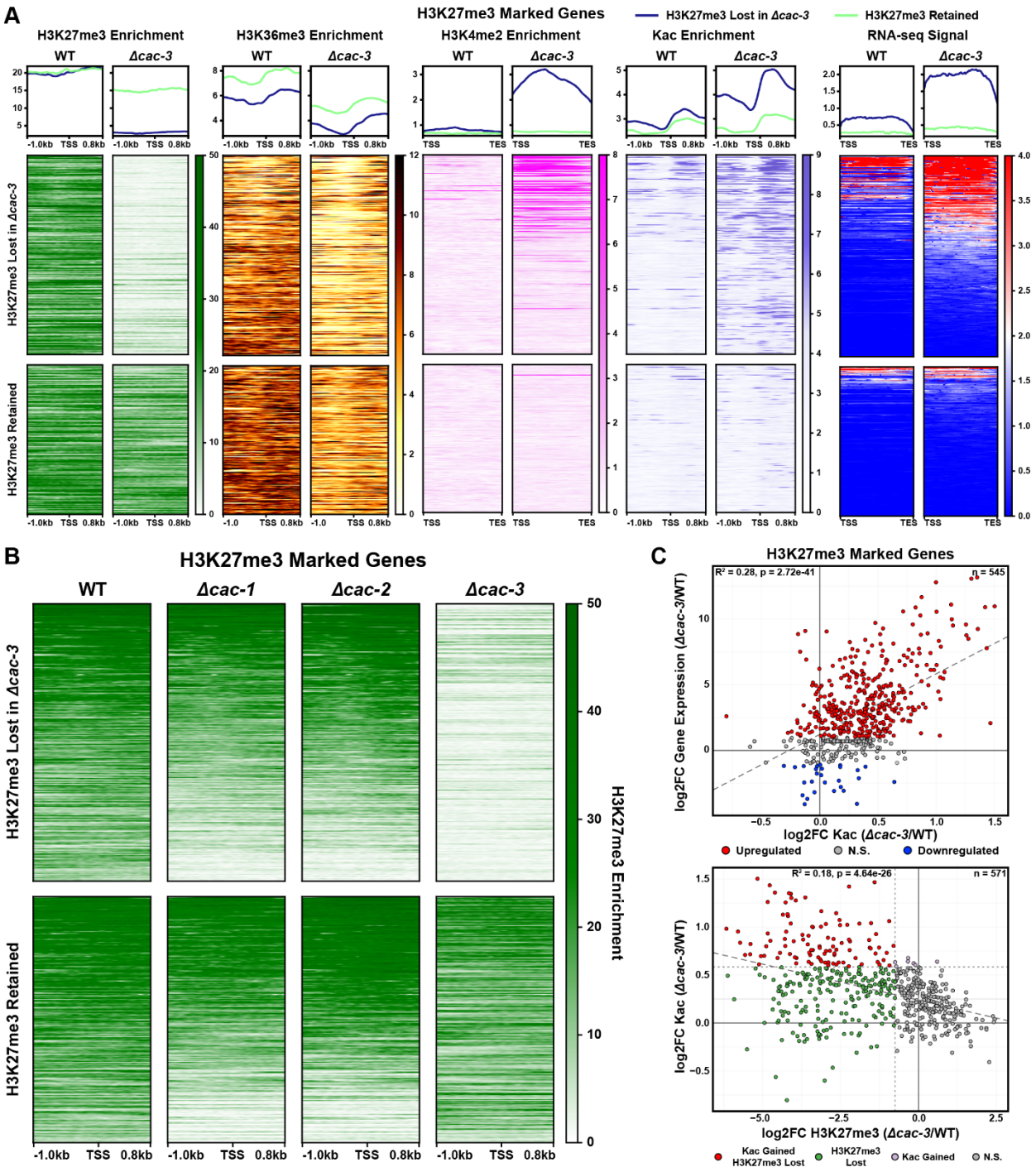
A
H3K27me3 Marked Genes
H3K27me3 Lost in Δcac-3
H3K27me3 Retained
H3K27me3 Enrichment
WT
Δcac-3
H3K36me3 Enrichment
H3K4me2 Enrichment
Kac Enrichment
RNA-seq Signal
H3K27me3 Lost in Δcac-3
H3K27me3 Retained
-1.0kb TSS 0.8kb
TSS TES
B
H3K27me3 Marked Genes
WT
Δcac-1
Δcac-2
Δcac-3
H3K27me3 Lost in Δcac-3
H3K27me3 Retained
H3K27me3 Enrichment
-1.0kb TSS 0.8kb
C
H3K27me3 Marked Genes
R² = 0.28, p = 2.72e-41
n = 545
log2FC Gene Expression (Δcac-3/WT)
log2FC Kac (Δcac-3/WT)
Upregulated
N.S.
Downregulated
R² = 0.18, p = 4.64e-26
n = 571
log2FC Kac (Δcac-3/WT)
log2FC H3K27me3 (Δcac-3/WT)
Kac Gained
H3K27me3 Lost
H3K27me3
Lost
Kac Gained
N.S.

Figure S3.13: *Δcac-3* experiences unique changes in the heterochromatin environment

(A) Heatmaps displaying enrichment of H3K27me3, H3K36me3, H3K4me2, Kac, and RNA-seq Signal at H3K27me3-marked genes in WT and *Δcac-3*. Genes are clustered by loss of H3K27me3 in *Δcac-3*. Clusters are individually sorted by RNA-seq signal. **(B)** Heatmap displaying enrichment of H3K27me3 in CAF-1-deficient mutants. Genes are clustered by loss of H3K27me3 in *Δcac-3*. Clusters are individually sorted by H3K27me3 enrichment. **(C)** Scatter plots displaying log2FC of Kac enrichment vs. log2FC of gene expression in *Δcac-3* vs WT (Top) and log2FC of H3K27me3 enrichment vs. log2FC of Kac in *Δcac-3* vs WT.

Table S3.1: Stains used in this study

Strain	Genotype	Source
S2	WT	FGSC
ETX27-6	*cac-1::hph*	This Study
ETX27-2	*cac-1::hph*	This Study
ETX14-5	*cac-2::hph*	This Study
ETX14-8	*cac-2::hph*	This Study
ETX15-9	*cac-3::hph*	This Study
ETX15-6	*cac-3::hph*	This Study
ETX25-5	*cac-1::hph*, *suz-12::hph*	This Study
ETX119-1	*cac-1*::*hph*, *his-3*$^{-}$::*cac-1*-3xFLAG::*his-3*$^{+}$	This Study
ETX119-2	*cac-1*::*hph*, *his-3*$^{-}$::*cac-1*-3xFLAG::*his-3*$^{+}$	This Study
ETX80-2	*cac-2*::*hph*, *his-3*$^{-}$::*cac-2*-3xFLAG::*his-3*$^{+}$	This Study
ETX82-2	*cac-2*::*hph*, *his-3*$^{-}$::*cac-2*-3xFLAG::*his-3*$^{+}$	This Study
S328	*set-7::hph*	FGSC
S375	*suz-12::hph*	FGSC
FGSC 12082	*naf-1::hph*	FGSC
FGSC 11778	*naf-2::hph*	FGSC
S537	*asf-1::hph*	FGSC
FGSC 19985	*atrx::hph*	FGSC

Table S3.2: Primers used in this study

Primer Name	Sequence	Description	Designed
Cac-1 Geno F	CCAGCTCCTCATC GAACTCC	cac-1 genotyping primer	This Study
Cac-1 Geno R	CTCCCGGTCGACA GAAGATG	cac-1 genotyping primer	This Study
Cac2_Geno_Forward	GGTGCTGGCTCCA CTAACTT	cac-2 genotyping primer	This Study
Cac2_Geno_reverse	GACAAAGAGTGC CCTTCGGA	cac-2 genotyping primer	This Study
Cac-3 Geno F	ATCTGGAAGGTG GCCAACAG	cac-3 genotyping primer	This Study
Cac-3 Geno R	AAGCGATTCATG GGCCTTCC	cac-3 genotyping primer	This Study
set-7_off_gene	GCATCACCCACTA CACGACA	set-7 genotyping primer	This Study
suz12_geno_F	TCCGTCTTTTGGG TAGCTAGAT	suz-12 genotyping primer	This Study
suz12_geno_R	GGGTTGTGCGAG GTGTGG	suz-12 genotyping primer	This Study
HPH_300_Universal	TAAAGGGAGGAA GGGCGAAC	hph genotyping primer	This Study
pBM61 Gibson cloning P2	GTGGACGGCTAA TGGGGTCTGAAT GCTAAA	his-3 complement plasmid cloning primer	This Study
pBM61 Gibson cloning P1	TTTGGTTGATGTG AGGGGTTGTGAA AGTGG	his-3 complement plasmid cloning primer	This Study
CDS_FP_cac-1_gibson	CAAGCTCGAAAT TAACCCTCACTAA AGTCGAAGACCA GCTCATCAGG	cac-1 CDS cloning primer	This Study
CDS_RP_cac-1_gibson	TCCGCCGCTACCT CCACCCGATCCGC CCTCCTTCCACTT CCAACCAC	cac-1 CDS cloning primer	This Study
UTR_FP_cac-1_gibson	ACGCGACTATAT ATTTGTCTCTAAT TGTACCGGTCTTT TTCTCTACATCC	cac-1 UTR cloning primer	This Study
UTR_RP_cac-1_gibson	TAATACGACTCAC TATAGGGCGAAT TGAACTGGAGGT GATTGTTTATG	cac-1 UTR cloning primer	This Study

CDS_FP_cac-2_gibson	CAAGCTCGAAATTAACCCTCACTAAAGGTCCACGACATTCACTGTCCT	cac-2 CDS cloning primer	This Study
CDS_RP_cac-2_gibson	TCCGCCGCTACCTCCACCCGATCCGCCCGCTTTAGCCACGTCGCT	cac-2 CDS cloning primer	This Study
UTR_FP_cac-2_gibson	ACGCGACTATATATTTGTCTCTAATTGTACGTCGCTAGGCGGTTGTTG	cac-2 UTR cloning primer	This Study
UTR_RP_cac-2_gibson	TAATACGACTCACTATAGGGCGAATTGGAGCCTGTACCTAAGCAGACCGATACC	cac-2 UTR cloning primer	This Study
NCU04869_qPCR_F	TGGTGCGTTCAACCTGAAAA	NCU04869 qPCR primer	This study
NCU04869_qPCR_R	TCACCATTTTCTTCCGCACAA	NCU04869 qPCR primer	This Study
NCU08834_qPCR_F	TCGAGGACATTTACCGCCAC	NCU08834 qPCR primer	This study
NCU08834_qPCR_R	CTCGCTTTCTGTGCAACACC	NCU08834 qPCR primer	This Study
NCU08085_qPCR_F	CACCAACTACCACACCATCC	NCU08085 qPCR primer	Kamei et al. 2019
NCU08085_qPCR_R	CGAGGGCTTCGGGTCTATG	NCU08085 qPCR primer	Kamei et al. 2019

Table S3.3: Antibodies used in this study

Antigen	Supplier	Catalog #
H3K27me3	Cell Signaling	C36B11
H3K27me3	Abcam	ab6002
H3K9me3	Active Motif	39161
H4K20me3	Active Motif	91108
H3K36me3	Abcam	ab9050
Pan-acetyl-lysine	Cell Signaling Technology	9441S
H3K4me2	Active Motif	39141
FLAG	Sigma-Aldrich	F1804

Table S3.4: Sequencing samples used in this study

Title	Type	SRA
WT rep 1	RNA	SRR8269825
WT rep 2	RNA	SRR8269775
WT rep 3	RNA	SRR8269782
WT rep 4	RNA	SRR8269810
Δcac-2 rep 1	RNA	SRR7970629
Δcac-2 rep 2	RNA	SRR7970630
Δcac-2 rep 3	RNA	SRR7970631
Δcac-3 rep 1	RNA	SRR7970598
Δcac-3 rep 2	RNA	SRR7970599
Δcac-3 rep 3	RNA	SRR7970600
Δset-7 rep 1	RNA	SRR10916163
Δset-7 rep 2	RNA	SRR10916164
Δset-7 rep 3	RNA	SRR10916165
Δsuz-12 rep 1	RNA	SRR9027658
Δsuz-12 rep 2	RNA	SRR9027759
Δsuz-12 rep 3	RNA	SRR9027689
Δasf-1 rep 1	RNA	SRR10916318
Δasf-1 rep 2	RNA	SRR10916319
Δasf-1 rep 3	RNA	SRR10916320
Δatrx rep 1	RNA	SRR9027727
Δatrx rep 2	RNA	SRR9027728
Δatrx rep 3	RNA	SRR9027730
Δnaf-1 rep 1	RNA	SRR8269830
Δnaf-1 rep 2	RNA	SRR8269647
Δnaf-1 rep 3	RNA	SRR8269650
Δnaf-2 rep 1	RNA	SRR7970603
Δnaf-2 rep 2	RNA	SRR7970606
Δnaf-2 rep 3	RNA	SRR7970610
ash-1(Y888F) rep 1	RNA	SRR7690267
ash-1(Y888F) rep 2	RNA	SRR7690268
ash-1(Y888F) H3K27me2/3 rep 1	ChIP	SRR7690295
ash-1(Y888F) H3K27me2/3 rep 2	ChIP	SRR7690296
ash-1(Y888F) H3K36me3	ChIP	SRR7690288

CHAPTER FOUR

DISCUSSION

The body of work presented in this dissertation represents a significant contribution to our understanding of the PcG repression pathway in fungal species. Employing the *N. crassa* model system, we conducted experiments that help uncover how PRC2 is directed to form and maintain facultative heterochromatin domains. First, we constructed a strain harboring an inducible PRC2 complex, with the ultimate goal of understanding how PRC2 is directly recruited to DNA genome wide. We used this tool to induce *de-novo* establishment of facultative heterochromatin domains, which revealed interesting insights into the molecular factors that promote PRC2 recruitment and H3K27me3 maintenance. This is the first system developed in *N. crassa* that enables the progressive measurement of genome-wide H3K27me3 recovery *de-novo*. We next turned my focus to analyzing the roles of histone chaperones in the maintenance of facultative heterochromatin in *N. crassa*. Through a large-scale histone chaperone mutant screen, we identified the CAF-1 complex as an important player in PRC2-mediated gene repression. We revealed that CAF-1 plays a role in maintaining gene repression that is distinct from PRC2, and that both complexes are required for proper maintenance of the facultative heterochromatin environment. The results of this study provide greater knowledge of the consequences of CAF-1 deficiency on heterochromatin maintenance and may help contextualize the role of CAF-1 in this process in other metazoan species. Collectively the research performed in this dissertation enhances our knowledge of the complex relationship between chromatin formation and gene regulation and motivates further studies to determine how PRC2 activity is regulated.

Measurement of *de-novo* H3K27me3 Establishment

The mechanisms that underlie PRC2 recruitment have been a topic of extensive research, yet our understanding of this process remains incomplete (Kahn et al., 2016; Laprell et al., 2017; Laugesen et al., 2019; Lee et al., 2007; Yu et al., 2019). Technical limitations and species-specific variation of PcG systems have made it difficult to establish general rules for how PRC2 recognizes its target loci across the genome (Baile et al., 2022; Bieluszewski et al., 2021; Fischer et al., 2022; Sharaf et al., 2022). We decided to leverage the minimal Polycomb repressive system of *N. crassa* to study the dynamics of PRC2 recruitment in greater detail (Jamieson et al., 2018; Jamieson et al., 2013). The absence of PRC1 homologs in this system limits the number of potential molecular factors capable of recruiting PRC2 activity (de Potter et al., 2023; Ridenour et al., 2020).

The development of a functional *qaP-suz-12* system allowed us to visualize recovery of H3K27me3 just hours after induction, showing that PRC2 recruitment occurs quickly *in vivo*. In an unexpected result, we observed that recovery of H3K27me3 at WT loci was incomplete, even after inducing *qaP-suz-12* over multiple days, and that novel H3K27me3 peaks emerged at ectopic loci. We ultimately revealed that this ectopic methylation coincided with downregulation of gene expression under quinic acid growth conditions. These results suggest that PRC2 recruitment and subsequent H3K27me3 maintenance is highly dependent on transcriptional activity. Interestingly, a WT strain grown under identical conditions did not experience a comparable shift in H3K27me3 patterns, suggesting that maintenance at native loci prevents H3K27me3 rearrangement, while *de-novo* establishment facilitates it. These results shed light on the importance of H3K27me3 establishment and maintenance in maintaining a proper facultative heterochromatin environment.

In addition to revealing insights into the dynamics of facultative heterochromatin establishment, the *qaP-suz-12* system allowed us to identify putative H3K27me3 nucleation sites in the *N. crassa* genome. We identified internal loci at which H3K27me3 was established hours post-induction and cloned them into an ectopic locus to ask if *N. crassa* possesses *cis*-regulatory elements capable of recruiting PRC2. We showed that the DNA sequence of a nucleation site on LGIII was able to induce establishment of an ectopic H3K27me3 domain, but only after perturbing maintenance through mutation of *epr-1*. These results support a model in which H3K27me3 maintenance at native loci prevents movement of the PTM to ectopic sites, and support the hypothesis that maintenance helps prevent H3K27me3 rearrangement in a WT strain grown in quinic acid-containing media. It will be interesting to test the ability of the *qaP-suz-12* system to re-establish and maintain H3K27me3 in strains with mutations of chromatin regulators known to be involved in these processes.

CAF-1 is Required for Proper Heterochromatin Formation

Research across various model systems has shown that DNA replication is a critical checkpoint in the maintenance of epigenetic marks (Alabert & Groth, 2012; Almouzni & Cedar, 2016; Fang et al., 2024; Li & Zhang, 2012; Serra-Cardona & Zhang, 2018; Wenger et al., 2023). Histone PTMs on parental histones become diluted 2-fold after DNA is replicated and must be faithfully re-established prior to cell division (Alabert et al., 2015; Jadhav et al., 2020; Petryk et al., 2018; Wenger et al., 2023). Multiple replication-associated proteins have been implicated in this process through experiments that have revealed defects in the epigenome in their absence (Fang et al., 2024; Green et al., 2005; Huang et al., 2015; Mello et al., 2002; Ray-Gallet et al., 2011; Yu et al., 2018; Zhang et al., 2000). The histone chaperone CAF-1 is one of the most well-

characterized proteins involved in chromatin assembly during DNA replication and has been shown to be required for proper heterochromatin maintenance across eukaryotes (Cheng et al., 2019; Dohke et al., 2008; Enomoto & Berman, 1998; Franklin et al., 2025; Huang et al., 2007; Murzina et al., 1999; Roelens et al., 2017; Song et al., 2007). We decided to use *N. crassa* as a model system to study the impact of CAF-1-deficiency on facultative heterochromatin formation.

Our results revealed a genome-wide redistribution of H3K27me3 in CAF-1-deficient mutants that was accompanied by activation of many PRC2-repressed genes. These same genes experienced a gain in enrichment of histone PTMs associated with active transcription, suggesting that the heterochromatin environment shifted to a more "euchromatin-like" state as a result of CAF-1 inhibition. Furthermore, generating a double mutant that inactivated both the CAF-1 and PRC2 complexes resulted in additive defects in gene repression and the chromatin environment. These results identified a unique role for CAF-1 in the PRC2 gene repression pathway and provided greater context as to why CAF-1 is important for heterochromatin maintenance in metazoans. Furthermore, this study represents the first evidence that histone chaperones are important for maintenance of facultative heterochromatin in *N. crassa*.

Studying CAF-1's involvement in facultative heterochromatin maintenance in higher-order eukaryotes has remained challenging due to crucial roles of both CAF-1 and PRC2 in organismal development and pluripotency exit (Cheloufi et al., 2015; Cheng et al., 2019; Houlard et al., 2006; Ishiuchi et al., 2015; O'Carroll et al., 2001; Piunti & Shilatifard, 2021; Ueda et al., 2016). However, conservation of both complexes across metazoans has enabled studies in fungal models that have revealed a clear connection between CAF-1 activity and heterochromatin maintenance. Despite the contributions of this study to our general knowledge of CAF-1's role in this process, the biological mechanisms involved remain incompletely

understood. Observed defects in ASH-1 mediated H3K36me3 deposition may hint at a direct interaction between CAF-1 and ASH-1, although this would likely not be conserved in non-fungal species. Furthermore, CAF-1 has been shown to directly interact with PRC2 in mammals and plants, although we were unable to recapitulate this interaction in *N. crassa*. Collectively, our results motivate further biochemical experiments to reveal the molecular factors that work in concert with CAF-1 to maintain gene repression.

Broader Impacts

The ultimate goal of biological research is to further our understanding of the natural world and uncover the mysteries of life. Furthermore, I believe a central value of biologists should be to improve the quality of life for humankind by expanding our knowledge of the factors involved in maintaining it, and how perturbing them results in harmful diseases and disorders. In previous chapters I have explained how my research has contributed to our general knowledge of chromatin regulation, and how the tools I developed will facilitate future studies. I will now briefly cover how my work is relevant to applications of biological research beyond the bench.

Epigenetic misregulation has been implicated in a multitude of genetic diseases and disorders, and most human cancers have been associated with epigenetic variants (Baylin & Jones, 2016; Piunti & Shilatifard, 2021). Yet the causal links between epigenetic change and disease remain incompletely understood, and current work is focused on determining the roles epigenetic regulators in disease prevention (Allis & Jenuwein, 2016; Lappalainen & Greally, 2017). PRC2 is a protein of particular interest, as perturbing the complex is associated with multiple genetic diseases and cancers (Blackledge & Klose, 2021; Margueron & Reinberg, 2011;

Parreno et al., 2022; Piunti & Shilatifard, 2021; Seong et al., 2010; Yu et al., 2019). Many therapeutics have been developed that inhibit PRC2 activity to prevent disease progression and alleviate harmful symptoms (Bao et al., 2024; Duan et al., 2020; Kim & Roberts, 2016; Velez et al., 2024). Furthermore, defective PRC2 repression has also been associated with increased oncogene expression (Lee et al., 2014; Parreno et al., 2022; Zhang et al., 2022).

Gaining a better understanding of how PRC2 and other PcG proteins are recruited to maintain gene repression may enable the development of tools that allow us to directly alter the epigenome. These tools could be applied in a similar fashion to regular gene editing to help treat symptoms of harmful genetic diseases, without the need to induce harmful DNA DSBs. Indeed, recent work has shown that epigenetic regulators can be ectopically recruited to sites of interest across the genome using CRISPR-Cas-based technology (Hilton et al., 2015; Nunez et al., 2021; Xu et al., 2025). Leveraging these types of technology will allow researchers to build an epigenetic "map" by determining which epigenetic modifications and chromatin-associated proteins interact with one another to maintain chromatin architecture. Expanding our knowledge of how the epigenetic environment is regulated across eukaryotes will be critical in solving many difficult biological problems that currently face our species.

References

Alabert, C., Barth, T. K., Reveron-Gomez, N., Sidoli, S., Schmidt, A., Jensen, O. N., Imhof, A., & Groth, A. (2015). Two distinct modes for propagation of histone PTMs across the cell cycle. *Genes Dev*, *29*(6), 585–590. https://doi.org/10.1101/gad.256354.114

Alabert, C., & Groth, A. (2012). Chromatin replication and epigenome maintenance. *Nat Rev Mol Cell Biol*, *13*(3), 153–167. https://doi.org/10.1038/nrm3288

Allis, C. D., & Jenuwein, T. (2016). The molecular hallmarks of epigenetic control. *Nat Rev Genet*, *17*(8), 487–500. https://doi.org/10.1038/nrg.2016.59

Almouzni, G., & Cedar, H. (2016). Maintenance of Epigenetic Information. *Cold Spring Harb Perspect Biol*, *8*(5). https://doi.org/10.1101/cshperspect.a019372

Baile, F., Gomez-Zambrano, A., & Calonje, M. (2022). Roles of Polycomb complexes in regulating gene expression and chromatin structure in plants. *Plant Commun*, *3*(1), 100267. https://doi.org/10.1016/j.xplc.2021.100267

Bao, Q., Kumar, A., Wu, D., & Zhou, J. (2024). Targeting EED as a key PRC2 complex mediator toward novel epigenetic therapeutics. *Drug Discovery Today*, *29*(6), 103986. https://doi.org/https://doi.org/10.1016/j.drudis.2024.103986

Baylin, S. B., & Jones, P. A. (2016). Epigenetic Determinants of Cancer. *Cold Spring Harb Perspect Biol*, *8*(9). https://doi.org/10.1101/cshperspect.a019505

Bieluszewski, T., Xiao, J., Yang, Y., & Wagner, D. (2021). PRC2 activity, recruitment, and silencing: a comparative perspective. *Trends Plant Sci*, *26*(11), 1186–1198. https://doi.org/10.1016/j.tplants.2021.06.006

Blackledge, N. P., & Klose, R. J. (2021). The molecular principles of gene regulation by Polycomb repressive complexes. *Nat Rev Mol Cell Biol*, *22*(12), 815–833. https://doi.org/10.1038/s41580-021-00398-y

Cheloufi, S., Elling, U., Hopfgartner, B., Jung, Y. L., Murn, J., Ninova, M., Hubmann, M., Badeaux, A. I., Euong Ang, C., Tenen, D., Wesche, D. J., Abazova, N., Hogue, M., Tasdemir, N., Brumbaugh, J., Rathert, P., Jude, J., Ferrari, F., Blanco, A.,…Hochedlinger, K. (2015). The histone chaperone CAF-1 safeguards somatic cell identity. *Nature*, *528*(7581), 218–224. https://doi.org/10.1038/nature15749

Cheng, L., Zhang, X., Wang, Y., Gan, H., Xu, X., Lv, X., Hua, X., Que, J., Ordog, T., & Zhang, Z. (2019). Chromatin Assembly Factor 1 (CAF-1) facilitates the establishment of facultative heterochromatin during pluripotency exit. *Nucleic Acids Res*, *47*(21), 11114–11131. https://doi.org/10.1093/nar/gkz858

de Potter, B., Raas, M. W. D., Seidl, M. F., Verrijzer, C. P., & Snel, B. (2023). Uncoupled evolution of the Polycomb system and deep origin of non-canonical PRC1. *Commun Biol*, *6*(1), 1144. https://doi.org/10.1038/s42003-023-05501-x

Dohke, K., Miyazaki, S., Tanaka, K., Urano, T., Grewal, S. I., & Murakami, Y. (2008). Fission yeast chromatin assembly factor 1 assists in the replication-coupled maintenance of heterochromatin. *Genes Cells*, *13*(10), 1027–1043. https://doi.org/10.1111/j.1365-2443.2008.01225.x

Duan, R., Du, W., & Guo, W. (2020). EZH2: a novel target for cancer treatment. *J Hematol Oncol*, *13*(1), 104. https://doi.org/10.1186/s13045-020-00937-8

Enomoto, S., & Berman, J. (1998). Chromatin assembly factor I contributes to the maintenance, but not the re-establishment, of silencing at the yeast silent mating loci. *Genes Dev*, *12*(2), 219–232. https://doi.org/10.1101/gad.12.2.219

Fang, Y., Hua, X., Shan, C. M., Toda, T., Qiao, F., Zhang, Z., & Jia, S. (2024). Coordination of histone chaperones for parental histone segregation and epigenetic inheritance. *Genes Dev*, *38*(3-4), 189–204. https://doi.org/10.1101/gad.351278.123

Fischer, S., Weber, L. M., & Liefke, R. (2022). Evolutionary adaptation of the Polycomb repressive complex 2. *Epigenetics Chromatin*, *15*(1), 7. https://doi.org/10.1186/s13072-022-00439-6

Franklin, R., Zhang, B., Frazier, J., Chen, M., Do, B. T., Padayao, S., Wu, K., Vander Heiden, M. G., Vakoc, C. R., Roe, J. S., Ninova, M., Murn, J., Sykes, D. B., & Cheloufi, S. (2025). Histone chaperones coupled to DNA replication and transcription control divergent chromatin elements to maintain cell fate. *Genes Dev*, *39*(9-10), 652–675. https://doi.org/10.1101/gad.352316.124

Green, E. M., Antczak, A. J., Bailey, A. O., Franco, A. A., Wu, K. J., Yates, J. R., 3rd, & Kaufman, P. D. (2005). Replication-independent histone deposition by the HIR complex and Asf1. *Curr Biol*, *15*(22), 2044–2049. https://doi.org/10.1016/j.cub.2005.10.053

Hilton, I. B., D'Ippolito, A. M., Vockley, C. M., Thakore, P. I., Crawford, G. E., Reddy, T. E., & Gersbach, C. A. (2015). Epigenome editing by a CRISPR-Cas9-based acetyltransferase activates genes from promoters and enhancers. *Nat Biotechnol*, *33*(5), 510–517. https://doi.org/10.1038/nbt.3199

Houlard, M., Berlivet, S., Probst, A. V., Quivy, J. P., Hery, P., Almouzni, G., & Gerard, M. (2006). CAF-1 is essential for heterochromatin organization in pluripotent embryonic cells. *PLoS Genet*, *2*(11), e181. https://doi.org/10.1371/journal.pgen.0020181

Huang, H., Stromme, C. B., Saredi, G., Hodl, M., Strandsby, A., Gonzalez-Aguilera, C., Chen, S., Groth, A., & Patel, D. J. (2015). A unique binding mode enables MCM2 to chaperone histones H3-H4 at replication forks. *Nat Struct Mol Biol*, *22*(8), 618–626. https://doi.org/10.1038/nsmb.3055

Huang, S., Zhou, H., Tarara, J., & Zhang, Z. (2007). A novel role for histone chaperones CAF-1 and Rtt106p in heterochromatin silencing. *EMBO J*, *26*(9), 2274–2283. https://doi.org/10.1038/sj.emboj.7601670

Ishiuchi, T., Enriquez-Gasca, R., Mizutani, E., Boskovic, A., Ziegler-Birling, C., Rodriguez-Terrones, D., Wakayama, T., Vaquerizas, J. M., & Torres-Padilla, M. E. (2015). Early embryonic-like cells are induced by downregulating replication-dependent chromatin assembly. *Nat Struct Mol Biol*, *22*(9), 662–671. https://doi.org/10.1038/nsmb.3066

Jadhav, U., Manieri, E., Nalapareddy, K., Madha, S., Chakrabarti, S., Wucherpfennig, K., Barefoot, M., & Shivdasani, R. A. (2020). Replicational Dilution of H3K27me3 in Mammalian Cells and the Role of Poised Promoters. *Mol Cell*, *78*(1), 141–151 e145. https://doi.org/10.1016/j.molcel.2020.01.017

Jamieson, K., McNaught, K. J., Ormsby, T., Leggett, N. A., Honda, S., & Selker, E. U. (2018). Telomere repeats induce domains of H3K27 methylation in Neurospora. *Elife*, *7*. https://doi.org/10.7554/eLife.31216

Jamieson, K., Rountree, M. R., Lewis, Z. A., Stajich, J. E., & Selker, E. U. (2013). Regional control of histone H3 lysine 27 methylation in Neurospora. *Proc Natl Acad Sci U S A*, *110*(15), 6027–6032. https://doi.org/10.1073/pnas.1303750110

Kahn, T. G., Dorafshan, E., Schultheis, D., Zare, A., Stenberg, P., Reim, I., Pirrotta, V., & Schwartz, Y. B. (2016). Interdependence of PRC1 and PRC2 for recruitment to Polycomb Response Elements. *Nucleic Acids Res*, *44*(21), 10132–10149. https://doi.org/10.1093/nar/gkw701

Kim, K. H., & Roberts, C. W. (2016). Targeting EZH2 in cancer. *Nat Med*, *22*(2), 128–134. https://doi.org/10.1038/nm.4036

Lappalainen, T., & Greally, J. M. (2017). Associating cellular epigenetic models with human phenotypes. *Nat Rev Genet*, *18*(7), 441–451. https://doi.org/10.1038/nrg.2017.32

Laprell, F., Finkl, K., & Muller, J. (2017). Propagation of Polycomb-repressed chromatin requires sequence-specific recruitment to DNA. *Science*, *356*(6333), 85–88. https://doi.org/10.1126/science.aai8266

Laugesen, A., Hojfeldt, J. W., & Helin, K. (2019). Molecular Mechanisms Directing PRC2 Recruitment and H3K27 Methylation. *Mol Cell*, *74*(1), 8–18. https://doi.org/10.1016/j.molcel.2019.03.011

Lee, M. G., Villa, R., Trojer, P., Norman, J., Yan, K. P., Reinberg, D., Di Croce, L., & Shiekhattar, R. (2007). Demethylation of H3K27 regulates polycomb recruitment and H2A ubiquitination. *Science*, *318*(5849), 447–450. https://doi.org/10.1126/science.1149042

Lee, W., Teckie, S., Wiesner, T., Ran, L., Prieto Granada, C. N., Lin, M., Zhu, S., Cao, Z., Liang, Y., Sboner, A., Tap, W. D., Fletcher, J. A., Huberman, K. H., Qin, L. X., Viale, A., Singer, S., Zheng, D., Berger, M. F., Chen, Y.,…Chi, P. (2014). PRC2 is recurrently inactivated through EED or SUZ12 loss in malignant peripheral nerve sheath tumors. *Nat Genet*, *46*(11), 1227–1232. https://doi.org/10.1038/ng.3095

Li, Q., & Zhang, Z. (2012). Linking DNA replication to heterochromatin silencing and epigenetic inheritance. *Acta Biochim Biophys Sin (Shanghai)*, *44*(1), 3–13. https://doi.org/10.1093/abbs/gmr107

Margueron, R., & Reinberg, D. (2011). The Polycomb complex PRC2 and its mark in life. *Nature*, *469*(7330), 343–349. https://doi.org/10.1038/nature09784

Mello, J. A., Sillje, H. H., Roche, D. M., Kirschner, D. B., Nigg, E. A., & Almouzni, G. (2002). Human Asf1 and CAF-1 interact and synergize in a repair-coupled nucleosome assembly pathway. *EMBO Rep*, *3*(4), 329–334. https://doi.org/10.1093/embo-reports/kvf068

Murzina, N., Verreault, A., Laue, E., & Stillman, B. (1999). Heterochromatin dynamics in mouse cells: interaction between chromatin assembly factor 1 and HP1 proteins. *Mol Cell*, *4*(4), 529–540. https://doi.org/10.1016/s1097-2765(00)80204-x

Nunez, J. K., Chen, J., Pommier, G. C., Cogan, J. Z., Replogle, J. M., Adriaens, C., Ramadoss, G. N., Shi, Q., Hung, K. L., Samelson, A. J., Pogson, A. N., Kim, J. Y. S., Chung, A., Leonetti, M. D., Chang, H. Y., Kampmann, M., Bernstein, B. E., Hovestadt, V., Gilbert, L. A., & Weissman, J. S. (2021). Genome-wide programmable transcriptional memory by CRISPR-based epigenome editing. *Cell*, *184*(9), 2503–2519 e2517. https://doi.org/10.1016/j.cell.2021.03.025

O'Carroll, D., Erhardt, S., Pagani, M., Barton, S. C., Surani, M. A., & Jenuwein, T. (2001). The polycomb-group gene Ezh2 is required for early mouse development. *Mol Cell Biol*, *21*(13), 4330–4336. https://doi.org/10.1128/MCB.21.13.4330-4336.2001

Parreno, V., Martinez, A. M., & Cavalli, G. (2022). Mechanisms of Polycomb group protein function in cancer. *Cell Res*, *32*(3), 231–253. https://doi.org/10.1038/s41422-021-00606-6

Petryk, N., Dalby, M., Wenger, A., Stromme, C. B., Strandsby, A., Andersson, R., & Groth, A. (2018). MCM2 promotes symmetric inheritance of modified histones during DNA replication. *Science*, *361*(6409), 1389–1392. https://doi.org/10.1126/science.aau0294

Piunti, A., & Shilatifard, A. (2021). The roles of Polycomb repressive complexes in mammalian development and cancer. *Nat Rev Mol Cell Biol*, *22*(5), 326–345. https://doi.org/10.1038/s41580-021-00341-1

Ray-Gallet, D., Woolfe, A., Vassias, I., Pellentz, C., Lacoste, N., Puri, A., Schultz, D. C., Pchelintsev, N. A., Adams, P. D., Jansen, L. E., & Almouzni, G. (2011). Dynamics of histone H3 deposition in vivo reveal a nucleosome gap-filling mechanism for H3.3 to maintain chromatin integrity. *Mol Cell*, *44*(6), 928–941. https://doi.org/10.1016/j.molcel.2011.12.006

Ridenour, J. B., Moller, M., & Freitag, M. (2020). Polycomb Repression without Bristles: Facultative Heterochromatin and Genome Stability in Fungi. *Genes (Basel)*, *11*(6). https://doi.org/10.3390/genes11060638

Roelens, B., Clemot, M., Leroux-Coyau, M., Klapholz, B., & Dostatni, N. (2017). Maintenance of Heterochromatin by the Large Subunit of the CAF-1 Replication-Coupled Histone Chaperone Requires Its Interaction with HP1a Through a Conserved Motif. *Genetics*, *205*(1), 125–137. https://doi.org/10.1534/genetics.116.190785

Seong, I. S., Woda, J. M., Song, J. J., Lloret, A., Abeyrathne, P. D., Woo, C. J., Gregory, G., Lee, J. M., Wheeler, V. C., Walz, T., Kingston, R. E., Gusella, J. F., Conlon, R. A., & MacDonald, M. E. (2010). Huntingtin facilitates polycomb repressive complex 2. *Hum Mol Genet*, *19*(4), 573–583. https://doi.org/10.1093/hmg/ddp524

Serra-Cardona, A., & Zhang, Z. (2018). Replication-Coupled Nucleosome Assembly in the Passage of Epigenetic Information and Cell Identity. *Trends Biochem Sci*, *43*(2), 136–148. https://doi.org/10.1016/j.tibs.2017.12.003

Sharaf, A., Vijayanathan, M., Obornik, M., & Mozgova, I. (2022). Phylogenetic profiling resolves early emergence of PRC2 and illuminates its functional core. *Life Sci Alliance*, *5*(7). https://doi.org/10.26508/lsa.202101271

Song, Y., He, F., Xie, G., Guo, X., Xu, Y., Chen, Y., Liang, X., Stagljar, I., Egli, D., Ma, J., & Jiao, R. (2007). CAF-1 is essential for Drosophila development and involved in the maintenance of epigenetic memory. *Dev Biol*, *311*(1), 213–222. https://doi.org/10.1016/j.ydbio.2007.08.039

Ueda, T., Nakata, Y., Nagamachi, A., Yamasaki, N., Kanai, A., Sera, Y., Sasaki, M., Matsui, H., Honda, Z., Oda, H., Wolff, L., Inaba, T., & Honda, H. (2016). Propagation of trimethylated H3K27 regulated by polycomb protein EED is required for embryogenesis, hematopoietic maintenance, and tumor suppression. *Proc Natl Acad Sci U S A*, *113*(37), 10370–10375. https://doi.org/10.1073/pnas.1600070113

Velez, J., Dale, B., Park, K. S., Kaniskan, H. U., Yu, X., & Jin, J. (2024). Discovery of a novel, highly potent EZH2 PROTAC degrader for targeting non-canonical oncogenic functions of EZH2. *Eur J Med Chem*, *267*, 116154. https://doi.org/10.1016/j.ejmech.2024.116154

Wenger, A., Biran, A., Alcaraz, N., Redo-Riveiro, A., Sell, A. C., Krautz, R., Flury, V., Reveron-Gomez, N., Solis-Mezarino, V., Volker-Albert, M., Imhof, A., Andersson, R., Brickman, J. M., & Groth, A. (2023). Symmetric inheritance of parental histones governs epigenome maintenance and embryonic stem cell identity. *Nat Genet*, *55*(9), 1567–1578. https://doi.org/10.1038/s41588-023-01476-x

Xu, D., Besselink, S., Ramadoss, G. N., Dierks, P. H., Lubin, J. P., Pattali, R. K., Brim, J. I., Christenson, A. E., Colias, P. J., Ornelas, I. J., Nguyen, C. D., Chasins, S. E., Conklin, B. R., & Nunez, J. K. (2025). Programmable epigenome editing by transient delivery of CRISPR epigenome editor ribonucleoproteins. *Nat Commun*, *16*(1), 7948. https://doi.org/10.1038/s41467-025-63167-x

Yu, C., Gan, H., Serra-Cardona, A., Zhang, L., Gan, S., Sharma, S., Johansson, E., Chabes, A., Xu, R. M., & Zhang, Z. (2018). A mechanism for preventing asymmetric histone segregation onto replicating DNA strands. *Science*, *361*(6409), 1386–1389. https://doi.org/10.1126/science.aat8849

Yu, J. R., Lee, C. H., Oksuz, O., Stafford, J. M., & Reinberg, D. (2019). PRC2 is high maintenance. *Genes Dev*, *33*(15-16), 903–935. https://doi.org/10.1101/gad.325050.119

Zhang, X., Lou, H. E., Gopalan, V., Liu, Z., Jafarah, H. M., Lei, H., Jones, P., Sayers, C. M., Yohe, M. E., Chittiboina, P., Widemann, B. C., Thiele, C. J., Kelly, M. C., Hannenhalli, S., & Shern, J. F. (2022). Single-cell sequencing reveals activation of core transcription factors in PRC2-deficient malignant peripheral nerve sheath tumor. *Cell Rep*, *40*(12), 111363. https://doi.org/10.1016/j.celrep.2022.111363

Zhang, Z., Shibahara, K., & Stillman, B. (2000). PCNA connects DNA replication to epigenetic inheritance in yeast. *Nature*, *408*(6809), 221–225. https://doi.org/10.1038/35041601